R-02-38

Nuclear data for accelerator-driven transmutation

Annual Report 2001/2002

J Blomgren, C Johansson, J Klug,
N Olsson, S Pomp, P-U Renberg

Department of Neutron Research
and The Svedberg Laboratory
Uppsala University

July 2002

Svensk Kärnbränslehantering AB
Swedish Nuclear Fuel
and Waste Management Co
Box 5864
SE-102 40 Stockholm Sweden
Tel 08-459 84 00
+46 8 459 84 00
Fax 08-661 57 19
+46 8 661 57 19

ISSN 1402-3091
SKB Rapport R-02-38

Nuclear data for accelerator-driven transmutation

Annual Report 2001/2002

J Blomgren, C Johansson, J Klug,
N Olsson, S Pomp, P-U Renberg

Department of Neutron Research
and The Svedberg Laboratory
Uppsala University

July 2002

Contents

Appendices:
Most of them are conference papers. Appendix XVI is PhL thesis.

IV. C. Johansson, J. Blomgren, A. Ataç, B. Bergenwall, S. Dangtip, K. Elmgren, J. Klug, N. Olsson, S. Pomp, A. Prokoev, T. R.onnqvist, U. Tippawan, O. Jonsson, L. Nilsson, P.-U. Renberg, P. Nadel-Turonski, A. Ringbom. Neutron-proton scattering at intermediate energies – recent, new and future measurements. International Conference on Nuclear Data for Science and Technology. Tsukuba, Japan, Oct. 7–12, 2001 (accepted).

V. S. Dangtip, B. Bergenwall, U. Tippawan, A. Ataç, J. Blomgren, K. Elmgren, C. Johansson, J. Klug, N. Olsson, S. Pomp, O. Jonsson, L. Nilsson, P.-U. Renberg, P. Nadel-Turonski, G. Alm Carlsson, J. Söderberg, C. Le Brun, J.F. Lecolley, F.R. Lecolley, M.Louvel, N. Marie, C. Schweitzer, C. Varignon, Ph. Eudes, F. Haddad, M. Kerveno, T. Kirchner, C. Lebrun, L. Stuttg e, I. Slypen. Experimental double-differential cross sections and kerma coefficients for carbon and oxygen at 95 MeV, International Conference on Nuclear Data for Science and Technology, Tsukuba, Japan, Oct. 7–12, 2001 (accepted).

VI. U. Tippawan, B. Bergenwall, S. Dangtip, A. Ataç, J. Blomgren, K. Elmgren, C. Johansson, J. Klug, N. Olsson, S. Pomp, O. Jonsson, L. Nilsson, P.-U. Renberg, P. Nadel-Turonski. Experimental double-differential light-ion production cross sections for silicon at 95 MeV, International Conference on Nuclear Data for Science and Technology, Tsukuba, Japan, Oct. 7–12, 2001 (accepted).

VII. A. Koning, J.P.M. Beijers, J. Benlliure, O. Bersillon, J. Blomgren, J. Cugnon, M. Duijvestijn, P. Eudes, D. Filges, F. Haddad, S. Hilaire, C. Lebrun, F.-R. Lecolley, S. Leray, J.-P. Meulders, R. Michel, R. Neef, R. Nolte, N. Olsson, E. Ostendorf, E. Ramström, K.-H. Schmidt, H. Schumacher, I. Slypen, H.-A. Synal, R. Weinreich. HINDAS – A European nuclear data program for accelerator-driven systems, International Conference on Nuclear Data for Science and Technology, Tsukuba, Japan, Oct. 7–12, 2001 (accepted).

VIII. Jean-Pierre Meulders, J. Blomgren and Nils Olsson, representing the HINDAS collaboration: HINDAS – A European Concerted Action on High and Intermediate Energy Nuclear Data for Accelerator-Driven Systems Nuclear Applications in the New Millennium, Reno, Nevada, USA, Nov. 11–15, 2001. (accepted)

IX. C. Johansson, J. Blomgren, A. Ataç, B. Bergenwall, S. Dangtip, K. Elmgren, J. Klug, N. Olsson, S. Pomp, A. Prokoev, U. Tippawan, O. Jonsson, L. Nilsson, P.-U. Renberg, P. Nadel-Turonski, C. Le Brun, J.F. Lecolley, F.R. Lecolley, M. Louvel, N. Marie, C. Varignon, Ph. Eudes, F. Haddad, M. Kerveno, T. Kirchner, C. Lebrun, L. Stuttge, I. Slypen. Neutrons for science and industry – the Uppsala neutron beam facility, Nuclear Applications in the New Millennium, Reno, Nevada, USA, Nov. 11–15, 2001. (accepted)

X. J. Klug, J. Blomgren, A. Ataç, B. Bergenwall, S. Dangtip, K. Elmgren, C. Johansson, N. Olsson, S. Pomp, A. Prokoev, U. Tippawan, O. Jonsson, L. Nilsson, P.-U. Renberg, P. Nadel-Turonski, C. Le Brun, J.F. Lecolley, F.R. Lecolley, M.Louvel, N. Marie, C. Varignon, Ph. Eudes, F. Haddad, M. Kerveno, T. Kirchner, C. Lebrun, L. Stuttg e, I. Slypen. SCANDAL – A facility for elastic neutron scattering studies in the 50–130 MeV range, Nuclear Applications in the New Millennium, Reno, Nevada, USA, Nov. 11–15, 2001. (accepted)

XI. H. Cond e, J. Blomgren, W. Gudowski, J.-O. Liljenzin, C. Mileikovsky, Nils Olsson, J. Wallenius, Swedish Expert Group on Transmutation, Nuclear Applications in the New Millennium, Reno, Nevada, USA, Nov. 11–15, 2001. (accepted)

XII. J. Blomgren, Experimental activities at high energies, Invited lecture at Workshop on Nuclear Data for Science & Technology: Accelerator Driven Waste Incineration, Trieste, Italy, Sept. 10-21, 2001.

XIII. J. Blomgren, B. Bergenwall, C. Johansson, J. Klug, S. Pomp, U. Tippawan, K. Elmgren, N. Olsson, O. Jonsson, L. Nilsson, A. Prokoev, P.-U. Renberg, M. Österlund, S. Dangtip, Neutrons for science and industry – The Uppsala neutron beam facility, Particle Beam and Plasma Interaction with Materials, Chiang Mai, Thailand, Jan. 31 – Feb. 2, 2002 (accepted).

XIV. S. Pomp, B. Bergenwall, J. Blomgren, C. Johansson, J. Klug, U. Tippawan, S. Dangtip, K. Elmgren, N. Olsson, O. Jonsson, L. Nilsson, A.V. Prokoev, P.-U. Renberg, M. Österlund, MEDLEY and SCANDAL – two facilities for studies of neutron-induced nuclear reactions, Particle Beam and Plasma Interaction with Materials, Chiang Mai, Thailand, Jan. 31–Feb. 2, 2002 (accepted).

XV. N. Olsson and T. Lefvert, Minnesanteckningar från möte med OECD/NEA Nuclear Science Committee (NSC), Paris, 2002-06-03 – 05.

XVI. C. Johansson, MCNP calculations of beta-gamma concidence detectors for monitoring of radioactive xenon, PhL thesis.

1 Background

The present project, supported as a research task agreement by Statens Kärnkrafts-inspektion (SKI), Svensk Kärnbränslehantering AB (SKB), Barsebäck Kraft AB (BKAB) and Vattenfall AB, started 1998-07-01. From 1999-01-01 the project also receives support from Totalförsvarets forskningsinstitut (FOI). The primary objective from the supporting organizations is to promote research and research education of relevance for development of the national competence within nuclear energy.

The aim of the project is in short to:

- promote development of the competence within nuclear physics and nuclear technology by supporting licenciate and PhD students,
- push forward the international research front regarding fundamental nuclear data within the presently highlighted research area “accelerator-driven transmutation”,
- strengthen the Swedish in uence within the mentioned research areaby expanding the international contact network,
- constitute a basis for Swedish participation in the nuclear data activities at IAEA and OECD/NEA.

The project is run by the Department of Neutron Research (INF) at Uppsala University, and is utilizing the unique neutron beam facility at the national The Svedberg Laboratory (TSL) at Uppsala University.

In this document, we give a status report after the fourth year (2001-07-01 – 2002-06-30) of the project.

The contract on financial support to the project was for four calendar years, during the period 1998-07-01 – 2002-06-30, and thereby the financial support has now been terminated. Two students were supposed to be educated to PhD exam within the project. Because PhD students cannot be accepted at Uppsala university until full funding has been guaranteed, they were accepted September 1, 1998 (Joakim Klug) and March 1, 1999 (Cecilia Johansson). In addition, they have been involved on a minor fraction of their time in teaching and outreaching activities, paid from other sources. Thereby, they still have some time left until dissertation for the PhD level, although the plan on four years total research time is unchanged. Both students have obtained licentiate degrees. Funding for the remaining time has been reserved, i.e., the total funding is adequate for completing the task. These modifications of the agenda have been presented to and agreed upon by the reference group.

Since the project financially has been terminated, this annual report also serves as the final report of the project. As will be presented below, a new project (NATT) with a similar scope supported by almost the same partners begins July 1, 2002. Thereby, information about the completion of the PhD work by Johansson and Klug will be given in the future NATT reports, which will be distributed to the partners of the present project.

2 Introduction

Transmutation techniques in accelerator-driven systems (ADS) involve high-energy neutrons, created in the proton-induced spallation of a heavy target nucleus. The existing nuclear data libraries developed for reactors of today go up to about 20 MeV, which covers all available energies for that application; but with a spallator coupled to a core, neutrons with energies up to 1–2 GeV will be present. Although a large majority of the neutrons will be below 20 MeV, the relatively small fraction at higher energies still has to be characterized. Above ~ 200 MeV, direct reaction models work reasonably well, while at lower energies nuclear distortion plays a non-trivial role. This makes the 20–200 MeV region the most important for new experimental cross section data.

Very little high-quality neutron-induced data exist in this energy domain. Only the total cross section (Finlay et al., 1993) and the np scattering cross section have been investigated extensively. Besides this, there are data on neutron elastic scattering from UC Davis at 65 MeV on a few nuclei (Hjort et al., 1994). Programmes to measure neutron elastic scattering have been proposed or begun at Los Alamos (Rapaport and Osborne) and IUCF (Finlay et al., 1992), with the former resulting in a thesis on data in the 5°–30° range on a few nuclei.

The situation is similar for (n,xp) reactions, where programmes have been run at UC Davis (Ford et al., 1989), Los Alamos (Rapaport and Sugarbaker, 1994), TRIUMF (Alford and Spicer, 1998) and TSL Uppsala (Olsson, 1995, Blomgren, 1997), but with limited coverage in secondary particle energy and angle. Better coverage has been obtained by the Louvain-la-Neuve group up to 70 MeV (Slypen et al., 1994).

Thus, there is an urgent need for neutron-induced cross section data in the region around 100 MeV, which is an area where very few facilities in the world can give contributions. By international collaboration within an EU supported Concerted Action, which has been followed by the full scale project HINDAS, the level of ambition for the present project has been increased, and the potential of the unique neutron beam facility at The Svedberg Laboratory in Uppsala can be fully exploited.

3 Experimental setup and techniques

3.1 The TSL neutron beam facility

At TSL, quasi-monoenergetic neutrons are produced by the reaction ^{7}Li(p,n)^{7}Be in a ^{7}Li target bombarded by 50 180 MeV protons from the cyclotron, as is illustrated in Fig. 1 (Condé et al., 1990, Klug et al., 2002). After the target, the proton beam is bent by two dipole magnets into an 8 m long concrete tunnel, where it is focused and stopped in a well-shielded Faraday cup, which is used to measure the proton beam current. A narrow neutron beam is formed in the forward direction by a system of three collimators, with a total thickness of more than four metres.

The energy spectrum of the neutron beam consists of a high-energy peak, having approximately the same energy as the incident proton beam, and a low-energy tail. About half of all neutrons appear in the high-energy peak, while the rest are roughly equally distributed in energy, from the maximum energy and down to zero. The thermal contribution is small. The low-energy tail of the neutron beam can be reduced using time-of-flight (TOF) techniques over the long distance between the neutron source and the reaction target (about 8 m).

The relative neutron beam intensity is monitored by integrating the charge of the primary proton beam, as well as by using thin film breakdown counters, placed in the neutron beam, measuring the number of neutron-induced fissions in ^{238}U (Prokofiev et al., 1999).

Two multi-purpose experimental setups are semi-permanently installed at the neutron beam line, namely MEDLEY and SCANDAL. These were described in detail in the annual report 1999/2000, and only a brief presentation is given here.

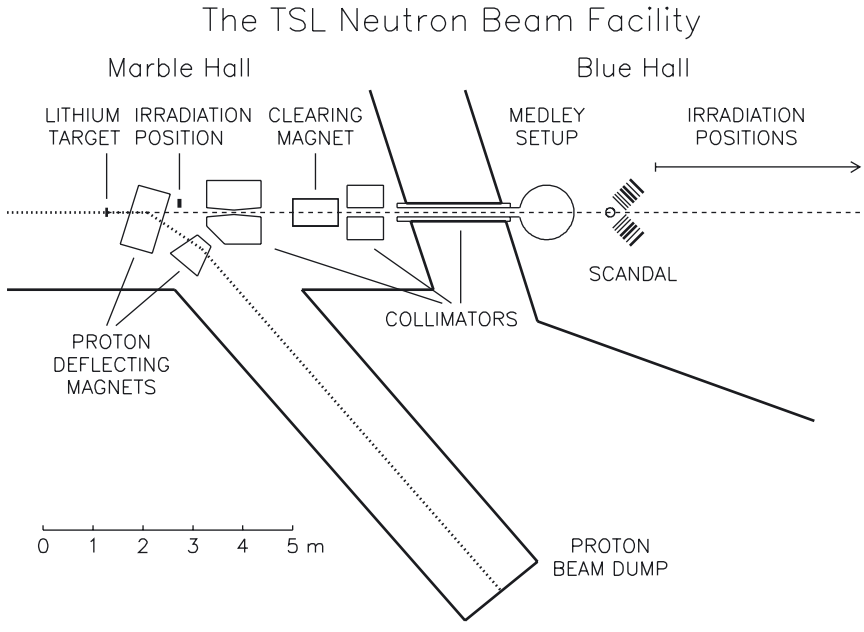

Figure 1. *The TSL neutron beam facility.*

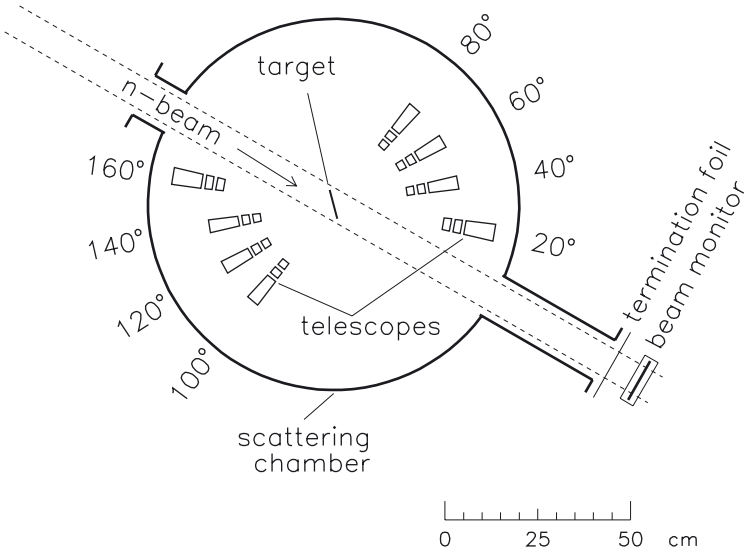

Figure 2. *The MEDLEY detector array.*

3.2 The MEDLEY setup

The MEDLEY detector array (Dangtip et al., 2000), shown in Fig. 2, is designed for measurements of neutron-induced light-ion production cross sections of relevance for applications within ADS and fast-neutron cancer therapy and related dosimetry. It consists of eight particle telescopes, installed at scattering angles of 20°–160° with 20° separation, in a 1 m diameterscatteringchamber, positioned directly after the last neutron collimator. All the telescopes are fixed on a turnable plate at the bottom of the chamber, which can be rotated without breaking the vacuum.

Each telescope is a $\Delta E - \Delta E - E$ detector combination, where the ΔE detectors are silicon surface barrier detectors with thicknesses of 50 or 60 μm and 400 or 500 μm, respectively, while the E detector is a 50 mm long inorganic CsI(Tl) crystal. $\Delta E - \Delta E$ or $\Delta E - E$ techniques are used to identify light charged particles (p, d, t, ^{3}He, α). The chosen design gives a sufficient dynamic range to distinguish all charged particles from a few MeV up to more than 100 MeV.

The solid angle of the telescopes is defined by active collimators, designed as thin hollow plastic scintillator detectors, mounted on small photomultiplier tubes. A signal from such a detector is used to veto the corresponding event, thereby ensuring that only particles that pass inside the collimator are registered.

3.3 The SCANDAL setup

The SCANDAL setup (Klug et al., 2002) is primarily intended for studies of elastic neutron scattering, i.e., (n,n) reactions. Neutron detection is accomplished via conversion to protons by the H(n,p) reaction. In addition, (n,xp) reactions in nuclei can be studied by direct detection of protons. This feature is also used for calibration, and the setup has therefore been designed for a quick and simple change from one mode to the other. The device is illustrated in Fig. 3. It consists of two identical systems, in most cases

located on each side of the neutron beam. The design allows the neutron beam to pass through the drift chambers of the right-side setup, making low-background measurements close to zero degrees feasible.

In neutron detection mode, each arm consists of a 2 mm thick veto scintillator for fast charged-particle rejection, a neutron-to-proton converter which is a 10 mm thick plastic scintillator, a 2 mm thick plastic scintillator for triggering, two drift chambers for proton tracking, a 2 mm thick ΔE plastic scintillator, which is also part of the trigger, and an array of 12 large CsI detectors for energy determination. The trigger is provided by a coincidence of the two trigger scintillators, vetoed by the front scintillator. The compact geometry allows a large solid angle for protons emitted from the converter. Recoil protons are selected using the ΔE and E information from the plastic scintillators and the CsI detectors, respectively.

The energy resolution is about 3.7 MeV (FWHM), which is sufficient to resolve elastic and inelastic scattering in several nuclei. The angular resolution is calculated to be about 1.4° (rms) when using a cylindrical scattering sample of 5 cm diameter.

When SCANDAL is used for (n,xp) studies, the veto and converter scintillators are removed. A multitarget arrangement can be used to increase the target content without impairing the energy resolution, which istypically 3.0 MeV (FWHM). This multitarget box allows up to seven targets to be mounted simultaneously, interspaced with multi-wire proportional counters (MWPC). In this way it is possible to determine in which target layer the reaction took place, and corrections for energy loss in the subsequent targets can be applied. In addition, different target materials can be studied simultaneously, thus facilitating absolute cross section normalization by filling a few of the multi-target slots with CH2 targets. The first two slots are normally kept empty, and used to identify charged particles contaminating the neutron beam.

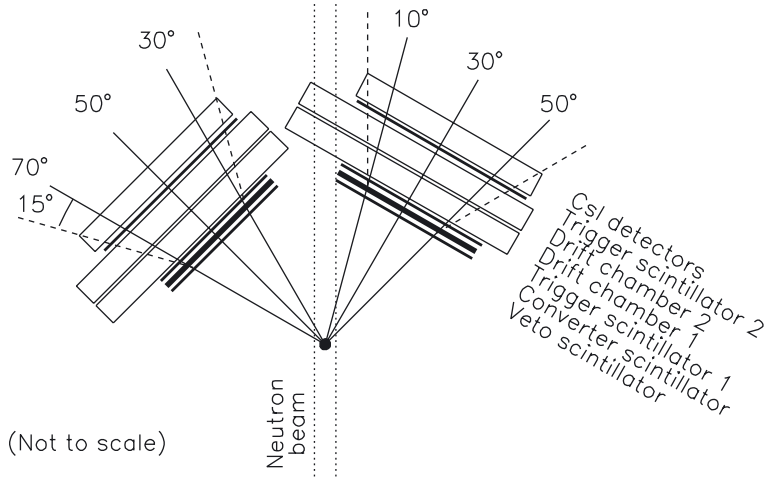

Figure 3. *The SCANDAL setup.*

3.4 New neutron beam facility atTSL

The rapidly increasing number of neutron beam users has motivated a new facility to be built. The overall design has been agreed upon, and at present details of the individual components are being designed. Practical work has begun during spring 2002, which includes re-building of beam line magnets, removal of obsolete heavy equipment and procurement of concrete for the new shielding walls. The experimental programme will face a down-period during autumn 2003 to allow for major installations.

4 Results and analysis

4.1 Elastic scattering

A one-week experiment was performed in February 2002 with SCANDAL on neutron scattering from iron. Data are under analysis, carried out by Michael Österlund. The analysis of the data on elastic scattering from ^{12}C and ^{208}Pb has now resulted in final data. A preliminary angular distribution of neutrons scattered from carbon and lead is shown in Fig. 4. Some minor work remains on data corrections. Publications of the results are underway. It will be very interesting to see how well these data can be described by recent optical model representations (Koning).

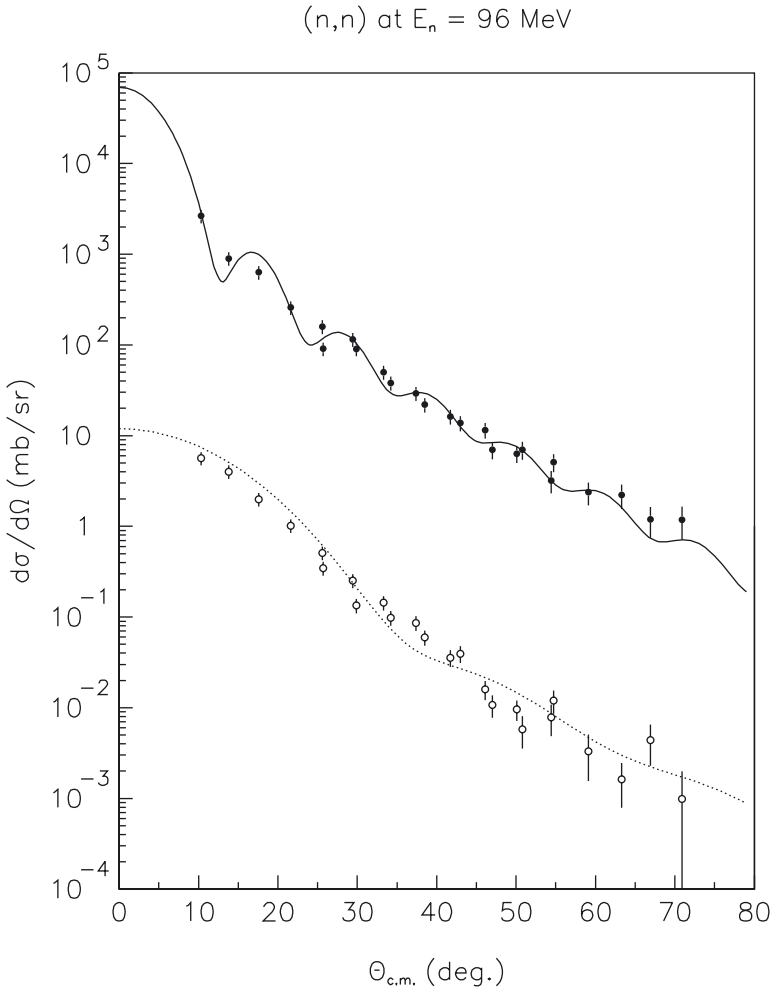

Figure 4. *Preliminary data on neutron elastic scattering from ^{12}C and ^{208}Pb. Filled and open circles refer to data on ^{208}Pb and ^{12}C, respectively. The curves are predictions by a model by Koning. The carbon data and the corresponding theory prediction have been multiplied by 0.01.*

4.2 (n,xlcp) reactions

In August–September 2001, we performed experiments with MEDLEY to measure double differential cross sections $d^2\sigma/d\Omega dE$ for protons and other light charged particles (d, t, ^{3}He, α) emitted in reactions of 100 MeV neutrons on ^{238}U targets. This was carried out in collaboration with a French group lead by Jean-François Lecolley, Caen, within the HINDAS collaboration. A second experimental run was performed in parallel with the elastic scattering measurement with SCANDAL in February 2002.

4.3 (n,xn) reactions

We have launched another collaboration project with the Caen group; (n,xn) reactions. For these studies, a modified SCANDAL converter (CLODIA) has been designed and built in Caen. It was tested and mounted at SCANDAL for the first time in April 2001. This test experiment provided guidance for further equipment development. In April 2002, an upgraded version of CLODIA was tested in beam. Preliminary analysis indicates that the performance of the equipment isnow satisfactory, and a second CLODIA device will be built.

4.4 Tagged neutron-proton scattering

Neutron-proton scattering is the reference cross section for fast-neutron reactions, i.e., it is the standard which all other cross sections are measured relative to. Experimental studies of this cross section have been undertaken at TSL as part of the present project, and they will form a major part of the thesis by Cecilia Johansson. We have also been involved in a similar experiment at Indiana University Cyclotron Facility (IUCF), Bloomington, Indiana, USA. The last experiment with that setup was carried out in July–August 2001, with Stephan Pomp and Udomrat Tippawan participating from Uppsala.

A large paper on the technical aspects of the project is in final form, and will be submitted early autumn 2002 to Nuclear Instruments and Methods A.

5 International activities

5.1 Collaboration

INF participates in the EU project HINDAS (High- and Intermediate Energy Nuclear Data for Accelerator-Driven Systems), which involves 16 European institutions from Belgium, France, Germany, The Netherlands, Spain, Sweden and Switzerland. The experimental work is performed at six European laboratories (UCL in Louvain-la-Neuve, TSL in Uppsala, KVI in Groningen, PSI in Villigen, COSY at Jülich and GSI in Darmstadt). Work on the theoretical interpretation of the experimental results is also included. The project, which started 2000-09-01 and runs over three years, is coordinated by Prof. Jean-Pierre Meulders, Louvain-la-Neuve, Belgium.

HINDAS has a total budget of 2.1 MEUR, whereof 210 kEUR falls on the Uppsala partner, while the collaborators that use the TSL neutron facility have received in total about 500 kEUR. Most of the money is intended for PhD students or postdocs. This means an increasing engagement for the Uppsala group and TSL, but also more focus on the activities here.

A substantial fraction of the Uppsala funding is used to employ Stephan Pomp, who acts as liaison between the Uppsala group and the collaborating groups, as well as supervisor for PhD students at INF.

To our judgement, HINDAS is well organized and focused. It involves a major part of the competence and equipment available in Europe, and will also contribute to the development of nuclear data activities in Europe, by bringing new scientists into this area.

Recently, an Expression of Interest (EoI) was submitted to the European Commission on a nuclear data project within the 6th framework program. The project is called Transmutation RElevant Nuclear Data (TREND), and is aimed to continue the work of the present HINDAS project. TREND, however, is larger, and it spans all energies from 1 eVup to1GeV.At present, about 25 European institutes are involved.

5.2 Meetings and conferences

Nils Olsson has taken on duty as Swedish representative in the OECD/NEA Nuclear Science Committee (NSC) and its Executive Group. He participated in a meeting with these bodies 2002-06-03 – 05. Notes from the meeting are enclosed in appendix XV.

Jan Blomgren was invited speaker at Workshop on Nuclear Data for Science and Technology: Accelerator Driven Waste Incineration, Trieste, Italy, September 2002. Although named “workshop”, it was in reality a summer school with a majority of the participants from the 3rd world. The lectures are enclosed in appendix XII.

The entire group participated in the Internation Conference on Nuclear Data for Science and Technology, Tsukuba, Japan, October 7–11. In total, 11 contributions with Uppsala authors were presented. Nils Olsson gave aninvited overview talk about the

Uppsala activities, and Cecilia Johansson and Joakim Klug gave oral presentations of their work. Relevant contributions are enclosed in appendix I–VII.

Jan Blomgren, Cecilia Johansson and Joakim Klug participated in the International Conference on Accelerator Driven Transmutation Technologies, Nuclear Applications in the New Millennium, Reno, Nevada, USA, November 11–15. Jan Blomgren gave a talk presenting the HINDAS collaboration, and Cecilia Johansson and Joakim Klug gave poster presentations of their work (appendix VIII–XI).

Stephan Pomp and Jan Blomgren participated in the International Workshop on Particle Beam and Plasma Interaction with Materials, Chiang Mai, Thailand, January 31–February 2, 2002. Two contributions were presented (appendix XIII–XIV). At the same time, a collaboration meeting was held with the Chiang Mai partners of the neutron beam group.

6 Administrative matters

6.1 Personnel and PhD students

During the project year, Jan Blomgren has been project leader. Stephan Pomp has worked full time within the project with research and student supervision. During the year, he got a new position as assistant professor (forskarassistent), which begins July 1, 2002. Nils Olsson, former project leader and now research director at FOI, is active within the project on a part-time basis (20%).

The loss of supervision capacity with Nils Olssons departure has partly been compensated by involving Michael Österlund and Somsak Dangtip, although both are financed by other sources than the present project. Österlund is associate professor at Jönköping university, with which we have reached an agreement on joint funding (25% each, making him available on 50% of his time). By this agreement, one more university is now involved in nuclear physics activities. Dangtip is assistant professor at Chiang Mai university, Thailand. He is involved in simulations of the experimental equipment of the project.

Two PhD students are directly connected to and financed by the present project, Cecilia Johansson and Joakim Klug, which both are connected to the research school AIM (Advanced Instrumentation and Measurements). Two other students, Bel Bergenwall who is financed by AIM, and Udomrat Tippawan with a scholarship from Thailand, have tasks strongly related to the present project, and especially to the line of development emerging from the collaboration with the French groups within HINDAS.

During this year, an agreement has been reached with SKB, SKI, Ringhals AB and FOI about a new project, which forms a natural continuation of the present. The new project, Neutron data for Accelerator-driven Transmutation Technologies (NATT), runs over 4 years, during 2002-07-01 – 2006-06-30. Two PhD students will be educated up to PhD exam within the project. The two students, Angelica Hildebrand and Philippe Mermod, have actually already been accepted, and begun their studies April 15. Both students have also been accepted to AIM.

Cecilia Johansson defended her licentiate thesis June 7. The title of thesis is “MCNP calculations of beta-gamma concidence detectors for monitoring of radioactive xenon”.

INF has had one PhD dissertation during the year, Klas Elmgren, who has worked on experimental studies of fission at intermediate energies.

During the year, Jan Blomgren has been director of studies of the Research School for Nuclear Technology, based at the Swedish Centre for Nuclear Technology. The main activity during the year has been to start a basic course on nuclear power technology. This has been accomplished by joining forces with Kärnkraftsäkerhet och Utbildning AB (KSU), which is an education company owned and operated by the nuclear power industry. An agreement has been reached between KSU and SKC that academic students can join the KSU courses, thereby establishing a direct link between industry and universities. KSU provides the infrastructure and the organization of the course, whilst young academic staff (Jan Blomgren, Uppsala university, Anders Nordlund, Chalmers and Mats Jonsson, KTH) contribute as teachers. A record number of students (32, whereof 10 academic) took the course. In addition, this has led to the involvement by Jan Blomgren in various other KSU courses, e.g., in the physics of radiation protection.

Members of our group participate in several courses on nuclear physics as well as on energy technology. Some of these include problems related to transmutation. Also a number of outreach talks, seminars, articles and interviews related to this project have been given.

6.2 Reference group

Reference group meetings, with participation by Per-Eric Ahlström (SKB), Benny Sundström (SKI), Thomas Lefvert (Vattenfall AB), Fredrik Winge (BKAB) and Anders Ringbom (FOA), were held in Uppsala 2001-09-20 and 2002-03-14. Scientic and administrative reports on the progress of the project were given at these meetings. In addition to the meetings, the progress of the work has continously been communicated to the reference group members by short, written, quarterly reports.

References

Alford W.P. and Spicer B.M., 1998. Nucleon charge-exchange reactions at intermediate energy, Advances in Nuclear Physics 24, 1.

Blomgren J, 1997. The (n,p) reaction – Not So Boring After All? Proceedings from International Symposium on New Facet of Spin Giant Resonances in Nuclei, Tokyo, p. 70. (Invited talk).

Cond e H., Hultqvist S., Olsson N., Rönnqvist T., Zorro R., Blomgren J., Tibell G., Hakansson A., Jonsson O., Lindholm A., Nilsson L., Renberg P.-U., Brockstedt A., Ekstr. om P., Österlund M., Brady P., Szeflinski Z., 1990. A facility for studies of neutron induced reactions in the 50–200 MeV range, Nucl. Instr. Meth. A292, 121.

Dangtip S., Ata¢ c A., Bergenwall B., Blomgren J., Elmgren K., Johansson C., Klug J., Olsson N., Alm Carlsson G., Söderberg J., Jonsson O., Nilsson L., Renberg P.-U., Nadel-Turonski P., Le Brun C., Lecolley F.-R., Lecolley J.-F., Varignon C., Eudes Ph., Haddad F., Kerveno M., Kirchner T., Lebrun C., 2000. A facility for measurements of nuclear cross sections for fast neutron cancer therapy, Nucl. Instr. Meth., in press.

Finlay R., Abfalterer W.P., Fink G., Montei E., Adami T., Lisowski P.W., Morgan G.L., Haight R.C., 1993. Neutron total cross sections at intermediate energies, Phys. Rev. C47, 237.

Finlay R., 1992. Proposal to the NSF for support of CHICANE/Spectrometer System for the IUCF Cooler Ring.

Ford T.D., Brady F.P., Castaneda C.M., Drummond J.R., McEachern B., Romero J.L., Sorenson D.S., 1989. A large dynamic range detector for measurement of neutron-induced charged particle spectra down to zero degrees, Nucl. Instr. Meth. A274, 253.

Hjort E.L., Brady F.P., Romero J.L, Drummond J.R., Sorenson D.S., Osborne J.H., McEachern B., 1994. Measurements and analysis of neutron elastic scattering at 65 MeV, Phys. Rev. C50, 275.

Klug J., Blomgren J., Ata¢ c A., Bergenwall B., Dangtip S., Elmgren K., Johansson C., Olsson N., Rahm J., Jonsson O., Nilsson L., Renberg P.-U., Nadel-Turonski P., Ringbom A., Oberstedt A., Tovesson F., Le Brun C., Lecolley J.-F., Lecolley F.-R., Louvel M., Marie N., Schweitzer C., Varignon C., Eudes Ph., Haddad F., Kerveno M., Kirchner T., Lebrun C., Stuttg e L., Slypen I., Proko˘ev A., Smirnov A., Michel R., Neumann S., Herpers U., 2002. SCANDAL – A facility for elastic neutron scattering studies in the 50 130 MeV range, accepted for publication in Nucl. Instr. Meth. A.

Koning A. private communication.

Olsson N., 1995. Studies of spin-isospin excitations at TSL in Uppsala, Nucl. Phys. News 5, no. 2, 28.

Prokofiev A.V., Smirnov A.N., Renberg P.-U., 1999. A monitor for intermediate-energy neutrons based on thin ˇlm breakdown counters, Report TSL/ISV-99-0203, Uppsala University.

Rahm J., Blomgren J., Condé H., Elmgren K., Olsson N., R.onnqvist T., Zorro R., Ringbom A., Tibell G., Jonsson O., Nilsson L., Renberg P.-U., Ericson T.E.O. and Loiseau B., 2001. np scattering measurements at 96 MeV, Phys. Rev. C63, 044001.

Rapaport J. and Sugarbaker E., 1994. Isovector excitations in nuclei, Annu. Rev. Nucl. Part. Sci. 44, 109.

Rapaport J., 1994. private communication, and Osborne J., thesis, unpublished.

Slypen I., Corcalciuc V., Ninane A., Meulders J.P. Charged particles produced in fast neutron induced reactions on ^{12}C in the 45 80 MeV energy range, Nucl. Instr. Meth. A337, 431.

Thun J., Blomgren J., Elmgren K., K.allne J., Olsson N., Lecolley J.-F., Lefebvres F., Varignon C., Borne F., Ledoux X., Patin Y., Jonsson O., Renberg P.-U., 2002. The response of a liquid scintillator detector to 21–100 MeV neutrons, Nucl. Instr. Meth. A478, 559.

SCANDAL - A Facility for Elastic Neutron Scattering Studies in the 50–130 MeV range

Joakim KLUG[1,*], Jan BLOMGREN[1], Ayse ATAÇ[1], Bel BERGENWALL[1], Somsak DANGTIP[1], Klas ELMGREN[1,2], Cecilia JOHANSSON[1], Nils OLSSON[1,2], Stephan POMP[1], Udomrat TIPPAWAN[1], Alexander PROKOFIEV[1,3], Olle JONSSON[3], Leif NILSSON[3], Per-Ulf RENBERG[3], Pawel NADEL-TURONSKI[4], Christian LE BRUN[5], Jean-François LECOLLEY[5], François-René LECOLLEY[5], Michel LOUVEL[5], Nathalie MARIE[5], Cyril VARIGNON[5], Philippe EUDES[6], Ferid HADDAD[6], Maëlle KERVENO[6], Thomas KIRCHNER[6], Claude LEBRUN[6], Louise STUTTGÉ[7], Isabelle SLYPEN[8]

[1] *Department of Neutron Research, Uppsala University, Sweden*
[2] *Swedish Defence Research Agency (FOI), Stockholm, Sweden*
[3] *The Svedberg Laboratory, Uppsala University, Sweden*
[4] *Department of Radiation Sciences, Uppsala University, Sweden*
[5] *LPC, ISMRA et Université de Caen, CNRS/IN2P3, France*
[6] *SUBATECH, Université de Nantes, CNRS/IN2P3, France*
[7] *IReS, Strasbourg, France*
[8] *Institute de Physique Nucleaire, Université Catholique de Louvain, Belgium*

Recently, a large number of applications involving high-energy (> 20 MeV) neutrons have become important. Examples are development of spallation sources, transmutation of nuclear waste, fast-neutron cancer therapy, as well as dose effects for airflight personnel and electronics failures due to cosmic-ray neutrons.

Elastic neutron scattering plays a key role for the understanding of all these areas. The most important reason is that it allows a determination of the optical potential, which plays a decisive role in every microscopic calculation including neutrons in either the entrance or exit channel. In addition, the elastic cross section is also the largest of the individual partial cross sections contributing to the total cross section.

A facility for detection of scattered neutrons in the energy interval 50–130 MeV, SCANDAL (SCAttered Nucleon Detection AssembLy), has recently been installed at the 20–180 MeV neutron beam facility of the The Svedberg Laboratory, Uppsala. It is primarily intended for studies of elastic neutron scattering, but can be used for the (n,p) and (n,d) reaction experiments as well.

The performance of the spectrometer is illustrated in measurements of the (n,p) and (n,n) reactions on ^{1}H and ^{12}C at 96 MeV.

KEYWORDS: neutron beam, neutron detection, active converter, CsI(Na) hodoscope, neutron scattering

I. Introduction

The recent development of high-intensity proton accelerators has resulted in ideas to use subcritical reactors, fed by externally produced neutrons, for transmutation of waste from nuclear power reactors or nuclear weapons material. This has the potential to simplify the requirements for long-term storage of such materials.

Conventional radiation treatment of tumours is carried out using photons or electrons. Some common types of tumours, however, cannot be treated successfully in this way. For some of these, very good treatment results have been reached with fast neutron therapy, making it the largest non-conventional therapy world-wide.

It has also become evident that electronics in aeroplanes suffer effects from cosmic-ray neutrons.[1,2)] These can induce nuclear reactions in the silicon substrate of a memory device, releasing free charges, which in turn can flip the memory content. This random re-programming is obviously not wanted.

Furthermore, neutrons at aircraft altitudes give a significant radiation dose to airplane personnel. This poses a relatively new dosimetry problem, which is currently under investigation.[3)]

All these applications involve neutrons at energies above 20 MeV. As there is very little data available in this region, the interest in new data is growing rapidly.

A facility for detection of scattered neutrons, SCANDAL (SCAttered Nucleon Detection AssembLy), has recently been installed at the 20–180 MeV neutron beam facility of The Svedberg Laboratory (TSL) in Uppsala, Sweden. It is primarily intended for studies of elastic neutron scattering, but can be used for the (n,p) and (n,d) reactions as well. The energy interval for detected neutrons is 50–130 MeV, i. e., of greatest relevance for the applications described above.

1. Why elastic scattering?

Neutron elastic scattering allows a determination of the optical potential, which plays a role in every microscopic calculation including neutrons in either the entrance or exit channel. In addition, the elastic cross section is also the largest of the individual partial cross sections contributing to the total cross section. In fact, a consequence of the optical model is that the elastic cross section must constitute at least half the

* Corresponding author, Tel. +46 18 471 3254, Fax. +46 18 471 3853, E-mail: joakim.klug@tsl.uu.se

total cross section. Thus, enhanced data on elastic scattering will improve the understanding of e. g. neutron transport in a spallation target.

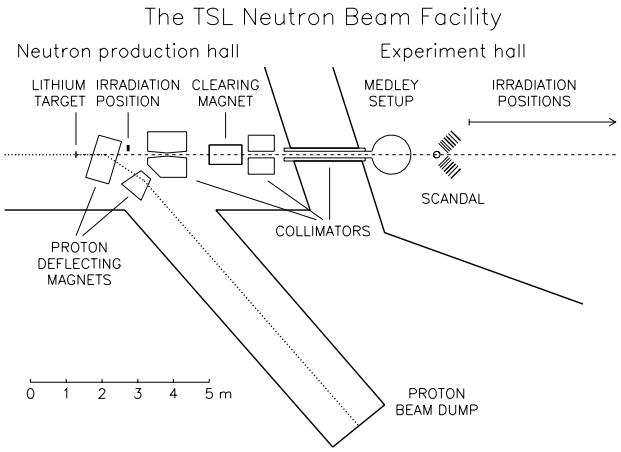

Fig. 1 The TSL neutron beam facility.

II. The neutron beam facility

1. Neutron production

At the neutron facility at TSL[4] (see **fig. 1**), almost monoenergetic neutrons are produced by the reaction ^{7}Li(p,n)^{7}Be in a target of 99.98 % ^{7}Li. After the target, the proton beam is bent into a tunnel, where it is stopped in a well-shielded carbon beam-dump. A narrow neutron beam is formed in the forward direction by three collimators.

The energy spectrum of the neutron beam consists of a full-energy peak, containing about half of all neutrons, and a low-energy tail ranging from maximum energy down to zero. This tail can be reduced by time-of-flight measurements. With a proton beam of 5 μA onto a 4 mm lithium target, the total neutron yield in the full-energy peak at the experimental position, 8 m from the production target, is about $5 \cdot 10^4$ cm^{-2}s^{-1}. The energy resolution of the full-energy peak depends on the choice of lithium target thickness. For most experiments a resolution of about 1 MeV (FWHM) has been selected.

2. Monitoring

For direct neutron monitoring, fission counters are available, which have been calibrated relative to *np* scattering. The absolute uncertainties in the measured neutron fluences are about 10 %.

Relative monitoring can be provided by charge integration of the primary proton beam. In addition, different experiments running simultaneously can provide signals to each other, also to be used as relative monitors.

III. The SCANDAL setup

1. General layout

The setup is primarily intended for studies of elastic neutron scattering, i. e., (n,n) reactions. The neutron detection is

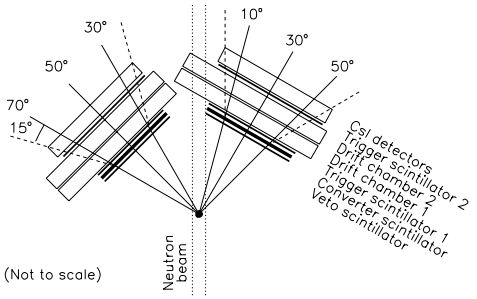

Fig. 2 Schematic figure of the SCANDAL setup

accomplished via conversion to protons by the H(n,p) reaction, which has a cross section of above 50 mb/sr at small angles. In addition, (n,p) reactions in nuclei can be studied by direct detection of protons. This is also used for calibration of the setup.

The device is illustrated in **fig. 2**. It consists of two identical systems, typically located on each side of the neutron beam. The design allows the neutron beam to pass through the drift chambers of the right-side setup, making low-background measurements close to zero degrees feasible.

In neutron detection mode, each arm consists of a 2 mm thick veto scintillator for fast charged-particle rejection, a neutron-to-proton converter which is a 10 mm thick plastic scintillator, a 2 mm thick plastic scintillator for triggering, two drift chambers for proton tracking, a 2 mm thick ΔE plastic scintillator which is also part of the trigger, and an array of CsI detectors for energy determination. The trigger is provided by a coincidence of the two trigger scintillators, vetoed by the front scintillator.

2. Design features

SCANDAL uses active converters, having the advantage that they can be thicker than passive converters, because the proton straggling on the way out of the scintillator can be measured and compensated for.

The converters contain hydrogen and carbon, which allows unambiguous measurements up to 12 MeV excitation energy. For higher excitation energies, the ^{12}C(n,p) channel opens in the converter, and therefore a unique identification of the target excitation is no longer possible. This is obviously not a problem for elastic scattering, or inelastic scattering to low-lying states, but complicates future developments, like neutron excitation of giant resonances, or quasielastic experiments.

The setup has in total 24 CsI detectors, 12 in each system.

The drift chambers serve two main purposes; they improve the angular resolution and they allow rejection of spurious events.

The H(n,p) cross section close to zero degrees is rather flat over several degrees in the lab system. This effect, combined with the rather large front-area of the CsI's, makes the effective subtended angular range for each detector quite large. This would be a major contribution to the angular resolution without proton tracking.

Furthermore, the Q-value for ^{12}C(n,p) is -12.6 MeV. Thus, at forward angles energy detection can isolate the protons

which are due to conversion via H(n,p). At about 20° conversion angle, the proton energies from the two processes are the same, and thereby it can no longer be determined whether the energy lost was due to excitations in the neutron scattering sample or in the conversion. By applying a 15° maximum opening angle criterion on the conversion (see fig. 2), such problems can be avoided.

3. Resolution

The energy resolution in neutron mode has contributions from the neutron beam (1.2 MeV at FWHM), the converter (1.4 MeV), the two trigger scintillators (0.3 MeV each), straggling in non-detector materials (0.3 MeV), kinematics (1.2 MeV), and the CsI detectors (3.0 MeV). This makes a total excitation-energy resolution of 3.7 MeV in elastic scattering measurements.

The angular resolution is solely due to the neutron beam and target width. With the present setup dimensions and a 5 cm wide sample, it is about 1.4° (rms). The angular resolution is most crucial at small angles, where the cross section is very large, and also falls very rapidly.

4. Solid angle and count rate

The solid angle subtended by each system in the proton detection mode is about 240 msr for a point target. Applying the maximum opening angle criterion on the second scattering in the converter (see above), required for neutron detection, makes the effective solid angle smaller—about 130 msr per setup at full coverage of the 15° cone. The conversion efficiency is then about $5 \cdot 10^{-4}$.

5. Normalization

Normalization of neutron-induced cross sections suffers from the difficulties in monitoring the absolute intensity of neutron beams. Precisions better than 10 % have very rarely been achieved. Therefore, most data have been measured relative to another cross section assumed to be known. Most often, the neutron-proton scattering cross section has been used as the primary standard.

Recent experimental investigations[5–8] have indicated that the *np* scattering cross section might have larger uncertainties than previously estimated. It seems now that the cross section can be uncertain by as much as 10-15 % in the energy range of 100 MeV and up.[9]

A recent high-precision measurement of *np* scattering at 96 MeV in the 74–180 degree range claims an absolute uncertainty of 1.9 %,[8] but this is outside our angular range. This is where a planned H(n,n) measurement comes in. By making a relative measurement of the angular distribution of H(n,n) from (close to) zero degrees and out to angles overlapping with the existing data, a normalization to the total cross section can be made with a very small uncertainty (about 1 %).[10]

The reason for this high precision is that the total cross section has been possible to determine with a very high precision (1 %), because knowledge of the absolute beam intensity is not required. Instead, it can be inferred from intensity ratio measurements in attenuation experiments. Furthermore, in the case of hydrogen, integration of the elastic scattering cross section accounts for more than 99 % of the total cross section, with very small corrections for capture and bremsstrahlung processes.

For practical experimental reasons, we plan to measure this in a CH_2-vs-C difference measurement. By this technique, we can normalize the C(n,n) cross section to the H(n,n) cross section. This is very useful, because thereby we can establish the much larger C(n,n) cross section as a secondary standard, allowing all other nuclei to be measured relative to C(n,n).

A second normalization method will be provided by comparisons with the total elastic cross section. This cross section has been derived from the difference of the total cross section and the total inelastic cross section. Both these quantities have been measured in attenuation experiments, and are therefore known to high precision, i. e. 1–2 %. (See for example ref.[11]). By covering 0–70 degrees, far more than 99 % of the contribution to the total elastic cross section will be accounted for, providing a second normalization technique. This method works the best with light nuclei, however, and is therefore well suited for e. g. C(n,n), but is not as reliable for ^{208}Pb(n,n). Hence, this is another reason to establish C(n,n) as a secondary standard. A detailed account of these issues is underway.[12]

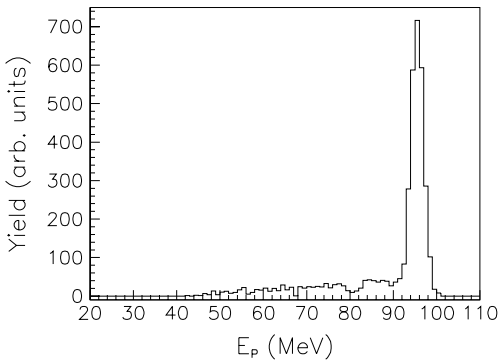

Fig. 3 Proton energy spectrum for (n,p) reactions in hydrogen, induced by 96 MeV neutrons, in the angular range 6–7°. The spectrum has been obtained by subtracting a ^{12}C(n,p) spectrum from a proton spectrum coming from CH_2, after normalization.

IV. Results

To investigate the characteristics of the SCANDAL setup and to develop the experimental procedures, measurements have been performed both in proton and in neutron detection mode, at a neutron beam energy of 96 MeV.

1. Proton detection

The proton mode runs were used for studies of the H(n,p) and ^{12}C(n,p) reactions, as well as for calibration purposes. By normalizing ^{12}C(n,p) spectra, obtained with a pure carbon sample, with respect to the carbon content in a CH_2 sample, carbon spectra can be subtracted from those of CH_2, giving pure *np* scattering spectra as illustrated in **fig. 5.**.

The resolution of the *np* scattering peak varies due to differences in intrinsic resolution in the CsI detectors, but an average

value of 3.7 MeV (FWHM) has been found. Apart from the CsI detectors, the main contributions to the resolution come from the neutron beam, the plastic scintillators and straggling in non-detector materials. These are estimated to be 1.2, 1.7 and 0.7 MeV (FWHM), respectively; implying an average intrinsic CsI resolution of 3.0 MeV.

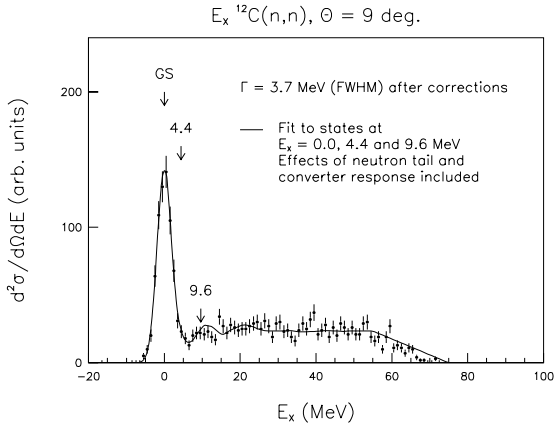

Fig. 4 Excitation energy spectra for ^{12}C(n,n) at 9°. See the text for details on the response function and its contributions.

2. Neutron detection

Figure 1. shows an excitation energy spectrum for ^{12}C(n,n) at 96 MeV and 9° scattering angle. The large peak at E_X = 0 MeV is due to elastic scattering, and the excited states at 9.6 MeV, and possibly at 4.4 MeV, are small but visible.

A response function for the SCANDAL setup has been constructed. A Gaussian has been fitted to the H(n,p) peak in the converter, reflecting elastic scattering from the ground state in ^{12}C, as well as to the excited states at 4.4 and 9.6 MeV. Knowing the relative cross section of ^{12}C(n,p) reactions in the converter with respect to that of (n,p) reactions in hydrogen, a ^{12}C(n,p) spectrum has been added. Also, a low-energy neutron tail has been included by knowing the ^{7}Li(p,n) cross section, again with respect to that of H(n,p) in the converter.

At an excitation energy of 75 MeV, the energy of the scattered neutron is 20 MeV, giving an energy of 0–10 MeV for the protons reaching the CsI detector. Protons with these energies are rejected in the analysis; thus there are no events in the E_X spectrum above 75 MeV. A straight line describing the cut-off at high excitation energies has been employed between E_X = 55 MeV, where all events are recorded, and 75 MeV.

Adding the contributions from the hydrogen peak, the ^{12}C(n,p) and the low-energy neutron backgrounds, as well as the cut-off at high E_X, gives the full response function shown.

It is concluded that the full spectrum can be explained in terms of the effects described here, and that no unexpected contributions are seen. In addition, the absolute rate is compatible with theory expectations. The energy resolution is 3.7 MeV (FWHM) for this experiment, in which a very large target was used to obtain high count rate at the expense of energy resolution.

V. Summary

The experiment setup SCANDAL, for detection of primarily neutrons in the energy interval 50–130 MeV, together with the quasi-monoenergetic 20–180 MeV neutron beam facility at the The Svedberg Laboratory (TSL), Uppsala, Sweden, will be used to provide elastic neutron scattering data for a wide range of applications, in an energy region which has been identified as very important, and in which there exist very little high-quality data.

First results, for ^{12}C(n,n), show that we can fully characterize the performance of the setup, and that an energy resolution of 3.7 MeV is possible to achieve.

Acknowledgements

This work was financially supported by Vattenfall AB, Swedish Nuclear Fuel and Waste Management Company, Swedish Nuclear Power Inspectorate, Barsebäck Power AB, Swedish Defence Research Agency, Swedish Natural Science Research Council, and the European Commission.

References

1) J.F. Ziegler, *IBM J. Res. Develop.* **40** (1996) 19.
2) H.H.K. Tang, *IBM J. Res. Develop.* **40** (1996) 91.
3) D. O'Sullivan, private communication. EU Cosmic Radiation and Dosimetry Group.
4) H. Condé, *et al.*, *Nucl. Instr. Meth.* **A292** (1990) 121.
5) T. Rönnqvist, *et al.*, *Phys. Rev. C* **45** (1992) R496.
6) T.E.O. Ericson, *et al.*, *Phys. Rev. Lett.* **75** (1995) 1046.
7) J. Rahm, *et al.*, *Phys. Rev. C* **57** (1998) 1077.
8) J. Rahm, *et al.*, *Phys. Rev. C* **63** (2001) 044001.
9) J. Blomgren, N. Olsson, J. Rahm, "How Strong is the Strong Interaction? – The πNN Coupling Constant and the Shape and Normalization of np Scattering Cross Sections", in *Proceedings of Workshop on Critical Issues in the Determination of the Pion-Nucleon Coupling Constant, Physica Scripta* T87 (2000) 33.
10) C. Johansson, *et al.*, to be published.
11) J. DeJuren and N. Knable, *Phys. Rev.* **77** (1950) 606.
12) J. Klug, *et al.*, to be published.

Neutron-Proton Scattering as a Primary Standard in the 100–1000 MeV Region

Jan BLOMGREN[1,*] and Nils OLSSON[1,2]

[1] *Department of Neutron Research, Uppsala University, Sweden*
[2] *Swedish Defence Research Agency (FOI), Stockholm, Sweden*

Neutron-proton scattering is used as standard cross section in neutron-induced nuclear data measurements. Recently, there has been an intense debate on the np scattering cross section above 100 MeV, indicating that this cross section might not be as well known as was previously thought.

The world data base on np scattering differential cross section data from 100 to 1000 MeV incident neutron energy has been reviewed. In addition, the status of the np total cross section and the $pp \rightarrow d\pi^+$ total cross section is discussed, as these have frequently been used to normalize np scattering data. It appears that the shapes of the largest np data sets tend to fall into two groups, with different steepness at backward angles. Also, it seems as the two major techniques for normalizing data yield incompatible results.

Both these effects have consequences not only for the cross section itself, but also for determinations of the absolute strength of the strong interaction in the nuclear sector, the pion-nucleon coupling constant, $g^2_{\pi NN}$. This fundamental constant is often derived from np scattering data, and the conflicting data situation has led to an intense debate about its exact value.

KEYWORDS: neutron-proton scattering, primary standard, cross section, pion-nucleon coupling constant

I. Introduction

The np scattering cross section - in particular at $180°$ (C.M.), which corresponds to proton emission at $0°$ in the lab - is used to normalize measurements of other neutron-induced cross sections, i.e., it is the primary standard cross section. Many emerging applications, like dosimetry for airplane crew, fast-neutron cancer therapy, studies of electronics failures induced by cosmic-ray neutrons, and accelerator-driven incineration of nuclear waste and energy production technologies, can benefit from various cross section measurements, where np scattering is typically used as reference. It also plays an important role in fundamental physics, because it has been used to derive a value of the pion-nucleon coupling constant, $g^2_{\pi NN}$, i.e., the absolute strength of the strong interaction in the nuclear sector (See Ref.[1)] for a review). Large uncertainties for such an important cross section are therefore unacceptable.

In this paper, we present a review of the world data base on np scattering differential cross sections from 100 to 1000 MeV incident neutron energy. In addition, the status of the np total cross section and of the $pp \rightarrow d\pi^+$ total cross section is discussed, since these have frequently been used to normalize np scattering data. We have found two major problematic features of the data base. First, it appears that the large data sets tend to fall into two groups, characterized by a different steepness at backward angles. Consequently, significantly different values of $g^2_{\pi NN}$ have been suggested. Second, the two major techniques for normalizing data yield incompatible results.

II. Brief survey of the np scattering data base

The differential np scattering cross section data base in the energy region $100 - 1000$ MeV is dominated by two large data sets, the LAMPF data (Bonner *et al.*,[2)] Evans *et al.*,[3,4)] Jain *et al.*[5)] and Northcliffe *et al.*[6)]) and the PSI data (previously Hürster *et al.*,[7)] recently replaced by Franz *et al.*[8)]). Until recently, the LAMPF data constituted almost 50 % of the data base. The recent publication of an extended PSI data set (Franz *et al.*) has resulted in that the PSI data now accounts for over 60 % of the statistical weight of the data base. These two large data sets are incompatible when statistical uncertainties only are considered.

We use the LAMPF and PSI data to illustrate the situation of the np scattering data. A thorough investigation of all data can be found in ref.[9)] To access data, we refer to the Nijmegen data base, which is easily accessed over www.[10)] For a list of references, see, e.g., Ref.[11)]

III. The np scattering angular distribution

For comparisons of different data sets, we have taken ourselves the liberty to use the Uppsala data at 162 MeV[12,13)] as a reference. To be able to compare data at different energies, we present the data in the c.m. system, plotted as $d\sigma/dt$ versus the Mandelstam variable $t = q^2$; see **Fig. 1**. Since we want to compare the shape, we have renormalized the different data sets to agree at $t = 0$ for the presentation below. To make this normalization in a reasonable way, we have fitted the data according to a two-exponential shape, a technique frequently used by previous authors when comparing different data sets. The fit to the Uppsala data is shown as a solid line, whereas the fits to other data are represented by dashed lines. The fits were performed up to $t = 0.08$ (GeV/c)^2, regardless of how far out in angle the data extend. The reason for this choice is somewhat arbitrary, but is not crucial; using a moderately wider range does not influence the conclusions of this study.

At low energies, the Bonner data are flatter than the Uppsala data, but this discrepancy decreases gradually in magnitude

* Corresponding author, Tel. +46 18 471 3788, Fax. +46 18 471 3853, E-mail: jan.blomgren@tsl.uu.se

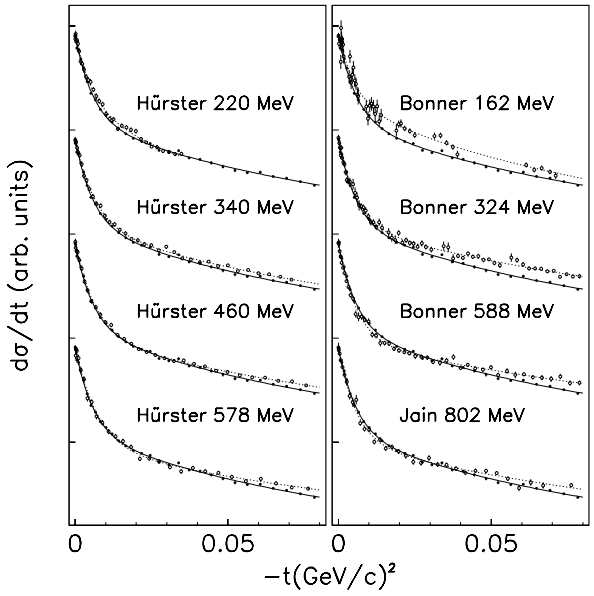

Fig. 1 Data of LAMPF and PSI data plotted as $d\sigma/dt$ versus t for a few energies. The Uppsala data at 162 MeV are shown for reference. (Linear scale)

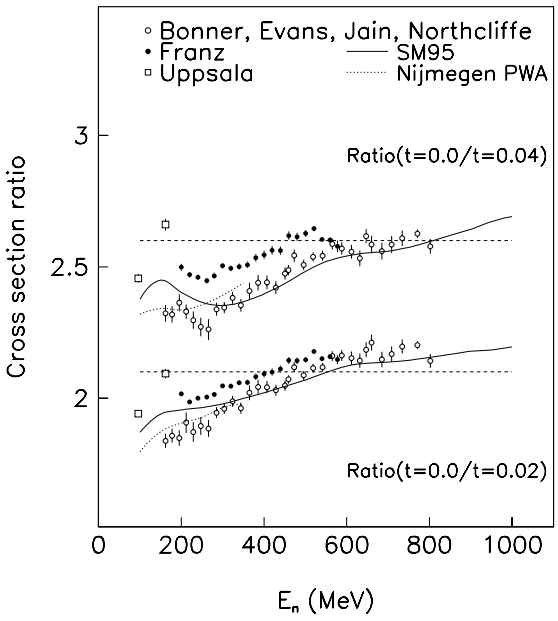

Fig. 2 The ratio of $d\sigma/dt$ at $(t = 0.00)/(t = 0.02)$, and $(t = 0.00)/(t = 0.04)$, respectively. The dashed horizontal lines are to guide the eye. If the np scattering process were due to one-pion exchange only, the data should fall on such straight lines.

with increasing energy, and the Jain data at 802 MeV (obtained with the Bonner setup) are in reasonably good agreement with the Uppsala 162 MeV data. At lower energies, the individual points scatter substantially. Above 400 MeV, the scatter is smaller, indicating a better precision in the data.

A similar comparison with the Hürster/Franz data from 220 to 578 MeV shows good agreement with the Uppsala data at all energies, at least up to $t = 0.05$ (GeV/c)^2. It is interesting to note that in the range $t = 0$ to 0.03 (GeV/c)^2, which corresponds to the angular region where the Uppsala data deviate the most from the Bonner data, the agreement with the Hürster/Franz data is almost perfect.

We have attempted another method to illustrate the steepness of the cross section. In **Fig. 2**, we have plotted the ratios $(d\sigma/dt)_{t=0}/(d\sigma/dt)_{t=0.02}$ and $(d\sigma/dt)_{t=0}/\ (d\sigma/dt)_{t=0.04}$, respectively. In such a plot, if the reaction mechanism is dominated by one-pion exchange, the data should appear as straight horizontal lines irrespective of at which value of t the comparison is being made. It can be noted that the Hürster/Franz data actually display such a rather flat behaviour (note that the scale in Fig. 2 is zero-suppressed). The Bonner data, on the other hand, display more of an energy dependence. At higher energies, the data sets agree well.

IV. Normalization of np scattering data

1. Normalization using pion production data

Both the LAMPF and PSI data were normalized by measuring np scattering simultaneously with the pion-production reaction $np \to d\pi^0$, when above the threshold energy of about 275 MeV. This reaction has never been measured on an absolute scale directly, but it is linked to the $pp \to d\pi^+$ reaction via isospin invariance. The Uppsala data have been normalized to the total cross section, which can be done by integrating the differential cross section, given that the inelastic channels are small or can be corrected for.

Normalization by pion production measurements are not without difficulties. There are several reasons why the $pp \to d\pi^+$ cross section is not a very good reference. First, the cross section as such is not known to better than 5% anywhere from threshold and up to 1 GeV. It is probably known *now* to better than 10% above 400 MeV, but not much better. What is even worse is that it has changed systematically by 10% in the $400 - 600$ MeV energy region since 1980. Thereby, the LAMPF and PSI data have been normalized to the same reaction, but at different times. Thus, the reference cross section is significantly different for the two experiments.

Moreover, the cross section shape as such induces additional problems. The cross section increases rapidly from the threshold and up to a maximum at about 600 MeV, and then it goes down steeply again. This means that small uncertainties in the absolute beam energy translates to large uncertainties in the cross section.

Finally, this normalization relies on that isospin invariance holds for the $pp \to d\pi^+$ and $np \to d\pi^0$ reactions. A recent theoretical investigation[14] indicates deviations of the several percent because of, e.g., mass differences in the two channels. These deviations are difficult to verify experimentally, and they have been taken into account only by the PSI group.

2. Normalization using total cross section data

If the entire np angular distribution were experimentally known at a certain energy, normalization to the total cross section would be trivial, because scattering is the only process contributing to the total cross section. There are two main sources of uncertainties with such a normalization. First, the entire angular distribution is not measured in most cases, and assumptions have to be made about the undetected part. Second, if above the pion-production threshold, the integrated differential elastic scattering cross section does not correspond to the experimental total cross section, but corrections must be applied for inelastic channels. A third uncertainty could be ascribed to how well the total cross section is known. All these effects are discussed below.

In most experiments only a part of the angular distribution is measured. The reliability of the total cross section normalization technique depends in such cases on the extrapolation techniques used for the unmeasured region. This has been studied by the Uppsala group, which has used different partial-wave analyses (PWAs) when normalizing the same data.[12,13,15,16] The distribution of the results has been used to estimate the uncertainty in this procedure. At 96 and 162 MeV, when covering the $120^\circ - 180^\circ$ angular region, a normalization uncertainty of 4% was given. After having extended the data sets to cover $74^\circ - 180^\circ$, the normalization uncertainty was estimated to 2%. The new value was compatible with the old one, given the uncertainties quoted.

The total cross section is dominated by elastic scattering, but in addition inelastic effects contribute. Below the pion-production threshold, the two largest are capture and np bremsstrahlung. Both these two inelastic processes impose sub-percent effects, which are negligible with present experimental precision.

Above the pion-production threshold at 275 MeV, the total cross section has to be corrected for contributions from pion-producing reactions. If such a correction could be made accurately, the total cross section data could be used for normalization also above the pion-production threshold. A recent investigation indicates that this can be done with a reasonable precision up to, say, 500 MeV.

The total cross section data situation is, however, not without complications. There are two large high-accuracy total cross section data sets available, by Lisowski *et al.*[17] from LAMPF, and by Grundies *et al.*[18] from PSI, which are in perfect agreement all over their common energy domain, i.e., $125 - 580$ MeV. The data of Keeler *et al.*[19] and Devlin *et al.*[20] are both systematically above the Grundies-Lisowski data (up to about 6%). The recent measurement by Abfalterer *et al.*[21] falls roughly in between.

3. Cross-check of the total cross-section and pion-production normalizations

At energies just above the pion-production threshold, a very small fraction of the total cross section comes from pion-production reactions. Therefore, normalizations using the total cross section and the $np \to d\pi^0$ reaction can be compared. To do this, a small correction of the total cross section is required.

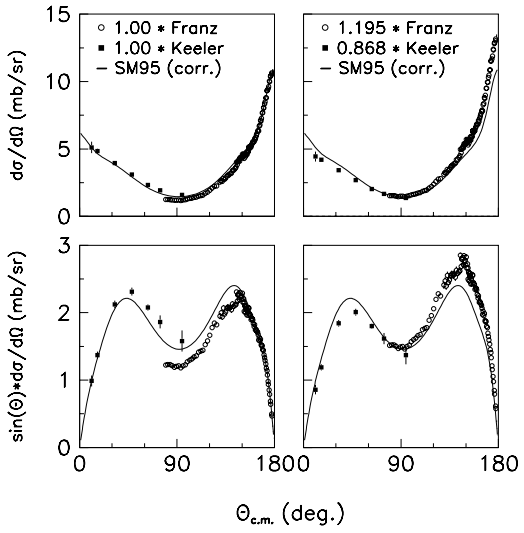

Fig. 3 Cross-check of the pion-production and total cross-section normalization methods. Upper left: the Keeler and Franz data with their original normalization. Lower left: the same data, but multiplied with the solid angle element $2\pi \sin\theta$. Right: the same data but renormalized to the total cross section. The PWA SM95 has been renormalized to the experimental total cross section. See the text for details.

We have made such a comparison using the Franz *et al.* data at 320 MeV.[8]

In **Fig. 3**, the Franz data with their original normalization, obtained from the $np \to d\pi^0$ cross section, are shown in the upper left panel. In addition, the Keeler small-angle data at 319 MeV[19] are plotted, also with their original normalization. In the lower left panel, the cross section multiplied with the solid angle element $2\pi \sin\theta$ is given, thus displaying how much each scattering angle bin contributes to the total cross section. It is evident that the two data sets are not in mutual agreement. We have taken ourselves the liberty to renormalize them to agree internally, applying Legendre polynomial fits to the two data sets and joining the fits in the overlap region. Finally, the combined set was normalized to the experimental total cross section by Lisowski *et al.*, with a 3% correction for the inelasticities obtained from SM95. The resulting set is presented in the right panels.

The renormalization factors are rather large. The Keeler set had to be reduced by 13%. However, the Keeler data were normalized to their own total cross section measurement, which is about 6% higher than the Lisowski and Grundies data. Our renormalization therefore accounts for additionally 7%. The Franz data need to be renormalized upwards by almost 20%! Apparently, the pion production and total cross section normalizations are inconsistent. The inconsistency is even larger than what can be explained from the previously discussed systematic shift of the $pp \to d\pi^+$ cross section. It is evident from Fig. 3 that there are large uncertainties involved in this procedure, because of the small overlap between the two data sets, and the large error bars of the Keeler data at about 90°. Nevertheless, it seems as relatively large renormalizations are

required to bring the differential and total cross section data into agreement.

4. Conclusion and discussion on normalization techniques

We find it evident that normalization using pion production has an inherent uncertainty on the $5-10\%$ level from the $pp \rightarrow d\pi^+$ data situation only. In addition, there are other complications, like the precision in absolute neutron energy and the conversion from $pp \rightarrow d\pi^+$ to $np \rightarrow d\pi^0$. Our conclusion is that it is presently impossible to normalize to better than 10% with this technique.

When using the total cross section for normalization, substantially better precision is reached if a wide-angle data set is used. With reasonable assumptions about the uncertainty in the angular distribution of the undetected region, an uncertainty in the normalization of the order of $2-4\%$ has been reached in a few recent experiments.

Our conclusion is that the total cross section is a more reliable technique than pion-production normalization. The total cross section is known with a precision superior to any other neutron-induced cross section. We believe that one of the best ways of avoiding the present normalization difficulties is to measure relative, differential np scattering cross sections, covering the full angular distribution, and normalize the result to the total cross section. Thus, an unambiguous normalization could be performed. Such efforts are underway.[22)]

A novel approach is attempted at IUCF.[23)] The idea is to use a tagged neutron beam to measure the absolute scale of the cross section at backward angles. This requires good absolute knowledge of virtually every component in the detection system, but if this can be achieved, it would open a new possibility to resolve the normalization discrepancy.

V. Summary, Discussion and Outlook

In this paper, we have examined the world data base on np differential scattering cross section data from 100 to 1000 MeV incident neutron energy. In addition, the status of the np total cross section and the $pp \rightarrow d\pi^+$ total cross section has been reviewed, because these have frequently been used to normalize np scattering data.

We have found two major problematic features of the data base. First, it appears that the shape of the large data sets tend to fall into either one of two mutually incompatible groups, with different steepness at backward angles. Second, it is not only the shape of the data that is under debate, but also the absolute scale. There are two major techniques for normalizing data, which yield incompatible results. Both these effects have implications for the determination of the pion-nucleon coupling constant, $g^2_{\pi NN}$, and not surprisingly, different opinions about its value appear.

One of our conclusions after this investigation is that there is still a great need for new, precision data, especially in the low energy range, i.e., up to about 500 MeV. In particular, the available data at backward angles for energies below 200 MeV are very scarce, and new data in this range should therefore be given high priority.

Normalization has been a problem for a long time, manifested in that some theoretical analyses are performed using floating normalization. This approach has made sense when using data with very unreliable absolute scale, but, evidently, important physics information has been lost in the process. Finding techniques to obtain precise, reliable normalization should therefore be given high priority. Our conclusion is that normalization to the total cross section has the best potential in this respect. Measurements covering the entire angular distribution would be of particular value for this purpose.

Furthermore, efforts should be put into some kind of evaluation of the existing data. By careful analysis of the experimental conditions, it might be possible to find systematic problems which can explain the deviations.

Acknowledgment

Numerous stimulating discussions with Torleif Ericson and Benoît Loiseau are gratefully acknowledged. We want to thank the The Svedberg Laboratory and the Uppsala neutron collaboration for its support, J.A. Niskanen for valuable discussions, and the PSI group for supplying data prior to publication. This work was supported by the Swedish Natural Science Research Council, Vattenfall AB, Swedish Nuclear Fuel and Waste Management Company, Swedish Nuclear Power Inspectorate, Barsebäck Power AB, the EU Council, and the Swedish Defence Research Agency.

References

1) Critical Issues in the Determination of the Pion-Nucleon Coupling Constant, ed. J. Blomgren, Phys. Scr. **T87** (2000).
2) B.E. Bonner, *et al.*, Phys. Rev. Lett. **41** (1978) 1200.
3) M.L. Evans, *et al.*, Phys. Rev. Lett. **36** (1976) 497.
4) M.L. Evans, *et al.*, Phys. Rev. **C26** (1982) 2525.
5) Mahavir Jain, *et al.*, Phys. Rev. **C30** (1984) 566.
6) L.C. Northcliffe, *et al.*, Phys. Rev. **C47** (1993) 36.
7) W. Hürster, *et al.*, Phys. Lett. **B90** (1980) 367.
8) J. Franz, *et al.*, Phys. Scr. **T87** (2000) 14.
9) J. Blomgren, N. Olsson, J. Rahm, Phys. Scr. **T87** (2000) 33.
10) The Nijmegen data base is easily accessed over www at http://nn-online.sci.kun.nl/. Data are listed in Ref..[11)]
11) V.G.J. Stoks, *et al.*, Phys. Rev. **C48** (1993) 792.
12) T.E.O. Ericson, *et al.*, Phys. Rev. Lett. **75** (1995) 1046.
13) J. Rahm, *et al.*, Phys. Rev. **C57** (1998) 1077.
14) J. Niskanen and M. Vestama, Phys. Lett. **B394** (1997) 253.
15) T. Rönnqvist, *et al.*, Phys. Rev. **C45** (1992) R496.
16) J. Rahm, *et al.*, Phys. Rev. **C63** (2001) 044001.
17) P.W. Lisowski, *et al.*, Phys. Rev. Lett. **49** (1982) 255.
18) V. Grundies, *et al.*, Phys. Lett. **B158** (1985) 15.
19) R.K. Keeler, *et al.*, Nucl. Phys. **A377** (1982) 529.
20) T.J. Devlin, *et al.*, Phys. Rev. **D8** (1973) 136.
21) W.P. Abfalterer, *et al.*, Phys. Rev. **C63** (2001) 044608.
22) C. Johansson, *et al.*, contribution to this conference.
23) T. Peterson, *et al.*, Nucl. Phys. **A 663&664** (2000) 1057c.

Cross Section Measurements for Science and Industry at Intermediate Energies

Nils OLSSON*

Swedish Defence Research Agency (FOI), Stockholm, Sweden, and
Department of Neutron Research, Uppsala University, Sweden

Applications involving intermediate-energy neutrons (> 20 MeV) are rapidly growing. These applications are to be found within nuclear energy research, medicine, reliability of electronics, etc. Cross section data are needed to develop these areas, and thus neutron beam facilities, as well as various spectrometers, are needed. The situation at TSL in Uppsala is used to illustrate the needs and the techniques. It is argued that a dedicated, quasi-monoenergetic neutron beam facility is well motivated in an international perspective.

KEYWORDS: neutron beams, detector systems, cross sections, applied research, energy, medicine, electronics

I. Introduction

A number of new applications involving intermediate-energy (> 20 MeV) neutrons have emerged over the last few years. Among these are the development of spallation sources, accelerator-driven systems (ADS) for transmutation of nuclear waste, fast-neutron cancer therapy, as well as dose effects for airflight personnel and electronic failures due to cosmic-ray neutrons.

This has led to intense experimental activities. Briefly, these activities can be divided into two main categories: measurements of basic nuclear data, i.e., cross sections, and direct testing or neutron irradiation of various objects, e.g., electronic circuits or dosemeter equipment. Of these, the nuclear data measurements is the by far largest activity, while the in-beam testing or irradiation activities are presently small, but rapidly growing.

A common feature of the applications mentioned is that neutrons, as well as the various particles they create by nuclear reactions, are transported in bulk matter, which can be a spallation target, a reactor, human tissue, detector material, material of electronic devices, etc. To simulate the processes in matter, cross sections are needed for transport calculations. The more detailed information that is used, e.g., double-differential cross sections, the better calculations can be made. More integral cross section measurements, as well as studies of phenomena as a whole, can in addition be used to verify the microscopic measurements. In many cases the processes in the applications are so complicated that both approaches are needed to get a deeper understanding.

To meet the requirements from these applications, wide programmes on neutron-induced cross section measurements is running or being started at several laboratories. Most often, these programmes are performed as international concerted activities, with support and follow-up from international bodies. A good example is the EU supported HINDAS project,[1)] which aims at establishing a high-energy data file for ADS studies.

Since a large energy region has to be covered, it is impossible to make complete experimental data bases. Thus, the measurements have to be chosen in such a way that they give the maximum contribution to the development of nuclear models, which in turn are used to create data files with full coverage in energy and mass number. It should be pointed out that nuclear quantities are difficult to describe in the intermediate-energy region, since compound nuclear processes, direct processes and intermediate, or pre-compound, processes are all important. Thus, nuclear reaction models must take them all into account and, where appropriate, the competition between them.

There is a lack, however, of relevant neutron facilities for this kind of programmes. Beams of intermediate-energy neutrons with sufficient intensity can only be produced at cyclotrons or linacs. With few exceptions, such accelerators have only been available at nuclear or particle physics laboratories for fundamental research, at which projects aiming for applications have faced tough competition. Over the past decade, the interest in nuclear and particle physics has diminished in most countries, resulting in closure of many accelerators and laboratories.

This is an unfortunate situation, since it coincides with the rapidly growing needs from the mentioned applications, which are of large economical and societal importance. It is thus important to join the forces of the fundamental and applied researchers, in order to obtain an output from the remaining facilities which is acceptable to society and to the public, especially in view of the often very large costs involved. To slightly move the centre-of-gravity in nuclear physics towards applications is probably the best way to take responsibility for the future competence within this branch of physics.

In this paper I will give a brief review of neutron-induced intermediate-energy cross section measurements, which are performed to satisfy the needs from a number of applied areas. The programme at the The Svedberg Laboratory (TSL) in Uppsala will specifically be used to illustrate these activities.

II. Neutron beam facilities

In the fifthies and early sixties, rather low-quality neutron beams were obtained using internal targets in cyclotrons or synchrotrons. These beams were in fact sometimes the first

* Corresponding author, Tel. +46 8 55 50 33 86, Fax. +46 8 55 50 34 94, E-mail: nils.olsson@foi.se

extracted beams of such machines. However, the targets were typically hit by several turns of the circulating ion beam, and thus the neutron beam characteristics, e.g., energy resolution, timing, etc, limited the usefulness.

The next generation of neutron beam facilities employed high-energy (several hundred MeV) cyclotrons or linacs to deliver a high intensity proton (or deuteron) beam onto a thick spallation target of some heavy material. In the spallation process, up to 30 neutrons can be produced by a single proton, and thus such facilities give high neutron fluxes. The neutron spectrum is continuous, and is to first order described by a $1/E_n$ function, extending up to the incident proton energy. The neutron energy of a single event can be determined from the time-of-flight (ToF) relative to the sharp beam burst. However, the highest intensity is found at low energy, and therefore such facilities are suitable for material science employing neutron scattering techniques. Around 100 MeV and above, the intensity per energy interval is very low, and hence it is difficult to obtain good statistics in cross section measurements at those energies. Well-known examples of spallation sources for intermediate-energy neutron research are found at Los Alamos, PSI and Gatchina. The recent ToF facility at CERN also belongs to this category.

To have good conditions for cross section measurements at intermediate energies, an intense monoenergetic source would be ideal. Unfortunately nature does not provide a suitable nuclear reaction for such a source. The best choice seems to be ^{7}Li(p,n)^{7}Be, which has a reasonable cross section for the direct reaction to the ground state and the first excited state (above 30 mb/sr). Thus, a full-energy peak, having a width of around 1 MeV and containing about half of the neutrons, is obtained together with a more or less flat low-energy tail. The neutron intensity in the peak at 100 MeV is typically two orders of magnitude higher at present quasi-monoenergetic facilities than the corresponding intensity per MeV in a reasonable experimental position at a spallation source.

Pioneering work on cross section measurements up to about 60 MeV using this reaction, both for fundamental and applied research, was performed at UC Davis. Such measurements were later extended to the several hundred MeV region at TRIUMF. At present, active programmes of neutron cross section measurements are run at UCL in Louvain (up to 70 MeV), TIARA at JAERI (up to 90 MeV), and TSL in Uppsala (up to 180 MeV).

III. The Uppsala neutron facility

At the neutron facility of the The Svedberg Laboratory (TSL) in Uppsala, Sweden[2,3] (see **Fig. 1**), quasi-monoenergetic neutrons are produced by the ^{7}Li(p,n)^{7}Be reaction[4] in a target of 99.98% ^{7}Li. After the target, the proton beam is bent by two dipole magnets into an 8 m concrete tunnel, where it is focused and stopped in a well-shielded carbon beam-dump. A narrow neutron beam is formed in the forward direction by a system of three collimators, with a total thickness of more than four metres.

The total neutron yield in the full-energy peak at the experimental position, 8 m from the production target, is at 100

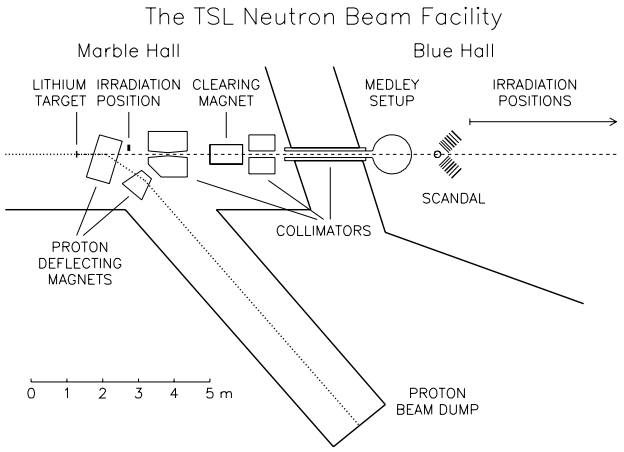

Fig. 1 The TSL neutron beam facility.

MeV typically about $5 \cdot 10^4$ cm^{-2}s^{-1}. The energy resolution of the peak depends on the choice of lithium target thickness. For most experiments a resolution of about 1 MeV (FWHM) is selected. The low-energy tail of the neutron beam can be reduced by ToF techniques, while the thermal contribution, which is equally spread over all times, is small.

At present, two major experimental setups for cross section measurements are semi-permanently installed. These are the MEDLEY detector telescope array,[5] housed in a 100 cm diameter scattering chamber (see **Fig. 2**). MEDLEY consists

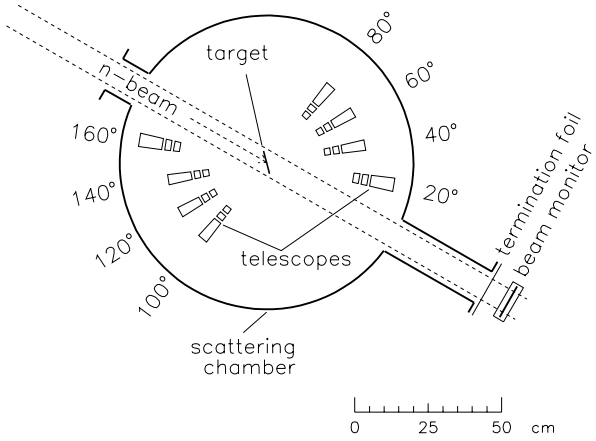

Fig. 2 The MEDLEY facility, showing the scattering chamber and the eight telescopes.

of eight particle telescopes, placed at $20° - 160°$, with $20°$ separation, and operated in vacuum. Each telescope is a $\Delta E - \Delta E - E$ detector combination, with sufficient dynamic range to distinguish all charged particles from a few MeV up to maximum energy, i.e., about 130 MeV. At the exit of the scattering chamber, a 0.1 mm stainless steel foil terminates the vacuum system, and from here and on the neutrons travel in air.

Immediately after MEDLEY follows SCANDAL (SCAt-

tered Nucleon Detection AssembLy),[3,6] a setup designed for large-acceptance neutron and proton detection (see **Fig. 3**). Neutron detection is accomplished via conversion to recoil

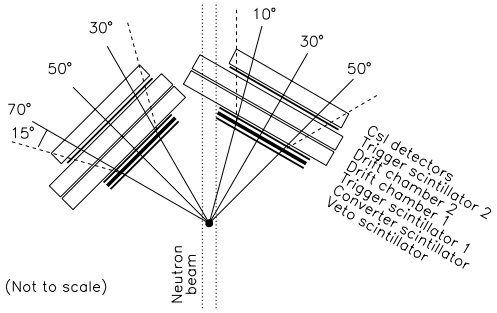

Fig. 3 Schematic figure of the SCANDAL setup.

protons by np scattering in a hydrogen-containing material. The device, shown in Fig. 3, consists of two identical systems, typically located on each side of the neutron beam. The design allows low-background measurements close to zero degrees. Each of the two systems consists of a thin veto scintillator for fast charged-particle rejection, an active neutron-to-proton converter, which is a 10 mm thick plastic scintillator, a thin plastic scintillator for triggering, two drift chambers for proton tracking, a thin plastic scintillator which is also part of the trigger, and an array of 12 CsI detectors for energy determination. For (n,xp) measurements, the veto and converter detectors are removed.

An high-intensity irradiation position[7] for small objects is available in the neutron production hall, less than 2 m from the Li target, while irradiations of large objects can be performed at lower intensity over a path of several meters after the SCANDAL setup.

Absolute normalization of the neutron flux is a notorious problem in all neutron-beam experiments. For direct neutron monitoring, fission counters are available,[8] which have been calibrated relative to np scattering, allowing an uncertainty of no more than 10%. Relative monitoring can be provided by many different means. Charge integration of the primary proton beam is one of the standard techniques. In addition, for most of the beam time periods, many different experiments (up to seven so far) can be running simultaneously, and then it is common to use signals from the other experiments as relative monitors.

IV. Nuclear data needs

1. Accelerator-driven systems (ADS)

Several of the proposed transmutation schemes involve neutrons of high energy, created in proton-induced spallation of a heavy target nucleus. Therefore, the neutron spectrum in a transmutation core will differ in one significant way compared to present reactors: the presence of neutrons at very high energies (up to $1 - 2$ GeV). The nuclear data libraries developed for reactors of today go up to about 20 MeV, which covers all available energies for that application, but not for a spallator coupled to a core. Although a large majority of the neutrons will be below 20 MeV, the relatively small fraction at higher energies still has to be characterized. The small number of neutrons at very high energies make such data not being as important as mid-range data. Above, say, 200 MeV direct reaction models assuming a single interaction (impulse approximation) works reasonably well, while at lower energies nuclear distortion plays a non-trivial role. This makes the $20-200$ MeV region the most important for new neutron data.

Very little high-quality neutron-induced data exist in this domain. Only the total cross section and the (n,p) reaction has been investigated extensively. There are high-quality neutron total cross section data on a series of nuclei all over this energy range. In addition, there are (n,p) data in the forward angular range at modest excitation energies available at a few energies and for a rather large number of nuclei.

Within the European HINDAS project,[1] we strive for obtaining an experimental data set for iron (construction material), lead (spallation target material) and uranium (core material), which is as complete as possible with regard to reaction channels. These data will be used to pin down the nuclear models, which are to be used to calculate the complete data base.

Today, several groups are working on transmutation-related cross section measurements at TSL, within the HINDAS frame. Neutron elastic scattering is being studied with the SCANDAL setup. Hydrogen and helium production is measured with a combination of SCANDAL and MEDLEY, production of residual activity by activation and accelerator mass spectroscopy techniques, and fast neutron-induced fission by thin-film breakdown counters and ionization chambers.

2. Medical applications and dosimetry

Cancer treatment with fast neutrons (up to about 70 MeV) is performed routinely at several facilities around the world, and today it represents the largest therapy modality besides the conventional treatments with photons and electrons (for an overview of this field, see, e.g., Ref.[9]).

The interaction of neutrons with tissue is very complex, and to a large extent unknown. Thus, the existing methods and techniques employed are based on experience, rather than on knowledge of fundamental processes. The lack of data bases at higher energies with sufficiently high precision (few %) makes it difficult to estimate correctly the dose given by the neutron beam and to plan and optimize the radiation therapy. With better microscopic cross section libraries available, the dose and radiation quality planning could be dramatically improved. A substantial improvement in the knowledge of fundamental nuclear cross sections is therefore needed.

About half the dose at 70 MeV comes from np scattering, $10 - 15\%$ from elastic neutron scattering and the remaining $35 - 40\%$ from neutron-induced emission of charged particles (p, d, t, ^{3}He and α) from nuclei. Double-differential cross sections for all these reactions in tissue-relevant elements, i.e., carbon, nitrogen, oxygen and calcium, are therefore of greatest relevance for fast neutron therapy.

Figure 4, which shows the total kerma coefficient (i.e., the energy transferred to charged particles per unit neutron

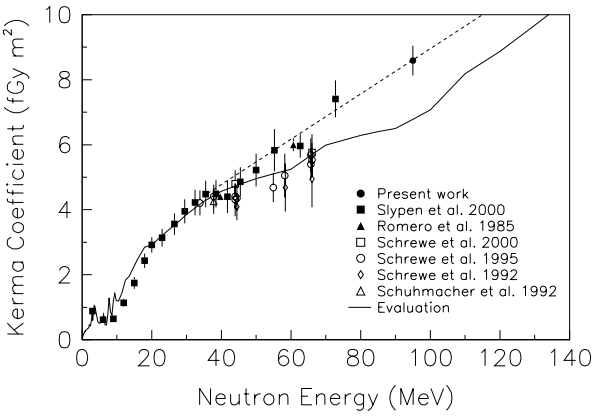

Fig. 4 Total kerma coefficient for ^{12}C vs. incident neutron energy. The dashed line is an eye-guide to the recent data at $50-100$ MeV. (From Ref.[10]).

fluence) in carbon, illustrates the difficulties in modelling witout constraining data.[10] The model prediction[11] (solid line) above 65 MeV, which was performed before any data were available, underestimates the recent experimental data up to 100 MeV by 25%.

Besides the applications in cancer treatment, the same type of data will improve the understanding of fast neutron dosimetry for radiation protection purposes, i.e., with a good enough cross section data base at hand, the response of various dosemeters can be calculated straight forward. Together with an in-beam calibration of the device, redundancy will be introduced to strengthen the reliability. The importance of such activities can be illustrated by the neutron dosimetry problems for airplane crew, which have recently received widespread attention.

3. Interference of radiation with electronics

Recently, the importance of cosmic radiation effects in aircraft electronics has been highlighted (see, e.g., Refs.[12,13] and references therein). When an electronic memory circuit is exposed to particle radiation, the latter can cause a flip of the memory content in a bit, which is called a single-event upset (SEU). This induces no hardware damage to the circuit, but evidently, unwanted re-programming of aircraft computer software can have fatal consequences.

At flight altitudes, as well as at sea level, the cosmic ray flux is dominated by neutrons and muons. The latter do not interact strongly with nuclei, and therefore neutrons are most important for SEU. Since neutrons have no charge, they can only interact via violent, nuclear reactions, in which charged particles or recoils are created, that occasionally induce an SEU. Thus, knowledge of the nuclear interactions of neutrons with silicon is needed to obtain a full understanding of the SEU problem. Measurements of neutron-induced charged particle-production cross sections are therefore of utmost importance.

Once the neutron-induced charged-particle production cross sections are known, and thus the energy deposition on a microscopic level, it might be possible to calculate the SEU rate with reasonable precision also for future components. Up to now, direct in-beam component testing has been carried out to characterize the effect.

Some insight has been gained by studying the energy dependence of the SEU rate. As can be seen in the upper panel of **Fig. 5**, the upset cross section rises slowly with neutron energy

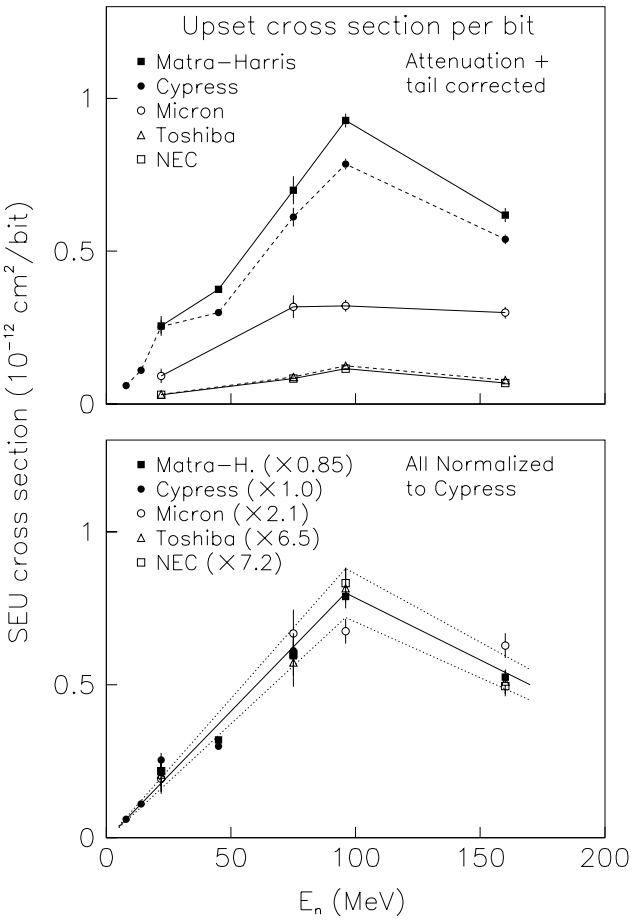

Fig. 5 The energy dependence of the SEU cross section for a few devices. See the text for details. (From Ref.[14]).

for all devices tested, up to a maximum at about 100 MeV.[14] It is notable that the most modern components (Matra-Harris and Cypress) are the most sensitive. This is because they use less charge to represent a digit, thereby making the component faster, but also more sensitive to this kind of perturbation. In the lower panel, all data have been normalized to the same relative rate to illustrate that the energy dependence is very similar for all of them.

Already from these simple measurements, important conclusions about the origin of the effect can be drawn. The fact that the rise is rather slow seems to indicate that heavy ions are primarily responsible. If the effect were mostly due to protons or alpha particles, the cross section should peak at a much lower energy.

There are plans to develop these studies further by measuring cross sections for production of light charged particles and

light heavy ions. For the light particles, the MEDLEY setup is being used. For light heavy ions, major modifications or different tecniques are needed because of the very short range of the ejectiles.

4. Fundamental physics

The TSL neutron beam facility has been running for about a decade. The main activity up to now has been studies of the (n,p) reaction at about 100 MeV, using a magnetic spectrometer, on a series of nuclei ranging from ^{9}Be to ^{208}Pb, and np scattering at 96 and 162 MeV.

Although carried out for other reasons, these fundamental studies on isospin and spin-isospin excitations have important consequences for applications. The (n,p) data on nuclei give partial contributions to theoretical model code developments. The np scattering cross section is being used to normalize other neutron-induced data, and thus a precise knowledge of this cross section is important also for applications.

Recently, the np scattering cross section in the intermediate-energy range has been under intense debate, motivated by the Uppsala results at 96 MeV[15] and 162 MeV,[16] which, together with recent data taken at PSI,[17] are steeper at backward angles than the bulk of previously published data. This is clearly illustrated by a comparison with various partial-wave analyses, which in principle are fits to the older data. The discrepancy at 180° typically amounts to 10%.

This discrepancy does not only influence the normalization of nuclear data for applications, but it is also of great fundamental importance. It is connected to the value of the pion-nucleon coupling constant, i.e., the absolute strength of the strong interaction, which is of great relevance not only to basic nuclear physics, but also to problems on a cosmological scale. If all other nucleon-nucleon potential information were known, a difference of only a few percent in the value of the coupling constant would be sufficient to either unbind the deuteron or to produce a bound diproton, in both cases with major consequences for the world as we know it.

These issues have motivated a critical re-examination of the entire np data situation, which were discussed extensively during a recent workshop in Uppsala.[18,19] New experiments are underway at TSL[20] and IUCF[21] to resolve the discrepancy.

V. Research programme

1. Elastic neutron scattering

Besides the fundamental importance of elastic neutron scattering as a laboratory for tests of isospin dependence in the nucleon-nucleon and nucleon-nucleus interactions, knowledge of the optical potentials derived from elastic scattering is important in virtually every application where nuclear reaction calculations are being performed. The reason for this is that the optical potential plays a role in defining the neutron wave function in either the entrance or exit channel. The elastic cross section is also the largest of the individual partial cross sections contributing to the total cross section. In fact, a consequence of the optical model is that the elastic cross section must be at least half the total cross section.

Our highest priority is to measure elastic scattering for nuclei of relevance for the HINDAS project, i.e., ^{56}Fe, ^{208}Pb and ^{238}U at 100 MeV. Next, it is obvious to study some magic or semi-magic nuclei, e.g., ^{12}C, ^{16}O, ^{40}Ca and ^{90}Zr. Here it is fortunate that zirconium is also an important material in future ADS, and carbon, oxygen and calcium are all of medical relevance, so the gain is twofold. Besides these elements, the H(n,n) reaction is also being studied for normalization purposes.

Up to now, we have taken data on ^{12}C(n,n) to characterize the SCANDAL facility. Data have also been taken on ^{208}Pb(n,n) and H(n,n), which are still under analysis. More details about the neutron elastic scattering project are given in Refs.[6,20]

2. Studies of (n,xn) reactions

In addition to elastic scattering cross sections, information about secondary neutron spectra are of great importance for many applications. In collaboration with LPC in Caen, we are therefore studying the feasibility of (n,xn) measurements at 100 MeV. The main idea is to use a secondary target to convert the neutrons from the primary target into recoil protons. To this end, a new setup (CLODIA) will be used in conjunction with parts of SCANDAL. If the tests turn out successful, measurements will be performed on the targets of relevance for HINDAS.

3. Charged-particle production

Double-differential cross sections for production of light ions (p, d, t, ^{3}He and α) in carbon, nitrogen, oxygen and calcium, which are of relevance for fast neutron therapy and dosimetry, are being measured using MEDLEY. Up to now, data have been taken on C and O at 100 MeV, those for the latter still being under analysis. For the oxygen measurements, we used a target made of quarts, with a pure silicon sample studied for background purposes. Since these "background" data in fact are "signal" data for the SEU problem, we spent some extra effort by using a sample in the form of a silicon detector. In this way the charged-particle energy loss in the target could be measured directly. The C, O and Si measurements are further discussed in Refs.[22,23]

Within the HINDAS collaboration, the production of hydrogen and helium in a transmutation environment is of interest. Besides the use of proton and alpha production data for benchmarking of precompound models, direct use of the data can provide limits on hydrogen and helium production, which has to be kept under control to avoid, e.g., safety concerns and material embrittlement. To this end we have up to now measured double-differential (n,xp) cross sections on iron and lead at 100 MeV, using SCANDAL in proton detection mode together with MEDLEY. These measurements are performed in collaboration with LPC, Caen, and University of Nantes.

4. Fast-neutron fission

Data on neutron-induced fission cross sections are of interest in fundamental nuclear physics (studies of competition

between different decay modes of excited nuclei; testing of theoretical nuclear models) as well as for applied nuclear research (ADS; standards). Until recently, there were only a few experimental studies of neutron-induced fission cross sections in the energy region above 20 MeV. In particular, very few measurements have been made for nuclei lighter than the actinides.

Scientists from the Khlopin Radium Institute (KRI), St Petersburg, have performed measurements of absolute and/or relative neutron-induced fission cross sections in the $20 - 180$ MeV region at TSL. Detector setups, based on thin-film breakdown counters and Frisch-gridded ionization chambers, have been used for fission fragment detection. Cross sections and fission fragment anisotropies at various energies have been measured for a range of nuclei, actinides as well as subactinides. More details are given in Refs.[24–27)]

5. Production of residual activity

An extensive program of neutron-induced residual nuclide production is being performed at TSL by a group from University of Hannover. The production cross sections are studied by activation techniques or accelerator mass spectroscopy, using the two target irradiation locations available.

These data are of importance within many areas of applied nucler physics, e.g., ADS techniques, dosimetry, medicine, space technology, astrophysics, geophysics, cosmology, etc. These activities are further described in Refs.[28, 29)]

6. Irradiation experiments

Nuclear data measurements for dosemeter modelling or for the SEU problem are being carried out using the SCANDAL and MEDLEY setups. In addition, direct testing of existing dosemeters are regularly undertaken, involving national radiation protection institutes from a number of European countries. Similarly, a number of electronics companies worldwide visit TSL to irradiate memory chips and other devices.

The large number of simultaneous users has been a great asset in this research, because it has provided good normalization possibilities, but also interdisciplinary collaboration. A good example of the latter is the development of dosemeters based on fission in bismuth, which has benefitted very much from the fast-fission programme. Another example is the silicon cross section measurement programme that was triggered by the frequent visitors irradiating electronic devices.

VI. Discussion and Outlook

As has been shown in this paper, there are numerous applications where intermediate-energy beams or nuclear data are needed. These applications are found within the energy sector, medicine, radiobiology, health physics, electronic technology, etc. Outreaching and open-minded nuclear physics activities can here contribute with very fundamental knowledge, which will boost the development within the applied areas.

The activities today are certainly only scratching the surface of the new research area. To increase the efficiency in cross section measurements, and to be able to deliver a large bulk of data, it is necessary to have access to a powerful quasi-monoenergetic neutron source. Such a facility, to be used for the mentioned activities, do not exist today. On a world scale, or maybe even on a European scale, there is probably room for one such dedicated facility. It should consist of a few hundred MeV separated-sector cyclotron, with large turn-separation for high proton intensities and flexible time structure, in conjunction with several target stations. The accelerator at NAC in Faure, South Africa, could be taken as a model for such a machine.

The funding for this facility, which will be on the order of 50 MUSD, probably has to come from several, and very different, sources, e.g., fundamental physics research, technology, medicine, etc, and also from industrial partners, which interest seems to be growing. Moreover, it has to be raised on an international level. To successfully run this fund raising process, in order to satisfy the most various applications, is a great challenge during the beginning of the new millennium!

Acknowledgment

The author wants to thank all colleagues from several disciplines for numerous stimulating discussions. The strong support from TSL to this programme is greatly acknowledged.

References

1) A. Koning *et al.*, this conference.
2) H. Condé *et al.*, *Nucl. Instr. Meth.* **A292**, 121.
3) J. Klug *et al.*, to be published.
4) A. Prokofiev *et al.*, this conference.
5) S. Dangtip *et al.*, *Nucl. Instr. Meth.* **A452**, 484 (2000).
6) J. Klug *et al.*, this conference.
7) R. Michel *et al.*, *TSL Progress Report 1998-99*, Uppsala, 20 (2000).
8) A. Smirnov *et al.*, *Rad. Meas.* **25**, 151 (1995).
9) M. Tubiana, J. Dutreix and A. Wambersie, *Introduction to Radiobiology*, Taylor & Francis, (1990).
10) S. Dangtip *et al.*, to be published.
11) *ICRU Report 63*, ICRU, Betsheda, MD, (2000).
12) J.F. Ziegler, *IBM J. Res. Develop.* **40**, 19 (1996).
13) H.H.K. Tang, *IBM J. Res. Develop.* **40**, 91 (1996).
14) K. Johansson *et al.*, *IEEE Trans. Nucl. Sci.* **45**, 2195 (1998).
15) J. Rahm *et al.*, *Phys. Rev.* **C63**, 044001 (2001).
16) J. Rahm *et al.*, *Phys. Rev.* **C57**, 1077 (1998).
17) J. Franz *et al.*, *Physica Scripta* **T87**, 14 (2000).
18) Workshop on np scattering and the πNN coupling constant, ed. J. Blomgren, *Physica Scripta* **T87** (2000).
19) J. Blomgren and N. Olsson, this conference.
20) C. Johansson *et al.*, this conference.
21) T. Peterson *et al.*, Nucl. Phys. **A 663&664**, 1057c (2000).
22) B. Bergenwall *et al.*, this conference.
23) U. Tippawan *et al.*, this conference.
24) V.P. Eismont *et al.*, this conference.
25) I.V. Ryzhov *et al.*, this conference.
26) A.N. Smirnov *et al.*, this conference.
27) G. Tutin *et al.*, this conference.
28) R. Michel *et al.*, this conference.
29) W. Glasser *et al.*, this conference.

Neutron-Proton Scattering at Intermediate Energies - Recent, New and Future measurements

Cecilia JOHANSSON[1], Jan BLOMGREN[1,*], Ayşe ATAÇ[1], Bel BERGENWALL[1], Somsak DANGTIP[1,2], Klas ELMGREN[1,3], Joakim KLUG[1], Nils OLSSON[1,3], Stephan POMP[1], Alexander PROKOFIEV[1,4], Tryggve RÖNNQVIST[1], Udomrat TIPPAWAN[1,2], Olle JONSSON[4], Leif NILSSON[4], Per-Ulf RENBERG[4], Pawel NADEL-TURONSKI[5], Anders RINGBOM[3]

[1] *Department of Neutron Research, Uppsala University, Sweden*
[2] *Fast Neutron Research Facility, Chiang Mai University, Thailand*
[3] *Swedish Defence Research Agency (FOI), Stockholm, Sweden*
[4] *The Svedberg Laboratory, Uppsala University, Sweden*
[5] *Department of Radiation Sciences, Uppsala University, Sweden*

A programme to investigate the neutron-proton scattering differential cross section at intermediate energies is active at the The Svedberg Laboratory, Uppsala, Sweden. Up to now, measurements of back angle differential np scattering cross sections have been undertaken at 96 MeV and 162 MeV. These high-precision data are well described by partial-wave analyses of other data sets over a wide angular range, but deviate at the most backward angles. However, they agree well in shape over the full angular range with another recent high-quality measurement from PSI.

These results have large consequences for measurements of nuclear data for applications, because back angle np scattering is used as a primary standard. A new setup, SCANDAL (SCAttered Nucleon detection AssembLy), has been developed and installed for measurements aiming at clarifying the situation at back angles, as well as for forward-angle experiments, resulting in a complete angular distribution.

KEYWORDS: neutron-proton scattering, primary standard, cross section, pion-nucleon coupling constant

I. Introduction

The neutron-proton scattering cross section - in particular at 180° (C.M.) - is of utmost importance for many applications of today, including medical applications, studies of electronics failures induced by cosmic-ray neutrons, and accelerator-driven transmutation of nuclear waste and energy production technologies. The reason is that this cross section is frequently used to normalize measurements of other neutron-induced cross sections. In addition, it plays an important role in fundamental physics, because it can be used to derive a value of the absolute strength of the strong interaction in the nuclear sector, commonly expressed as the pion-nucleon coupling constant, $g^2_{\pi NN}$. (See Ref.[1)] for a review.) Large uncertainties for such an important cross section are therefore unacceptable.

Unfortunately, there are severe discrepancies in the data base on np scattering in the 100–1000 MeV range. This is discussed in a separate contribution to this conference.[2)] In this paper, we present recent and planned activities aiming at determining this cross section by purely experimental techniques, and to establish this cross section as a primary standard with a small uncertainty.

A notorious problem of all neutron physics is to determine the intensity of a neutron beam. This might sound like an innocent problem, but it is rather difficult to overcome it.

A charged particle interacts with the electrons of the atom. Thereby it is possible to build systems where *every* particle gives a signal when passing through a detector, and hence it is a relatively simple task to determine the beam intensity by just counting pulses. Another option is to stop particles via their energy loss - which is also an effect of interaction with the atomic electrons - and finally measure the collected charge in a Faraday cup.

Neutrons interact by the strong interaction only, and they are uncharged. This means that it is intrinsically impossible to build a device which produces a signal for each particle that passes. Detection of neutrons *always* has to proceed via a nuclear reaction, releasing charged particles, which can subsequently be detected. The problem is that there is no way to determine a nuclear cross section from theory only with a reasonable precision. This means we end up in circular reasoning.

Let us assume we want to use np scattering for neutron detection. Counting the protons is a relatively simple task, but we need to know the cross section to derive the number of incoming neutrons. To measure that cross section, however, we need to know the number of incident neutrons. Thus, this constitutes a vicious circle.

There are two common techniques to solve this dilemma; combination of total and elastic np data, and tagged neutron beams.

The total cross section, i.e., the probability that a neutron interacts at all with a target nucleus, is a quantity which can be determined without knowledge of the absolute beam intensity. This integral cross section is related to the attenuation of a neutron beam, which means that a relative measurement of the beam intensity before and after a target is sufficient.

In the case of hydrogen, the total cross section is completely dominated by elastic scattering, which accounts for more than

* Corresponding author, Tel. +46 18 471 3788, Fax. +46 18 471 3853, E-mail: jan.blomgren@tsl.uu.se

99% of the total cross section. A relative measurement of the np scattering angular distribution can thereby be normalized to agree with the total cross section, and thus an absolute np differential cross section can be obtained.

For a few reactions, detection of the residual nucleus can be used to verify the neutron production. An example is the D(d,n)^{3}He reaction. By detecting the kinetic energy and direction of the residual ^{3}He nucleus, the energy and angle of the neutron is known. In addition, the detection of a ^{3}He nucleus implies that there *must* be a neutron, i.e., the ^{3}He nucleus serve as a "tag" on the neutron. With this technique, "beams" of really low - but known - intensity can be produced.

II. Back angle neutron-proton scattering measurements with LISA

Back angle np data have previously been measured by proton detection in the magnetic spectrometer LISA (Light Ion Spectrometer Assembly) at 96 MeV[3,4] and 162 MeV.[5,6] The experimental setup and procedure have been described in detail recently,[4,7] and therefore only a brief summary will be given here.

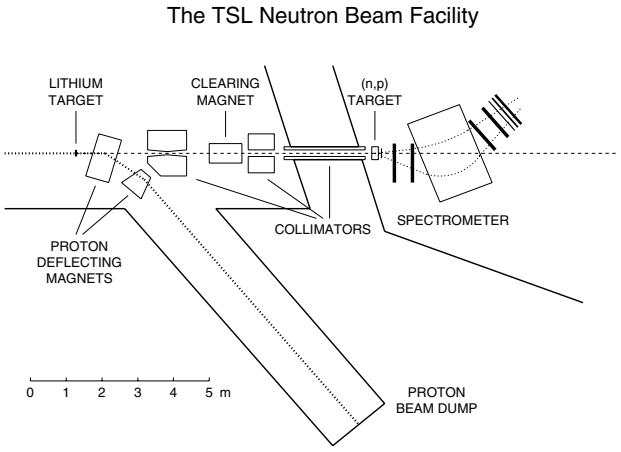

Fig. 1 Overview of the Uppsala neutron beam facility. The neutron production, shielding and collimation are shown, as well as the magnetic spectrometer arrangement.

The TSL neutron beam facility is shown in **Fig. 1**. Protons from the cyclotron impinge on the neutron production target from the left in the figure. Neutrons are produced by the ^{7}Li(p,n)^{7}Be reaction, using a lithium target enriched to 99.98% in ^{7}Li. After the target, the proton beam is bent into a well-shielded beam dump. The neutron beam is defined by a 1.1 m long iron collimator, with two other collimators serving as beam scrapers. The neutron yield is on the order of $10^5 - 10^6$ s^{-1} over the full target area.

To maximize the count rate without impairing the energy resolution, a sandwiched multi-target system is used. It consists of thin target layers interspaced by nine multi-wire proportional chambers (MWPCs), each having an efficiency of $\geq 99\%$. In this way, it is possible to determine in which target the scattering or reaction takes place, so that corrections for energy losses in the subsequent targets can be applied. The np data were obtained from the difference of CH_2 and C target data.

The momentum determination of the charged particles emitted from the targets is performed with a spectrometer consisting of a dipole magnet and four drift chambers (DCHs),[8] two in front of and two behind the magnet.

The trigger signal is generated by a small 1 mm thick plastic scintillator, located immediately after the multi-target box and an array of large plastic scintillators, positioned behind the last DCH. The entire setup can be rotated around a pivot point, located below the centre of the multi-target box.

The energy resolution in the measured spectra is typically in the range $3 - 7$ MeV (FWHM). The relative cross section data from the different spectrometer settings, all treated as relative cross sections, are matched pairwise in the overlapping regions using a minimum χ^2 criterion.[4] Thus, relative angular distributions in the range 74°/72° (96/162 MeV, resp.) to 180° (c.m.) were obtained.

Absolute np scattering cross sections are obtained by normalization to the total np cross section. The total cross section σ_T has been experimentally determined around 100–160 MeV by several groups, and is considered to be well known (about 1 % uncertainty). If the entire angular range, i.e., from $0°$ to $180°$, had been measured in the present experiment, it would have been possible to normalize the data to the total cross section directly by integration. Since that is not the case, we consider our angular distribution as a measurement of a *fraction* (F) of the total cross section, i.e., the part between 74°/72° and 180°. By using a number of partial-wave analyses (PWA's) or potential models, it is possible to estimate the magnitude of this fraction, to which the data should be normalized.

The spread in F for the various PWA's and NN potential models can be used to estimate the precision of this normalization procedure, which was found to be $\pm 1.9\%$ and $\pm 2.3\%$ at 96 and 162 MeV, respectively.

The final data are presented in **Fig. 2**. A general feature is that our data are about 10% higher at 180° and have a steeper slope in the $150° - 180°$ angular region than most of the older data in the same energy region. As a consequence, the slope is also steeper than several of the current PWA's and NN potential models, because these were to some extent fitted to the older data. A similar situation is also present at higher energies, where large data sets disagree significantly in shape. The shape of the present data is, however, in very good agreement with the new Franz *et al.* data.[19]

The np scattering cross section at $180°$ is used as a primary standard for normalization of most other neutron-induced cross sections. Uncertainties of the order of 10% in this cross section are therefore unacceptable. Remeasuring the absolute np scattering cross sections with high precision and at several energies should be of high priority.

III. Back angle np measurements with SCANDAL

Recently, the SCANDAL facility has been installed at the TSL neutron beam (see **Fig. 3**). SCANDAL is presented in detail in another contribution to this conference[20] and therefore

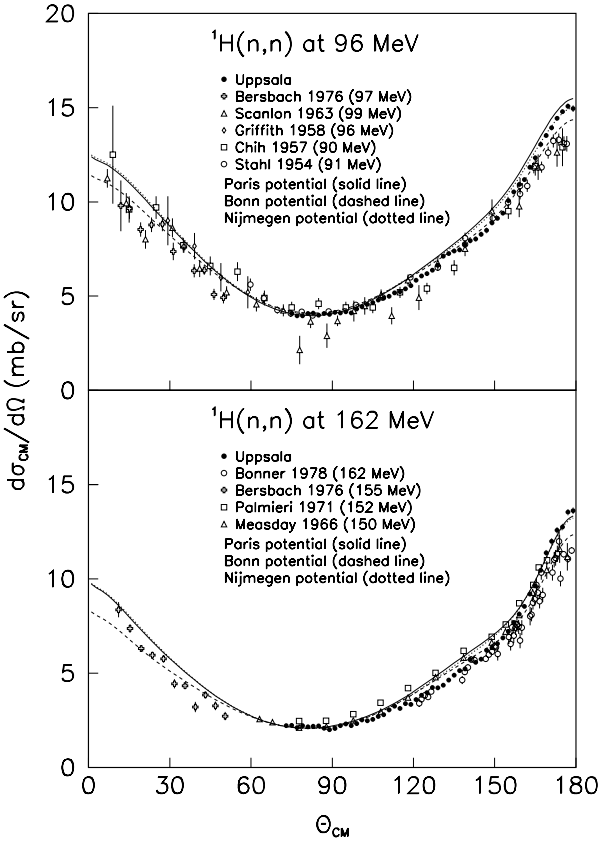

Fig. 2 Differential np scattering cross sections at 96 and 162 MeV (filled circles). Also plotted are other data from the literature at energies close to 96 MeV[9–12] (upper panel) and 162 MeV[12–15] (lower panel). The lines show predictions for the Paris[16] (solid), Bonn[17] (dashed) and Nijmegen[18] (dotted) NN potentials.

only a brief description is given here.

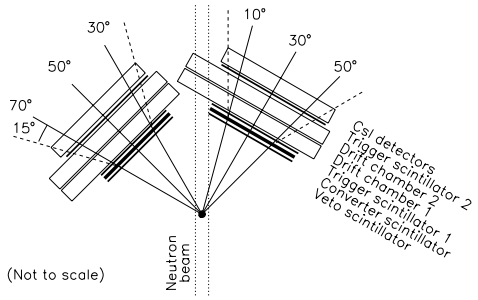

Fig. 3 Schematic figure of the SCANDAL setup.

SCANDAL was originally designed for neutron elastic scattering measurements, but it works also as proton detector. It consists of two identical detection arms. Neutrons are detected by conversion to protons in a plastic scintillator, after which the protons are energy analyzed by a CsI array. Tracking is obtained using drift chambers, and two plastic scintillators are used for triggering as well as particle identification by energy loss measurements. A plastic scintillator acts as veto for charged particles from the scattering target.

Recently, a back angle np experiment with SCANDAL was undertaken. In this run, the converter and veto scintillators were dismounted, and SCANDAL thus acted as a proton detector. The aim was to study the np angular distribution with different systematic effects than for a magnetic spectrometer. The results are in good agreement with the previously published data with LISA. The full uncertainties, including both statistical and systematic, are about 4 %. This is not sufficiently precise to provide new evidence in the debate about the steepness of the back angle np scattering cross section, but instead it gave a good confidence check of SCANDAL, as well as corroborating estimations of uncertainties in the LISA measurements (part of the equipment has been used at both setups).

IV. Forward angle np measurements with SCANDAL

If the entire angular range, i.e., from 0° to 180°, were known, it would have been possible to normalize the data to the total cross section directly by integration. This has motivated a recent experiment on forward angle np scattering.

Since energy resolution is not critical in this measurement, but statistics are, a converter thicker than standard was used (3 cm instead of 1 cm). The two SCANDAL arms were covering nominally 10–50° and 30–70°, corresponding to coverage of 20–140° in the c.m. system. The lower limit of the angular range can, however, be moved to even smaller angles by analyzing data with limited acceptance.

Subtraction of data obtained with CH_2 and carbon targets has been used to obtain the np differential cross section. Data analysis is in progress. The ambition is to provide a full angular distribution from 10° to 180° (c.m.), thereby obtaining a purely experimental np scattering cross section as reference for future measurements of neutron-induced cross sections.

This method provides a second, purely experimental normalization method. By measuring CH_2 and carbon in the same experiment, the elastic cross section ratio of hydrogen versus carbon can be obtained. The elastic cross section of carbon can be determined absolutely by a combination of total and reaction cross section measurements. Both the total cross section and the reaction cross section can be determined in relative measurements of beam attenuation. The only important difference is the geometry used (see, e.g., Ref.[21]) The integrated elastic cross section can then be determined as the difference of the total and reaction cross sections. The elastic differential cross section on carbon falls dramatically with angle. With the present SCANDAL setup, essentially all the elastic differential cross section is covered. Thereby, the differential cross section can be related to the integrated elastic cross section, and a second, independent normalization can be established.

As a byproduct of this, it is possible to obtain the C(n,n) elastic cross section as a secondary standard. This is very useful in elastic scattering experiments on heavier nuclei, because the C(n,n) cross section is relatively large, which allows good statistics for normalization in a rather short beam time, and

carbon is easy to handle.

V. Tagged neutrons

Tagging provides another technique to obtain absolute normalization of neutron-induced cross sections. Such a facility has recently been developed at the cooler storage ring at Indiana University Cyclotron Facility (IUCF)[22] (see **Fig. 4**).

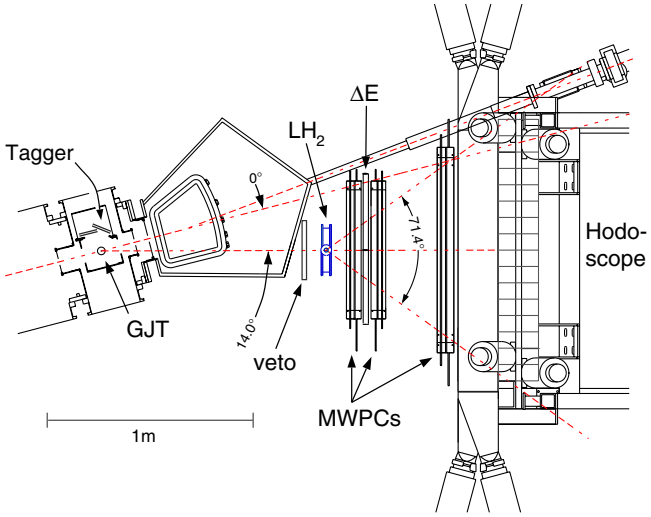

Fig. 4 Overview of the IUCF tagged neutron setup.[22]

A circulating proton beam impinges on a deuterium gas-jet target (GJT). Neutrons are produced in the D(p,n)^{2}He reaction, where ^{2}He denotes two unbound protons in a relative $^1S_0$ state. By detection of these two low-energy protons, the neutron energy and angle is determined, which makes absolute cross section measurements feasible.

A setup for back angle np cross section measurements is located close to the tagging facility. Test data have been obtained, and recently a large production run was performed.

It is interesting to compare the back angle np measurements with LISA and the tagging experiment. The former is relatively easy experimentally, while the latter is very complicated. There is, however, a tradition at IUCF of successful completion of technically very challenging experiments.

It is tempting to speculate about the possible impact of the IUCF experiment. If it turns out to agree with the TSL data, a new standard will be established, which would deviate significantly from the old one. If, on the other hand, the IUCF experiment corroborates the older measurements (and thereby the PWAs and NN models built upon those data), the TSL experiment has to be scrutinized or even repeated. If the IUCF data falls somewhere in between the TSL and old data, a re-evaluation of the systematic uncertainties in all measurements would probably be undertaken.

Acknowledgments

Numerous stimulating discussions with Torleif Ericson and Benoît Loiseau are gratefully acknowledged. We want to thank the The Svedberg Laboratory for its support. This work was supported by the Swedish Natural Science Research Council, Vattenfall AB, Swedish Nuclear Fuel and Waste Management Company, Swedish Nuclear Power Inspectorate, Barsebäck Power AB, the EU Council, and the Swedish Defence Research Agency.

References

1) Critical Issues in the Determination of the Pion-Nucleon Coupling Constant, ed. J. Blomgren, Phys. Scr. **T87** (2000).
2) J. Blomgren and N. Olsson, contribution to this conference.
3) T. Rönnqvist, *et al.*, Phys. Rev. **C45** (1992) R496.
4) J. Rahm, *et al.*, Phys. Rev. **C57** (1998) 1077.
5) T.E.O. Ericson, *et al.*, Phys. Rev. Lett. **75** (1995) 1046.
6) J. Rahm, *et al.*, Phys. Rev. **C63** (2001) 044001.
7) H. Condé, *et al.*, Nucl. Instr. and Meth. **A292** (1990) 121.
8) B. Höistad, *et al.*, Nucl. Instr. and Meth. **A295**, 172 (1990).
9) R.H. Stahl and N.F. Ramsey, Phys. Rev. **96**, 1310 (1954).
10) C.Y. Chih and W.M. Powell, Phys. Rev. **106**, 539 (1957).
11) J.P. Scanlon, *et al.*, Nucl. Phys. **41**, 401 (1963).
12) A.J. Bersbach, R.E. Mischke, and T.J. Devlin, Phys. Rev. **D13** (1976) 535.
13) B.E. Bonner, *et al.*, Phys. Rev. Lett. **41**, 1200 (1978).
14) J.N. Palmieri and J.P. Wolfe, Phys. Rev. C **3**, 144 (1971).
15) D.F. Measday, Phys. Rev. **142** (1960) 584.
16) M. Lacombe, *et al.*, Phys. Rev. C **21**, 861 (1980).
17) R. Machleidt, K. Holinde, and Ch. Elster, Phys. Rep. **149**, 1 (1987), and R. Machleidt, private communication.
18) V.G.J. Stoks, *et al.*, Rev. C **49**, 2950 (1994).
19) J. Franz, *et al.*, Phys. Scr. **T87** (2000) 14.
20) J. Klug, *et al.*, contribution to this conference.
21) J. DeJuren and N. Knable, Phys. Rev. **77** (1950) 606.
22) T. Peterson, *et al.*, Nucl. Phys. **A 663&664** (2000) 1057c.

Cross Section Data and Kerma Coefficients at 95 MeV Neutrons for Medical Applications

Bel BERGENWALL[1,*], Somsak DANGTIP[1,2], Ayse ATAÇ[1], Jan BLOMGREN[1], Klas ELMGREN[1,3], Cecilia JOHANSSON[1], Joakim KLUG[1], Nils OLSSON[1,3], Stephan POMP[1], Udomrat TIPPAWAN[1,2], Olle JONSSON[4], Leif NILSSON[4], Per-Ulf RENBERG[4], Pawel NADEL-TURONSKI[5], Jonas SÖDERBERG[6], Gudrun ALM CARLSSON[6], Christian LE BRUN[7], Jean Francois LECOLLEY[7], Francois René LECOLLEY[7], Michel LOUVEL[7], Nathalie MARIE[7], Cathy SCHWEITZER[7], Cyril VARIGNON[7], Philippe EUDES[8], Ferid HADDAD[8], Maëlle KERVENO[8], Thomas KIRCHNER[8], Claude LEBRUN[8], Louise STUTTGÉ[9], Isabelle SLYPEN[10]

[1] *Department of Neutron Research, Uppsala University, Sweden*
[2] *Fast Neutron Research Facility, Chiang Mai University, Thailand*
[3] *Swedish Defence Research Agency (FOI), Stockholm, Sweden*
[4] *The Svedberg Laboratory, Uppsala University, Sweden*
[5] *Department of Radiation Sciences, Uppsala University, Sweden*
[6] *Department of Radiology and Radiation Physics, Linköping University, Sweden*
[7] *LPC, ISMRA et Université de Caen, CNRS/IN2P3, France*
[8] *SUBATECH, Université de Nantes, CNRS/IN2P3, France*
[9] *IReS, Strasbourg, France IReS, Strasbourg, France*
[10] *Institute de Physique Nucleaire, Université Catholique de Louvain, Belgium*

Motivated by the need of data on neutron-induced reactions with biologically relevant materials, e.g., carbon and oxygen, we have constructed and installed the MEDLEY detector array at the neutron beam facility of the The Svedberg Laboratory in Uppsala. The central detection elements of MEDLEY are three-detector telescopes, consisting of two silicon detectors and a CsI crystal. To cover wide energy and angle ranges, we have mounted eight such telescopes at 20° intervals. We have used $\Delta E - \Delta E - E$ techniques to obtain good particle identification for protons, deuterons, tritons, ^{3}He and α particles over an energy range from a few MeV up to 100 MeV. To define the detector solid angle, plastic scintillators were employed to serve as active collimators.

We have up to now measured double-differential cross sections of inclusive light-ion production induced by 95 MeV neutrons on carbon and oxygen. From these data production cross sections, as well as partial kerma coefficients, are being determined. We have found that especially the proton kerma coefficient for carbon is substantially larger than that of a recent evaluation, leading to a larger total kerma coefficient. The obtained data supports a trend observed for similar data at lower energies.

KEYWORDS: Fast neutron radiotherapy, LET, dosimetry, double-differential cross section

I. Introduction

Today, nuclear radiotherapy, alone or in combination with other treatment modalities, is playing a crucial role in coping with cancer tumours. Two out of three cancer patients in Europe receive some form of radiation therapy,[1)] where sparsely ionising particles (also referred to as low Linear Energy Transfer (LET) radiation), i.e., Bremsstrahlung photons and electrons are predominant. This form of radiation is often known as conventional therapy.

However, due to different factors such as the tumour growth rate, the oxygen content and the repair mechanism on the one hand, and the damage mechanism caused by the ionising particle on the other hand, some tumours are very resistant to conventional therapy.

Owing to their highly ionising ability, i.e., high LET, caused by secondary particles along their tracks in tissue, neutrons can be biologically advantageous over photons, electrons and protons. It has therefore been advocated that for some resistant tumours, fast neutrons should offer a better treatment.[2,3)]

Salivary gland, prostate and soft tissue tumours, as well as cartilaginous sarcomas, are among the tumours that have been successfully treated by fast neutron radiation.[4–6)]

Another area where fast neutrons come into play, and which is of concern from a radioprotection viewpoint, is the neutron flux that cosmic ray particles give rise to at altitudes where commercial air flights operate. Cosmic ray particles, mainly protons and α particles, interact with the atmospheric atoms and generate a radiation field, which is significant at these altitudes. In this region the essential contribution to the dose rate is due to neutrons, to which crews and passengers are subject.

To further develop the quality in neutron dosimetry and therapy, the microscopic cross section database has to be improved. This has been highlighted recently by the International Nuclear Data Committee (INDC) of IAEA, which in a recent summary report recommended that future scientific activities should focus on fast neutron cross sections, and attempts should be made to remove deficiencies in the data on neutron interactions with biologically relevant nuclei.[7)]

Microscopic cross sections for neutron induced reactions on C, N, O and Si are also much needed for neutron-induced

* Corresponding author, Tel. +46 18 471 3254, Fax. +46 18 471 3853, E-mail: bel@tsl.uu.se

reaction models, since these have to be tested and improved by experimental data, whose scarcity has been repeatedly emphasised.[8–10)]

A step in this direction has been taken by the Louvain-la-Neuve group. In a number of publications, the group reports on measurements of double-differential cross sections for fast neutrons and derived kerma coefficients for carbon[11,12)] up to 75 MeV, for oxygen[13)] up to 65 MeV and for hydrogen[14)] in the range $25 - 75$ MeV.

The construction of the MEDLEY setup[15)] at the The Svedberg Laboratory (TSL) in Uppsala is a further step to meet the needs mentioned above. The first data set for carbon obtained using the MEDLEY facility is already in the publishing process.[16)] Additional data for carbon, oxygen and silicon are in the analysis stage, and will be published in the near future. In this paper we discuss the carbon and oxygen measurements, while data for silicon is presented by Tippawan *et al.*[17)]

II. Experiment and Methods

1. The neutron beam facility

The neutron beam facility at TSL offers quasi-monoenergetic neutrons, produced by the ^{7}Li(p,n)^{7}Be reaction in a target of 99.98% ^{7}Li. Deflecting magnets mounted after the Li target direct the proton beam into a well shielded beam dump. A set of collimators shapes the neutron beam prior to delivery to the experimental hall, where MEDLEY is located. A clearing magnet, located after the first collimator, deflects charged particles created in the shaping of the neutron beam. At the target position, the neutron beam diameter is 8 cm and the achieved neutron flux, using a 100 MeV proton beam of 5 μA and a 4 mm Li target, is $3 \cdot 10^4$ n s^{-1} cm^{-2}.

In order to monitor the neutron flux, the proton beam current is measured by means of a Faraday Cup located in the beam dump. In addition, a thin film breakdown counter[18)] (TFBC), mounted after the MEDLEY exit, is used to monitor the number of neutron-induced fissions in ^{238}U. Further details about the neutron beam facility are found elsewhere.[19–21)]

2. The MEDLEY setup

Eight detector telescopes, placed at 20° intervals, covering scattering angles from 20° to 160° simultaneously, are housed in an evacuated cylindrical chamber with a diameter of 1 m and a height of 24 cm (see **Fig. 1**). Up to three different reaction targets with diameters of typically 25 mm, can be mounted at the centre of the chamber and can be engaged in the beam or away from it without breaking the vacuum.

The detector telescopes are placed at distances between 20 and 28 cm from the target and consist of two fully depleted surface barrier silicon detectors, thickness 50 or 60 μm for the first and 400 or 500 μm for the second, and one CsI detector, thickness 5 cm, diameter 40 mm, see **Fig. 2**. This arrangement has proven to allow good particle separation, by means of $\Delta E - \Delta E - E$ techniques, over a wide dynamic range, i.e., from a few MeV α particles to 100 MeV protons.

We have mounted a thin, active plastic scintillator collimator in front of each telescope in order to obtain a well-defined acceptance. Each collimator has a 19 mm diameter hole at the centre and is mounted concentrically with the telescope axis. A signal from a hit in a collimator is used to reject the related event. The thickness (1 mm) is chosen as to allow a reasonable pulse height for 100 MeV protons.

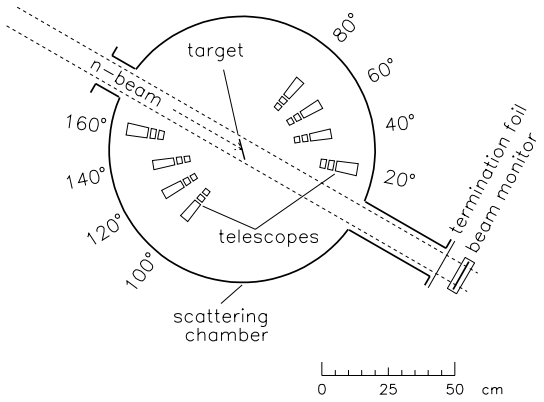

Fig. 1 The arrangement of the MEDLEY elements in the chamber. Depicted are: the target, the detectors, the chamber termination foil and the TFBC neutron monitor.

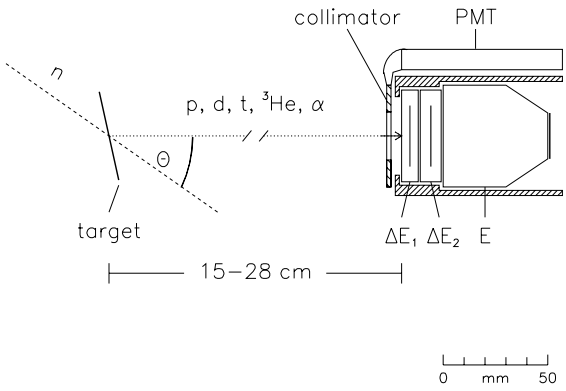

Fig. 2 Detailed sketch of the telescope. Depicted are the thin detector (ΔE_1), the thick detector (ΔE_2) CsI detector (E), PM tube (PMT), the collimators and the detector housing.

3. Measurements

We have measured neutron-induced light ion production in carbon and oxygen at $E_n = 95$ MeV. Two carbon targets of different thickness (0.5 mm and 0.15 mm, respectively) with a diameter of 22 mm were utilized. The thick target was used in order to get reasonable count rate and the thinner one to allow control of the energy losses of low-energy particles.

For oxygen, two targets were employed, a fused quartz target (SiO_2) and a pure silicon (Si) target. The data obtained using the pure Si target constitutes the SiO_2 background events, which, when subtracted from the SiO_2 events, give the pure oxygen data. By proceeding in this way, we also obtained data for silicon, which is needed for assessment of the damage caused by neutrons to electronic equipment. This phenomenon is discussed in Refs. 17 and 19, where more details are provided. Data on np scattering, used for normalisation, has been collected using a 1 mm thick CH_2 target.

III. Analysis and results

1. Detector calibration and event selection

For the energy calibration of the Si detectors, we have used the punch-through energies of the measured particles, which are known from the detector thickness. The measured energy loss in the Si detectors was then used to calculate the remaining energy deposited in the CsI crystals. The latter were then calibrated by comparing the measured signal with the calculated energy. Two different parameterisations for the CsI response function have been used, one for the hydrogen isotopes and one for the helium isotopes.[15] We have verified the validity of the calibration by making use of peaks in the spectra corresponding to ground-state and low excitation-energy transitions in the ^{12}C(n,p)^{12}B and ^{12}C(n,d)^{11}B reactions. As a further check of the calibration of the first silicon detector, we have used a 5.48 MeV α source (^{241}Am).

By employing time-of-flight techniques, events produced by neutrons in the low-energy tail of the neutron spectrum could be rejected. The background data was measured during runs with target out and was analysed in the same way as the signal runs. Thereafter corrections were made for differences in the data acquisition dead time and the data was normalised to the same neutron flux. A Monte Carlo code has been developed to correct the distortions of the charged-particle spectra caused by energy and particle losses in the reaction targets.

We found that the background is dominated by protons, which are believed to originate from neutrons in the beam halo causing reactions in the beam tube wall at the chamber entrance. This affects mostly the 20° telescope, for which the signal-to-background ratio is about 5:1 for protons and about 7:1 for deuterons. For tritons and α particles, however, the background is negligible.

2. Absolute cross section normalisation

Absolute, double-differential cross sections were obtained from the data by comparison with the number of recoil protons detected from a CH_2 target, after correction for differences in the neutron flux, and assuming that the np cross section is well known.[22] The pure hydrogen proton spectrum was obtained by subtracting the proton spectrum obtained with the carbon target. We estimate that the total absolute normalisation uncertainty is about 3.5%, with equal contributions of 2% each from uncertainties in the target thickness, the relative neutron beam fluence and the np cross section. The last uncertainty is based on a recent measurement made at 96 MeV.[22]

3. Cross sections and kerma coefficients

We have up to now deduced the double-differential cross section, $d^2\sigma/d\Omega dE(\theta, E)$, for proton, deuteron and triton production in carbon at angles ranging from 20° to 160° in steps of 20°. The low energy threshold is about $3 - 4$ MeV for protons and slightly higher for deuterons.

For angles above 40°, the charged particle energy spectra agree well with the recent evaluation[23] and exhibit a monotonically decreasing behaviour as expected for particle emission after statistical equilibrium of the absorbed particle energy. However, for the most forward angle (20°) we observe that the proton spectrum exhibits a broad bump in the mid-energy region, and deviates from the evaluation by up to a factor of two. This deviation is observed also at 40°, although smaller and located at lower energies.

A similar behaviour has been observed in the Louvain-la-Neuve data at 72.8 MeV, and could be attributed to a strong component of a direct or semi-direct reaction mechanism. Also, quasi-elastic scattering, whose contribution becomes increasingly important at higher energies, is in accordance with the shape and the position of the bump.

The deuteron data shows a a marked structure at higher energy, which can be understood as direct (n,d) pick-up reactions where the residual nucleus is in the ground state or in a low-lying excited state. This is well described by the evaluation. The triton spectra, on the other hand, show a decreasing behaviour with energy in all energy bins.

The double-differential cross sections were integrated over energy and scattering angle to obtain the total cross sections. The angular integration was performed by fitting Legendre polynomials to the data for each energy bin i, while the energy integration was done by summing over all energy bins. Below the low-energy threshold, i.e., about 5 MeV, the evaluated data, Ref. 23, was used.

With the energy-weighted double-differential cross sections for protons, deuterons and tritons at hand, we could calculate the partial kerma coefficients (k_Φ), i.e., the energy transferred to charged particles per unit fluence, for production of specific charged particles,

$$k_\Phi = N \sum_{i=1}^{i_{max}} E_i \frac{d\sigma}{dE}(E_i)\Delta E_i \qquad (1)$$

where N is the number of target nuclei per unit mass, E_i is the mean energy of bin i, having a bin width of ΔE_i. **Fig. 3** shows the obtained values for protons, deuterons and tritons, as well as a comparison with other experimental data and the evaluation.

There are in principle two ways to measure the total kerma coefficient: 1) from direct measurements of the absorbed dose by means of a cavity chamber,[24] also known as integral measurements, or, 2) by adding all partial kerma coefficients obtained from the basic information contained in experimental microscopic cross section data.

In the present work we made an effort to estimate the total kerma coefficient for carbon at 95 MeV by summing the measured partial kerma coefficients for protons, deuterons and tritons, together with the evaluated coefficients for α particles, heavier recoils (A>4) and elastic recoils, Ref. 23. The obtained value, see **Fig. 4**, confirms the trend of the previous microscopic data (filled symbols), while the evaluation (continuous line) underestimates the data by approximately 25%. However, the integral measurements (open symbols) are well in accordance with the evaluation up to 70 MeV.

IV. Discussion, conclusion and Outlook

We have in this paper reported on new results on double-differential cross sections for inclusive proton, deuteron and triton production in carbon at 95 MeV. The data was obtained

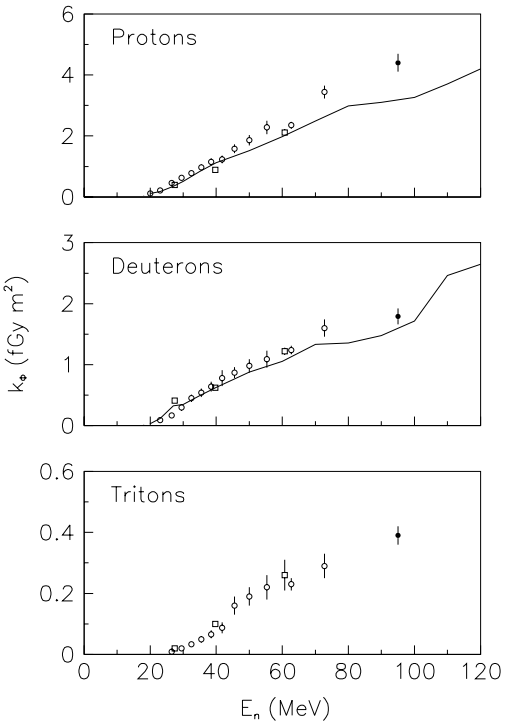

Fig. 3 Partial kerma coefficients for production of protons, deuterons, and tritons in carbon vs. incident neutron energy. The filled circles represent the present data, open circles are from Louvain-la-Neuve,[11] open squares from UC Davis[25] and the solid curve is the evaluation.[23] (From Ref.[16]). The error bars denote total uncertainties.

using a new facility constructed for measurements of neutron-induced light charged-particle production. We have deduced both the partial and the total kerma coefficients for carbon at the same energy. When compared to the evaluation,[23] the partial kerma coefficient for protons is about 35% higher, leading to a 25% higher total kerma coefficient, which can be explained by the fact that protons account for the largest contribution to the total kerma at 95 MeV.

The integrated cross section data as well as the kerma coefficients for protons, deuterons and tritons agree well with the trend of the Louvain-la-Neuve data[11] obtained at lower energies.

In general, the kerma coefficients obtained so far by different groups, agree well with the evaluations up to 40 MeV. Above this energy the microscopic data (Fig. 4, filled symbols) starts to deviate from the integral data (empty symbols) and from the evaluation (solid line). Thus, it is important to understand the origin of this discrepancy and to improve the evaluation in order to achieve agreement with the experimental data.

Newly collected data on carbon, oxygen and silicon, which are currently under analysis, will, hopefully, contribute to that and also bring more clarification and understanding of the different mechanisms involved in neutron reactions and their im portance in the energy range around 100 MeV. Other experiments on additional nuclei are planned as well as measurements intended to extend the available experimental data towards higher energies. Our ambition is that all these efforts will ultimately enable a more accurate dose delivery to the patient.

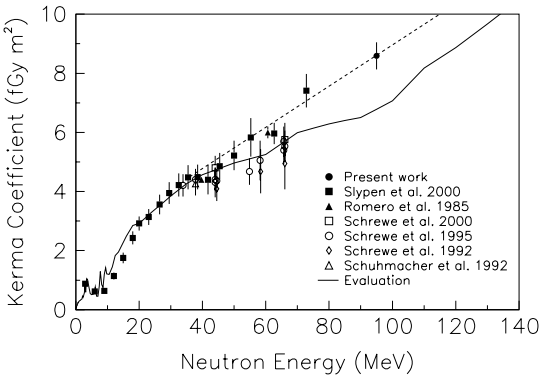

Fig. 4 Comparison between evaluated and measured total kerma factors for ^{12}C + n reaction vs. incident neutron energy. The dashed line is for guiding the eye, only. (From Ref.[16]).

Acknowledgment

The authors whish to thank the The Svedberg Laboratory, the Advanced Instrumentation and Measurement School (AIM) at Uppsala University, the Swedish Research Council and the Swedish Cancer Foundation for their support.

References

1) U. Amaldi Nucl. Phys. **A654** (1999) 375c.
2) R. Orecchia *et al.*, Eur. J. Cancer, **34** (1998) 459.
3) D. Schwartz *et al.*, Int. J. Radiat. Oncol. Biol. Phys. **50** (2001) 449.
4) G. Laramore *et al.*, Int. J. Radiat. Oncol. Biol. Phys. **32** (1995) 879.
5) A. Wambersie *et al.*, Radiat. Prot. Dosim. **31** (1990) 421.
6) M. Tubiana *et al.*, Introduction to Radiobiology, Taylor and Francis, London, 1990.
7) INDC Report, INDC(NDS)-423, May 2001.
8) M. B. Chadwick *et al.*, Radiat. Prot. Dosim. **70** (1997) 421.
9) P. M. DeLuca Jr. *et al.*, ICRU News, June (1996), 14.
10) R. White *et al.*, Radiat. Prot. Dosim. **44** (1992) 11.
11) I. Slypen *et al.*, Phys. Med. Biol. Rev. **45** (2000) 577.
12) I. Slypen *et al.*, Phys. Med. Biol. Rev. **40** (1995) 73.
13) S. Benck *et al.*, Phys. Med. Biol. Rev. **43** (1998) 3427.
14) V. Coralciuc *et al.*, Phys. Med. Biol. Rev. **44** (1999) 719.
15) S. Dangtip *et al.*, Nucl. Instr. and Meth. **A452** (2000) 484.
16) S. Dangtip *et al.*, to be published.
17) U. Tippawan *et al.*, contribution to this conference.
18) A. V. Prokofiev *et al.*, TSL Report, TSL/ISV-99-0203.
19) N. Olsson *et al.*, contribution to this conference.
20) H. Condé *et al.*, Nucl. Instr. and Meth. **A292** (1990) 121.
21) J. Klug *et al.*, to be published.
22) J. Rahm *et al.*, Phys. Rev. **C63** (2001) 044001.
23) M. B. Chadwick *et al.*, Med. Phys. **26** (1999) 974.
24) U. J. Schrewe *et al.*, Phys. Med. Biol.Rev. **45** (2000) 651.
25) T. S. Subramanian *et al.*, Phys. Rev. **C28**, 521 (2001).

Experimental Double-Differential Light-Ion Production Cross Sections for Silicon at 95 MeV Neutrons

Udomrat TIPPAWAN[1,2,*], Bel BERGENWALL[1], Somsak DANGTIP[1,2], Ayse ATAÇ[1], Jan BLOMGREN[1], Klas ELMGREN[1,3], Cecilia JOHANSSON[1], Joakim KLUG[1], Nils OLSSON[1,3], Stephan POMP[1], Olle JONSSON[4], Leif NILSSON[4], Per-Ulf RENBERG[4], Pawel NADEL-TURONSKI[5]

[1] *Department of Neutron Research, Uppsala University, Sweden*
[2] *Fast Neutron Research Facility, Chiang Mai University, Thailand*
[3] *Swedish Defence Research Agency (FOI), Stockholm, Sweden*
[4] *The Svedberg Laboratory, Uppsala University, Sweden*
[5] *Department of Radiation Sciences, Uppsala University, Sweden*

The importance of cosmic radiation effects in aircraft electronics has recently been highlighted. At commercial flight altitudes, as well as at sea level, the most important particle radiation is due to neutrons, created in the atmosphere by spallation of nitrogen and oxygen nuclei, induced by cosmic-ray protons. When, e.g., an electronic memory circuit is exposed to neutron radiation, charged particles can be produced in a nuclear reaction. The charge released by ionization can cause a flip of the memory content in a bit, which is called a single-event upset (SEU). A similar logic error in one of the storage registers of a microprocessor may trigger an unanticipated loop that cannot be escaped without turning the unit off.

To get a deeper understanding of these phenomena, more detailed cross section information on neutron-induced charged-particle production at intermediate energies is needed. To this end, double-differential cross sections of inclusive light-ion production in silicon, induced by 95 MeV neutrons, have been measured. The experiment was performed using the MEDLEY setup, which consists of eight three-element particle telescopes, covering the angular range $20^\circ - 160^\circ$. The charged particles were identified using $\Delta E - \Delta E - E$ techniques. By using an active target, consisting of a 300 μm thick Si detector, the energy loss in the target itself could be measured and corrected for.

KEYWORDS: Charged-particle spectrometer array, active silicon target, double-differential cross section, SEU

I. Introduction

In recent years, the importance of cosmic radiation effects in microelectronic devices on board aircraft[1,2] and satellites[3,4] has been highlighted. At commercial flight altitudes, as well as at sea level, the most important particle radiation is due to neutrons, created in the atmosphere by cosmic-ray protons causing spallation of nitrogen and oxygen nuclei. The spallation neutron spectrum shows a typical $1/E$ dependence, extending to energies of several GeV. When a neutron collides with a silicon nucleus, light and heavy charged particles can be produced in a nuclear reaction. If the charge released by ionization passes a critical threshold, the memory content in a bit flips. This is called a single-event upset (SEU). In some cases, two or more bits in a single memory word may flip, which is called single-word multi-bit upset (SMU).[5–7]

Light charged particles (p, d, t, ^{3}He and α) are normally not considered in SEU calculations since the energy deposited by these particles within the sensitive volume is very small. The memory residing in highly integrated microchip devices are today formed by very small charges. With the expected advances in technology, the development towards higher scale integration includes reducing the operation voltage which also means that the critical threshold is decreased. For this reason, also the contribution from light ions, such as α particles, is expected to become significant for SEU, and it might also affect the SMU rate.[5)]

Since it is difficult to have access to sufficient machine-time for in-beam accelerated testing, and in-field testing is time consuming, many codes[8–12)] for neutron-induced SEU simulation have been developed. However, the lack of experimental neutron cross sections at intermediate energies makes the precision of such codes uncertain. In some codes nuclear models are used, e.g., the quantum-molecular dynamics (QMD) or the antisymmetrized molecular dynamics (AMD) models, to calculate the neutron-nucleus reaction cross sections. The results are most often verified by comparison with the corresponding proton-induced reaction data on ^{27}Al.

Recently, active personal neutron dosemeters, based on silicon diodes, have been developed for space flight applications.[13–15)] The silicon diodes are covered by plastic material with different contents of boron and ^{6}LiF, in order to get some spectral sensitivity. Contrary to the case of SEU, light charged particles, e.g., protons, play a key role for radiation dosimetry at high energies. Furthermore, the neutron spectrum inside the shielding of a spacecraft[16)] peaks at energies of about 1 and 100 MeV, just as it does at aircraft altitudes.[17)] This is a relatively new dosimetry issue, which is currently under investigation.

In this contribution, we present data obtained with the MEDLEY setup, which has been constructed with the goal to measure double-differential light-ion production cross sections.

* Corresponding author, Tel. +46 18 471 3254, Fax. +46 18 471 3853, E-mail: tippawan@tsl.uu.se

II. Experimental setup and Methods

1. The neutron beam

The Svedberg Laboratory (TSL) offers a neutron beam facility (see Fig. 1 in Ref.[18]), using the ^{7}Li(p,n)^{7}Be reaction. Quasi-monoenergetic neutrons are produced at 0° together with an almost flat low-energy tail is obtained. The low-energy neutrons can be suppressed using time-of-flight (TOF) techniques. The proton beam is bent out from the neutron beam by two dipole magnets into a lead-shielded water-cooled beam dump.

2. Beam Monitoring

For absolute normalization of the neutron fluence, the neutron beam is directly monitored by a thin-film breakdown counter (TFBC), measuring the number of neutron-induced fissions in ^{238}U. Relative monitoring can be obtained by charge integration of the proton beam from the Faraday cup in the beam dump.

3. The MEDLEY setup

The MEDLEY detector setup[19] consists of a 100 cm diameter evacuated chamber, containing eight three-element particle telescopes and the reaction target (see Figs. 1 and 2 in Ref[20]). The telescopes are mounted to cover scattering angles from 20° to 160° in 20° intervals.

Each telescope consists of two ΔE detectors and one thick E detector. We have found in previous studies that two ΔE detectors with different thickness yield good separation between the different particle types and give a large dynamic range, i.e., from a few MeV up to 100 MeV.

The ΔE detectors are fully depleted standard ORTEC silicon surface barrier detectors. The thickness of the front ΔE detector (ΔE_1) is either 50 or 60 μm, while the second one (ΔE_2) is 400 or 500 μm. CsI(Tl) crystals are used as E detectors, because of several superior properties, e.g., high density and large light conversion yield. Furthermore, the crystals are only slightly hygroscopic. This allows a window-less construction and we avoid dead layer effects.

To obtain a well-defined acceptance, collimators are placed in front of the telescopes. To avoid the problem of in-scattering or particle reactions before reaching the first detector, which is difficult to avoid in conventional (thick) collimators, we have instead chosen to employ thin, active collimators, where the signal from a hit can be used to veto the related event. The plastic scintillator collimators have a 40x40 mm^2 square shape, with a 19 mm diameter hole at the centre and a thickness of 1 mm. This thickness is sufficient also for the most penetrating 100 MeV protons to produce a reasonable pulse height.

To measure the energy loss of charged particles in the silicon target, we have chosen a PIPS Si detector as active target, manufactured by CANBERRA, without frame or other mounting assemblies. It has a 30x30 mm^2 square shape and is 300 μm thick. It is suspended on a thin aluminium target frame, using thin threads and small springs. The measured energy resolution is 120 keV (FWHM) for 5.48 alpha particles from a ^{241}Am source.

4. Electronics and data acquisition

For each detector, the output signal is processed by a charge-sensitive preamplifier, and outputs are generated for energy (E) and timing (T). The E branch is further amplified and shaped, and the pulse height is registered by an ADC. For the other branch (T), only signals from the silicon detectors of each telescope are fed to CFDs and a logic OR to define an event. The MASTER triggering signal for the data acquisition system is produced by a logic OR between all eight telescopes. The MASTER signal is fed to all TDCs as common start. The RF signal from the cyclotron is used as reference for the TOF, and is registered as a stop signal in one of the TDCs, as is the T signal from all the silicon detectors.

The raw data are stored on an event-by-event basis and split into two independent branches, one for on-line monitoring and the other to magnetic tape for subsequent analysis.

III. Data analysis

In the measurement of light-ion production in silicon induced by 95 MeV neutrons, the active silicon target was used for the main data acquisition. Background runs were performed by moving the target frame out of the neutron beam. Furthermore, a 25 mm diameter by 1.0 mm thick CH_2 target

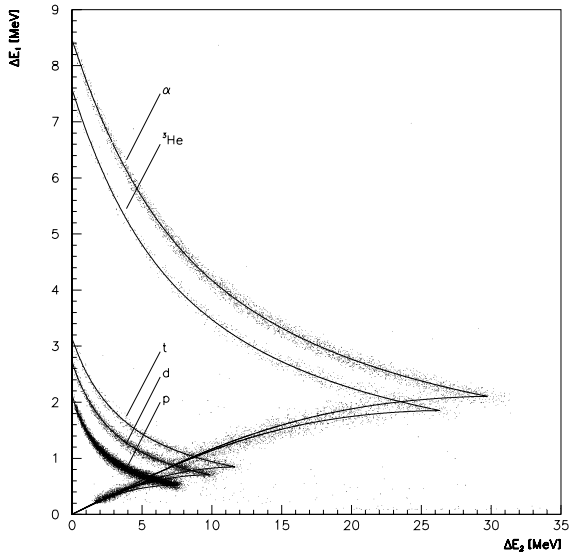

Fig. 1 Pulse height of the 50 μm ΔE_1 versus the 400 μm ΔE_2 detector.

was used for absolute cross-section normalization. The data analysis is done on an event-by-event basis, where the data are first sorted into separate files for each telescope, and subsequently into parameter matrices for each file.

1. Particle identification and Energy calibration

The $\Delta E - \Delta E - E$ technique is used to identify light ions from protons up to ^{6}Li. **Figures 1** and **2** show two-dimensional plots for ΔE_1 versus ΔE_2 and ΔE_2 versus E, respectively, for a scattering angle of 20°. The separation between different particles is very good, and thus the particle identification procedure is straight forward.

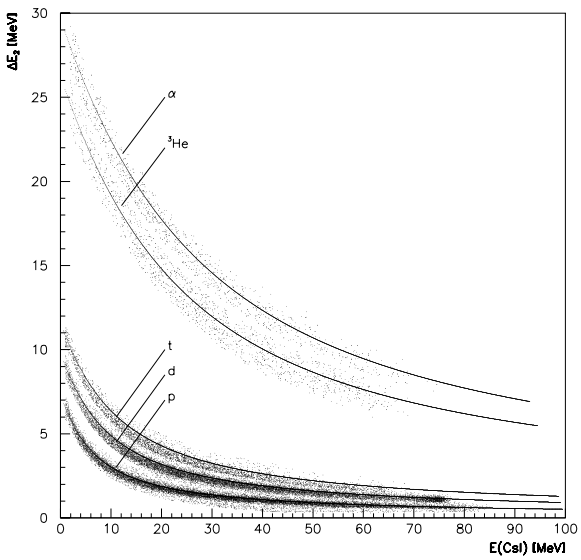

Fig. 2 Pulse height of the ΔE_2 versus the CsI E detector.

Energy calibration of all detectors is obtained from the data itself, using a user-supplied FORTRAN program, combined with HBOOK and MINUIT software. When running the program, events in the bands are fitted with respect to the energy deposited in both Silicon detectors. This energy is determined from the detector thicknesses and calculations of energy loss in silicon. The ΔE_1 detectors are further calibrated and checked using a 5.48 MeV α source.

Due to the non-linear correspondence between pulse height (or light output L) and deposited energy in a CsI detector for various particles, we used the following parameterisations;[19)]

$$E = a + bL + c(bL)^2 \qquad \text{for hydrogen isotopes,}$$

$$E = a + bL + c\ln(1 + dL) \quad \text{for helium isotopes.}$$

The parameters a,b,c and d are obtained by the fitting procedure.

To further check the calibration at high energy, we used the distinct peaks corresponding to ground-state and low excitation-energy transitions in the ^{28}Si(n,d)^{27}Al and ^{12}C(n,d)^{11}B reactions. The energies of these peaks can be calculated from the neutron energy and the reaction kinematics, taking the energy loss in the silicon target and in the silicon detectors into account.

The program performs identification for every event, the ejectile energy is obtained by adding the energy deposited in the three-element telescope, and the charged-particle TOF can be calculated since the energy and mass are determined, and the flight path from target to detector for each telescope is known.

2. Low energy neutron rejection and background subtraction

In order to reject events due to low-energy neutrons, the neutron TOF has to be constructed. The time difference between the MASTER signal and the cyclotron RF is registered in a TDC for each telescope and each ΔE detector of that telescope. The time difference is the sum of the flight times for the neutron and the charged particle. Subtraction of the charged particle TOF from the total TOF then yield the neutron TOF for every event. After creation of a two-dimensional plot of the neutron TOF versus the charged-particle ejectile energy, as is shown in **Fig. 3**, one can make a contour for selection of particles associated with the full-energy neutron peak only.

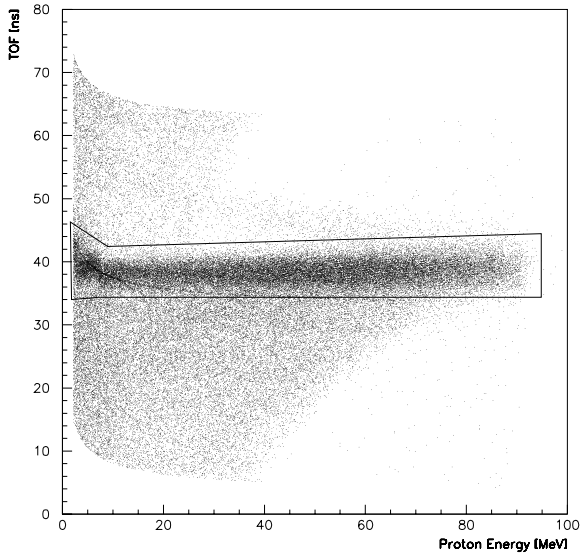

Fig. 3 Neutron TOF versus proton energy for the ^{28}Si(n,p)^{28}Al. A selection of protons associated with the full-energy neutron peak is illustrated with the full line contour.

From this point, events are sorted into different histograms according to the type of particle. The histograms represent both the energy and angular distribution of the different particles induced by the monoenergetic neutrons.

The background (target-out) runs are analysed in the same conditions as the silicon (target-in) runs, each histogram being normalized to the same neutron fluence and corrected for dead time. Finally, the background run histograms are subtracted from the silicon ones.

3. Absolute cross-section normalization

Absolute double-differential cross sections are obtained by normalizing the silicon data to the number of recoil protons emerging from a CH_2 target, and assuming that the np scattering cross section is well known.

The CH_2 runs are analysed in the same conditions as the silicon and background runs. After proper subtraction of the sample-out background and the ^{12}C(n,p) contribution, the cross section per count and incident neutron is determined from the pure recoil proton peak, using previous experimental cross section data from TSL.[21)]

This method can only be used for telescopes at forward angles, i.e., $\theta = 20° - 40°$. At larger angles, the kinematics of the recoil protons make the elastic np peak too diffuse. Thus, the CsI crystals of these telescopes are assumed to have the same intrinsic efficiency as those at forward scattering angles.

Furthermore, the energy dependence of the intrinsic efficiency is not very large in the energy range of interest here.

IV. Results, discussion and outlook

Preliminary energy spectra for proton and deuteron production at an angle of 20° are shown in **Figs. 4** and **5**, respectively.

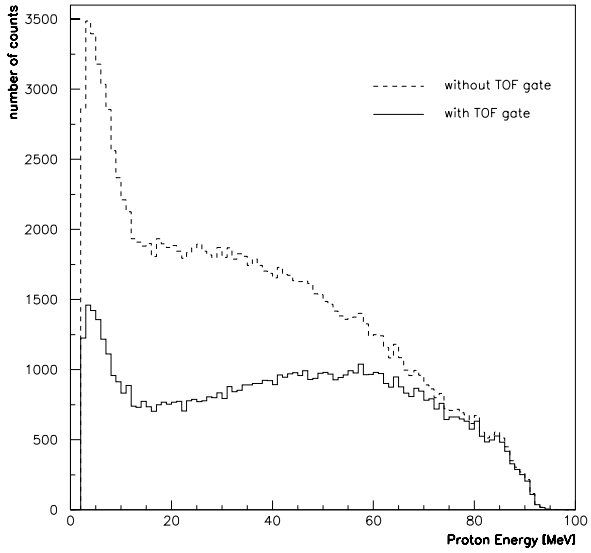

Fig. 4 Preliminary energy spectrum for protons at 20°.

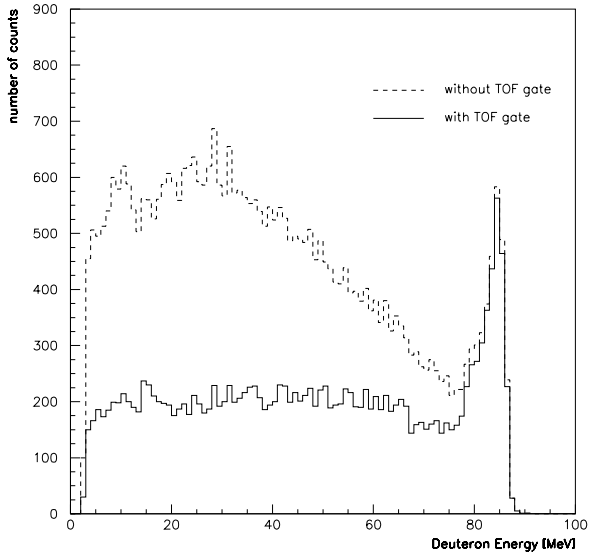

Fig. 5 Preliminary energy spectrum for deuterons at 20°.

Clear peaks, corresponding to transitions to low-lying states in the residual nucleus, can be seen at the highest energies for deuterons. The effect of applying the TOF gate in Fig. 3 is clearly seen; the spectra reduces from the dashed curve to the solid one. These data still have to be normalized, and in addition, corrections have to be applied for the solid angle acceptance, the CsI efficiency and the energy loss in the active silicon target. Comparisons will be made with Monte Carlo simulations.

We have been able to identify ^{6}Li events, however with poor statistics. Therefore we plan to use the QMD model to calculate the cross sections for the contributions from heavy ions. The total cross section is experimentally well known. By subtracting the elastic and inelastic cross sections calculated using a state-of-the-art optical model, and the measured cross sections for production of light ions, the calculated heavy-ion cross sections can be renormalized to a realistic magnitude. This will be a great improvement compared to most other approaches.

Acknowledgment

The authors wish to thank the The Svedberg Laboratory, the Thai Ministry of University Affairs and the International Program in the Physical Sciences for the fellowship arrangement, the Thailand Research Fund, the Swedish Research Council and the Swedish Cancer Foundation for their support.

References

1) H. Kanata *et al.*, Proc. IEEE 1999 Int. Conf. on Microelectronic Test Structures. **12**, 184 (1999).
2) P. Hazucha and C. Svensson, IEEE J. Solid-State Circuits. **35**, 1422 (2000).
3) V.F. Bashkirov *et al.*, Radiat. Meas. **30**, 427 (1999).
4) S. Buchner *et al.*, IEEE Trans. Nucl. Sci. **47**, 705 (2000).
5) K. Johansson *et al.*, IEEE Trans. Nucl. Sci. **46**, 1427 (1999).
6) S. Satoh *et al.*, IEEE Electron Device Lett. **21**, 310 (2000).
7) P. Hazucha and C. Svensson, IEEE Trans. Nucl. Sci. **47**, 2595 (2000).
8) M.B. Chadwick and E. Normand, IEEE Trans. Nucl. Sci. **46**, 1386 (1999).
9) Y. Tosaka *et al.*, IEEE Trans. Nucl. Sci. **46**, 774 (1999).
10) C.S. Dyer *et al.*, IEEE Trans. Nucl. Sci. **46**, 1486 (1999).
11) T. Ikeuchi *et al.*, Proc. of the 2000 Symposium on Nuclear Data, Nov. 16-17, 2000, JAERI, Tokai, Japan, no. JAERI-Conf **2001-006**, 327 (2001).
12) P.-M Palau *et al.*, IEEE Trans. Nucl. Sci. **48**, 225 (2001).
13) M. Luszik-Bhadra *et al.*, Radiat. Meas. **33**, 305 (2001).
14) R.C. Singleterry *et al.*, Radiat. Meas. **33**, 355 (2001).
15) G.D. Badhwar and P.M. O'Neil, Nucl. Instr. Meth. **A466**, 464 (2001).
16) T.W. Armstrong and B.L. Colborn, Radiat. Meas. **33**, 299 (2001).
17) D. O'Sullivan, Final Report January1996-June 1999, Contract F14P-CT950011, Report 99–9–1, The Dublin Institute for Advanced Studies School of Cosmic Physics (1999).
18) J. Klug *et al.*, contribution to this conference
19) S. Dangtip *et al.*, Nucl. Instr. Meth. **A452**, 484 (2000).
20) B. Bergenwall *et al.*, contribution to this conference
21) J. Rahm *et al.*, Phys. Rev. **C63**, 044001 (2001).

HINDAS
A European Nuclear Data Program for Accelerator-Driven Systems

Arjan Koning[1,*], Hans Beijers[2], Jose Benlliure[3], Olivier Bersillon[4], Joseph Cugnon[5], Marieke Duijvestijn[1], Philippe Eudes[6], Detlef Filges[7], Ferid Haddad[6], Claude Lebrun[7], Francois-Rene Lecolley[8], Sylvie Leray[9], Jean-Pierre Meulders[10,**], Rolf Michel[11], Ralf Neef[7], Ralf Nolte[12], Nils Olsson[13], Elisabet Ramström[13], Karl-Heinz Schmidt[14], Helmut Schuhmacher[12], Isabelle Slypen[10], Hans-Arno Synal[15], Regin Weinreich[16]

[1] *Nuclear Research and consultancy Group, P.O. Box 25, NL-1755 ZG Petten, the Netherlands*
[2] *Kernfysisch Versneller Instituut, University of Groningen, Zernikelaan, NL-9737 AD Groningen, the Netherlands*
[3] *Universidad de Santiago de Compostela, Fisica de Particulas, E-15706 Santiago de Compostela, Spain*
[4] *Commissariat à l'Energie Atomique, Service de Physique Nucléaire, BP 12, 91680 Bruyères-le-Châtel, France*
[5] *Université de Liége, Physique Nucléaire Théorique, Institut de Physique au Sart Tilman, B5, 4000 Liège, Belgium*
[6] *Laboratoire SUBATECH, 4, Av. Alfred Kastler, 44037 Nantes, France*
[7] *Forschungszentrum Jülich, Institut für Kernphysik, D-52425 Jülich, Germany*
[8] *Université de Caen, LPC-ISMRA, 6 Bld du Marechal Juin, 14050 Caen Cedex, France*
[9] *Commissariat á l'Energie Atomique, Service de Physique Nucléaire Saclay, 91191 Gif-sur-Yvette Cedex, France*
[10] *Université Catholique de Louvain, Chemin du Cyclotron, B-1348 Louvain-la-Neuve, Belgium*
[11] *Zentrum für Strahlenshutz und Radioökologie, Am Kleinen Felde 30, D-30167 Hannover, Germany*
[12] *Physikalisch-Technische Bundesanstalt, Bundesallee 100, D-38116 Braunschweig, Germany*
[13] *Department of Neutron Research, Uppsala University, Box 535, S-75121 Uppsala, Sweden*
[14] *Gesellschaft für Schwerionenforschung mbH, Planckstrasse 1, D-64291 Darmstadt, Germany*
[15] *Institute of Particle Physics, Eidgenüssische Technische Hochschule, Hönggerberg, CH-8093 Zürich, Switzerland*
[16] *Laboratory for Radio- and Environmental Chemistry, Paul Scherrer Institute, CH-5232 Villigen-PSI, Switzerland*

In the HINDAS program, nuclear data in the 20-2000 MeV range are evaluated by means of a combination of nuclear models and well-selected intermediate- and high-energy experiments. A panoply of European accelerators is utilized to provide complete sets of experimental data for Iron, Lead and Uranium over a large energy range. Nuclear model codes are being improved and validated against these new experimental data. This should result in enhanced ENDF-formatted data libraries up to 200 MeV, and cross sections for high-energy transport codes above 200 MeV. The impact of the new data libraries and high-energy models will be directly tested on some important parameters of an accelerator-driven system (ADS). Here, we report the recent progress of the various experimental and theoretical activities in HINDAS.

KEYWORDS: intermediate energy, measurement program, ADS, 20-1500 MeV, double-differential, elastic , residual production cross section, multiplicity, inverse kinematics, nuclear models, TALYS, INC, data library

I. Introduction

HINDAS (High and Intermediate energy Nuclear Data for Accelerator-driven Systems) is a project supported by the European Commission, from September 2000 - August 2003, and involves 16 European laboratories. Its objective is to obtain a thorough understanding and complete modeling of nuclear reactions in the 20-2000 MeV region, in order to build reliable and validated computational tools for the detailed design of the spallation module of an accelerator driven system. To achieve this, an ambitious experimental and theoretical program has been launched.

Six European facilities, listed in **Table 1**, are participating in the measurement of the following observables:

- double-differential $(p, xn...x\alpha)$ and $(n, xn...x\alpha)$ cross sections,
- residual nuclide production, by activation and inverse kinematics techniques, and residual kinetic energies,
- neutron elastic scattering angular distributions,
- neutron and charged-particle multiplicity distributions,
- thick target neutron spectra.

The diversity of the used accelerators is such that the complete energy region between 20 and 2000 MeV is covered. A suitable coverage of the periodic table of elements is obtained with the choice of target elements: Fe, Pb and U. Lead and iron are representative of materials used in ADS, while uranium represents the actinide region.

Parallel to the measurement program, theoretical models are under development. For energies from zero up to 200 MeV, the new nuclear model code TALYS has been designed. It includes the optical model, direct, pre-equilibrium, fission and statistical models and thereby gives a prediction for all the open reaction channels. In addition, for energies up to 2000 MeV, a new intranuclear cascade model is under development.

* Corresponding author, Tel. +31-224-564051, Fax. +31-224 -568490, E-mail: koning@nrg-nl.com
** Coordinator, Tel. +32-10-473273, Fax. +31-10-452183 Email: Meulders@fynu.ucl.ac.be

During the measurement program, the nuclear model codes are directly benchmarked against the new experimental data. The intermediate energy models will be used to create ENDF-libraries up to 200 MeV, while the high-energy nuclear models will be implemented in high-energy transport codes. Finally, calculations of several quantities important in the design of ADS target or window, such as activity, radiation damage, gas production, etc., will be performed in order to assess the improvements brought by the new data and models.

The HINDAS project is divided into 8 work-packages (WP), which together aim to cover all aforementioned objectives. In this contribution, a general description of the program and the first results will be presented.

Table 1 European facilities participating in HINDAS

Institute	Accelerator	Energy range (MeV)
UCL-Louvain-la-Neuve	CYCLONE	20-70 (p and n)
UU-Uppsala	TSL	20-180 (p and n)
KVI-Groningen	AGOR	130-190 (p)
PSI-Villigen	cyclotron	45-70 (p)
FZ-Jülich	COSY	50-2500 (p)
GSI-Darmstadt	SIS	300-1000 (MeV.A)

II. Experimental program up to 200 MeV

1. Light charged-particle production induced by neutrons and protons (WP1)

The main objective of WP1 is to measure double-differential production cross sections for light charged particles (lcp), i.e. protons, deuterons, tritons, Helium-3, alpha's, in nuclear reactions induced by protons and neutrons in the incident energy range 20-200 MeV. The goal is to provide precise experimental data over a complete angular range (20 to 160 degrees) with an overall uncertainty better than 15%.

The $(p, xlcp)$ reactions on Pb and U have been measured by the partners of UCL-Louvain-la-Neuve, SUBATECH-Nantes and LPC-Caen at 65 MeV at the CYCLONE cyclotron (UCL), and the same reactions on Fe, Pb and U at 135 MeV are planned by the partners of SUBATECH, LPC and KVI-Groningen at KVI. For these measurements, 8 triple telescopes (Si-Si-CsI) allow to measure the light charged-particles from a low energy threshold up to 160 MeV.

The $(n, xlcp)$ reactions on Fe, Pb and U will be measured at 65 MeV at the CYCLONE cyclotron (UCL). Six $\Delta E - E$ telescopes (NE-102 plastic scintillator - CsI(Tl) detector) detect the charged particles produced by the neutrons on the target. The information from the telescopes coupled to the time of flight method with excellent time resolution (less than 1 ns) allows to reconstruct, event by event, the energy spectra for each ejectile. Double-differential cross sections are obtained for the neutron monoenergetic peak (∼63 MeV) and also for energies from the continuum of the neutron energy spectrum[1)] (from 30 to 57 MeV). In **Figure 1**, the recently obtained 62.7 MeV Pb(n, xp) cross sections for the whole angular range are shown. Results for the other nuclides are still under analysis.

The $(n, xlcp)$ reactions on Fe and Pb at 100 MeV will be measured at the Svedberg cyclotron (Uppsala), with the same detection setup as for the proton induced-reactions. Partners of SUBATECH, LPC and UU-Uppsala are involved.[2)]

In addition, a series of experiments devoted to the measurement of light-charged particle multiplicity distributions from proton-induced reactions for projectile energies between 130 and 200 MeV will be performed at KVI.

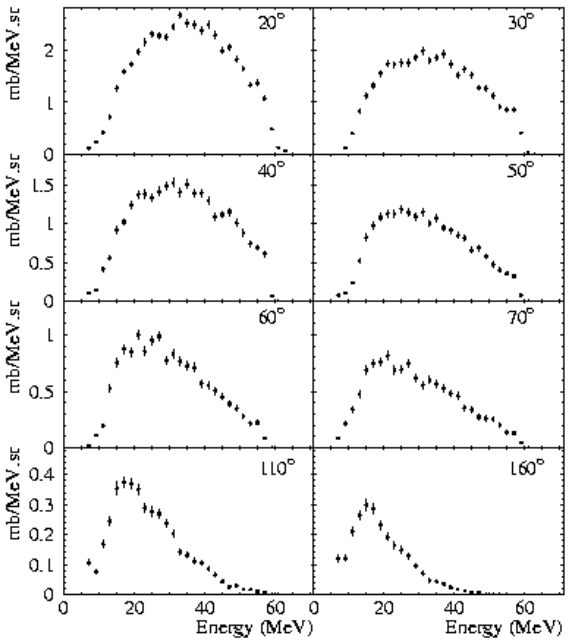

Fig. 1 Double-differential cross sections for 62.7 MeV Pb(n, xp).

2. Neutron production induced by neutrons and protons (WP2)

Elastic neutron scattering angular distributions at 100 MeV for Fe and Pb will be measured[3)] in Uppsala by UU-Uppsala and LPC-Caen. Such data are important to determine the nuclear optical potential to high precision in an energy range where data are essentially lacking. With this model, cross sections for elastic scattering, which is the most important reaction channel in the moderation and transport of the source neutrons, can be calculated. Moreover, the optical potential is a necessary component in the description of many other reaction channels, since it accounts for the behavior of a neutron entering or emerging from a nucleus. Optical models developed in WP7 will be used to analyze the measurements.

The measurements will be performed using a recently developed detector setup, consisting of two identical detector sets, which can be arranged to cover, e.g., the 10-50 and 30-70 degree ranges. Each detector set consists of a front veto scintillator, a 1 cm thick plastic scintillator for conversion into recoil protons, two drift chambers with x-y position sensitivity for proton tracking, and an array of 12 large CsI detectors for proton energy measurement. Absolute cross sections will be determined by comparison with the reasonably well known

neutron-proton scattering cross section.

Also, the measurement of double-differential spectra from (p, xn) reactions in Pb and U, using a 65 MeV proton beam will be performed by partners of LPC-Caen, SUBATECH and UCL. In these experiments the emitted neutrons will be detected by well shielded NE-213 neutron detectors, placed around the scattering centre to measure angular distributions. The neutron energy distribution will be determined using time-of-flight techniques. Neutrons will be distinguished from gamma-rays using the pulse shape discrimination properties of this kind of detectors. Note that the energy is chosen such that a data set consistent with that of WP1 is formed.

3. Residual nuclide production induced by neutrons and protons and production of long-lived radionuclides (WP3)

WP3 comprises measurements of integral cross sections for the production of residual nuclides from Fe and U by protons with energies up to 2.6 GeV and 70 MeV, respectively,[4] and by neutrons with energies between 30 and 170 MeV,[5] measurements of the ^{235,238}U, ^{209}Bi and ^{nat}Pb fission cross sections for neutrons with energies from 30 MeV to 150 MeV[6] and measurement of production cross sections of long-lived radionuclides from Fe and Pb after chemical separation.

Irradiation experiments with protons[7] are performed at PSI using the stacked-foil technique and off-line γ-spectrometry. Long-lived radionuclides are measured after chemical separation via AMS at the PSI/ETH Tandem AMS at ETH.

Experiments with quasi-monoenergetic neutrons produced by the ^{7}Li(p,n)^{7}Be reaction are performed at UCL,[8] Uppsala[9,10] and NAC-Cape Town, South Africa. Residual nuclides are measured by off-line γ-spectrometry. Neutron cross sections are determined by unfolding methods from the experimental response integrals determined in a series of irradiation experiments with different neutron energies. Fission cross sections are measured using parallel-plate fission chambers (PPFC). While the U- and the Bi- PPFC's were already used in earlier experiments, the ^{nat}Pb-PPFC was specially developed within the HINDAS project.

The data to be determined in this work package will provide an experimental basis to calculate inventories of the spallation target, of shielding and structural materials for an accelerator driven system after shut-down. Also, it will aid in validating theoretical work which is needed for calculations on very short-lived radionuclides, which make up an essential part of the spallation target during operation of a facility. With respect to the long-term behavior and the final disposal of spallation targets and structural materials, the precise modeling of long-lived radionuclides will be essential.

III. Experimental program above 200 MeV

1. Light charged-particle production (WP4)

Light charged-particle production data are important to probe the high-energy nuclear models. In the latter, the competition between neutrons and charged-particles and the emission of composite particles (deuterons, alphas) are not yet treated satisfactorily. Moreover, the production yields of hydrogen and helium are essential for estimation of gas production in the window or structure materials of an ADS.

Production cross-sections for hydrogen and helium are being measured using a 4π silicon ball detector, see **Figure 2**. So far, experiments have been performed at 0.8, 1.2, 1.8 and 2.5 GeV on several targets.[11] These measurements are also performed in coincidence with neutron multiplicity distributions using the neutron detector mentioned in WP5 (see below). This allows to study the production rates of protons and alphas as a function of the excitation energy in the nucleus remaining at the end of the intranuclear cascade stage. All these data will be analysed and compared to high-energy nuclear models. A careful analysis of the light charged-particle

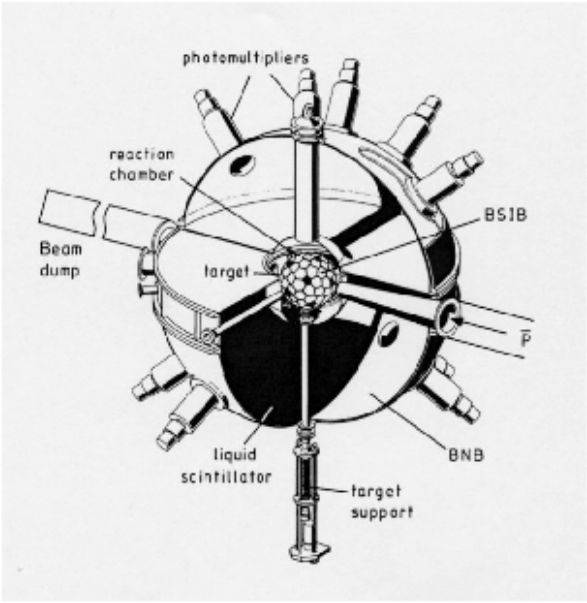

Fig. 2 The Berlin ball detector system.

production data at high energies has shown that experimental data are scarce and often limited to a small range of energy. In particular, the high energy part of the out-going proton spectrum, which contributes as much as neutrons to the propagation of the inter-nuclear cascade inside a thick target, is not well known. In WP4, the partners will join to develop a new magnetic spectrometer able to measure, with a high resolution, double-differential cross-sections for the production of light charged-particles over a broad energy range. This apparatus will also be used in coincidence with a neutron scintillator detector measuring low energy neutron multiplicities. This will permit to disentangle the intra-nuclear cascade and the de-excitation stages in the reaction mechanism. These second generation experiments will provide a deeper understanding of the mechanisms that will be necessary to definitively tune all the parameters of the nuclear models. Simulations of the expected results with the high-energy nuclear models from WP8 will be done.

2. Neutron production induced by protons in thin and thick targets (WP5)

In this work-package, different types of neutron production data measured in both thin and thick targets will be collected, intercompared and compared with models. Neutron energy spectra and complete angular distributions using two complementary experimental techniques have been measured: time-of-flight for the low energy part of the neutron spectrum and neutron-proton scattering on a liquid hydrogen converter with a magnetic spectrometer measuring the momentum of the recoiling proton for high energy neutrons. This has allowed to obtain energy spectra of (p, xn) reactions with a high resolution from 2 MeV to the incident energy, on several targets at 800, 1200 and 1600 MeV.[12] The same apparatus was used to measure neutron energy spectra from thick targets with different length and diameters.

The multiplicity of neutrons up to 150 MeV on both thin and thick targets of different length and diameter for incident proton energies of 0.4, 0.8, 1.2, 1.8 and 2.5 GeV over a wide range of structural and target materials has been measured. This was performed with a 4π liquid scintillator detector able to measure event-wise. The neutron multiplicity distribution in thin targets reflects the excitation energy distribution of the nucleus left at the end of the intranuclear cascade stage and is therefore important to understand the reaction mechanism.

Results will be used to assess the remaining deficiencies in the codes to be improved in WP8. Simulation of thick target results will also be realized using a 200 MeV evaluated data file instead of the standard 20 MeV file. Direct applications of the thick target experiments such as average neutron multiplicities or high energy neutron leakage for shielding estimation will be investigated.

3. Residual nuclide production in inverse kinematics (WP6)

In spallation reactions of heavy nuclei induced by protons of about 1 GeV, mostly short-lived radioactive nuclei are produced. The spallation residues are stopped inside the target. They decay towards stable isobars predominantly by beta decay. After irradiation, long-lived radioactive residues are identified in mass and atomic number by gamma spectroscopy and by accelerator mass spectrometry. These methods are used in WP3 of HINDAS and provide reliable and comprehensive data on cumulative yields, from which long-lived activities and final element yields can be deduced. In addition, these techniques allow for measurements over a large range of bombarding energies. A previous intercomparison with available data has revealed that the calculations with nuclear reaction models are not realistic enough, but it is difficult to pin down the deficiencies of the models on the basis of cumulative yields. For this purpose, a complete systematic of isotopic production cross sections emerging from the nuclear reaction is required.

In particular for proton energies above 200 MeV, a substantially different technique, based on the use of inverse kinematics,[14] has been developed recently which allows to identify all short-lived radioactive nuclides produced as spallation residues prior to beta decay. Heavy nuclei are provided as projectiles, impinging on a liquid-hydrogen target. The spallation residues are identified in-flight in a high- resolution magnetic spectrometer. These experiments allow a much more direct insight into the reaction mechanism than experiments in normal kinematics and therefore are best suited to improve nuclear-reaction models which are known to be unable to reproduce available data. In addition, this technique allows to determine the kinetic energies of the spallation residues,[13] an information of highest importance for estimating radiation damages in structure materials of an ADS. That means that these experiments provide unique and valuable information which complements the results obtained in normal kinematics. Due to electronic interactions in the spallation target, the primary protons loose energy and induce nuclear reactions in a wide energy range. However, the higher energies are particularly important for residual-nuclide productions, since more than 75% of the primary protons of 1 GeV undergo nuclear reactions in the spallation source in an energy range above 700 MeV. Additional measurements with a liquid deuterium target are aimed to provide information on spallation reactions induced by neutrons.

The experiments in inverse kinematics and the data analysis being rather complex, only few projectile species and energies can be investigated. Therefore, the measurements are restricted to ^{208}Pb, ^{238}U and ^{56}Fe at 1 A GeV and partly at 500 A MeV. It is expected that the full isotopic distributions and kinetic energies obtained in inverse kinematics provide sufficient information to develop substantially improved nuclear-reaction models.

IV. Theoretical/Evaluation program

1. Nuclear data libraries and related theory (WP7)

1. TALYS. TALYS[15] is a computer code system for the simulation and analysis of nuclear reactions, created by NRG Petten and CEA Bruyères-le-Châtel. The basic objective behind the construction of TALYS is the ability to give a complete description of nuclear reactions that involve neutrons, photons, protons, deuterons, tritons, ^{3}He- and alpha-particles, for target nuclides of mass 12 and heavier. To achieve this, a suite of nuclear reaction models has been implemented into a single code system. This enables to evaluate nuclear reactions from the unresolved resonance region up to intermediate energies. As specific features of TALYS we mention

- In general, a non-approximative implementation of many nuclear models for direct, compound, pre-equilibrium and fission reactions.
- A continuous, smooth description of reaction mechanisms over a wide energy range (0.001- 200 MeV).
- Completely integrated optical model and coupled-channels calculations through the ECIS code, with incorporation of new (global and local) optical model parameterizations for many nuclei.[16]
- Total and partial cross sections, energy spectra, angular distributions, double-differential spectra and an exact

modelling of exclusive cross sections and spectra. Excitation functions for residual nuclide production, including isomeric cross sections.

- Automatic reference to nuclear structure parameters as masses, discrete levels, resonances, level density parameters, deformation parameters, fission barrier and gamma-ray parameters, mostly from the RIPL library.[17)]

- Various phenomenological and microscopical level density models, such as Gilbert-Cameron, Ignatyuk and combinatorial state densities built on Hartree-Fock-Bogoliubov based single-particle states.

- Semi-classical and quantum-mechanical (multi-step direct/compound) models for pre-equilibrium reactions.

- Use of systematics if an adequate theory for a particular reaction mechanism is not yet available or implemented, or simply as a predictive alternative for nuclear models.

TALYS is used for the analysis of all sub-200 MeV experiments in HINDAS. In **Figure 3**, residual production cross sections calculated by TALYS are compared with experimental data. For this calculation, pre-equilibrium reactions were modeled with a two-component exciton model, while multiple compound emission was treated with the Hauser-Feshbach model. As two important ingredients we mention nucleus-tailored optical potentials and energy-dependent shell effects in the level density.

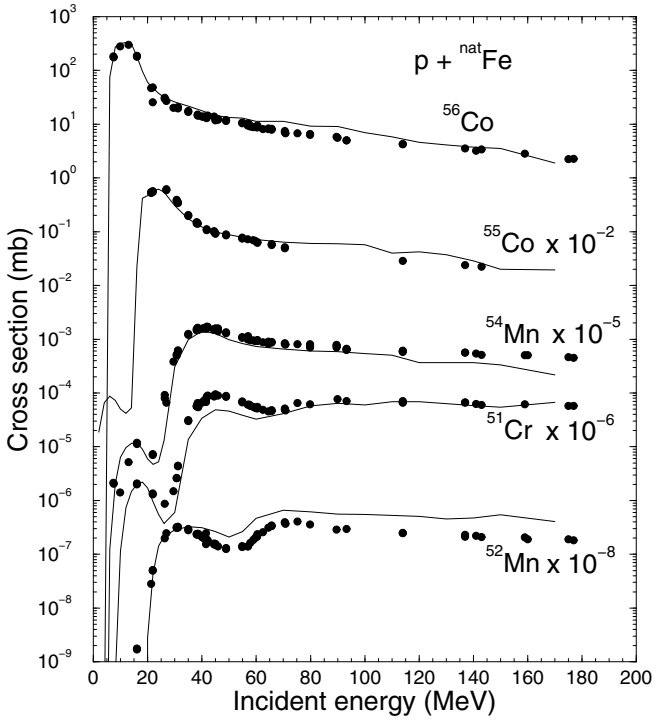

Fig. 3 TALYS-0.36 calculation for residual production cross sections of $p + {}^{nat}$Fe, compared with experimental data.[18)]

2. Tamura-Udagawa-Lenske model. In this part of WP7 the quantum-mechanical multistep direct reaction model according to Tamura-Udagawa-Lenske (TUL) is used to describe nucleon-induced reactions at intermediate energies.[19)] It will be applied for the calculation of the double-differential cross sections measured in WP1 and WP2 . Furthermore, it will be used for predictions of unmeasured data in this energy range. For ADS applications it is important that the magnitude of the calculated cross sections is free of any adjustable parameters and is strictly related to known physical parameters and quantities such as effective interactions and applied optical potentials. Consequently, knowledge of dedicated optical potentials for the different isotopes is extremely important. Another objective is to include this option in TALYS.

3. Quasi-particle code DYWAN. DYWAN[20)] has been optimized by Univ. Nantes for nucleon and charged composite particle production in the 20-200 MeV range. In this code, the quasi-particles can occupy a set of discrete single-particle states, with some probability. The phase space extension of these single-particle states is described with the help of a wavelet basis, in a way which minimizes the loss of information contained in the whole quantal wave-function. Equations of motion for the relevant degrees of freedom have been derived and solved numerically. The code is now in a state which allows a comparison with the measurements of WP1.

2. High energy models and codes (WP8)

1. Intranuclear cascade (INC) code. An enhanced INC code, INCL4, is under construction at the University of Liège and CEA Saclay. Although the previous version, INCL3,[21)] gave reasonable predictions for proton-induced neutron cross-sections and residual mass distributions, the model suffered from some shortcomings: (*i*) it systematically underestimates the intensity of the quasi-elastic peak in neutron spectra (*ii*) it underestimates the cross-section for the production of residues with mass close to the target mass. This was attributed to the neglect of the diffuseness of the nuclear surface in INCL3. Currently, a density distribution with a smooth surface, of the Wood-Saxon type, is taken into account. Some additional new features have been implemented in INCL4: (i) Consistent dynamical Pauli blocking: The baryon-baryon collisions are allowed stochastically according to the estimated occupation of the phase space around the outgoing particles. In addition, the possible final state of a binary collision is checked for the energy content in the original Fermi sphere. This eliminates spurious emission due to the otherwise stochastic treatment of the Pauli blocking, (ii) Improvement of the pion dynamics. The lifetime attributed to the delta particles has been lengthened for small delta mass, reflecting the small decay probability governed by the reduction of the phase space in pion-nucleon channel, (iii) The angular momentum of the remnant is delivered by the code. This offers a microscopic alternative to phenomenological formulae like the one of de Jong et al,[22)] (iv) Inclusion of incident light ions: d, t, ^{3}He, ^{4}He, (v) The stopping time has been revisited. It is still determined by the observed changes of rate in the time variation of the average values of some key physical quantities, like the target

excitation energy. However, the impact parameter and incident energy dependences are considerably weakened when a smooth surface is introduced.

A complete and usable version of INCL4 is under construction.[23] As an example, **Figure 4** shows that the quasi-elastic peak in neutron spectra is satisfactorily reproduced.

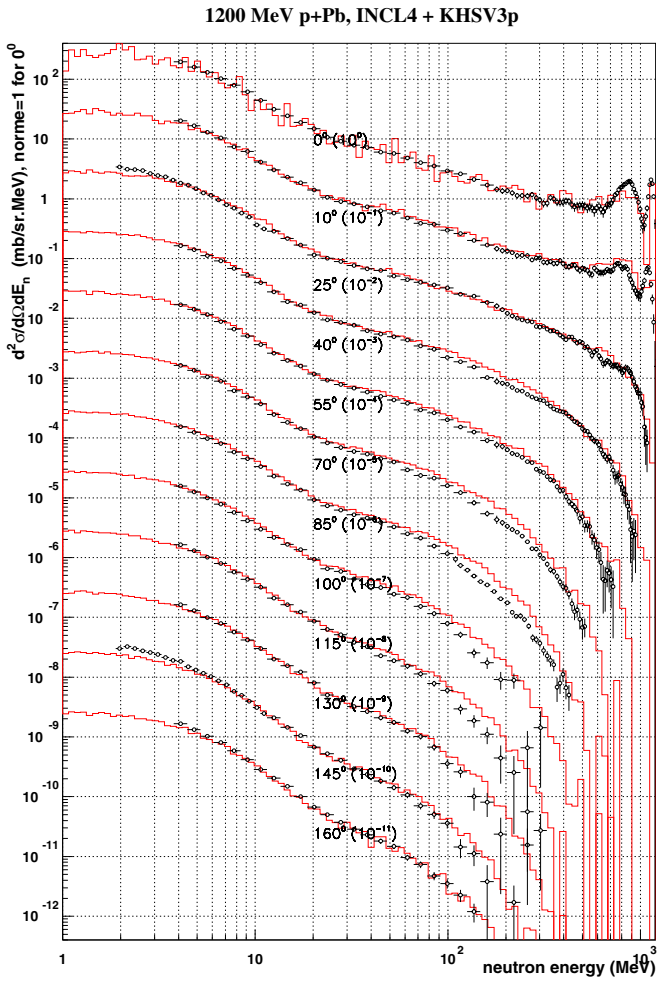

Fig. 4 Neutron production double differential cross-sections for 1200 MeV protons *Pb*. Comparison between the Liège INC model plus the KHSV3p evaporation-fission model (histograms) with the experimental data (dots) of WP5[12]

2. Evaporation code. The latest version of the KHS evaporation code,[24] KHSv3p, has been completed by GSI and CEA Saclay. It differs from the preceeding versions on three points. First, effective barriers for proton and alpha evaporation have been preferred to potential ones in order to account for penetration effects and have been adjusted to reproduce properly the isotopic distributions of residues. Second, the fission barriers have been adjusted from those of Ref.[25] by a factor f_B=0.9 to account for the reduction of the fission barrier with increasing temperature. Finally, dissipative effects are simulated by forbidding fission until some transient time has passed. This model, together with the INCL4 code, satisfactorily describes the residue production data from WP6.

V. Conclusions

The HINDAS project is now well underway. High quality experimental data, representing all important channels (for neutron, light charged particle and residual nuclide production) of proton- and neutron-induced reactions above 20 MeV on Fe, Pb and U are measured and compared with the state-of-the-art nuclear models. Data will be measured at the European facilities that are the best equipped for the reaction under consideration. Theoretical nuclear models will be developed (optical model, pre-equilibrium, fission, direct and statistical models at energies in the 20-200 MeV region; intra-nuclear cascade, fission and evaporation models above 200 MeV) and then benchmarked against the new experimental data. Intermediate energy models will be used to create evaluated data libraries up to 200 MeV, both for incident neutrons and protons, whereas the high energy nuclear models will be implemented in transport codes to generate the necessary cross-sections. The combination of these new high- and low energy transport codes will be probed on macroscopic quantities.

Acknowledgment

HINDAS is a Fifth Framework project supported by the European Commission (EC). We are grateful to Dr. V. Bhatnagar of the EC for his continuous involvement.

References

1) S. Benck et al., *Eur. Phys. J.* **A3**, 149 (1998)
2) S. Dangtip et al., *Nucl. Instrum. Meth. Phys. Res.* **A452**, 484 (2000).
3) J. Klug et al., this conference.
4) R. Michel et al., this conference.
5) Glasser et al., this conference.
6) R. Nolte et al., this conference.
7) M. Gloris et al., *Nucl. Instr Meth. Phys. Res.* **A463**, 593 (2001).
8) H. Schuhmacher et al., *Nucl. Instr Meth. Phys. Res.* **A421**, 284
9) H. Condé et al., *Nucl. Instr Meth. Phys. Res.* **A292**, 121 (1990).
10) V.P. Eismont et al., *Phys. Rev.* **C53** 2911 (1996).
11) A. Letourneau et al., *Nucl. Intrum. Meth. Phys. Res.* **B170**, 299 (2000).
12) X. Ledoux et al., *Phys. Rev. Lett.* **82**, 4412 (1999).
13) W. Wlazlo et al., *Phys. Rev. Lett.* **84**, 5736 (2000).
14) T. Enqvist et al., this conference.
15) A.J. Koning and S. Hilaire, to be published.
16) A.J. Koning and J.P. Delaroche, to be published.
17) Reference Input Parameter Library, *IAEA-TECDOC-1034*, August 1998.
18) R. Michel, private communication, available from the Nuclear Energy Agency; http://www.nea.fr.
19) E. Ramström, this conference.
20) B. Jouault et al., *Nucl. Phys* **A628**, 119 (1998).
21) J. Cugnon, *Nucl. Phys.* **A620**, 475 (1997).
22) M. de Jong et al., *Nucl. Phys.* **A531**, 709 (1991).
23) A. Boudard, J.Cugnon, S. Leray and C. Volant, to be published.
24) A.R. Junghans et al., *Nucl. Phys.* **A629**, 635 (1998).
25) A.J. Sierk, *Phys. Rev.* **C33**, 2039 (1986).

HINDAS - A European project on High- and Intermediate-energy Nuclear Data for Accelerator-driven Systems

The HINDAS collaboration

J.P.M. Beijers[a], J. Benlliure[b], O. Bersillon[c], J. Blomgren[d,§], J. Cugnon[e], P. Eudes[f], D. Filges[g], A. Koning[h], J.-F. Lecolley[i], S. Leray[j], J.-P. Meulders[k,*], R. Michel[l], N. Olsson[d], K.-H. Schmidt[m], H. Schuhmacher[n], I. Slypen[k], H.-A. Synal[o], R. Weinreich[p]

HINDAS partners:

a) Rijksuniversiteit Groningen, the Netherlands
b) Universidade de Santiago de Compostela, Spain
c) Commisariat à l'Energie Atomique, Bruyères-le-Châtel, France
d) Department of Neutron Research, Uppsala University, Sweden
e) Université de Liège, Belgium
f) Subatech, Nantes, France
g) Forschungszentrum Jülich, Germany
h) Nuclear Research and consultancy Group, Petten, the Netherlands
i) LPC, ISMRA and Université de Caen, France
j) Commisariat à l'Energie Atomique, Saclay, France
k) Université Catholique de Louvain, Louvain-la-Neuve, Belgium
l) Zentrum für Strahlenshutz und Radioökologie, Hannover University, Germany
m) Gesellschaft für Schwerionenforschung, Darmstadt, Germany
n) Physikalisch-Technische Bundesanstalt, Braunschweig, Germany
o) Eidgenössische Technische Hochschule, Zürich, Switzerland
p) Paul Scherrer Institute, Villigen, Switzerland

*) Project coordinator
§) Presenter

Abstract

The available commercial reactors as well as fusion research has motivated extensive programs on nuclear data up to 20 MeV. Accelerator-driven transmutation will make use of neutrons up to GeV energies. Although only a minor fraction of the neutrons will be at these high energies, they nevertheless need to be well characterized.

Measuring all relevant data is impossible; even if all existing laboratories on earth would be dedicated to this, it would take centuries. Therefore, the work has to be focused on measuring key data for theory development.

HINDAS – High- and Intermediate-Energy Nuclear Data for Accelerator-Driven Systems – is a European coordinated effort for accomplishing this goal for energies above 20 MeV. The collaboration consists of 16 universities or institutes, whereof 6 laboratories, from seven EU countries. The work is divided into two energy ranges, 20–200 MeV and 200–2000 MeV. In each of these ranges, there are three experimental work packages, on light charged-particle production, neutron production and production of residual nuclei, resp. In addition, there are work packages on data libraries and theory development, making a total of 8 work packages.

HINDAS is coordinated by UCL, Louvain-la-Neuve, Belgium. The total EU funding is about 2 MUSD. To this should be added matching funding, equipment and infrastructure from the participating countries.

1 Introduction

One of the outstanding new developments in the field of Partitioning and Transmutation (P&T) concerns Accelerator-Driven Systems (ADS), which consist of a combination of a high-power, high-energy accelerator, a spallation target for neutron production, and a sub-critical reactor core.

The development of the commercial critical reactors of today motivated a large effort on nuclear data up to about 20 MeV, and presently several million data points can be found in various data libraries. At higher energies, data are scarce or even non-existent. With the development of nuclear techniques based on neutrons at higher energies, there is nowadays a need also for higher-energy nuclear data.

The nuclear data needed for transmutation in an ADS can roughly be divided into two main areas. First, the initial proton beam produces neutrons via spallation reactions. This means that data on proton-induced neutron production is needed. In addition, data on other reactions are needed to assess the residual radioactivity of the target. Second, the produced neutrons can induce a wide range of nuclear reactions, and knowledge of these are useful in the design of an ADS. Among these reactions, some cross sections can be used directly. Examples are elastic scattering for neutron transport, proton and alpha production for assessment of the hydrogen and helium gas production in the target window or core, and fission for obvious reasons.

In most cases, however, direct data determination is not the ultimate goal. The global capacity for such measurements is insufficient to obtain complete coverage of important data. It is even impossible in theory to supply all relevant data. In a reactor core, large quantities of short-lived nuclides affect the performance of the core during operation, but measuring cross sections for these nuclides is impossible because experiment targets cannot be made. A good example is ^{135}Xe, the well-known villain of the Chernobyl disaster, with its half-life of 9 h.

This means that the experimental work must be focused on providing benchmark data for theory development, making it possible to use theoretical models for unmeasured parameters in a core environment.

2 The HINDAS project

HINDAS is a joint European effort, which gathers essentially all European competence on nuclear data for transmutation in the 20–2000 MeV range. The program has been designed to obtain a maximal improvement in high-energy nuclear data knowledge for transmutation. This goal can only be achieved with a well-balanced combination of basic cross section measurements, nuclear model simulations and data evaluations. The three elements iron, lead and uranium have been selected to give a representative coverage of typical materials for construction, target and core, respectively, especially relevant to ADS, as well as a wide coverage of the periodic table of elements.

In total, 16 universities or laboratories participate. Of these, 6 have experimental facilities. This means that HINDAS involves essentially all relevant European laboratories in its energy range. This distribution and coordination of experiments at many laboratories makes the work very efficient. What is noteworthy is that HINDAS involves many partners and even laboratories which have previously not been involved at all in activities on nuclear data for applications. Thus, HINDAS has already widened the field of applied nuclear physics.

HINDAS is coordinated by UCL, Louvain-la-Neuve, Belgium. The total EU funding is about 2 MUSD. To this should be added matching funding, equipment and infrastructure from the participating countries. The coordinator represents the collaboration versus the European Commission. In the internal work, he is assisted by a management committee and a scientific committee.

3 Organization of the research work

The project is carried out in eight work packages (WP). WP 1–3 concerns experiments in the 20–200 MeV range, WP 4–6 deals with 200–2000 MeV experiments, and WP 7 and 8 are devoted to theory for the 20–200 and 200–2000 MeV regions, resp.

The division into two energy ranges is natural, since there appear to be a transition region around 200 MeV for the theoretical models. Below this energy the theoretical calculations have to include direct interactions, as well as preequilibrium, fission and statistical models, whereas at higher energies the intra-nuclear cascade model, together with fission and evaporation models, have to be considered. As a coincidence, the experimental facilities and the measurement techniques are also different below and above about 200 MeV.

The experimental WPs are structured according to type of particles produced. This means that for each energy range, there are WPs on production of light ions, neutrons and residues, resp. Below, the WPs are described in some more detail:

1) Light charged-particle production induced by neutrons or protons between 20 and 200 MeV (Lead contractor: Université Nantes, France).

The double-differential cross sections for proton- and neutron-induced production of hydrogen and helium ions on iron, lead and uranium isotopes is being measured at UCL-Louvain, TSL-Uppsala and KVI-Groningen. These measurements aim at providing essentially complete data in both emission angle and ejectile energy. Such double differential cross sections constitute a very stringent test for theoretical models in this energy domain. In addition, charged-particle multiplicities in proton-induced reactions are measured at KVI.

2) Neutron production induced by neutrons or protons between 20 and 200 MeV (Lead contractor: Uppsala University, Sweden).

Neutron elastic scattering measurements (see the contribution by Klug *et al.* in these proceedings), (p,xn) and (n,xn) measurements on iron, lead and uranium are performed at UCL-Louvain and TSL-Uppsala. Elastic scattering measurements are useful not only for optical model development, but can also be used directly for neutron transport calculations. The (n,n) and (n,xn) measurements make use of novel detection techniques, while (p,xn) reactions are studied using NE213 detectors with time-of-flight techniques.

3) Residual nuclide production induced by neutrons and protons between 20 and 200 MeV and production of long-lived radionuclides (Lead contractor: Hannover University, Germany)

Measurements of proton-induced production of residual nuclei are carried out at PSI,

while neutron-induced production is studied at UCL-Louvain and TSL-Uppsala, where also neutron-induced fission is measured. For the short-lived residual radionuclides, cross sections are determined using activation techniques. The production of long-lived radionuclides is studied by Accelerator-Mass Spectroscopy (AMS) after chemical separation at ETH.

4) Light charged-particle production above 200 MeV (Lead contractor: FZ Jülich, Germany)

The proton- and deuteron-induced production cross sections of protons and alpha particles are measured with a 4π silicon ball detector at the COSY accelerator in Jülich. Experiments on thin targets aim for tests of the intra-nuclear cascade model, while thick-target studies are focused on benchmarking transport codes. These measurements will also help to evaluate gas production in the window and structure materials of an ADS, which will give implications for the lifetime of such components. With the PISA setup, it will also be possible to measure total and double-differential cross sections for production of spallation products.

5) Neutron production induced by protons above 200 MeV in thin and thick targets (Lead contractor: CEA-Saclay, France)

Double-differential neutron production cross sections, for both thin and thick targets, have recently been measured at CEA-Saclay using time-of-flight or magnetic spectrometer techniques. At FZ Jülich, multiplicities of neutrons up to 150 MeV are being studied event-wise with a 4π liquid scintillator, using both thin and thick targets. The two experiments are complementary, both for technical and physics reasons. E.g., comparisons can be made between the directly measured multiplicities with those inferred from integration of the double-differential data.

6) Residual nuclide production above 200 MeV in inverse kinematics (Lead contractor: GSI, Germany)

Proton- and deuteron-induced nuclide production is measured in inverse kinematics, i.e., a lead or uranium beam hits a liquid hydrogen or deuterium target, and the spallation products are identified in flight using a high-resolution magnetic spectrometer. In this way all spallation products, irrespective of half-life, can be measured. These new data will be useful when calculating the radioactive inventory, the radiotoxicity and the breeded impurities in a realistic spallation target of an ADS.

7) Nuclear data libraries and related theory (Lead contractor: NRG, Netherlands)

This work package concerns nuclear model calculations for analysis of the experimental data provided by WP 1–3, i.e., between 20 and 200 MeV. Special emphasis will be put on providing as complete information as possible on cross sections for all possible outgoing channels of iron, lead and uranium, and to construct improved nuclear data libraries, extending to 200 MeV.

8) High energy models and codes (Lead contractor: Université de Liège, Belgium)

This work package is devoted to theory for WP 4–6, i.e., above 200 MeV, and regards mainly intra-nuclear cascade models and evaporation and fission models. The main objective is the development of powerful and accurate tools to calculate nucleon-nucleus spallation reactions.

4 Dissemination of results

All results will be published in regular refereed physics journals. In addition, all relevant data will be implemented into the regular nuclear data bases. Continuous contacts are kept with nuclear data evaluators; in fact some of the collaboration members are also established data evaluators themselves.

5 Collaboration with other EU projects

Two other EU projects deal with aspects of nuclear data for transmutation, the NTOF-ND-ADS project at CERN and MUSE in Cadarache. These two projects are primarily devoted to lower energies. The three data-related projects are clustered as a sub-group, BASTRA (Basic STudies on TRAnsmutation), of a wider cluster linking all EU projects on P&T.

6 Summary

HINDAS is a joint European effort, which gathers essentially all European competence on nuclear data for transmutation in the 20–2000 MeV range. It contains a combination of basic cross section measurements, nuclear model simulations and data evaluations on iron, lead and uranium. In total, 16 universities or laboratories participate, whereof 6 have experimental facilities. This means that HINDAS involves essentially all relevant European laboratories in its energy range.

NEUTRONS FOR SCIENCE AND INDUSTRY - THE UPPSALA NEUTRON BEAM FACILITY

C. Johansson[a], J. Blomgren[a], A. Ataç[a], B. Bergenwall[a], S. Dangtip[a], K. Elmgren[a], J. Klug[a], N. Olsson[a], S. Pomp[a], A. Prokofiev[a], U. Tippawan[a], O. Jonsson[b], L. Nilsson[b], P.-U. Renberg[b], P. Nadel-Turonski[c], C. Le Brun[d], J.F.Lecolley[d], F.R. Lecolley[d], M. Louvel[d], N. Marie[d], C. Varignon[d], Ph. Eudes[e], F. Haddad[e], M. Kerveno[e], T. Kirchner[e], C. Lebrun[e], L. Stuttgé[f], I. Slypen[g]

[a] *Department of Neutron Research, Uppsala University, Sweden*
[b] *The Svedberg Laboratory, Uppsala University, Sweden*
[c] *Department of Radiation Sciences, Uppsala University, Sweden*
[d] *LPC, ISMRA et Université de Caen, CNRS/IN2P3, France*
[e] *SUBATECH, Université de Nantes, CNRS/IN2P3, France*
[f] *IReS, Strasbourg, France*
[g] *Institute de Physique Nucleaire, Université Catholique de Louvain, Belgium*

Abstract

A number of new applications involving high-energy neutrons have emerged over the last few years. Among these are the development of spallation sources, accelerator-driven systems (ADS) for transmutation of nuclear waste, fast-neutron cancer therapy, as well as dose effects for airflight personnel and electronics failures due to cosmic-ray neutrons.

To meet the requirements from these applications, a wide programme on neutron-induced cross section measurements is running at the $20-180$ MeV neutron beam facility at the The Svedberg Laboratory, Uppsala. Two new multi-purpose experimental devices have recently been installed; SCANDAL (SCAttered Nucleon Detection AssembLy), primarily intended for neutron elastic scattering, but also useful for (n,p) reaction studies, and MEDLEY, aiming at studies of charged-particle production, ranging from protons to alpha particles.

SCANDAL is used for a series of experiments to provide data for optical model analysis, with C, Ca, Fe, Zr and Pb as first targets. MEDLEY is used to measure charged-particle production in light nuclei (C, N, O) for use in dosimetry and neutron therapy, as well as in heavy nuclei (Fe, Pb, U) for ADS systems. Ion production in silicon will also be important for modeling of single-event upsets in electronics.

In addition to the studies with SCANDAL and MEDLEY, fast fission cross sections are measured, as well as cross sections for production of residual activity in a wide range of nuclei. Such data are of importance in, e.g., ADS, astrophysics, etc.

Most of the ADS-relevant measurements performed in Uppsala are part of the EC supported HINDAS project. A number of projects have been performed within ISTC.

Besides fundamental cross section measurements, the neutron beam is used to test and calibrate dosemeters, as well as to verify the sensitivity of various electronic circuits to neutron irradiation. Several national radiation institutes and commercial electronics companies are involved in such activities.

From our experiences, we conclude that a new, dedicated facility for production of intermediate-energy neutrons, to be used solely for applications of the mentioned type, is well motivated.

1 Introduction

Recently, a large number of applications involving high-energy (20 MeV) neutrons have become important. Transmutation - the subject of this conference - is an obvious example, but also fast-neutron cancer therapy, dose effects for airflight personnel due to cosmic-ray neutrons, as well as electronics failures induced by the same cosmic-ray neutron flux have all got increasing attention.

This has led to intense experimental activities. Briefly, this can be divided into two main categories: measurements of nuclear data, and direct testing. Of these, nuclear data measurements is the largest activity, while the in-beam testing of electronics circuits is presently smaller, but rapidly growing.

2 The neutron beam facility

2.1 Neutron production

At the neutron facility at the The Svedberg Laboratory (TSL), Uppsala, Sweden [1] (see fig. 1), almost monoenergetic neutrons are produced by the reaction ^{7}Li(p,n)^{7}Be in a target of 99.98 % ^{7}Li. After the target, the proton beam is bent by two dipole magnets into an 8 m concrete tunnel, where it is focused and stopped in a well-shielded carbon beam-dump. A narrow neutron beam is formed in the forward direction by a system of three collimators, with a total thickness of more than four metres.

The energy spectrum of the neutron beam is shown in fig. 2. About half of all neutrons appear in the high-energy peak, at about 2 MeV below the incident proton energy, while the rest are roughly equally distributed in energy, from the maximum energy and down to zero. The thermal contribution is small. The low-energy tail of the neutron beam can be reduced by time-of-flight measurements (see fig. 2). With a proton beam of 5 μA onto a 4 mm lithium target, the total neutron yield in the full-energy peak at the experimental position, 8 m from the production target, is about $5 \cdot 10^4$ cm^{-2}s^{-1}. The energy resolution of the full-energy peak depends on the choice of lithium target thickness. For most experiments a resolution of about 1 MeV (FWHM) has been selected.

2.2 Base equipment

Two major experimental setups are semi-permanently installed. These are the MEDLEY detector telescope array, housed in a scattering chamber and operated in vacuum (see fig. 3). At the exit of this chamber, a 0.1 mm stainless steel foil terminates the vacuum system, and from here and on the neutrons travel in air. Immediately after MEDLEY follows SCANDAL (SCAttered Nucleon Detection AssembLy), a setup designed for large-acceptance neutron and proton detection (see fig. 4).

2.3 Monitoring

Absolute normalization of the neutron flux is a notorious problem in all high-energy neutron-beam applications. For direct neutron monitoring, fission counters are available, which have been calibrated relative to *np* scattering, allowing an uncertainty of no more than 5 % [2].

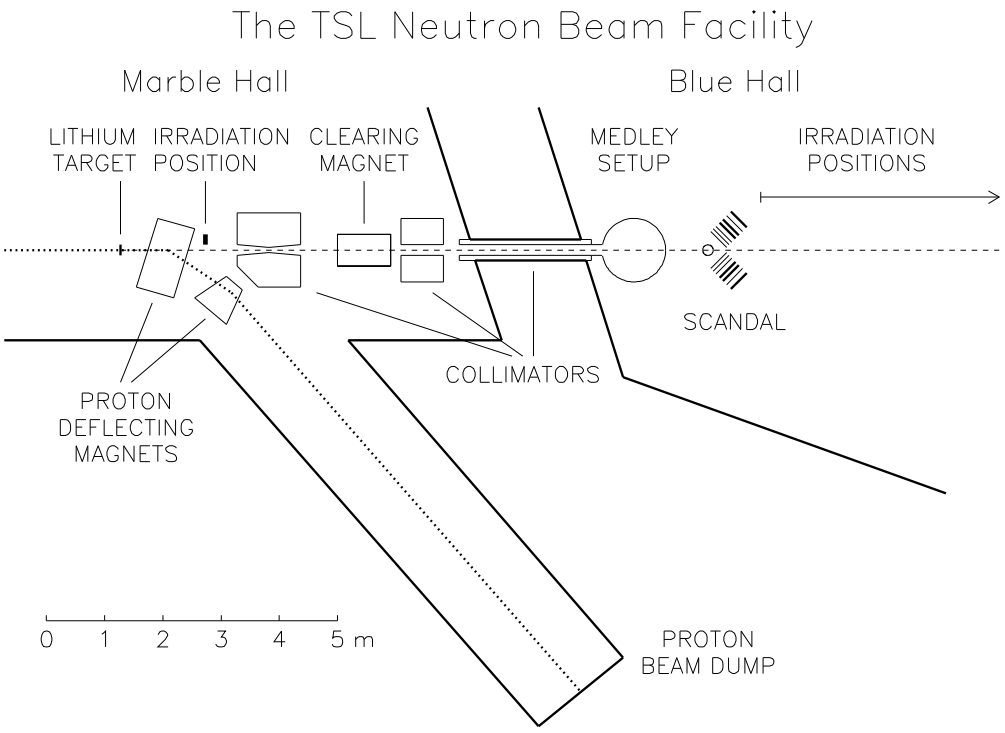

Figure 1: The TSL neutron beam facility.

Relative monitoring can be provided by many different means. Charge integration of the primary proton beam is one of the standard techniques. In addition, for most of the experiment periods, many different experiments (up to seven so far) can be running simultaneously, and then it is common to use signals from the other experiments as relative monitors.

3 Nuclear data for applications

3.1 Transmutation

Almost all proposed transmutation techniques involve high-energy neutrons created in proton-induced spallation of a heavy target nucleus. Therefore, the neutron spectrum in a transmutation core will contain one significant difference compared to present reactors: the presence of neutrons at very high energies. The nuclear data libraries developed for reactors of today go up to about 20 MeV, which covers all available energies for that

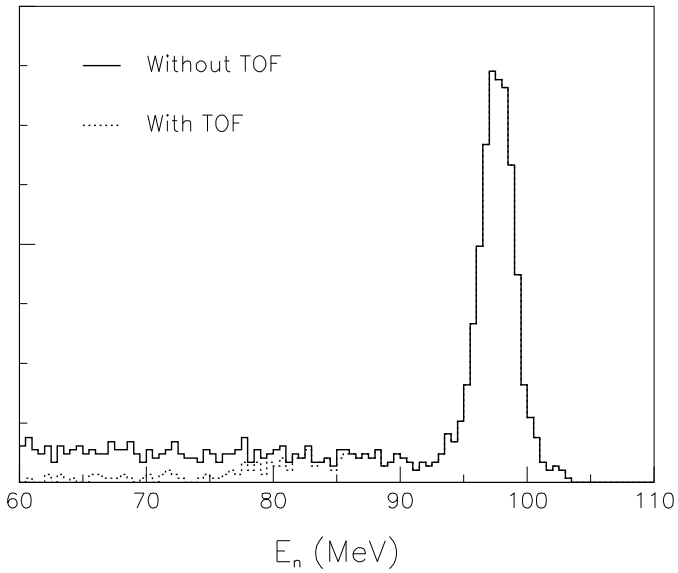

Figure 2: The neutron energy spectrum with and without time-of-flight rejection of low-energy neutrons.

application, but with a spallator coupled to a core, neutrons with energies up to 1-2 GeV will be present. Although a large majority of the neutrons will be below 20 MeV, the relatively small fraction at higher energies still has to be characterized. Spallation results in neutron spectra with an intensity distribution roughly like $1/E_n$. The small number of neutrons at very high energies make such data not being as important as mid-range data. Above about 200 MeV direct reaction models assuming a single interaction (impulse approximation) works reasonably well, while at lower energies nuclear distortion plays a non-trivial role. This makes the $20 - 200$ MeV region the most important for new data.

Very little high-quality neutron-induced data exist in this domain. Only the total cross section and the (n,p) reaction has been investigated extensively. There are high-quality neutron total cross section data on a series of nuclei all over this energy range. In addition, there are (n,p) data in the forward angular range at modest excitation energies available at a few energies and for a rather large number of nuclei.

Today, several groups are working at TSL on transmutation-related cross sections. Neutron elastic scattering is being studied with the SCANDAL setup (see the contribution by Klug *et al.* in these proceedings, and sect. 4.1). Hydrogen and helium production is measured with a combination of SCANDAL and MEDLEY, residue production by activation techniques, and fast-neutron fission by thin-film breakdown counters and ionization chambers.

3.2 Medical applications

Cancer treatment with fast neutrons is performed routinely at several facilities around the world, and today it represents the largest therapy modality besides the conventional treatments with photons and electrons. For a review of this field, see e.g. ref. [3].

The interaction of neutrons with tissue is very complex, and to a large extent unknown.

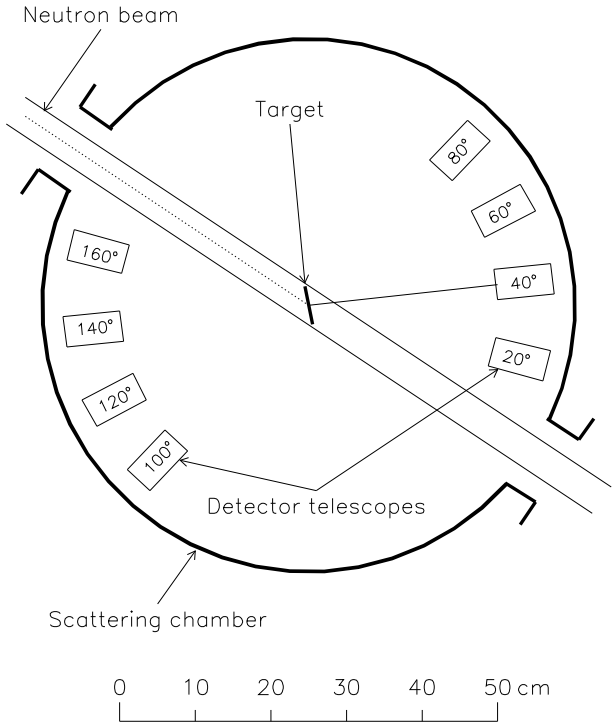

Figure 3: The MEDLEY facility, showing the scattering chamber and the eight telescopes.

Thus, the existing methods and techniques employed are based on experience, rather than on knowledge on fundamental physics. Because of the recent development of neutron beams with good intensity and energy resolution, it is today possible to study all the processes involved in detail, and thus dramatically improve the dose and radiation quality planning in connection with tumour therapy. The neutron facility at the The Svedberg laboratory (TSL) in Uppsala has unique properties in this respect.

In the commonly used energy range (up to about 70 MeV), it is unfortunately difficult to describe nuclear processes theoretically in a simple way, and in addition, the data base is meagre. In this energy region, compound nuclear processes, direct processes and intermediate or pre-compound processes are important and nuclear reaction models must take into account all these processes and, where appropriate, the competition between them. Most of the evaluated databases were compiled to be used in the development of nuclear fission and fusion energy sources and do therefore have a 20 MeV upper energy limit. The lack of extensive data bases at higher energies makes it difficult to estimate correctly the dose given by the neutron beam and to plan and optimize the radiation therapy.

A substantial improvement in the knowledge of fundamental nuclear data is therefore needed for a better understanding of the processes occuring on a cellular level. Besides the applications in cancer treatment, the same data will improve the understanding of fast neutron dosimetry for radiation protection purposes, e.g. for a future transmutation facility. In addition, neutron dosimetry problems for airplane crew have recently received widespread attention (see sect. 4.7).

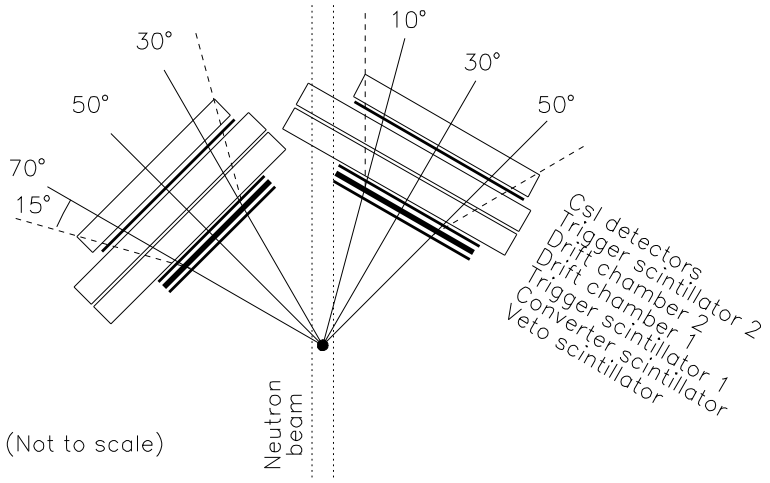

Figure 4: Schematic figure of the SCANDAL setup.

3.3 Fundamental physics

The TSL neutron beam facility has now been running for about a decade. The main activity up to now has been studies of the (n,p) reaction at about 100 MeV on a series of nuclei ranging from ^{9}Be to ^{208}Pb [4, 5, 6, 7, 8, 9, 10, 11], and *np* scattering at 96 and 162 MeV [12, 13, 14, 15].

Although carried out for other reasons, these fundamental studies have important consequences for applications. The (n,p) data on nuclei give partial contributions to code developments for transmutation core design. The *np* scattering cross section has been used to normalize other neutron-induced data, and thus a precise knowledge of this cross section is important also for applications.

Recently, the *np* scattering cross section in this energy range has been under intense debate, motivated by the Uppsala results presented in fig. 5, which are steeper at backwards angles than the bulk of previously published data. This is clearly illustrated by a comparison with the partial-wave analyses represented by the lines in the figure; the analyses are fits to the older data.

This discrepancy does not only influence the normalization of nuclear data for applications, but it is also of great fundamental importance, because *np* scattering data are being used for determinations of the pion-nucleon coupling constant, i.e. the absolute strength of the strong interaction in the nuclear sector. This coupling constant is of great relevance not only to basic nuclear physics, but also on a cosmological scale. Its strength governs the properties of the deuteron to a very high degree. If all other nucleon-nucleon potential information were known, the value of it could be determined very accurately, because then a difference of only a few percent in its value would be sufficient to either unbind the deuteron or to produce a bound diproton, in both cases with major consequences for the world as we know it.

These issues have motivated a critical re-examination of the entire *np* data situation [16]. A workshop was recently held in Uppsala in to address these problems [17]. New experiments are underway to resolve the discrepancy [18, 19].

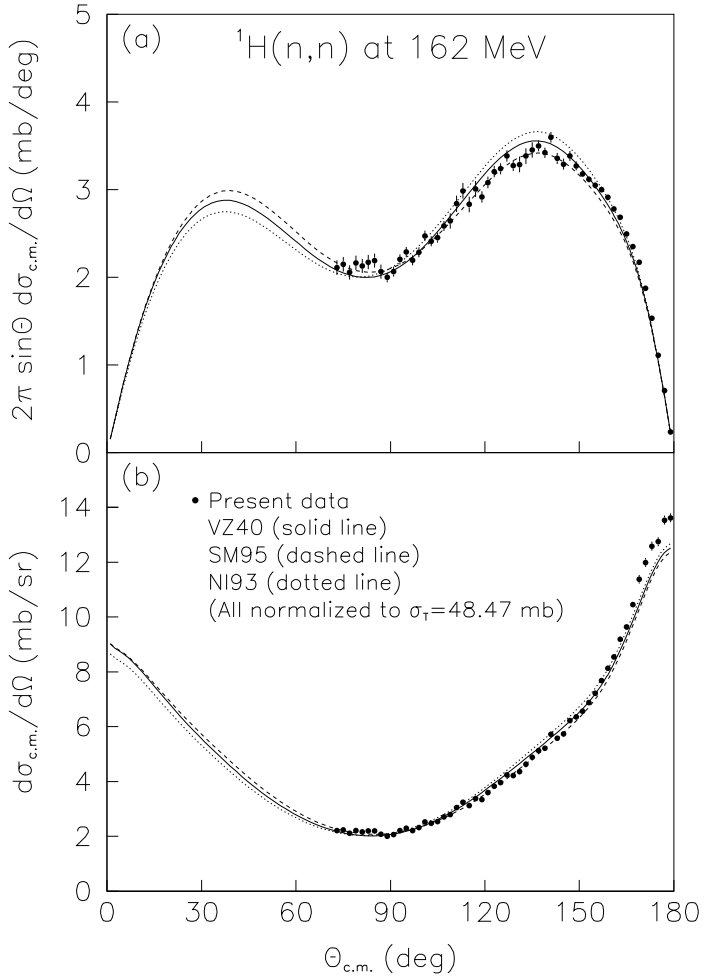

Figure 5: *np* scattering at 162 MeV.

4 Research programme

4.1 Elastic neutron scattering

Elastic neutron scattering is of utmost importance for a vast number of applications. Besides its fundamental importance as a laboratory for tests of isospin dependence in the nucleon-nucleon, and nucleon-nucleus, interaction, knowledge of the optical potentials derived from elastic scattering come into play in virtually every application where a detailed understanding of nuclear processes are important.

After thorough investigation, we have arrived at the conclusion that for transmutation purposes, neutron elastic scattering is the single most important intermediate-energy quantity still to be measured. There are several reasons for this, the most important being that it allows a determination of the optical potential, which plays a role in every calculation including neutrons in either the entrance or exit channel. The elastic cross section is also the largest of the individual partial cross sections contributing to the total cross section. In fact, a consequence of the optical model is that the elastic cross section must be at least half the total cross section.

Given the time and cost to carry out such experiments, the main focus must be on

developing theoretical models rather than systematically measuring all nuclei. The obvious nuclei to study are then the magic or semi-magic nuclei, i.e. ^{12}C, ^{16}O, ^{40}Ca, ^{90}Zr and ^{208}Pb. Here it is fortunate that lead and zirconium are also important materials in future transmutation facilities, and carbon, oxygen and calcium are all of medical relevance, so the gain is twofold. Besides the elements above, H(n,n) is being studied for normalization purposes. Important materials for transmutation cores, like iron, chromium, bismuth, thorium and uranium are planned to be investigated in a second phase.

Elastic neutron scattering is important also for fast-neutron cancer therapy, because the nuclear recoils account for 10–15 % of the dose. For a detailed description of the elastic neutron scattering project, we refer to the contribution to this conference by Klug *et al.*

4.2 Neutron production

Recently, a programme to measure the cross section for neutron-induced emission of neutrons, i.e. the (n,xn') reaction, has started at TSL. Of the total cross section, elastic neutron scattering is responsible for about half, and alpha production accounts for about 10%, while the rest is due to proton production and inelastic neutron scattering to roughly equal fractions. Inelastic neutron scattering is the last of these reactions to be measured. this is not surprising, because it poses outstanding experimental challenges. The technique will be to use a modified version of SCANDAL (sse below), equipped with a number of passive converters, for high-energy particles, and time-of-flight measurements for low energies [20].

4.3 Charged-particle production

About half the dose in fast-neutron cancer therapy comes from np scattering, 10-15 % from elastic neutron scattering and the remaining 35-40 % from neutron-induced emission of charged particles, such as protons, deuterons, tritons, ^{3}He- and α-particles. Double-differential cross sections for all these reactions in tissue-relevant nuclei, i.e., carbon, nitrogen, oxygen and calcium, are to be measured with the MEDLEY setup in an energy region of greatest relevance for fast neutron therapy, i.e., up to $70 - 100$ MeV [21].

Although intended for medical purposes, the requirements from these led to a multi-purpose detector design, which has turned out to be useful for many different applications. One of these is hydrogen and helium production in a transmutation environment. Besides the use of proton and alpha production data for benchmarking of precompound models, direct use of the data can provide limits on hydrogen and helium production, which has to be kept under control because of safety concerns and material embrittlement.

To study proton production for transmutation applications, MEDLEY and SCANDAL have been used together. A combination of the two setups allows for good statistics at all energies and angles. Experiments on lead and iron are already under analysis, and experiments on uranium are underway.

The MEDLEY detector array consists of eight particle telescopes, placed at $20 - 160$ degrees with 20 degrees separation. Each telescope is a $\Delta E - \Delta E - E$ detector combination, with sufficient dynamic range to distinguish all charged particles from a few MeV up to maximum energy, i.e., about 100 MeV. All the equipment is housed in a 100 cm diameter scattering chamber, so that the charged particles can be transported in vacuum.

The SCANDAL setup has two identical arms which together covers 0 – 70 degrees in the lab system. Each arm consists of a removable veto scintillator, a neutron-to-proton converter scintillator, two trigger scintillators, two drift chambers for proton tracking, and an array of CsI detectors for energy determination. When operated in neutron mode, the veto scintillators reject charged particles, and when used for proton production measurements, the vetos are removed.

4.4 Radiation damage of materials

So far, the knowledge on radiation damage in materials has been based on empirical studies in existing reactors, and the underlying mechanisms are not very well known. Two types of damages seem to occur due to reactor-energy neutrons, swelling and cracking. A future transmutation facility with a high flux of high-energy neutrons might be subject to severe radiation damage which cannot be assessed beforehand. In order to correctly understand the processes behind radiation damage and build a working theory model, it is necessary to have better neutron cross section data. These data are elastic neutron scattering, inelastic neutron scattering, and charged particle (mainly alpha and proton) production.

4.5 Fast-neutron fission

Although the main fission power in a transmutation facility arise from neutrons at lower energies, the high-energy neutron fission gives significant contributions to the power released, and to the residual activity created. Very little data exist on high-energy fission, but the situation is under rapid improvement. This can be exemplified by ongoing work at the TSL neutron beam [22].

4.6 Residue production

Production of residual nuclei in neutron-induced nuclear reactions are studied by activation techniques [23]. These experiments are carried out at two target locations. Besides placing the targets to be irradiated in the experiment hall, a second target station has been installed in the neutron production hall, much closer to the neutron production target, thereby allowing higher flux.

4.7 Neutron-induced electronics failures

Recently, the importance of cosmic radiation effects in aircraft electronics has been highlighted. (For reviews, see e.g. refs. [24, 25] and references therein.) When an electronic memory circuit is exposed to particle radiation, the latter can cause a flip of the memory content in a bit, which is called a single-event upset (SEU). This induces no hardware damage to the circuit, but evidently, unwanted re-programming of aircraft computer software can have fatal consequences. As components become smaller, the problem increases, and in the near future SEU might become a major computer reliability concern.

At flight altitudes, as well as at sea level, the cosmic ray flux is dominated by neutrons and muons. The latter do not interact strongly with nuclei, and therefore neutrons are most important for SEU.

Since neutrons have no charge, they can only interact via violent, nuclear reactions, in which charged particles are created, that occasionally induce an SEU. Thus, knowledge of the nuclear interaction of neutrons with silicon is needed to obtain a full understanding of

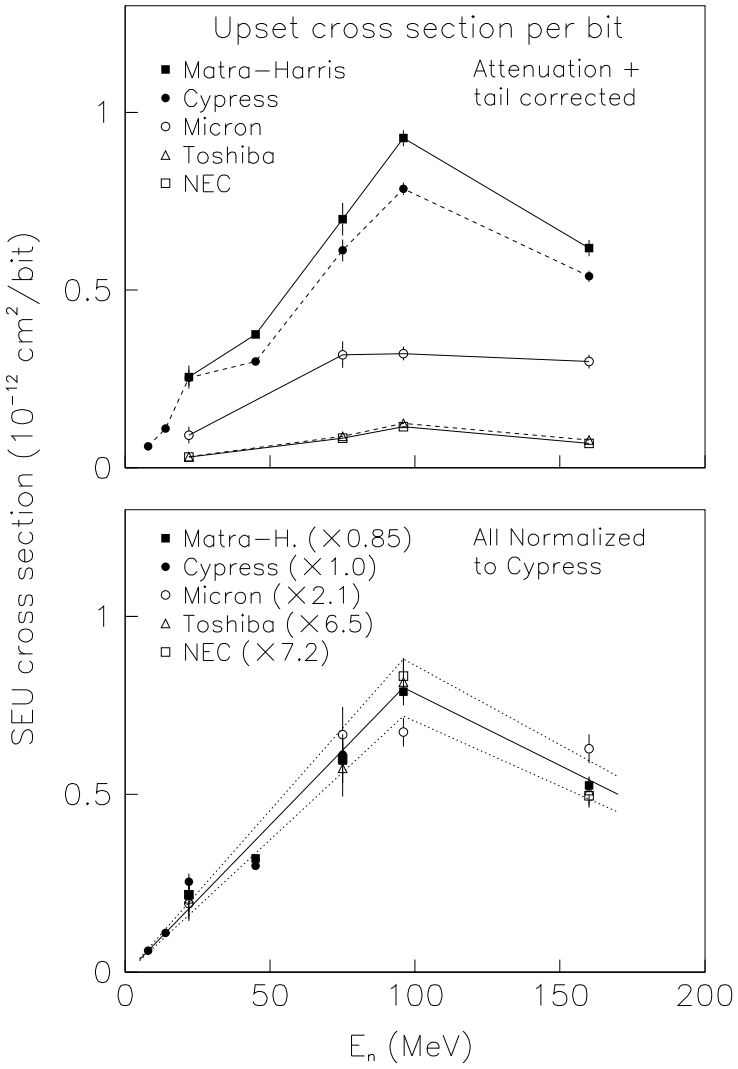

Figure 6: The energy dependence of the SEU cross section for a few devices. See the text for details.

the SEU problem. Firm experimental information about neutron-induced cross sections is very scarce. Thus, one has had to rely heavily on calculations based on nuclear models, which have a poor and essentially unknown precision. Measurements of neutron-induced charged particle-production cross sections are therefore of utmost importance for a full understanding of the SEU problem in aviation electronics.

If the neutron-induced charged-particle production cross sections were known, and thus the energy deposition on a microscopic level, it might be possible to calculate the SEU rate with reasonable precision also for any future components. Up to now, direct in-beam component testing has been carried out to characterize the effect, especially its neutron energy dependence [26, 27].

As can be seen in the upper panel of fig. 6, the upset cross section rises slowly with neutron energy for all devices tested, up to a maximum at about 100 MeV. It is notable that the most modern components (Matra-Harris and Cypress) are the most sensitive. This is because they use less charge to represent a digit, thereby making the component

faster, but also more sensitive to this kind of perturbation. In the lower panel, all data have been normalized to the same relative rate, to illustrate that the energy dependence is very similar for all of them.

Already from these simple measurements, important conclusions about the origin of the effect can be drawn. The fact that the rise is rather slow seems to indicate that heavy ions are primarily responsible. If the effect were mostly due to protons or alpha particles, the cross section should peak at a much lower energy.

There are plans to develop these studies further by measuring cross sections for production of light charged particles and light heavy ions. For the light particles, the MEDLEY setup (see above) should be used. For light heavy ions, major modifications will probably be needed because of the very short range of the ejectiles.

4.8 Dosimetry research

Nuclear data measurements for dosemeter modelling are to be carried out using the SCANDAL and MEDLEY setups. In addition, direct testing of existing dosemeters are regularly undertaken, involving national radiation protection institutes from a number of European countries. The large number of simultaneous users has been a great asset in this research, because it has provided good normalization possibilities, but also interdisciplinary collaboration. A good example of the latter is the development of dosemeters based on fission in bismuth, which has benefitted very much on the fast-fission programme.

5 Summary

The quasi-monoenergetic 20 – 180 MeV neutron beam at the The Svedberg Laboratory (TSL), Uppsala, Sweden, has been - and will be - used to provide data for a large number of applications. These involve transmutation, fundamental physics, medicine, dosimetry and electronics effects. The comparatively high flux, good energy resolution, precise monitoring and easy access to the beam has resulted in a large user community (presently about 70 users from about 10 countries). Two major multi-purpose experiment setups, MEDLEY and SCANDAL, are available, as well as a magnetic spectrometer (LISA).

The largest research programmes involve studies of elastic neutron scattering, neutron-induced light ion production, fast-neutron fission and in-beam testing of electronics devices.

This work was financially supported by Vattenfall AB, Swedish Nuclear Fuel and Waste Management Company, Swedish Nuclear Power Inspectorate, Barsebäck Power AB, Swedish Defence Research Agency, Swedish Cancer Society, EU, and Swedish Natural Science Research Council.

References

[1] H. Condé, *et al.*, Nucl. Instr. Meth. **A292** (1990) 121.

[2] A. Prokofiev, *et al.*, TSL report, TSL/ISV-99-0203.

[3] M. Tubiana, J. Dutreix and A. Wambersie, Introduction to Radiobiology, (Taylor & Francis, 1990).

[4] H. Condé, *et al.*, Nucl. Phys. **A545** (1992) 785.

[5] N. Olsson, *et al.*, Nucl. Phys. **A559** (1993) 368.

[6] T. Rönnqvist, *et al.*, Nucl. Phys. **A563** (1993) 225.

[7] A. Ringbom, *et al.*, Nucl. Phys. **A617** (1997) 316.

[8] S. Dangtip, *et al.*, Nucl. Phys. **A677** (2000) 3.

[9] N. Olsson, Nucl. Phys. News **5** (1995) 28.

[10] N. Olsson, Nucl. Phys. **A599** (1996) 185c.

[11] J. Blomgren, Proceedings from International Symposium on New Facet of Spin Giant Resonances in Nuclei, Tokyo, 1997, p. 70.

[12] T. Rönnqvist, *et al.*, Phys. Rev. C **45** (1992) R496.

[13] T.E.O. Ericson, *et al.*, Phys. Rev. Lett. **75** (1995) 1046.

[14] J. Rahm, *et al.*, Phys. Rev. C **57** (1998) 1077.

[15] J. Rahm, *et al.*, Phys. Rev. C **63** (2001) 044001.

[16] J. Blomgren, N. Olsson, J. Rahm, Phys. Scr. **T87** (2000) 33.

[17] Workshop on "Critical Points in the Determination of the Pion-Nucleon Coupling Constant", Uppsala, June 7-8, 1999. Proceedings published in Phys. Scr. **T87** (2000), ed. J. Blomgren.

[18] C. Johansson, *et al.*, to be published.

[19] T. Peterson, *et al.*, Nucl. Phys. **A 663 & 664** (2001) 1057c.

[20] J. F. Lecolley, *et al.*, TSL proposal (2000).

[21] S. Dangtip, *et al.*, Nucl. Instr. Meth. **A452** (2000) 484.

[22] V.P. Eismont, *et al.*, Phys. Rev. C **53** (1996) 2911.

[23] R. Michel, *et al.*, Nucl. Instr. Meth. **B129** (1997) 153.

[24] J.F. Ziegler, IBM J. Res. Develop. **40** (1996) 19.

[25] H.H.K. Tang, IBM J. Res. Develop. **40** (1996) 91.

[26] K. Johansson, *et al.*, IEEE transactions on Nuclear Science I **45** (1998) 2195.

[27] K. Johansson, *et al.*, IEEE transactions on Nuclear Science I **46** (1999) 1427.

SCANDAL - A facility for elastic neutron scattering studies in the 50–130 MeV range

J. Klug[a], J. Blomgren[a], A. Ataç[a], B. Bergenwall[a], S. Dangtip[a], K. Elmgren[a,b], C. Johansson[a], N. Olsson[a,b], S. Pomp[a], A. Prokofiev[a,c], U. Tippawan[a], O. Jonsson[c], L. Nilsson[c], P.-U. Renberg[c], P. Nadel-Turonski[d], C. Le Brun[e], J.F. Lecolley[e], F.R. Lecolley[e], M. Louvel[e], N. Marie[e], C. Varignon[e], Ph. Eudes[f], F. Haddad[f], M. Kerveno[f], T. Kirchner[f], C. Lebrun[f], L. Stuttgé[g], I. Slypen[h]

[a]Department of Neutron Research, Uppsala University, Sweden
[b]Swedish Defence Research Agency (FOI), Stockholm, Sweden
[c]The Svedberg Laboratory, Uppsala University, Sweden
[d]Department of Radiation Sciences, Uppsala University, Sweden
[e]LPC, ISMRA et Université de Caen, CNRS/IN2P3, France
[f]SUBATECH, Université de Nantes, CNRS/IN2P3, France
[g]IReS, Strasbourg, France
[h]Institute de Physique Nucleaire, Université Catholique de Louvain, Belgium

1 Introduction

A facility for detection of scattered neutrons, SCANDAL (SCAttered Nucleon Detection AssembLy), has recently been installed at the 20–180 MeV neutron beam facility of The Svedberg Laboratory (TSL) in Uppsala, Sweden. It is primarily intended for studies of elastic neutron scattering, but can be used for the (n,p) and (n,d) reactions as well. The energy interval for detected neutrons is 50–130 MeV, which makes the setup suitable for studies of transmutation-related cross sections.

1.1 Nuclear data for transmutation

As transmutation techniques involve high-energy neutrons created in proton-induced spallation of a heavy target nucleus, the neutron spectrum in a transmutation core will contain one significant difference compared to standard nuclear reactors: the presence of neutrons at much higher energies. The nuclear data libraries developed for reactors of today go up to about 20 MeV, which covers all available energies for that application; but with a spallator coupled to a core, neutrons with energies up to 1–2 GeV will be present. Although a large majority of the neutrons will be below 20 MeV, the relatively small fraction at higher energies still has to be characterized. Spallation results in neutron spectra with an intensity distribution roughly like $1/E_n$. The small number of neutrons at very high energies, say above 200 MeV, make such data not being as important as mid-range data. Above 200 MeV, direct reaction models based on the free interaction (impulse approximation) work reasonably well, while at lower energies nuclear distortion plays a non-trivial role. This makes the 20–200 MeV region the most important for new data.

Very little high-quality neutron-induced data exist in this domain. Only the total cross section [1] and the (n,p) reaction has been investigated extensively [2, 3]. There are high-quality neutron total cross section data on a series of nuclei all over this energy range. In addition, there are (n,p) data in the forward angular range at modest excitation energies available at a few energies and for a rather large number of nuclei.

Besides this, there are data on neutron elastic scattering from UC Davis at 65 MeV on a few nuclei [4]. Programmes to measure neutron elastic scattering have been proposed or begun at Los Alamos [5] and IUCF [6], with the former resulting in a thesis on data in the 5–30° range on a few nuclei [5]. The design of SCANDAL has been inspired by the latter two projects.

1.2 Why elastic scattering?

For transmutation purposes, neutron elastic scattering is the single most important intermediate-energy quantity that remains to be measured. There are several reasons for this, the most important being that it allows a determination of the optical potential, which plays a role in every microscopic calculation including neutrons in either the entrance or exit channel. In addition, the elastic cross section is also the largest of the individual partial cross sections contributing to the total cross section. In fact, a consequence of the optical model is that the elastic cross section must constitute at least half the total cross section. Thus, enhanced data on elastic scattering will improve the understanding of neutron transport in a spallation target, as well as fast neutron dosimetry for radiation protection purposes.

In addition, elastic cross sections are the most important partial cross sections needed to assess radiation damage due to high-energy neutrons. Investigations along this line are planned.

Given the time and cost to carry out elastic scattering experiments, the main focus must be on developing theoretical models rather than systematically measuring all nuclei. The obvious nuclei to study are then the magic or semi-magic nuclei, i. e. ^{12}C, ^{16}O, ^{40}Ca, ^{90}Zr and ^{208}Pb. Here it is fortunate that lead and zirconium are also important materials in future transmutation facilities, and carbon, oxygen and calcium are all of direct medical and dosimetric relevance, so the gain is twofold. Besides the elements above, H(n,n) will be studied for normalization purposes. Important materials for transmutation cores, like iron, chromium, bismuth, thorium and uranium might be investigated in a second phase.

In addition to the elastic scattering measurements to be done, there is an ongoing project with groups from Caen and Nantes in France and Louvain-la-Neuve in Belgium, to measure (n,xp) reactions at 100 MeV at the neutron beam in Uppsala.

1.3 Elastic scattering for other applications

Elastic scattering is a common denominator for transmutation and several other applications. One example is fast-neutron cancer therapy, where 10–15 % of the dose comes from elastic neutron scattering, ~50 % from *np* scattering, and the remaining part from neutron-induced emission of charged particles, such as protons, deuterons, tritons, ^{3}He- and α-particles. Double-differential cross sections for all these reactions in tissue-relevant nuclei, i. e. carbon, nitrogen, oxygen and calcium, are to be measured with another setup at TSL, called MEDLEY. This will be done in an energy region of greatest relevance for fast neutron therapy; i. e., up to 70–100 MeV [7, 8].

Although these investigations were originally motivated by fast-neutron cancer therapy, they also have transmutation applications. At possible future spallation facilities, these are the most important processes when it comes to health-related radiation effects for the personnel.

Recently, the importance of cosmic radiation effects in aircraft electronics has been

highlighted. (For reviews, see e.g. refs. [9, 10] and references therein.) When an electronic memory circuit is exposed to particle radiation, the latter can cause a flip of the memory content in a bit, which is called a single-event effect (SEE). This induces no hardware damage to the circuit, but evidently, unwanted re-programming of aircraft computer software can have fatal consequences.

At flight altitudes, as well as at sea level, the cosmic ray flux is dominated by neutrons and muons. The latter do not interact strongly with nuclei, and therefore neutrons are most important for SEE. Since neutrons have no charge, they can only interact via violent, nuclear reactions, in which charged particles are created, that occasionally induce an SEE. Thus, knowledge of the nuclear interaction of neutrons with silicon is needed to obtain a full understanding of the SEE problem.

If the neutron-induced charged-particle production cross sections were known, and thus the energy deposition on a microscopic level, it might be possible to calculate the SEE rate with reasonable precision also for any future components. Up to now, direct in-beam component testing has been carried out to characterize the effect, especially its neutron energy dependence [11, 12]. There are plans to develop these studies further by measuring cross sections for production of light charged particles and light heavy ions; where, for the light particles, the MEDLEY setup (see above) can be used.

Furthermore, neutrons at aircraft altitudes give a significant radiation dose to airplane personnel. This poses a relatively new dosimetry problem, which is currently under investigation [13].

2 The neutron beam facility

2.1 Neutron production

At the neutron facility at TSL [14] (see fig. 1), almost monoenergetic neutrons are produced by the reaction ^{7}Li(p,n)^{7}Be in a target of 99.98 % ^{7}Li. After the target, the proton beam is bent by two dipole magnets into an 8 m concrete tunnel, where it is focused and stopped in a well-shielded carbon beam-dump. A narrow neutron beam is formed in the forward direction by a system of three collimators, with a total thickness of more than four metres.

The energy spectrum of the neutron beam is shown in fig. 2. About half of all neutrons appear in the high-energy peak, while the rest are roughly equally distributed in energy, from the maximum energy and down to zero. The thermal contribution is small. The low-energy tail of the neutron beam can be reduced by time-of-flight measurements (see fig. 2). With a proton beam of 5 μA onto a 4 mm lithium target, the total neutron yield in the full-energy peak at the experimental position, 8 m from the production target, is about $5 \cdot 10^{4}$ cm^{-2}s^{-1}. The energy resolution of the full-energy peak depends on the choice of lithium target thickness. For most experiments a resolution of about 1 MeV (FWHM) has been selected.

2.2 Monitoring

Absolute normalization of the neutron flux is a notorious problem in all high-energy neutron-beam applications. For direct neutron monitoring, fission counters are available, which have been calibrated relative to *np* scattering. The absolute uncertainties in the measured neutron fluences are about 10 %.

Relative monitoring can be provided by many different means. Charge integration of the primary proton beam is one standard technique. In addition, for most of the experiment periods, different experiments can be running simultaneously, and then it is common that they use signals from each others experiments as relative monitors.

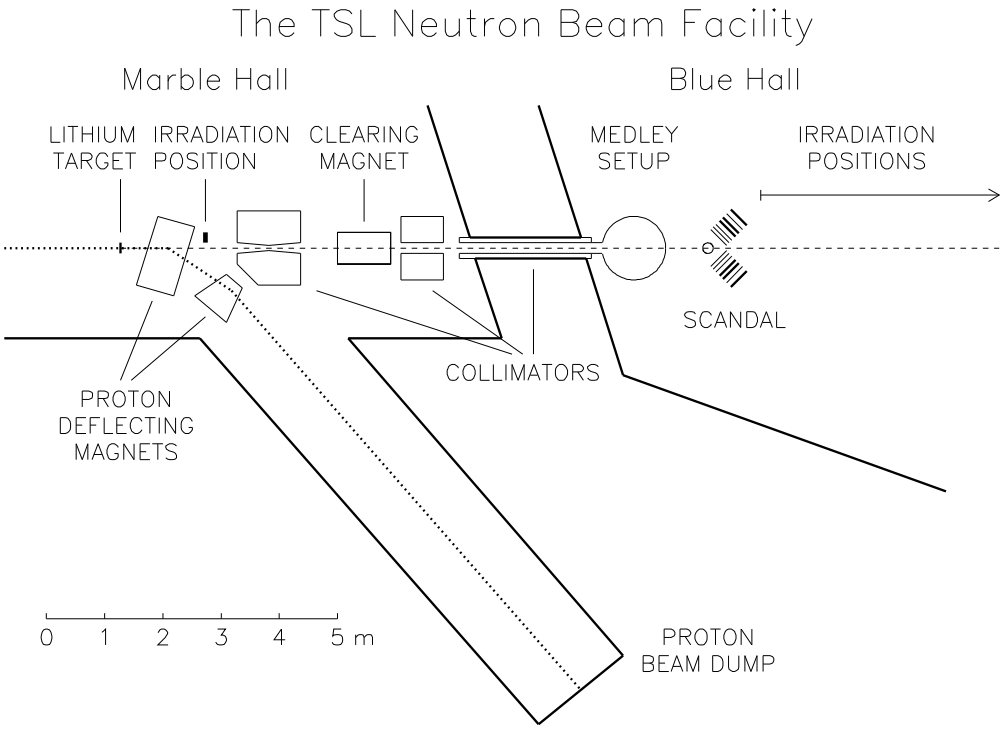

Figure 1: The TSL neutron beam facility.

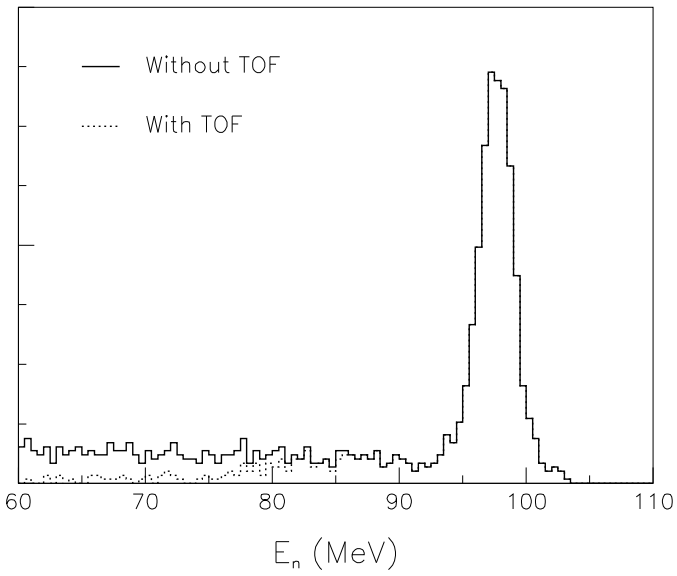

Figure 2: The neutron energy spectrum with and without time-of-flight rejection of low-energy neutrons.

3 The SCANDAL setup

3.1 General layout

The setup is primarily intended for studies of elastic neutron scattering, i.e., (n,n) reactions. The neutron detection is accomplished via conversion to protons by the H(n,p) reaction. In addition, (n,p) reactions in nuclei can be studied by direct detection of protons. This is also used for calibration of the setup. Therefore, it has been designed for a quick and simple change from one mode to the other.

The device is illustrated in fig. 3. It consists of two identical systems, typically located on each side of the neutron beam. The design allows the neutron beam to pass through the drift chambers of the right-side setup, making low-background measurements close to zero degrees feasible.

In neutron detection mode, each arm consists of a 2 mm thick veto scintillator for fast charged-particle rejection, a neutron-to-proton converter which is a 10 mm thick plastic scintillator, a 2 mm thick plastic scintillator for triggering, two drift chambers for proton tracking, a 2 mm thick ΔE plastic scintillator which is also part of the trigger, and an array of CsI detectors for energy determination. The trigger is provided by a coincidence of the two trigger scintillators, vetoed by the front scintillator. If used for (n,p) studies, the veto and converter scintillators can be removed, and additional drift chambers can be mounted if desired.

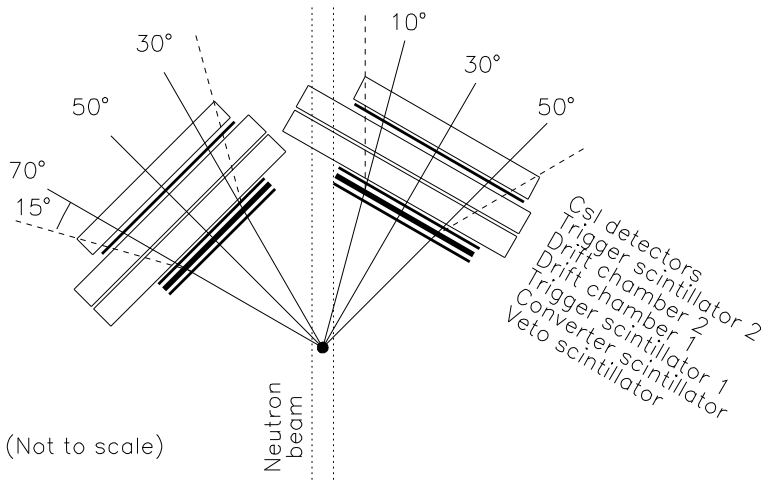

Figure 3: Schematic figure of the SCANDAL setup

3.2 Design features

The only realistic neutron-to-proton conversion reaction is H(n,p), which has a cross section of above 50 mb/sr at small angles. Two main approaches can in principle be used; passive or active converters.

Active converters have the advantage that they can be thicker, because the proton straggling on the way out of the scintillator can be measured and compensated for. The

maximum thickness of an active converter is thereby set by the energy resolution of the detector. A typical plastic scintillator has a resolution in the 10 % range, and the proton energy loss is about 1 MeV/mm for 100 MeV protons. Thereby, a converter thickness of 10 mm gives up to 10 MeV deposited energy, and the resolution contribution is henceforth up to 1 MeV.

The most frequently used converters contain hydrogen and carbon, which allows unambiguous measurements up to 12 MeV excitation energy. For higher excitation energies, the ^{12}C(n,p) channel opens in the converter, and therefore a unique identification of the target excitation is no longer possible. This is obviously not a problem for elastic scattering, or inelastic scattering to low-lying states, but complicates future developments, like neutron excitation of giant resonances, or quasielastic experiments. This problem is the same for active and passive converters.

The problems above can be circumvented by using a passive liquid hydrogen converter, but the technique is both non-trivial and expensive. Another prize to pay is that the converter must be an order of magnitude thinner for the same resolution. Based on these discussions, we have chosen to use active plastic scintillator converters.

The setup has in total 24 CsI detectors, 12 in each system. An average energy resolution of 3.0 MeV has been demonstrated for 77 MeV protons.

The drift chambers serve two main purposes; they improve the angular resolution and they allow rejection of spurious events.

The H(n,p) cross section close to zero degrees is rather flat over several degrees in the lab system. This effect, combined with the rather large front-area of the CsI's, makes the effective subtended angular range for each detector quite large. This would be a major contribution to the angular resolution without proton tracking.

Furthermore, the Q-value for ^{12}C(n,p) is -12.6 MeV. Thus, at forward angles energy detection can isolate the protons which are due to conversion via H(n,p). At about 20° conversion angle, the proton energies from the two processes are the same, and thereby it can no longer be determined whether the energy lost was due to excitations in the neutron scattering sample or in the conversion. By applying a 15° maximum opening angle criterion on the conversion (see fig. 3), such problems can be avoided.

Sufficient angular information is obtained by placing drift chambers between the converter and the CsI's. Hence, the conversion point is well determined. This has also the potential of allowing rejection of spurious events. With this technique, the remaining contribution to the angular resolution is the width of the neutron beam (or the scattering sample). The only way to improve the angular resolution further would be to use a narrower beam or target, but that would be at the expense of count rate.

3.3 Resolution

The energy resolution in neutron mode has contributions from the neutron beam (1.2 MeV at FWHM), the converter (1.4 MeV), the two trigger scintillators (0.3 MeV each), straggling in non-detector materials (0.25 MeV), kinematics (1.2 MeV), and the CsI detectors (3.0 MeV). This makes a total excitation-energy resolution of 3.7 MeV in elastic scattering measurements. This resolution is comparable with the distance from the ground state to the first excited state in most of the nuclei of interest, e. g., ^{12}C (4.4 MeV), ^{16}O (6.1 MeV), ^{40}Ca (3.3 MeV), ^{90}Zr (1.8 MeV), and ^{208}Pb (2.6 MeV).

The angular resolution is solely due to the neutron beam and target width. With the present setup dimensions and a 5 cm wide sample, it is about 1.4° (rms). The angular

resolution is most crucial at small angles, where the cross section falls very rapidly. For these angles, the cross section is also very large, and thereby a narrow strip target could be used to improve the angular resolution, without making the total beam time considerably longer.

3.4 Solid angle and count rate

The solid angle subtended by each system in the proton detection mode is about 240 msr for a point target. Applying the maximum opening angle criterion on the second scattering in the converter (see above), required for neutron detection, makes the effective solid angle smaller – about 130 msr per setup at full coverage of the 15° cone. The conversion efficiency is then about $5 \cdot 10^{-4}$.

In a typical experiment, the two arms will be located such as to cover 10–50°, and 30–70°, respectively. For a one-week run on ^{208}Pb, the total number of counts for a one-degree angular bin is expected to be about 5 000 at 10°, and 1 at 70°, illustrating that the cross section falls off rapidly with angle.

3.5 Normalization

Normalization of neutron-induced cross sections is a notorious problem because of the difficulties in monitoring the absolute intensity of neutron beams. Precisions better than 10 % have very rarely been achieved. Therefore, most data have been measured relative to another cross section assumed to be known. Most often, the neutron-proton scattering cross section has been used as the primary standard.

Recent experimental investigations [15, 16, 17, 18] have indicated that the *np* scattering cross section might have larger uncertainties than previously estimated. It seems now that the cross section can be uncertain by as much as 10-15 % in the energy range of 100 MeV and up [19].

A recent high-precision measurement of *np* scattering at 96 MeV in the 74–180 degree range claims an absolute uncertainty of 1.9 % [18], but this is outside our angular range. This is where the planned H(n,n) measurement comes in. By making a relative measurement of the angular distribution of H(n,n) from (close to) zero degrees and out to angles overlapping with the existing data, a normalization to the total cross section can be made with a very small uncertainty (about 1 %) [20].

The reason for this high precision is that the total cross section has been possible to determine with a very high precision (1 %), because knowledge of the absolute beam intensity is not required. Instead, it can be inferred from intensity ratio measurements in attenuation experiments. Furthermore, in the case of hydrogen, integration of the elastic scattering cross section accounts for more than 99 % of the total cross section, with very small corrections for capture and bremsstrahlung processes.

For practical experimental reasons, we plan to measure this in a CH_2-vs-C difference measurement. By this technique, we can normalize the C(n,n) cross section to the H(n,n) cross section. This is very useful, because thereby we can establish the much larger C(n,n) cross section as a secondary standard, allowing all other nuclei to be measured relative to C(n,n).

A second normalization method will be provided by comparisons with the total elastic cross section. This cross section has been derived from the difference of the total cross section and the total inelastic cross section. Both these quantities have been measured

in attenuation experiments, and are therefore known to high precision, i.e. 1-2 %. (See for example ref. [21]). By covering 0–70 degrees, far more than 99 % of the contribution to the total elastic cross section will be accounted for, providing a second normalization technique. This method works the best with light nuclei, however, and is therefore well suited for e.g. C(n,n), but is not as reliable for ^{208}Pb(n,n). Hence, this is another reason to establish C(n,n) as a secondary standard. A detailed account of these issues is underway [22].

4 Results

To investigate the characteristics of the SCANDAL setup and to develop the experimental procedures, measurements have been performed both in proton and in neutron detection mode, at a neutron beam energy of 96 MeV.

4.1 Proton detection

The proton mode runs were used for studies of the H(n,p) and ^{12}C(n,p) reactions, as well as for calibration purposes. By normalizing ^{12}C(n,p) spectra, obtained with a pure carbon sample, with respect to the carbon content in a CH_2 sample, carbon spectra can be subtracted from those of CH_2, giving pure *np* scattering spectra as illustrated in fig. 4.

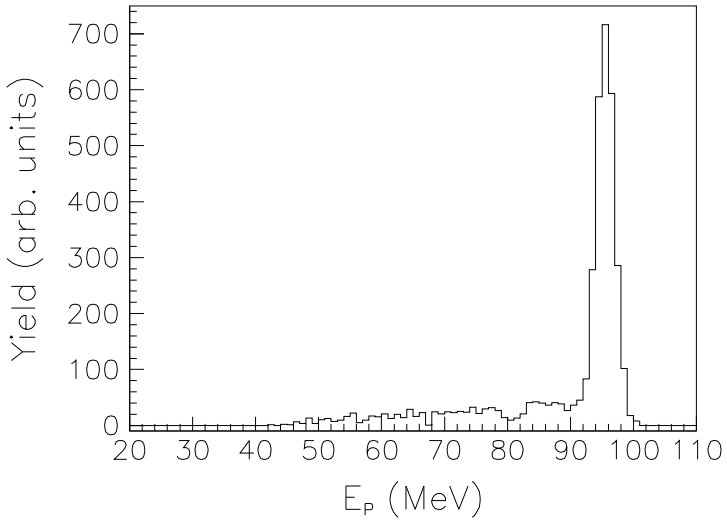

Figure 4: Proton energy spectrum for (n,p) reactions in hydrogen, induced by 96 MeV neutrons, in the angular range 6–7°. The spectrum has been obtained by subtracting a ^{12}C(n,p) spectrum from a proton spectrum coming from CH_2, after normalization.

The resolution of the *np* scattering peak varies due to differences in intrinsic resolution in the CsI detectors, but an average value of 3.7 MeV (FWHM) has been found. Apart from the CsI detectors, the main contributions to the resolution come from the neutron beam, the plastic scintillators and straggling in non-detector materials. These are estimated to be 1.2, 1.7 and 0.7 MeV (FWHM), respectively; implying an average intrinsic CsI resolution of 3.0 MeV.

In fig. 5, SCANDAL ^{12}C(n,p) data are compared with data collected on the same reaction with the magnetic spectrometer LISA (Light Ion Spectrometer Assembly) [23]. For this purpose, LISA data have been folded with a Gaussian representing the resolution in SCANDAL, and data from the SCANDAL measurement have been normalized to the LISA cross section scale. It is evident that SCANDAL reproduces the data. The errors are statistical.

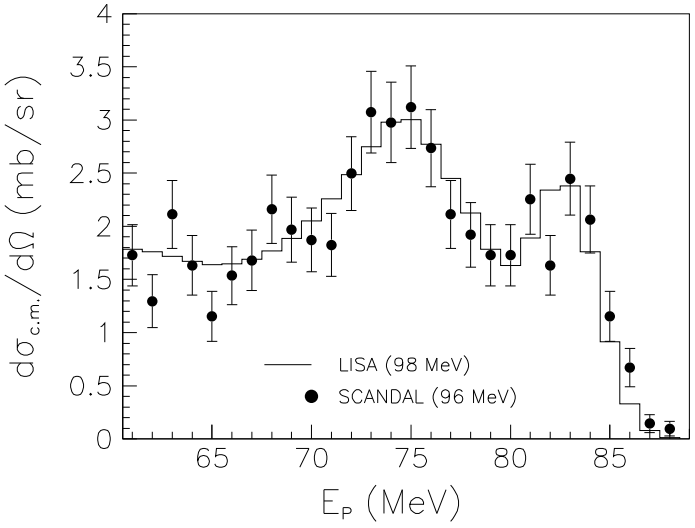

Figure 5: Comparison of SCANDAL and LISA proton energy spectra, from (n,p) reactions in carbon. LISA data have been folded with the SCANDAL resolution, while SCANDAL data have been normalized to the cross section scale of the LISA measurement.

4.2 Neutron detection

Fig. 6 shows excitation energy spectra for ^{12}C(n,n) at 96 MeV and 9° scattering angle. The large peak at E_X = 0 MeV is due to elastic scattering, and the excited states at 9.6 MeV, and possibly at 4.4 MeV, are small but visible.

A response function for the SCANDAL setup has been constructed. The upper plot of fig. 6 shows different components of this function. A Gaussian has been fitted to the H(n,p) peak in the converter, reflecting elastic scattering from the ground state in ^{12}C. Knowing the relative cross section of ^{12}C(n,p) reactions in the converter with respect to that of (n,p) reactions in hydrogen, a ^{12}C(n,p) spectrum has been added. Also, a low-energy neutron tail has been included by knowing the ^{7}Li(p,n) cross section, again with respect to that of H(n,p) in the converter.

At an excitation energy of 75 MeV, the energy of the scattered neutron is 20 MeV, giving an energy of 0–10 MeV for the protons reaching the CsI detector. Protons with these energies are rejected in the analysis; thus there are no events in the E_X spectrum above 75 MeV. For E_X = 55 MeV, the resulting proton energies are high enough for all events to be recorded. Thus, a straight line describing the cut-off at high excitation energies has been employed between E_X = 55 and 75 MeV.

Adding the contributions from the hydrogen peak, the ^{12}C(n,p) and the low-energy neutron backgrounds, as well as the cut-off at high E_X, gives the full response function

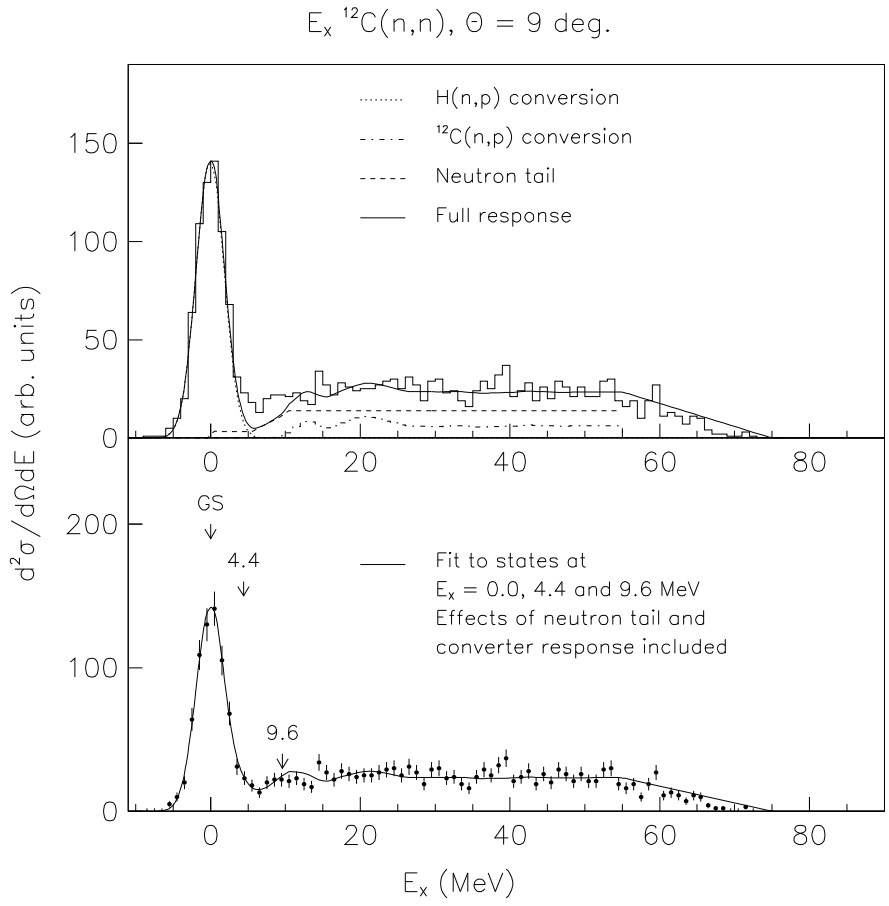

Figure 6: Excitation energy spectra for ^{12}C(n,n) at 9°. See the text for details on the response function and its contributions.

shown in the upper plot.

In the lower plot of fig. 6, Gaussians have been fitted to the excited states at 4.4 and 9.6 MeV, in addition to the ground state fit. Contributions from ^{12}C(n,p) reactions in the converter and from the low-energy neutron tail, relative to these states, have been included in the response function.

It is concluded that the full spectrum can be explained in terms of the effects described here, and that no unexpected contributions are seen. In addition, the absolute rate is compatible with theory expectations. The energy resolution is 3.7 MeV (FWHM) for this experiment, in which a very large target was used to obtain high count rate at the expense of energy resolution.

5 Summary

The experiment setup SCANDAL, for detection of primarily neutrons in the energy interval 50–130 MeV, together with the quasi-monoenergetic 20–180 MeV neutron beam facility at the The Svedberg Laboratory (TSL), Uppsala, Sweden, will be used to provide elastic neutron scattering data for transmutation applications. This will be done in

an energy region which has been identified as very important for characterizing neutron transport in a spallation target, and in which there exist very little high-quality data.

The magic or semi-magic nuclei ^{12}C, ^{16}O, ^{40}Ca, ^{90}Zr and ^{208}Pb will be studied for developing theoretical models. As lead and zirconium are important materials in future transmutation facilities, modelling of neutron transport in these materials will also benefit directly from our measurements. There are plans to study H(n,n) for normalization purposes, and in a second phase other materials for transmutation cores might be investigated.

First results, for ^{12}C(n,n), show that we are able to separate the ground state and first excited states reasonably well in closed-shell nuclei.

This work was financially supported by Vattenfall AB, Swedish Nuclear Fuel and Waste Management Company, Swedish Nuclear Power Inspectorate, Barsebäck Power AB, Swedish Defence Research Agency, Swedish Natural Science Research Council, and the European Commission.

References

[1] R. Finlay, *et al.*, Phys. Rev. C **47** (1993) 237.

[2] J. Rapaport and E. Sugarbaker, Annu. Rev. Nucl. Part. Sci. **44** (1994) 109.

[3] W.P. Alford and B.M. Spicer, Advances in Nuclear Physics **24** (1998) 1.

[4] E.L. Hjort, *et al.*, Phys. Rev. C **50** (1994) 275.

[5] J. Rapaport, private communication and J. Osborne, thesis, unpublished.

[6] R. Finlay, *et al.*, in *Proposal to the NSF for support of CHICANE/SPECTROMETER SYSTEM FOR THE IUCF COOLER RING*, (1992).

[7] S. Dangtip, *et al.*, Proc. Int. Conf. on Nuclear Data for Science and Technology, Trieste, Italy, 1997, p. 1652.

[8] S. Dangtip, *et al.*, Medical & Biological Engineering & Computing **35** (1997) 978.

[9] J.F. Ziegler, IBM J. Res. Develop. **40** (1996) 19.

[10] H.H.K. Tang, IBM J. Res. Develop. **40** (1996) 91.

[11] K. Johansson, *et al.*, Proc. Int. Conf. on Nuclear Data for Science and Technology, Trieste, Italy, 1997, 1497.

[12] K. Johansson, *et al.*, IEEE transactions on Nuclear Science I **45** (1998) 2195.

[13] D. O'Sullivan, private communication. EU Cosmic Radiation and Dosimetry Group.

[14] H. Condé, *et al.*, Nucl. Instr. Meth. **A292** (1990) 121.

[15] T. Rönnqvist, *et al.*, Phys. Rev. C **45** (1992) R496.

[16] T.E.O. Ericson, *et al.*, Phys. Rev. Lett. **75** (1995) 1046.

[17] J. Rahm, *et al.*, Phys. Rev. C **57** (1998) 1077.

[18] J. Rahm, *et al.*, Phys. Rev. C **63** (2001) 044001.

[19] J. Blomgren, N. Olsson, J. Rahm, How Strong is the Strong Interaction? – The πNN Coupling Constant and the Shape and Normalization of np Scattering Cross Sections, in Proceedings of Workshop on Critical Issues in the Determination of the Pion-Nucleon Coupling Constant, Physica Scripta T87 (2000) 33.

[20] C. Johansson, *et al.*, to be published.

[21] J. DeJuren and N. Knable, Phys. Rev. **77** (1950) 606.

[22] J. Klug, *et al.*, to be published.

[23] N. Olsson, *et al.*, Nucl. Phys. **A559** (1993) 368.

Appendix XI

Swedish Expert Group on Transmutation

H. Condé*, J. Blomgren*, W. Gudowski**, J.-O. Liljenzin***, C. Mileikowsky****,
N. Olsson*, and J. Wallenius**

** Dept. of Neutron Research, Uppsala University, Box 520, SE-751 25 Uppsala*
*** Dept. of Neutron and Reactor Physics, Royal Institute of Technology, SE-100 44 Stockholm*
**** Dept. of Nuclear Chemistry, Chalmers University of Technology, SE-412 96 Göteborg*
***** Avenue de Rochettaz 14A, 1009 Pully, Switzerland*

Abstract

An informal expert group on transmutation of nuclear waste was formed a few years ago in Sweden. The Group is a forum for discussion of Swedish national research and cooperation in international research in the field. The Group has members from the Chalmers Technical University, the Royal Technical Institute and the Uppsala University with Observers from the Ministry of Environment, Swedish Nuclear Power Inspectorate (SKI) and the Swedish Nuclear Fuel and Waste Management Co (SKB). Mostly basic research on partitioning, reactor and neutron physics, and material research is made at the named Universities with financial support from SKB and by participating in P&T projects within the European research framework programs.

The Group has actively participated in discussions with Russian laboratories about applications for research on transmutation to the International Scientific and Technical Centre (ISTC) in Moscow. In particular, a 1 MW Pb/Bi neutron spallation source has been designed and manufactured at IPPE, Obninsk with ISTC financial support by Sweden, USA and the European Union.

I. INTRODUCTION

Sweden has today 11 nuclear power reactors in operation. Until recently it was twelve reactors but one was shut down as a first step to move out of nuclear energy until about 2010. The nuclear reactors produce 40-50 percent of the electric power consumption in Sweden. The other 50 percent is mainly produced by hydro power.

The nuclear power reactors in Sweden will up till 2010 produce about 8000 tons of spent nuclear fuel. According to the Swedish Act on Nuclear Activities, the companies licensed to operate nuclear power plants have full responsibility for safely managing all nuclear production waste and for waste resulting from the dismantling of the facility. The financing system is based on a fee charged per generated kilowatt hour of electricity and is paid to the Government. There is a specific law – the Act on the Financing of Future Expenses for Spent Nuclear Fuel – regulating the way in which the expenses are calculated and how they should be met. The total estimated cost for the Swedish program for managing all nuclear waste and for dismantling nuclear power plants are about SEK 50 billion ($ 5 billions). The nuclear power utilities have formed a jointly owned company, the Swedish Nuclear Fuel and Waste Management Company (SKB) to fulfil the obligations of the power utilities regarding nuclear waste. The research and development (R&D) for waste management is carried out by SKB. The R&D program is evaluated each third year by the National Council for Nuclear Waste (KASAM), the Swedish Nuclear Power Inspectorate (SKI) and the Swedish Radiation Protection Institute (SSI) followed by a final decision taken by the Government

The present Swedish program for managing nuclear waste contains the following steps. The spent nuclear fuel is shipped to an interim storage (CLAB) for a 40 years cooling down period. Subsequently, the spent fuel will be put in a deep geological repository. The Government has accepted, as the main alternative, that the spent fuel will be encapsulated in canisters of steel and copper, which are placed in crystalline bedrock, at a depth of 500 meters, surrounded by highly absorbent clay in the repository. A demonstration repository will be built. When 5-10 percent of the spent fuel has been lowered in the repository, an evaluation of the method will be made and a definite decision will be taken by the Government if the rest of the spent fuel can continue to be deposited in the repository.

As one of the alternative options to the direct deposition of the total nuclear waste in a repository, the Government has responded positively on the proposal by SKB to study partitioning and transmutation (P&T) of the nuclear waste in combination with geological deposition of the remaining waste. This proposal has resulted in a limited support on P&T research from SKB to three different universities in Sweden, the Chalmers University of Technology, the Royal Institute of Technology and the Uppsala University. Furthermore, the same university research groups are also actively taking part in P&T research projects within the European 5th framework program.

An informal expert group on P&T with members from the above mentioned university research groups was formed in the early 90-ties to establish a forum for discussions on research strategies, means to find support for doing research, research coordinating and collaboration, and information exchange. One early activity of the expert group was to consult Russian nuclear weapon experts in their ambition to apply for support of civilian research projects on transmutation from the International Scientific and Technical Centre (ISTC) in Moscow. The ISTC was set up by the USA, Russia, Japan and the European Union to support civilian research activities at the weapons laboratories in the former Soviet Union. Sweden contributed directly to the ISTC fund when it was set up, but since Sweden became a member of the European Union the contribution is channelled through this organisation.

The present report gives the background, the members and the agenda for the Expert Group on Transmutation. It also shortly describes the P&T research in progress by the university groups, which are represented in the Expert Group, including the ongoing ISTC projects with Swedish involvement.

II. THE SWEDISH EXPERT GROUP ON TRANSMUTATION

A renewed interest of partitioning and transmutation of nuclear waste was raised in the early 90-ties mainly due to the technical developments of large accelerators, which made the accelerator driven transmutation concepts more likely to be realized. This interest initiated basic research on partitioning and accelerator driven transmutation at a few Swedish universities namely at the Chalmers University of Technology (partitioning), the Royal Institute of Technology (reactor physics) and the Uppsala University (nuclear data). An informal group was formed with members representing the research groups of the named three universities.

At the early 90-ties the International Scientific and Technical Centre (ISTC) was set up in Moscow as a joined undertaking of US, Japan, Russia and the European Union as reported above. The aim was to financially support civilian projects at nuclear weapon laboratories in the former Soviet Union. Sweden joined this effort by contributing to the ISTC fund, first directly and later, when Sweden became a member of EU, through that organisation. Accelerator driven transmutation was a civilian research area to which the Russian experts could give an important contribution. Thus, discussions started about transmutation research projects that could be made in Russia with support from ISTC. A workshop was arranged at Saltsjöbaden in Sweden in 1991 with participation mainly from US, Russia and Sweden. Following that meeting a number of ISTC funded projects in Russia has been initiated through the years with Swedish collaboration. The Expert Group was charged to report on those projects to the Swedish Nuclear Power Inspectorate (SKI) and subsequently got financial support for travelling expenditures to fulfil that task from the same organisation.

Nowadays, an international Contact Expert Group (CEG) has been established to advice the ISTC on which projects related to the research on accelerator driven systems should be supported. The CEG works with subgroups, one for each supporting partner to ISTC, namely US, Japan, EU and Korea. The Swedish Expert Group has close links to the EU subgroup within CEG and channel its recommendations on ISTC projects through that body.

The international R&D on transmutation is closely followed. The university research groups participate in international P&T research projects mainly within the EU framework programs and collaborate in ISTC projects. Members of the Expert Group are actively engaged in international working groups, advisory committees, and project steering committees. The Group is arranging conferences, symposia and expert meetings on ADS among those were the 2nd International ADTT Conference in Kalmar, Sweden in 1996.

The present members of the Swedish Expert Group, which are the named authors of this report, represent a broad know-how in scientific disciplines of importance for R&D of accelerator driven systems. Observers at the regular meetings of the Group, about 4 per year, come from the Ministry of Environment, the Nuclear Power Inspectorate

(SKI), and the Nuclear Fuel and Waste Management Co (SKB).

III. SWEDISH REASERCH ON PARTIONING AND TRANSMUTATION

A remarkable increase in the international research and development on transmutation has taken place during the last few years. This is in particular true for many of the countries within EU. A European road-map for producing an ADS demonstration facility within about the next decade has been produced by a working-group with members from 9 European countries among them Sweden. EU has given a strong support to practical demonstrations of the key issues according to the road-map like the spallation target experiment MEGAPIE at the cyclotron of the Paul Scherrer Institute, Switzerland and the preliminary design study of an demonstration accelerator driven system (PDS-XADS) but also to several basic studies of a wide range of technical and scientific problems for partitioning and transmutation.

I. Chalmers University of Technology

The Department of Nuclear Chemistry, CTH participates in the project PARTNEW within the EU 5th framework programme. The project is a continuation of NEWPART (4th EU FP) to study the extraction of lanthanides and actinides using pyridins or similar nitrogen-based molecules. The work to be carried out concerns the design of solvent extraction processes of Am(III) and Cm(III) that are contained within the acidic high active raffinates (HARs) or concentrates (HACs) from the reprocessing of spent nuclear fuels. The work to be done is sorted out in eight Work Packages (WPs) corresponding to 3 research domains:

· the actinides (III) (An(III)) + lanthanides (III) (Ln(III)) co-extraction from acidic HARs or HACs (DIAMEX processes)

· the An(III)/Ln(III) group separation from actinide feeds (SANEX processes)

· the Am(III)/Cm(III) separation system

For each domain, basic research and limited flowsheet developments will be carried out.

II. Royal Institute of Technology

The Department of Neutron and Reactor Physics at the Royal Institute of Technology, Stockholm participates in a number of projects under the 5th Framework Programme of the European Commission. The group coordinates the CONFIRM project aiming to manufacture and test nitride fuel. Irradiaton tests will be made at the R2 reactor at Studsvik. The group also participates in the SPIRE and MUSE projects, in which studies are made of radiation damage effects in martensitic steels and of the coupling between an accelerator driven neutron source and the subcritical assembly MASURCA at CEA/Cadarache, respectively.

The aspects of severe accidents in transmutation systems have been studied together with a group at the EURATOM Joint Research Centre at ISPRA, Italy. Furthermore, the use of Pb-Bi eutectic as the coolant of an accelerator driven system has been studied together with a group at the Technical University, Bilbao, Spain.

Extended studies have been made of a Pb/Bi cooled ADS concept (Sing-Sing) for transmutation of the nuclear waste from the Swedish reactors.

III. Uppsala University

The transmutation related research at Uppsala University is mainly performed by the Department of Neutron Research and makes use of the unique 20-180 MeV quasi-monoenergetic neutron beam at the The Svedberg Laboratory in Uppsala.

Since 1998 a project is run, with the aim to measure elastic neutron scattering from some nuclei at 100 MeV. Such data are crucial to improve existing nuclear models, and in this way improve the existing data libraries and extend them to higher energies. These libraries are needed to reliably calculate neutron and other particle transport in a transmutation target and blanket. The differential elastic scattering cross sections for carbon and lead have been measured using the detector facility, SCANDAL.

The group also participates in an EU supported project HINDAS. Within HINDAS, all kinds of reaction channels for incident neutrons and protons are considered, both experimentally and theoretically. The ultimate goal is to construct a new data library for the energy range 20-2000 MeV, which can be used for engineering design of transmutation devices. Several of the European experimental groups use the Uppsala neutron beam for their work. Studies linked to the HINDAS project are also made of nuclear models and code developments for ADS at the Department of Radiation Sciences.

IV. ISTC PROJECTS

Short information is given on a few ISTC research projects in progress related to ADS of special Swedish interest due to initiative in formulating the project and/or close cooperation with Swedish research groups. A general recommendation has been given by the officials of the European Commission who are responsible for the ADS research within the framework programs, that one should seek close links between corresponding EU and ISTC projects.

I. Measurements and Comparison of Proton- and Neutron-Induced Fission Cross Section of Lead and Neighbouring Nuclei in the 20-200 MeV Energy Region (ISTC project #1309)

Project leader: Vilen P. Eismont, V.G. Khlopin Radium Institute, S:t Petersburg

Proton- and neutron-induced fission cross sections of isotopes and elements in the lead region are being measured. The neutron experiments are made at the neutron beam facility of the 200 MeV cyclotron of the The Svedberg Laboratory,.Uppsala in collaboration with the Department of Neutron Research, Uppsala University. The produced database is partly unique and will put light on existing discrepancies between model calculations and experiments. A follow-up project on measurements of proton- and neutron-induced fission cross sections of separated tungsten isotopes and natural tungsten in 50-200 MeV energy region is planned

II. Pilot Flow Lead-Bismouth Target of 1 MWth for Accelerator-Based Systems (ISTC project # 559)

Project leader: Boris F. Gromov, Institute of Physics and Power Engineering (IPPE), Obninsk

The Expert Group took originally the initiative to this project, which was supported by Sweden but also became strongly supported by USA and EU.

The purpose of the project was to develop a heavy metal flow target which possesses the best features for producing neutrons at a high power proton accelerator. Thus, the technical key problems of a flowing lead-bismuth 20 MWth-power target should be investigated. The technical base should be established by the design of a pilot lead-bismuth 1 MWth-power target (TC-1). It was planned that the pilot target was going to be tested at the linear proton accelerator (LANSCE, 800 MeV, 1.5 mA proton beam) of the Los Alamos National Laboratory.

The project benefited from the broad experience of specialists at IPPE and Research and Development Bureau (RDB) "Gidropress", whose experience was developed by designing and operating the Russian nuclear submarines with lead-bismuth cooled reactors. The target design was a result of a close cooperation primarily between IPPE and LANL but was also discussed at several technical meetings with the participants from Sweden (Swedish collaborator: Department of Neutron and Reactor Physics, Royal Institute of Technology, Stockholm) and France (EU collaborator: CEA/Cadarache).

The target past the final delivering tests and was accepted by the Los Alamos National Laboratory, the CEA/Cadarache and the Royal Institute of Technology in the Spring of 2001. The Russian Authorities (MINATOM) has given clearance for exportation of the target. Decisions are still pending on the site for an irradiation test and the financing of that test if any.

III. Experimental Research of Transmutation of Fission Products and Minor Actinides in a Subcritical System Driven by a Neutron Generator. (ISTC project B-70, Belarus)

Project leader: S. E. Chigrinov, Radiation Physics & Chemistry Institute, Minsk-Sosny

The Yalina facility consists of an accelerator driven 14 MeV neutron source surrounded by a sub-critical blanket. The planned experiments will yield information in the following fields.:

- physics of sub-critical systems driven by a neutron generator,
- transmutation rates of fission products and minor actinides,
- spatial kinetics of sub-critical systems with external neutron sources
- experimental techniques for sub-criticality monitoring
- dynamical characteristics of sub-critical systems with an external neutron source (pulse mode operation of the neutron generator)

The Department of Neutron and Reactor Physics at the Royal Institute of Technology contributes to the project with the development of computer codes for simulation of the neutronics of the facility.

IV. Experimental Mock-up of Molten Salt Loop of Accelerator-Based Facility for Transmutation of Radioactive Waste and Conversion of Military Plutonium (ISTC project # 1606)

Project Manager: K. F. Grebyonkin, Russian Federal Nuclear Centre – Institute of Technical Physics (VNIITF), Snezhinsk, Chelyabinsk reg.

Project Scientific Leader: V. V. Ignatiev, Kurchatov Research Centre, Moscow

The mission of the project is to perform an integral reevaluation of the Molten Salt (MS) Nuclear Fuel Technology potential as applied to safe, low-waste and proliferation resistant treatment of RadWaste and Plutonium management as well as to develop a comprehensive program plan of the Technology commercialisation.

Members of the Swedish Expert Group were actively engaged in the planning of the ISTC project #1606. The Department of Nuclear Chemistry, Chalmers University of Technology and the Department of Neutron and Reactor Physics, Royal Institute of Technology will both be project collaborators. Furthermore, a close link will be established with the 5th European Framework project on Molten Salt Reactors (MOST) with 12 participating European institutes.

V. Combined Radiochemical and Activation Analysis of Long-Lived Nuclear Waste Transmuted in Fast Reactors and High Energy Accelerators (ISTC project # 1372)

Project manager: E. Ya. Smetanin, Institute of Physics and Power Engineering (IPPE), Obninsk

The project will include radiochemical analysis and activation measurements of the isotopic composition changes of minor actinide samples irradiated in fast reactors and by the radiation field from a massive lead spallation neutron source. Comparative analysis of the radioactive isotope transmutation efficiency in fast neutron reactors and accelerator driven systems. The Department of Neutron and Reactor Physics, Royal Institute of Technology will be the Swedish collaborator of the project.

VI. Experimental and Theoretical Studies of the Yields of Residual Product Nuclei Produced in Thin Pb and Bi Targets Irradiated by 40-2600 MeV Protons (ISTC project #2002)

Project manager: Yu. E. Titarenko, Institute of Theoretical and Experimental Physics, (ITEP), Moscow

The project is aimed at experimental and theoretical studies of the independent and cumulative yields of residual product nuclei in high energy proton irradiation of thin targets of highly enriched isotopes and natural Pb and natural Bi. Information exchange will be made with similar projects in progress at Univ. of Hannover and GSI, Darmstadt within the 5th EU Framework program HINDAS.

Preliminary contacts have been taken between ITEP and the Department of Neutron Research, Uppsala University to see if some of the experiments within the project can be made at the accelerator facilities of the The Svedberg Laboratory in Uppsala.

VII. The Subcritical Assembly in Dubna (SAD)

Joint Institute of Nuclear Research (JINR), Dubna

The planning of the "Subcritical Assembly in Dubna – SAD – project" is in a final stage with participation of the Department of Neutron and Reactor Physics, Royal Institute of Technology (RIT). The project goals are: to design and construct a small power subcritical system fueled with MOX and driven by the 660 MeV cyclotron, development and validation of techniques for measurements of subcriticality and neutronic properties of the assembly, validation of relevant computer codes and data libraries, dosimetry of high energy neutrons (above 20 MeV) The project is scheduled for 3 years and will use existing infrastructure of institutes in Dubna. A pre-ISTC project is discussed with financial support from ForschungsZentrum Karlsruhe, CIEMAT Madrid, RIT Stockholm, and CEA Cadarache.

V. SUMMARY

A direct disposal of the total spent reactor fuel in a deep geological repository after a cooling period of about 40 years is the option with highest priority of treating the Swedish reactor waste.

A limited research effort is devoted to partitioning and transmutation of the waste mainly to keep track of the international R&D in the field if that should pave the road to transmutation concepts which would be technical and economical applicable for the Swedish reactor waste within a foreseeable future.

An informal Expert Group on P&T with members from three universities in Sweden has been formed to establish a forum for discussions of research strategies, means to find support for doing research, research coordination and collaboration, and information exchange.

The university research groups actively participate in many of the research projects on P&T within the on-going 5th EU Framework Program but also collaborate with transmutation research projects in Russia financed by ISTC.

Experimental Activities at High Energies

J. Blomgren[†*]

[†] *Department of Neutron Research, Uppsala University, Sweden.*

Lecture given at the:
Workshop on Nuclear Data for Science & Technology:
Accelerator Driven Waste Incineration
Trieste, 10-21 September 2001

LNS

[*]jan.blomgren@tsl.uu.se

Abstract

Measurements of nuclear data for accelerator-driven systems at energies above 20 MeV presents major experimental challenges. In this presentation, some of the common problems are outlined, as well as techniques to overcome them. Ongoing experimental work is surveyed.

Keywords: Nuclear data.
PACS numbers: 64.60.Ak, 64.60.Cn, 64.60.Ht, 05.40.+j

Contents

1 Why nuclear data for accelerator driven waste incineration?

Before plunging into the subject - experimental nuclear data activities at high energies for applications within accelerator-driven waste incineration - it might be suitable to ask a most general question: why are we doing this at all?

There is no doubt that waste from present nuclear power reactors or nuclear weapons material can *in principle* be converted into less long-lived material. This means that small quantities can be treated in laboratories to high costs. Thus, the required laws of nature are there, and there is no real need for additional nuclear data to find out whether the fundamental mechanisms will work. They do.

This is, however, not enough when we discuss *realistic* treatment at a scale of interest to society. Going from laboratory-scale incineration at research-scale costs to industry-scale handling at a cost acceptable to society at large, with important boundary conditions like political acceptance, good environmental aspects, both concerning the working conditions for the personnel and losses in the process, etc., nuclear data at high energies play an important role.

The present situation resembles the development of critical power reactors. The first man-made reactor was tested by Fermi and collaborators in Chicago in 1942. At that time, very little was known about relevant cross sections. The ^{235}U fission cross section was reasonably well known, and the existence of beta-delayed neutrons had been established, but this was more or less all information at hand. The first reactors supplying electricity to a grid came into operation around 1955, and their power was about 50 MW electricity. Less than 30 years later, reactors of 1200 MW_e were commonplace. This enormous increase - a factor 25 in 30 years - was largely due to improved nuclear data conditions.

When assessing the safety of a critical reactor system, cross sections for a wide range of reactions have to be known. Fission cross sections are obviously required to know the energy release, scattering cross sections are needed to know the spatial distribution of neutrons in the core, hydrogen and helium production reaction probabilities should be under control for safety and materials issues, capture cross sections must be known to estimate losses, etc.

If a certain cross section is poorly known, or even unknown, it has to be estimated some way. If unknown, it has to be exaggerated to the extent that it cannot be that large, just for safety. Often total cross sections are known although a certain reaction is poorly known, which means that when calculating the safety margins, the total cross section can be used. With such an approach, you are sure you have at least not underestimated the effect.

There is always a balance between safety and cost. If you overestimate the need for safety margins, it will induce excessive costs for extra shelding, additional emergency systems, etc. Thereby, the better known a cross section is, the less it costs to arrive at a given safety level. It is therefore not very meaningful to talk about the safety of a system. What makes more sense is to assess the safety for a given cost, or the cost for a given safety level.

This reasoning was the driving force behind a large worldwide nuclear data campaign during the heydays of nuclear power development, and it resulted in about 3 million experimental nuclear data points, which are accessible in nuclear data libraries.

The present situation on accelerator-driven incineration strongly resembles the development of self-sustained reactors. The main use of nuclear data is not to prove the principle,

but to make it possible to go from laboratory to industry, i.e., to build large systems with a reasonable safety to an acceptable cost. Thus; *the main role of nuclear data is to improve the balance of safety versus economy.*

2 Why neutrons?

All large-scale applications of nuclear physics involve neutrons, and accelerator-driven incineration is no exception. Why is this the case? Well, there are good reasons for this, governed by the laws of nature.

Atomic nuclei contain enormous energies. A typical nuclear reaction can involve energy changes which are many million times larger than for any chemical reactions. There are, however, some important boundary conditions when we want to utilize this energy.

First, these large energy releases are due to the strong interaction. Thus, we need a strong interaction probe if we want to make nuclear reactions with a reasonable efficiency. Second, atomic nuclei are positively charged and very small, and thus the Coulomb effects are enormous. In addition, nuclei are surrounded by electrons. Although the strong force is some 100–1000 times stronger than electromagnetism, the cross section area of the atom is of the order of 10^{10} times larger than that of the nucleus, so any charged probe will mostly interact with the electrons, and not the nucleus. The only realistic solution to this dilemma is to use an uncharged probe. Third, this probe needs to have a reasonable life time. It should at least be able to travel from one nucleus to another before decaying. The only particle fulfilling these conditions is the neutron. [1]

3 Which reactions are of interest for waste incineration?

The discussion in section 2 concluded that neutron-induced reactions are necessary for a large-scale application. Thus, here we embark to find suitable neutron-induced nuclear reactions for incineration.

The fact that the neutron is uncharged makes it possible for it to enter a nucleus at any energy. Neutrons produced at whatever energy will lose energy in collisions, which finally results in really low-energy (thermal) neutrons. This means that in any reactor, thermal neutrons will almost inevitably comprise a sizeable fraction of the neutrons.

At these low energies, there are essentially three possible reactions; fission (in actinides), capture and elastic scattering. Of these, fission is by far the best reaction, and will always be the choice if possible at all. It releases lots of energy (200 MeV), which can help paying the bill, and it releases 2–4 neutrons, which can induce additional reactions, thereby lowering the demands for costly external neutron production. For really heavy elements, which often have large fission cross sections, this is the preferred method.

The second best alternative is capture. It also releases energy, but much less (8 MeV) and of the wrong type (photons, which do not induce chain reactions). Thus, capture is the

[1] The "second best" would probably be the K_L^0 meson, but its lifetime of 50 ns and the requirement of associated production due to its strangeness properties makes it completely useless for practical purposes.

choice only for elements which cannot fission, like the rest products after fission, for instance technetium or iodine.

Finally, scattering plays a major role for low-energy neutrons. This makes no elemental change, but is needed to know anyway when calculating the spatial distribution of neutrons.

At still low - but not extremely low - energies, other reaction channels open, like (n,p) or (n,α). Most of them are useless for our purposes, or even detrimental. There are only a few reactions which are of interest. The ^{3}He(n,p) reaction was planned to be utilized for tritium production in the APT (Accelerator-based Production of Tritium) project, which at present is considered a backup option in the US. The "classical" tritium production reaction is ^{6}Li(n,α)t which has been run in special tritium production reactors, but it also plays a vital role in thermonuclear weapons.

Here I cannot resist the temptation to tell the story of when Shrimp went like gangbusters [1]. It is really a good illustration of the need to know nuclear reaction data in general, and what can happen if you do not know them in particular. The first hydrogen bomb, Mike in 1952, was essentially a huge dewar of liquid deuterium, ignited by a conventional fission bomb. This demonstrated that the fusion bomb principle works, but its total weight of 82 tons made it useless as a combat weapon. The next development was the Shrimp device of the Castle Bravo series. It consisted of ^{6}LiD, where energy is released in a two-step process. Tritons and deuterons fuse into alpha particles and a neutron, and the neutron subsequently produces new tritium by the ^{6}Li(n,α)t reaction. With this technique, bombs sufficiently light to be airborne are feasible.

What the construction crew had missed altogether was the relatively large ^{7}Li(n,2n) reaction. The lithium was not pure ^{6}Li, but enriched to 40 % (it is 7.5 % naturally) and thereby the rest was ^{7}Li. The ^{7}Li(n,2n)^{6}Li reaction increses the explosion yield in two ways; it increses the number of neutrons and it produces additional ^{6}Li, which can subsequently produce more tritium. The expected yield was 5 MT, but it went off with 15 MT, which makes it the largest US bomb ever. A Japanese fishing boat, *Fukuryu Maru* (the *Lucky Dragon*) was hit by radioactive fallout, and the crew members got ill, whereof one subsequently died from secondary infections. For obvious reasons, this event caused political complications in the relations between USA and Japan.

4 Why accelerator-driven systems?

Next question to ask is why accelerators should be used. Why not convert the waste in standard critical reactors?

Let us first give the wrong answer! There are examples of proponents of accelerator-driven systems (ADS) who claim that the key issue of ADS is that they are sub-critical and therefore inherently safe. That argument is not very well founded, because critical water-moderated power reactors have been run almost 10 000 production years by now, and up to now there has been only one serious incident. This was the Three-Mile Island accident in 1979, which destroyed a reactor and made the owners unhappy because of a lost investment, but it did not seriously injure a single person. In fact, to this very day, not a single person has died due to problems in a commercial water-moderated reactor. This makes them maybe the most safe technical systems ever built by man, and superior as safe technical systems for energy production [2].

The real reasons are that some elements are very difficult or impossible to incinerate in a critical reactor, but possible to handle in ADS. This is because of the (non-)existence of delayed neutrons. In a standard critical power reactor, ^{235}U is used as fuel. On average, thermal fission of ^{235}U results in 2.43 neutrons. Of these, exactly one should induce new fission events, and the remaining 1.43 should be removed by capture in, e.g., control rods. Suppose something happens that increases the power in the reactor, so that more neutrons are produced, leaving not 1.00 but 1.01 neutrons for new fission per neutron generation. The average time between neutron release and next fission is of the order of 10^{-6} s. In one second, this should result in $1.01^{1000000}$ neutrons, which is a number larger than the number of electrons in the universe. Without some way to slow down things, a 1 % mistake would blow up the reactor in fractions of a second, i.e., much faster than a normal human being can react.

Nature is kind enough to provide a solution: delayed neutrons. All the 2.43 neutrons are not released simultaneously. Almost all are emitted very rapidly, but a small fraction, about 0.7 %, are emitted after beta decay to neutron-unstable states, and are therefore released after anywhere from fractions of a second up to a few minutes. This makes it possible to build a less "nervous" system. The reactor can then be designed in such a way that 0.993 prompt neutrons are available for next fission generation, i.e., the reactor is slowly stopping, but 0.007 additional neutrons appear a few seconds later. Now the neutron economy balances, and the characteristic time constant is slow. A mistuned knob will then result in a slow change of the reactor.

Now back to the original issue. ^{235}U is a very favourable case. Most elements have fewer delayed neutrons, and some elements we want to get rid of have virtually no delayed neutrons at all. This means that, e.g., some americium isotopes are very difficult to burn in critical reactors. A way out of this dilemma is to build a sub-critical system, in which every fission chain is slowly dying, but new chains are initiated by externally produced neutrons. The role of the delayed neutrons is now replaced by the accelerator-produced ones.

5 Which data are of interest for accelerator-driven systems?

5.1 Direct measurements or data for theory?

In section 3, the useful reactions for waste incineration were discussed. This does not mean, however, that these reactions are the only ones to be studied. Many unwanted reactions will also take place, and these need to be known as well. In addition, it is even possible that completely different reactions are even more interesting for our application, although they do not contribute at all (!). How can this be the case?

We have to realize that the task to measure everything that will happen in a future transmutation plant is an insurmountable one. First of all, this is because of practical limitations. At high energies, above 50 MeV or so, *one* cross section for *one* nucleus at *one* energy typically requires about a week of beam time at an international accelerator laboratory. Loosely calculated by industry standards, one week represents a cost of the order of 1 MUSD. Covering all relevant reactions for all relevant elements at moderate energy intervals would not only present costs approaching national budgets in size, it would

also literally take centuries to accomplish with the presently available laboratories.

Furthermore, even if the practical obstacles could be overcome, the situation would still not be satisfactory. In a reactor core, large quantities of short-lived elements can affect the operation, but these isotopes can be impossible to study in experiments. A good example is ^{135}Xe, the well-known villain of the Chernobyl accident with a half-life of 9 h, which makes it impossible in practice to make targets of it for in-beam measurements of cross sections.

All these conditions imply that all important data cannot be measured; instead theory has to be used for unmeasured regions. This in turn gives priority to measurements that are decisive for theory development, rather than direct measurements of specific cross sections. Hence, it is possible that reactions not even present in the system, or indirect quantities, should still be measured for theory development reasons.

5.2 Constraints imposed by accelerator-driven systems

In figure 1, a simplified accelerator-driven system (ADS) is illustrated. It consists of an accelerator producing a proton beam, a spallation target for neutron production, and a surrounding core for waste incineration and/or energy production. This simple picture illustrates the main areas for new nuclear data. First, proton-induced neutron production, i.e., (p,n) reactions, has to be known, and second, whatever these neutrons end up doing has to be investigated.

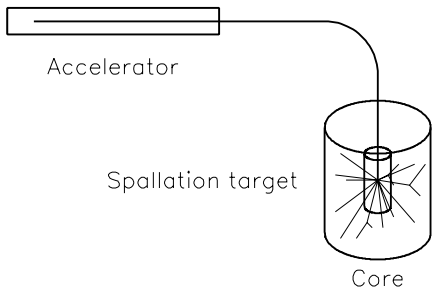

Figure 1: The basic ingredients of an accelerator-driven transmutation system.

The (p,n) reaction at small angles was extensively studied during the 1980's on a wide range of elements for completely other reasons [3], so that particular basic information is at hand. This is unfortunately not sufficient for spallation target modelling. When protons of more than 1 GeV hit a thick target, direct production is not the only neutron production process. Instead, a cascade of nuclear reactions can take place, with processes like (p,d) followed by (d,n), etc. A 1 GeV proton on a thick lead target produces about 20 neutrons via many such reaction chains.

Experimental studies of proton-induced neutron production has the interesting feature that the results depend on the target thickness. The optimal goal would be to disentangle the individual reactions and to calculate the total neutron yield as a sum of all possible reaction cascades. Since so many processes are involved, it is very difficult to measure them all with the technically required precision. Instead, integral measurements of the total number of neutrons are carried out, but then the result depends on the target thickness. Therefore,

some caution has to be used when estimating the neutron yield from a spallation target, based on experimental data on proton-induced neutron production.

If it is pretty evident which proton-induced reactions should be studied, i.e., (p,xn) at a few realistic energies for future ADS, the situation on neutron-induced reactions is less focused. Many reactions play important roles and at a very wide energy range. In most present design studies, the accelerator-produced neutrons comprise typically 5 % of the total number of neutrons. The rest are due to fission chain reactions. Thus, 95 % of all neutrons are at low energies, i.e., released at 2–3 MeV and rapidly thermalized to a few hundred keV in a lead(-bismuth) cooled system. Spallation results in a neutron spectrum with a roughly $1/E_n$ shape, peaking at only a few MeV. Hence, about 20% of the spallation neutrons are below 20 MeV already when coming out from the spallation target, which means that less than 1 % of all neutrons are above 20 MeV in the reactor core, even before moderation.

Thus, the bulk of neutrons are below 20 MeV. The present nuclear data libraries were originally motivated by data needs in power fission reactors or fission weapons (below 8 MeV), or in fusion research or thermonuclear weapons (14 MeV). The 20 MeV range was to large degree dictated by the presence at that time of tandems which could produce neutron beams up to about 20 MeV. Due to this, the data situation at low energies is rather satisfactory. Most elements have been thoroughly studied, but not all. Some isotopes remain to be investigated, and for others there are discrepancies in the data bases. These issues have motivated renewed interest in low-energy measurements, which will be covered by another contribution at this workshop [4].

At the highest energies, the number of neutrons is very small. In addition, theory works reasonably well above, say, 200 MeV. The reason is that at lower energies, the incident neutron has a de Broglie wave length corresponding to the radius of the nucleus. This implies that the entire nucleus, with all its structural properties participate in the reaction, making it exceedingly complex. At higher energies, the de Broglie wave length is about the size of individual nucleons, and the incident neutron interacts just once with a single nucleon. Accordingly, the reaction has a much simpler character, and can be described reasonably well with simple theory. (Well, simple for being nuclear theory...) Another way of illustrating the same effect is to note that a nucleon is typically bound by 8 MeV in a nucleus. This constitutes a major factor when a 10 MeV incident neutron interacts with it, but not when a 1000 MeV neutron shows up. The very high energies are the subject of a special session at this workshop [5].

There is a mid-range (often denoted "intermediate energy nuclear physics") from 20 to 200 MeV where data for applications are rather scarce, and where theory is not in a very good condition. This range is therefore a prime candidate for new measurements. In fact, in the EUropean joint project on high-energy data, HINDAS, the efforts on the 20–200 and 200–2000 MeV ranges are about equally large (see section 8), in spite of the latter being an order of magnitude larger in energy.

Throughout this paper, high energy means 20 MeV and up, unless something else is stated. The reasons are the ones given above; the availability of large data sets motivated by the classical nuclear applications up to about 20 MeV, and the virtual lack above 20 MeV, which has to be overcome now, when emerging applications demand such data.

5.3 Classification of data

To summarize; not even close to all data can be measured. Therefore, we have to make tough selections. The efforts should be concentrated along a few major lines:

1. **Data for theory development.** Such data need not to be strong reactions in a transmutation core, and they do not even need to be direct quantities. The optical model, which is the prime tool in nuclear models for these kind of systems, relies essentially on three types of experimental information; elastic scattering, and total and reaction cross sections.

   The elastic scattering cross section is the most important measurement when determining the optical model, which in turn is the standard representation of the force between a nucleon (proton or neutron) and a nucleus. The optical model is used as input in virtually every cross section calculation where a nucleon is present either in the incident or exit channel, and is therefore of major importance for theory development. This makes, e.g., neutron elastic scattering measurements much more important than they would be if they were only useful for direct use in calculations of the spatial distribution of neutrons in a core.

   The total cross section is the sum of all possible interactions, i.e., the probability that anything happens at all. The reaction cross section is the sum of all interactions except elastic scattering. These quantities can both be measured directly even if all the partial cross sections constituting it are unknown. Moreover, they can serve as guidance when different optical models all describe the same elastic scattering data well, but result in different rection cross sections.

2. **Strong reaction channels.** Elastic scattering is again a good example. At high energies, quantum mechanics requires elastic scattering to constitute at least 50 % of the total cross section, i.e., at least half of all what happens is elastic scattering. For high-energy neutrons, it turns out that elastic scattering in most cases constitutes about 50 %. Other strong reaction channels are (n,xp), (n,xn) and (n,xα). These four reaction channels (including (n,n)) typically accounts for about 99 % of all neutron-induced reactions.

3. **Data for special, important purposes.** Fission is a prime example. It is neither top-of-the-list for theory development nor a strong channel (except for some actinides), but its profound consequences makes it important for the overall assessment of the system. For instance, fission products account for a sizeable fraction of the residual radioactivity of the spallation target.

   Other examples are (n,xp) and (n,xα) cross sections for hydrogen and helium production. Since hydrogen is explosive, the production has obviously to be kept under control, or at least be known. In addition, hydrogen embrittles steel. Helium makes structural materials like steel swell, and data are therefore required for material aspects.

4. **Overall quantities.** For example, measurements of the total radioactivity after irradiation by residue detection are useful for cooling assessment.

6 The black magic of neutron experiments

A large majority of the experimental work for ADS concerns neutrons one way or the other, either in neutron production or neutron-induced reactions, or even both. In general, there are major additional experimental challenges when working with neutrons, compared to charged particles.

6.1 How many neutrons are there in the beam?

To measure a cross section, the intensity of the beam has to be known. A most notorious problem is how to determine the intensity of a neutron beam. This might sound like an innocent problem, but it is close to impossible to overcome it (!).

A charged particle interacts with the electrons of the atom. Thereby it is possible to build systems where *every* particle gives a signal when passing through a detector, and hence it is a relatively simple task to determine the beam intensity by just counting pulses. Another option is to stop particles via their energy loss - which is also an effect of interaction with the atomic electrons - and finally measure the collected charge. This is performed in every Faraday cup at every laboratory.

Neutrons interact by the strong interaction only, and they are uncharged. This means that there is no way you can build a device which produces a signal for each particle that passes, and you cannot stop neutrons in a controlled way. Detection of neutrons *always* has to proceed via a nuclear reaction, releasing charged particles, which can subsequently be detected. The problem is that there is no way to determine a nuclear cross section from theory only with a reasonable precision. This means we end up in circular reasoning.

Let us assume we want to use neutron-proton (np) scattering for neutron detection. Counting the protons emanating from a hydrogenous material is a simple task, but we need to know the cross section to derive the number of incoming neutrons. To measure that cross section, however, we need to know the number of incident neutrons. Are there no ways out of this vicious circle?

In fact, there are a few tricks which can be used, but they are all associated with large difficulties. The standard procedure is therefore to determine a single cross section using all these painstaking methods, and subsequently this cross section is used as *reference*, i.e., other cross section measurements are measured relative to it.

The standard reference cross section at our energies is np scattering. Suppose we want to measure ^{12}C(n,p). Instead of trying to measure the cross section on an absolute scale (which is virtually impossible), a typical experiment would be designed to measure the *ratio* of ^{12}C(n,p) versus np scattering. This facilitates the experimental work immensely.

A major risk with such an approach is that if the reference cross section is uncertain (or even wrong), all other data measured relative to it will be equally off. Such a case might in fact be at hand for neutrons above 50 MeV, where np differential cross section data display significant inconsistencies [6]. Not surprisingly, major experimental work is presently devoted to find agreement about the exact value of this reference cross section [7, 8, 9, 10] (see section 10).

The techniques used in these ongoing experiments are - as you could expect - the main tricks used to obtain absolute reference cross sections for neutron-induced reactions. Below, these techniques are described.

6.1.1 Tagged beams

The methodologically simplest method is probably to use tagged beams, but this does not necessarily mean it is the simplest technique in real life. Neutrons do not exist freely in nature (the life time is about 15 minutes) but have to be produced by nuclear reactions. For a few reactions, detection of the residual nucleus can be used to verify the neutron production. An example is the D(d,n)^{3}He reaction. By detecting the kinetic energy and direction of the residual ^{3}He nucleus, the energy and angle of the neutron is known. In addition, the detection of a ^{3}He nucleus implies that there *must* be a neutron, i.e., the ^{3}He nucleus serves as a "tag" on the neutron. With this technique, "beams" of really low intensity, but with known intensity can be produced. This beam can subsequently be used for cross section measurements.

Using this method for every cross section measurement is, however, not an option because of the extreme beam times required. Instead, it is used for precision determination of a reference cross section, which is subsequently used in other, relative, experiments (see above).

6.1.2 Combination of total and differential hydrogen cross sections

The total cross section, i.e., the probability that a neutron interacts at all with a target nucleus, is a quantity which can be determined without knowledge of the absolute beam intensity. This integral cross section is related to the attenuation of a neutron beam, which means that a relative measurement of the beam intensity before and after a target is sufficient.

In the case of hydrogen, the total cross section is completely dominated by elastic *np* scattering, which accounts for more than 99% of the total cross section. The only other reaction channels possible are capture (np $\rightarrow$ dγ) and bremsstrahlung (np $\rightarrow$ npγ), which both are orders of magnitudes weaker.

A relative measurement of the *np* scattering angular distribution can thereby be normalized to agree with the total cross section, and thus an absolute ^{1}H(n,p) cross section can be obtained.

6.1.3 Combination of total and reaction cross sections

The differential elastic cross section of a nucleus can be determined absolutely by a combination of total and reaction cross section measurements, together with a relative measurement of the differential elastic cross section. Both the total cross section and the reaction cross section can be determined in relative measurements of beam attenuation. The only important difference is the geometry used. The integrated elastic cross section can then be derived as the difference of the total and reaction cross sections. The elastic differential cross section on almost any nucleus falls dramatically with angle. Thus, by covering a moderately wide range at forward angles, essentially all the elastic differential cross section is covered. Thereby, the differential cross section can be related to the integrated elastic cross section. This technique works best for light nuclei, where there are only a few excited states with large separation in excitation energy. The reason is that the reaction cross section measurements often are plagued with a poor energy resolution, which results in contamination of inelastic scattering into the data.

6.1.4 Theoretically "known" reactions

Above 275 MeV, pion production opens up in neutron-proton reactions. The np $\rightarrow$ dπ^0 reaction should have exactly half the cross section of the pp $\rightarrow$ dπ^+ reaction, if isospin were a good symmetry, all particle masses were the same and there were no Coulomb effects. The latter reaction involves charged particles only, and should therefore be possible to determine accurately.

This technique has been frequently used for normalization of *np* scattering experiments above the pion production threshold, where protons from np $\rightarrow$ pn reactions and deuterons from np $\rightarrow$ dπ^0 reactions are detected simultaneously. Assuming the latter cross section to be known, using the relation between neutron- and proton-induced pion production can then provide an absolute cross section. This method is the least exact of the ones presented here, however, because it involves rather large, and partly unknown, corrections.

6.2 How large is a neutron detector?

In any experiment aiming at measuring a cross section, knowledge of the solid angle subtended by the detector is required. In charged-particle measurements, it is common to define the solid angle by either a passive collimator in front of the detector, which physically stops the particles, or by an active collimator, i.e., a detector with a hole so that particles hitting the collimator produce signals, which in turn are used for event rejection.

At really low neutron energies, passive collimators can sometimes be used, because there are a few elements (e.g., boron and cadmium) which possess huge capture cross sections, and thus very efficiently remove neutrons. These large capture cross sections are present only up to a few eV energies though. At slightly higher energies, collimation can still be obtained by having a moderator (like paraffin) doped with, e.g., boron. Thus, neutrons are moderated and then captured.

Above 20 MeV, such techniques are completely useless. There are no strong capture cross sections, and the scattering cross sections needed for moderation are so small that any reasonably well-working collimator has a thickness of the order of metres (!). In addition, at these energies many particle-production channels are available. Thereby, a collimator can sometimes produce almost as many particles as it removes. The bottom line of this discussion is that in most cases detectors without front collimation is the preferred choice. This is often referred to as "naked" detectors, which is a truth with qualification. Often the detectors have very heavy sheilding at the sides and back to protect them from ambient room background.

Since collimators cannot be successfully used, it is sometimes very difficult to know the effective size of a detector. A good example is provided by a recent state-of-the-art determination of the efficiency of a liquid scintillator detector, which has been used in proton-induced neutron production experiments for ADS [11]. The efficiency of this detector was measured in a tagged neutron experiment (see above), where the position and direction of the incident neutron was well known. Thereby, the detection efficiency for different physical parts of the detector could be determined. It was found that the efficiency was constant over most of the area, and that it dropped close to the edges, which was expected. It was also found, however, that some signals in the detector corresponded to neutrons not even hitting the detector. The reason for this weird effect was that there is a plastic front layer in the

detector, which extends outside the active area of the detector. Thus, neutrons which would have barely missed the detector had been scattered into the detector, raising its apparent efficiency significantly. This illustrates that the effective area of a neutron detector might not be straight forward to establish, and the question in the headline of this section might not be as stupid as it sounds at first.

7 How are high-energy neutron experiments carried out?

Rather than presenting a long list of different kinds of experiments, we are going to go through a case study: elastic neutron scattering. The choice of reaction is partly dictated by convenience (the author has some experience of it) but it is also a good illustration of all the problems associated with high-energy neutron work, because it involves neutrons both in the incident and exit channel. Thus, it gives you all the trouble...

7.1 Neutron production

The first obstacle is neutron production. At low energies (below 20 MeV or so) monoenergetic neutron beams can be produced. There are a few light-ion reactions, like D(d,n)^{3}He and T(d,n)^{4}He, which have positive Q-values and sizeable cross sections. The most widely used reaction is T(d,n)^{4}He, where deuterons of only a few hundred keV can produce 14 MeV neutrons.

Such a beam is strictly monoenergetic up to about 2 MeV incident deuteron energy. Above this energy, there is a possibility that the deuteron breaks up (it has a 2.2 MeV binding energy) into a proton and a neutron. Hence, strictly monoenergetic neutron beams are only possible up to about 16 MeV (i.e., 2 MeV beam plus 14 MeV Q-value). In reality, this is not a major obstacle until you get up to about 30 MeV or so, because the T(d,n)^{4}He cross section is so large that the breakup neutrons form only a small low-energy tail. At even higher energies though, the T(d,n)^{4}He cross section is smaller, making the total yield too low for most measurements.

The breakup effect is there in all nuclei, and in almost all nuclei neutrons are bound by about 8 MeV. The largest neutron separation energy is about 20 MeV. The consequence of this is that truly monoenergetic beams are impossible to produce above that energy. What is available at higher energies are quasi-monoenergetic beams, i.e., beams where a single energy dominates, but it is always accompanied by a low-energy tail.

If we go to energies at 50 MeV and up, three production reactions give reasonably monoenergetic beams. These are D(p,n), ^{6}Li(p,n) and ^{7}Li(p,n). The first has a large cross section, but the drawback that the energy resolution of the full-energy neutrons cannot be better than 3 MeV due to the Fermi motion of the neutron inside the deuteron. If a sharper energy definition is required, one of the two reactions using lithium is selected. They are about equally good, but there is a major practical difference: ^{6}Li is used in hydrogen bombs and is therefore not easily obtained, while ^{7}Li is provided more or less for free. As one could expect, ^{7}Li(p,n) is the most common production reaction for monoenergetic neutron beams. At 100 MeV, about 50 % of the neutrons fall within 1 MeV at maximum energy, while the

remaining half are distributed about equally from maximum energy down to zero. This is the closest to monoenergetic conditions nature provides.

There is also a completely different approach to the whole production. Instead of trying to get the neutrons as well gathered in energy as possible, all energies are produced simultaneously. A high-energy proton beam hits a thick (mostly stopping) target and lots of neutrons of all energies are produced, with typically a $1/E_n$ spectrum. If the incident proton beam is bunched and the experiment target is placed at a rather large distance from the neutron production target, time-of-flight (TOF) methods can be used to determine the energy of the incident neutron on an event-by-event basis.

The advantage of such so called white beams is the total intensity, which is larger than for monoenergetic beams, but instead the intensity per energy interval is much lower at high energies. This can partly be compensated by summing data over limited energy intervals, but still the intensity per such interval is lower. The advantage of being able to measure at many energies simultaneously is not worth much if you get insufficient statistics everywhere. As a consequence, white beams are restricted to experiments at low energies, where the intensities are large, or to high-energy reactions where the cross sections are rather large. Another feature is that white sources require event-by-event measurements. Experiments of effects with an energy dependence where the individual events cannot be distinguished cannot be performed at white beams. For experiments fulfilling the requirements above, white sources can, however, provide large quantities of very valuable information. This is especially true when excitation functions, i.e., the energy dependence of a cross section, is of particular interest.

The total cross section data from Los Alamos could serve as an example [12], where many thousand data on a wide range of nuclei in the energy range from a few MeV up to over 500 MeV have been acquired. Producing data of similar quality at monoenergetic beams would be extremely time-consuming.

7.2 Neutron detection

Just detecting a neutron at all can be hard enough, but isolating a certain final nuclear state is even more difficult, because it requires energy measurement of the neutron. Since the neutron must be converted to a charged particle via a nuclear reaction to be detected at all, we easily run into trouble. Most nuclear reactions can produce charged particles at many different energies, and hence there is not direct correspondence between the detected charged-particle energy and the incident neutron energy. This restricts the possible techniques for neutron spectrometry immensely.

At low energies, where the T(d,n) reaction is used for neutron production, the standard technique for elastic scattering measurements is time-of-flight. A pulsed deuteron beam hits a tritium target, thereby producing pulsed neutrons. These neutrons are scattered from a target and hit a fast detector, almost always a liquid scintillator, with an intrinsic efficiency of the order of 10 %. This detector only needs to register that a neutron hit it, and at which moment. Thereby, the energies of the released charged particles in the detector do not need to be well known. The flight time is provided by the time difference between the deuteron pulse hitting the tritium target and the stop pulse from the neutron detector.

At these energies, the deuteron beam stops in a thin metal foil. The beam stop is then made of an element with a high threshold for neutron emission, so that all neutrons emanate

from the tritium target. The scattering target can be located very close to the neutron production, and the total flight path needed to resolve nuclear final states is a few metres. If a large hall is available, the detection system with its shielding can be placed on a rotating system. If not, it is customary to use a fixed flight path and instead rotate the incident beam at the neutron production with a beam swinger, consisting of a moveable magnet system.

When going above 50 MeV, the conditions change significantly. Time-of-flight techniques become gradually more difficult to use with increasing energy in a more than linear fashion. With a total time resolution of 1 ns, one will get an energy resolution of 0.5 MeV with a flight path of 5 m at 20 MeV, while for the same energy resolution at 100 MeV, 60 m is needed. This would require a very large array of neutron detectors to preserve a reasonable solid angle and count rate. Even if accepting a 2 MeV resolution, the flight path is 15 m, which is too long for a rotating detector system. This leaves a beam swinger as the only alternative.

This will not solve all problems, however. At these high energies, the beam stop for the incident charged beam needs to be many centimetres thick, and we are above the neutron production thresholds for any material. This means that a vast majority of all neutrons produced come from the beam stop and not the production target. A solution to this dilemma is to move the beam stop away from the neutron production by a second beam swinger system. This does not only cost lots of money; it also costs count rate, because it increases the production-to-target distance, and the neutron intensity at target falls with the square of this distance.

One way out of this dilemma is to use a completely different approach. If we skip the time-of-flight technique altogether, and instead detect neutrons by conversion to charged particles, where the energy of the latter is measured, we can shorten the distance from the scattering target to detection to about 1 m. A typical converter is a material containing hydrogen, with conversion via *np* scattering. Detection of the direction and energy of secondary protons can the be used to determine the energy and direction of neutrons hitting the converter. Now it is relatively easy to get a large detection solid angle, but this is also a pre-requisite, because the conversion efficiency is inherently low, far smaller than 1 %. With such a technique, we can allow a longer (and fixed) distance from neutron production to scattering target which makes a nice dumping of the initial beam feasible.

It should be pointed out that for all other reactions than elastic scattering, we get an additional problem. The beam is not truly monoenergetic, and therefore TOF measurements are needed to reject the low-energy neutrons in the beam. This means that, e.g., inelastic scattering cannot be measured at all with TOF techniques at these energies, because TOF information is needed twice (production to scattering target and scattering target to detector) but only one TOF measurement is available (production to detector).

8 The HINDAS project

As has been described already, the data needs for development of accelerator-driven systems can never be satisfied by measurements only. Theory has to be used for unmeasured (or unmeasurable) regions. Even with an optimum coordination between experiment and theory, the data requirements would require large efforts at many laboratories over a long time. Thus, some kind of structure and organization is called for. Such a framework exists, and below it

is briefly outlined. In section 9, the ongoing work is described in more detail.

HINDAS (High- and Intermediate-energy Nuclear Data for Accelerator-driven Systems) is a joint European effort, which gathers essentially all European competence on nuclear data for transmutation in the 20-2000 MeV range. The program has been designed to obtain a maximal improvement in high-energy nuclear data knowledge for transmutation. This goal can only be achieved with a well-balanced combination of basic cross section measurements, nuclear model simulations and data evaluations. The three elements iron, lead and uranium have been selected to give a representative coverage of typical materials for construction, target and core, respectively, especially relevant to ADS, as well as to supply a wide coverage of the periodic table of elements.

In total, 16 universities or laboratories participate. Of these, 6 have experimental facilities. This means that HINDAS involves essentially all relevant European laboratories in its energy range. This distribution and coordination of experiments at many laboratories makes the work very efficient. What is noteworthy is that HINDAS involves many partners and even laboratories which have previously not been involved at all in activities on nuclear data for applications. Thus, HINDAS has already widened the field of applied nuclear physics.

HINDAS is coordinated by UCL, Louvain-la-Neuve, Belgium. The total EU funding is about 2 MUSD. To this should be added matching funding, equipment and infrastructure from the participating countries.

Two other EU projects deal with aspects of nuclear data for transmutation, the NTOF-ND-ADS project at CERN and MUSE in Cadarache. These two projects are primarily devoted to lower energies. The three data-related projects are clustered as a sub-group, BASTRA (Basic Studies on Transmutation), of a wider cluster linking all EU projects on partitioning and transmutation.

8.1 Organization of the research work

The project is carried out in eight work packages (WP). WP 1-3 concerns experiments in the 20–200 MeV range, WP 4-6 deals with 200–2000 MeV experiments, and WP 7 and 8 are devoted to theory for the 20–200 and 200–2000 MeV regions, respectively.

The division into two energy ranges is natural, since there appear to be a transition region around 200 MeV for the theoretical models. Below this energy the theoretical calculations have to include direct interactions, as well as preequilibrium, fission and statistical models, whereas at higher energies the intra-nuclear cascade model, together with fission and evaporation models, have to be considered. As a coincidence, the experimental facilities and the measurement techniques are also different below and above about 200 MeV.

The experimental WPs are structured according to type of particles produced. This means that for each energy range, there are WPs on production of light ions, neutrons and residues, resp. Below, the WPs are described briefly:

1. **Light charged-particle production induced by neutrons or protons between 20 and 200 MeV (Lead contractor: Université Nantes, France).**

   The double-differential cross sections for proton- and neutron-induced production of hydrogen and helium ions on iron, lead and uranium isotopes are being measured at UCL-Louvain, TSL-Uppsala and KVI-Groningen. These measurements aim at providing essentially complete data in both emission angle and ejectile energy. Such double

differential cross sections constitute a very stringent test for theoretical models in this energy domain. In addition, charged-particle multiplicities in proton-induced reactions are measured at KVI.

2. **Neutron production induced by neutrons or protons between 20 and 200 MeV (Lead contractor: Uppsala University, Sweden).**

   Neutron elastic scattering measurements, (p,xn) and (n,xn) measurements on iron, lead and uranium are performed at UCL-Louvain and TSL-Uppsala. Elastic scattering measurements are useful not only for optical model development, but can also be used directly for neutron transport calculations. The (n,n) and (n,xn) measurements make use of novel detection techniques, while (p,xn) reactions are studied using liquid scintillator detectors with time-of-flight techniques.

3. **Residual nuclide production induced by neutrons and protons between 20 and 200 MeV and production of long-lived radionuclides (Lead contractor: Hannover University, Germany)**

   Measurements of proton-induced production of residual nuclei are carried out at PSI, while neutron-induced production is studied at UCL-Louvain and TSL-Uppsala, where also neutron-induced fission is measured. For the short-lived residual radionuclides, cross sections are determined using activation techniques. The production of long-lived radionuclides is studied by Accelerator-Mass Spectroscopy (AMS) after chemical separation at ETH-Zürich.

4. **Light charged-particle production above 200 MeV (Lead contractor: FZ Jülich, Germany)**

   The proton- and deuteron-induced production cross sections of protons and alpha particles are measured with a 4π silicon ball detector at the COSY accelerator in Jülich. Experiments on thin targets aim for tests of the intra-nuclear cascade model, while thick-target studies are focused on benchmarking transport codes. These measurements will also help to evaluate gas production in the window and structure materials of an ADS, which will give implications for the lifetime of such components. With the PISA setup, it will also be possible to measure total and double-differential cross sections for production of spallation products.

5. **Neutron production induced by protons above 200 MeV in thin and thick targets (Lead contractor: CEA-Saclay, France)**

   Double-differential neutron production cross sections, for both thin and thick targets, have recently been measured at SATURNE using time-of-flight or magnetic spectrometer techniques. At FZ Jülich, multiplicities of neutrons up to 150 MeV are being studied event-wise with a 4π liquid scintillator, using both thin and thick targets. The two experiments are complementary, both for technical and physics reasons. E.g., comparisons can be made between the directly measured multiplicities with those inferred from integration of the double-differential data.

6. **Residual nuclide production above 200 MeV in inverse kinematics (Lead contractor: GSI, Germany)**

Proton- and deuteron-induced nuclide production is measured in inverse kinematics, i.e., a lead or uranium beam hits a liquid hydrogen or deuterium target, and the spallation products are identified in flight using a high-resolution magnetic spectrometer. In this way all spallation products, irrespective of half-life, can be measured. These new data will be useful when calculating the radioactive inventory, the radiotoxicity and the breeded impurities in a realistic spallation target of an ADS.

7. **Nuclear data libraries and related theory (Lead contractor: NRG, Netherlands)**

   This work package concerns nuclear model calculations for analysis of the experimental data provided by WP 1-3, i.e., between 20 and 200 MeV. Special emphasis will be put on providing as complete information as possible on cross sections for all possible outgoing channels of iron, lead and uranium, and to construct improved nuclear data libraries, extending to 200 MeV.

8. **High energy models and codes (Lead contractor: Université de Liège, Belgium)**

   This work package is devoted to theory for WP 4-6, i.e., above 200 MeV, and regards mainly the intra-nuclear cascade model and the evaporation and fission models. The main objective is the development of powerful and accurate tools to calculate nucleon-nucleus spallation reactions.

9 Survey of ongoing experimental work

9.1 Elastic neutron scattering

Every physics student has to take a course on basic optics. In all such courses, the diffraction of light by slits and grids is treated. In a two-slit diffraction setup, the intensity versus angle shows a chacteristic pattern, with intensity maxima and minima overlayed on an overall intensity decrease. This effect is due to constructive and destructive interference of waves passing through the two slits.

When neutrons are scattered elastically from a nucleus, a similar effect occurs due to interference of neutron waves on each side of the nucleus. The nucleus itself is strongly absorbing, being almost "black" for incident neutrons. There is hence a direct analogy between optics and neutron scattering.

A real potential can only cause scattering. This is because a real potential conserves the flux, i.e., the number of incident and emitted particles has to be the same (and they have to be of the same type). Nuclear reactions, on the other hand, violates this conservation. This means we need an imaginary potential to account for particle changes or losses.

This is another analogy with optics. A real refraction index can only describe scattering of light, but not intensity losses. For that, an imaginary refraction index has to be used.

When we want to describe the interaction between a neutron and a nucleus, the simplest potential we can use has two components, one imaginary and one real, and this is called *optical potentials* because the approach was inspired by optics. Such optical potentials are

true work horses of nuclear physics. Whenever a neutron impinges on, or is being emitted from, a nucleus, an optical potential is used to describe the motion.

The major features of these optical potentials are derived from elastic scattering data. Such data are therefore not only needed for calculations of neutron transport and moderation, but they are also a necessary component in the description of many other reaction channels.

In addition, the elastic cross section is also the largest of the individual partial cross sections contributing to the total cross section. In fact, a consequence of the optical model is that the elastic cross section must constitute at least half the total cross section.

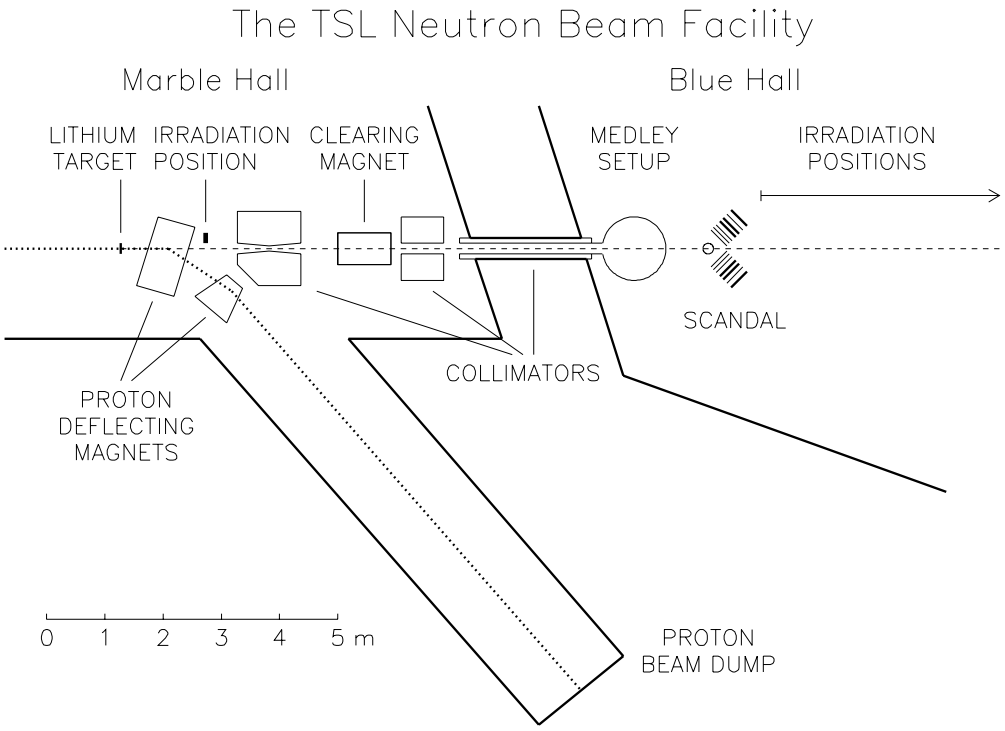

Figure 2: The TSL neutron beam facility.

Given the time and cost to carry out elastic scattering experiments, the main focus must be on developing theoretical models rather than systematically measuring all nuclei. The obvious nuclei to study are then the magic or semi-magic nuclei, i. e. ^{12}C, ^{16}O, ^{40}Ca, ^{90}Zr and ^{208}Pb. Here it is fortunate that lead (cooling) and zirconium (cladding) are also important materials in future transmutation facilities, so the gain is twofold.

A facility for detection of scattered neutrons, SCANDAL (SCAttered Nucleon Detection AssembLy), has recently been installed at the The Svedberg Laboratory (TSL) in Uppsala, Sweden. It is primarily intended for studies of elastic neutron scattering, but can be used for the (n,p) and (n,d) reactions as well. The energy interval for detected neutrons is 50–130 MeV, which makes the facility suitable for studies of transmutation-related cross sections.

At the neutron facility at TSL [14, 15] (see fig. 2), neutrons are produced by the ^{7}Li(p,n) reaction. After the target, the proton beam is bent by two dipole magnets into an 8 m concrete tunnel, where it is focused and stopped in a well-shielded carbon beam-dump. A narrow neutron beam is formed in the forward direction by a system of collimators.

The setup is primarily intended for studies of elastic neutron scattering, i. e., (n,n) reactions. The neutron detection is accomplished via conversion to protons by neutron-proton scattering. In addition, (n,p) reactions in nuclei can be studied by direct detection of protons (see section 9.2). This is also used for calibration of the setup.

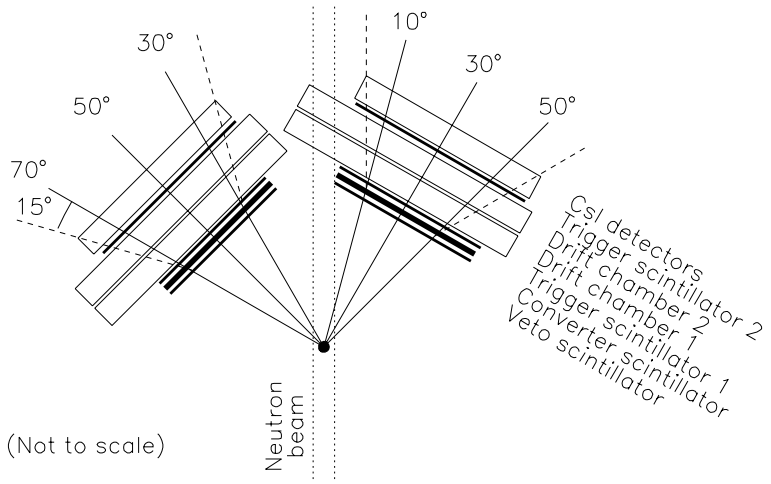

Figure 3: Schematic figure of the SCANDAL setup

The device is illustrated in fig. 3. It consists of two identical systems, typically located on each side of the neutron beam. The design allows the neutron beam to pass through the drift chambers of the right-side setup, making low-background measurements close to zero degrees feasible.

In neutron detection mode, each arm consists of a 2 mm thick veto scintillator for fast charged-particle rejection, a neutron-to-proton converter which is a 10 mm thick plastic scintillator, a 2 mm thick plastic scintillator for triggering, two drift chambers for proton tracking, a 2 mm thick ΔE plastic scintillator which is also part of the trigger, and an array of CsI detectors for energy determination. The trigger is provided by a coincidence of the two trigger scintillators, vetoed by the front scintillator. If used for (n,p) studies, the veto and converter scintillators can be removed, and additional drift chambers can be mounted if desired.

In a typical experiment, the two arms will be located such as to cover 10–50°, and 30–70°, respectively. For a one-week run on ^{208}Pb, the total number of counts for a one-degree angular bin is expected to be about 5 000 at 10°, and 1 at 70°, illustrating that the cross section falls off rapidly with angle.

At present, data have been taken on ^{12}C and ^{208}Pb. In addition, ^{1}H has been studied for normalization purposes. The full resolution is in the 3–4 MeV range.

9.2 Neutron-induced charged-particle production reactions

Production of protons and α particles have to be known in an ADS, because protons finally end up as hydrogen, which is explosive and causes embrittlement, and α particles can cause swelling of structural materials, like steel.

Data on (n,xp) reactions are also useful for model development. This is particularily true for precompound (or preequilibrium, that is essentially the same) reactions. When a low-energy neutron (or whatever particle) hits a nucleus, it is absorbed and moves around inside the compound nucleus in a chaotic fashion. In this process, the incident energy is dissipated on many nucleons in the nucleus, and the "memory" of the incoming particle is lost. Eventually, a particle is emitted, but this can now be described by purely statistical parameters. At much higher energies, the incident neutron interacts with just one single nucleon in a direct reaction, where all the other nucleons act more or less like spectators. This makes reaction theory relatively simpler above about 200 MeV.

There is an intermediate region from, say, 20 to 200 MeV where both direct and compound processes have to be taken into account. Moreover, there are also processes which are some kind of compromises between the two extremes; the incident neutron interacts a few times with a few nucleons. This is called precompuond reactions. Direct reactions typically result in emitted particles of high energies, while compound processes produce low-energy ejectiles. Preequilibrium reactions are found somewhere half the way, at intermediate ejectile energies.

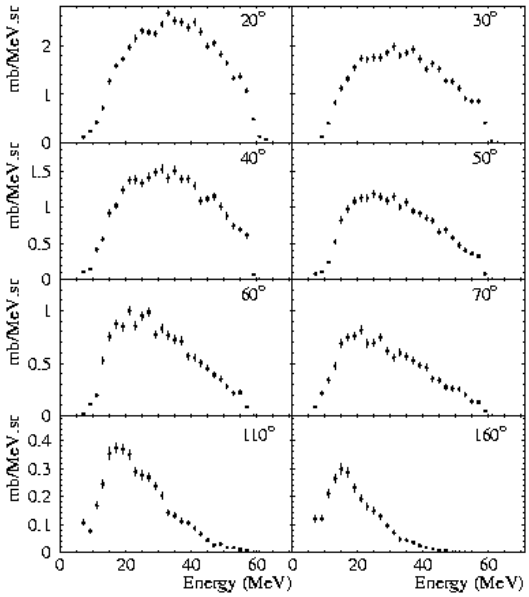

Figure 4: Double-differential cross sections for the Pb(n,xp) reaction at 62.7 MeV neutron energy, measured at Louvain-la-Neuve [13].

For precompound model development, measurements of (n,xp) reactions at these intermediate ejectile energies are therefore of high priority. In real experiments, however, it is even better to cover as complete emission energy ranges as possible. If all secondary particle energies are measured, the interplay between compound, precompound and direct processes can be studied. An example is given in figure 4, where Pb(n,xp) data from Louvain-la-Neuve at 62.7 MeV neutron energy are displayed [13].

Typically, such measurements are carried out using particle telescopes. Energy determination is not sufficient by itself to know the particle type, but a combined energy loss and full energy measurement is needed. The standard technique is to use a thin ΔE and a thick

(stopping) E detector. When you go to higher incident energies, the range of ejectile energies also gets larger, but even more so the range of stopping powers. This makes it very difficult to construct two-detector telescopes which makes a good job all the way. This is because the ΔE detector must be thin enough to allow low-energy particles to punch through, but then the signal from high-energy protons becomes so small that it drowns in the electronic noise. Three-detector telescopes are then a way out of this dilemma. An example of such a facility is MEDLEY [16], which uses eight telescopes, each being a Si-Si-CsI stack. The silicon detectors are about 50 and 500 μm thick, respectively, and the CsI detector is 3 cm thick, sufficient for stopping 100 MeV protons. With this setup, a very wide dynamic range, from 3 MeV α particles up to 100 MeV protons, can be covered.

Such a telescope setup has the advantage that it can provide data of a wide energy and angular range, but with the drawback that the solid angle of each telescope is rather limited, with statistics limitations as a consequence. Recently, a series of (n,xp) experiments have been carried out using both the MEDLEY and SCANDAL setups. SCANDAL has a very large solid angle, and it can be used as proton detector. Its dynamic range is, however, smaller. The combined setup thus produces both wide-range data with moderate statistics, and moderate-range data with superior statistics.

9.3 Proton-induced charged-particle production reactions

The motivations for studies of proton-induced charged-particle production reactions are essentially the same as for neutron-induced ditto, however with the extra pre-requisite that measurements in coincidence with low-energy neutrons are of special interest.

This is because one of the weak spots in modelling of ADS is the neutron production cascade in the spallation target. The final result of this cascade has been studied experimentally, by neutron multiplicity measurements. These studies, albeit valuable by their own merits, still do not disentangle the very complex chain of events resulting in neutrons. If the ambition is to get such a full understanding, cross sections for each step in the chain have to be known. If such measurements are carried out in coincidence with neutron multiplicity studies, the possibilities to link the bulk effects and individual cross sections are improved.

A 4π silicon ball for charged-particle detection for incident proton energies up to 2.5 GeV is shown in figure 5. Up to now, it has been used at 0.8, 1.2, 1.8 and 2.5 GeV on several targets [17]. Development of a magnetic spectrometer setup for similar studies is underway.

9.4 Production of residues

Measurements of elementary reactions, like (p,n) or elastic scattering, can provide very essential information to guide theory development. The ultimate goal would be to have such a successful nuclear theory that all the complex phenomena taking place in an ADS could be modelled based on elementary theory only. This is, however, not the case (yet). Such models are relatively good at describing, e.g., neutron production in the spallation target, but they are notoriously unreliable when it comes to describe the production of residual nuclei, i.e., what is left over after neutron production. Such information is of great technological significance, because the radioactivity of the core after shutdown largely depends on this.

There are two main techniques for measurements of residual nuclide production; measurements of induced activity and inverse kinematics studies. Induced actitivy studies are

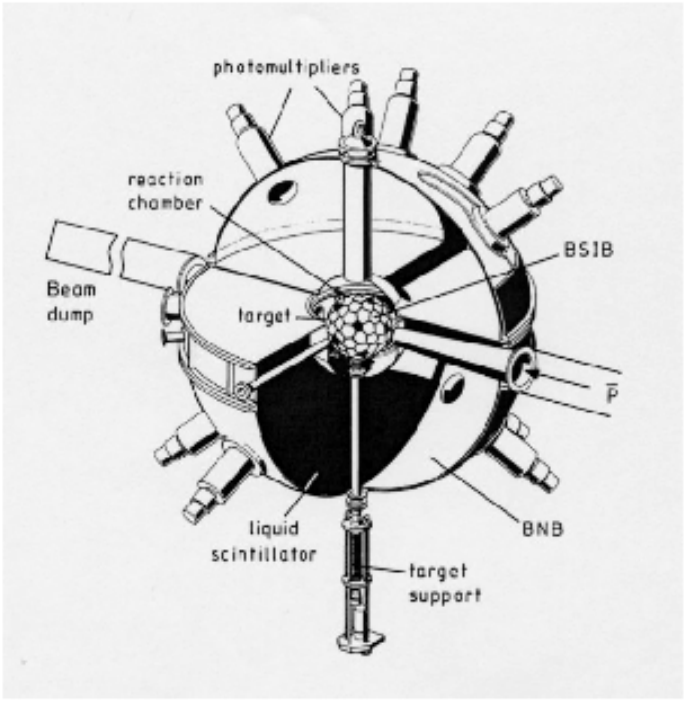

Figure 5: The Berlin ball detector system [17].

typically out-of-beam experiments [18]. They are performed by irradiation of a target, where the radioactive residual nuclei are detected afterwards by, e.g., γ spectrometry. These experiments often require long irradiation time, but since very little technology is needed during the actual irradiation, they can often be run as parasites on other experiments. This is particularily true for neutron beam experiments, where most often only a very small fraction of the beam is consumed by the primary experiment, which allows plenty of parasitic experiments further downstream in the beam. The long irradiation time needed can also be compensated by having many targets exposed simultaneously.

After irradiation, short-lived (minutes to years) radioactive nuclides are detected, most often with γ spectrometry using germanium detectors. This technique allows a very large number of integrated production cross sections to be determined, because all γ-emitting products can be detected. An example is shown in figure 6, where cross sections for production of various residues for protons on natural iron are presented [19].

With this technique, the stable products cannot be detected. This is, however, not such a terrible loss, because most nuclides are radioactive, and these studies are motivated by determining the induced activity. Another restriction is that radioactive nuclei with γ-free decay are missed. An example is ^{90}Sr, which contributes with a significant activity to spent fuel from standard power reactors of today, but it β decays by an electron (and neutrino) only, without γ emission. These restrictions of the method can be overcome by accelerator mass spectrometry (AMS), in which all residual nuclei, radioactive or not, are identified.

In particular for proton irradiation experiments above 200 MeV, a significantly different

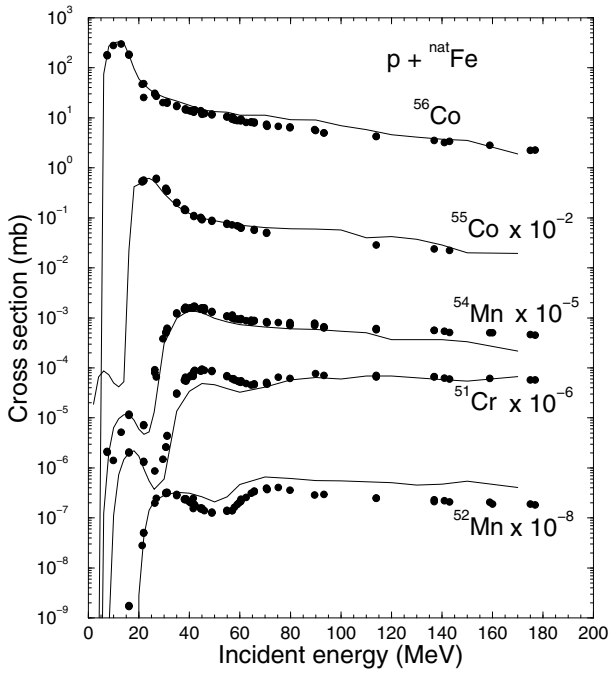

Figure 6: Cross sections for production of various residues for protons on natural iron [19]. The solid lines are predictions by the TALYS-0.36 model [20].

technique has been developed during the last few years [21]. Instead of sending a 1 GeV proton beam on a lead target, a 1 GeV per nucleon lead beam is impinging on a liquid hydrogen target. With this technique, the spallation products, which often have energies close to zero in standard experiments and therefore stop already inside the target, now move with about 1 GeV per nucleon. Thereby, they can be directly detected with standard techniques used in heavy-ion physics. Combinations of magnetic spectrometers, time-of-flight and energy loss measurements can provide unique identification of the emerging products.

An advantage with this method is that what you detect are the direct products, while in standard irradiation measurements, only the remaining elements after a waiting period can be determined. This makes the inverse kinematics method very useful for theory benchmarking when insight into the reaction mechanism is desired. In addition, it is possible to determine the kinetic energy of the products with this technique, which is of great value for assessment of structural damage in an ADS.

A disadvantage is that only one element can be studied at the time, which is not the case for induced-activity experiments. Moreover, interaction with neutrons cannot be studied directly. Instead, it has to be inferred from studies comparing liquid hydrogen and deuterium targets. Another limitation is that this technique is difficult to use at low energies.

The two techniques for measurements of residual nuclide production are not competitors. Rather, they complement each other and to some extent they can be used to verify results from the other.

9.5 High-energy neutron production

A central issue in ADS is the neutron production at the spallation target. This has been studied using two complementary techniques for the neutron detection. Time-of-flight has been used for low neutron energies, and conversion to protons in combination with a magnetic spectrometer at high energies. Thereby, the choice of techniques resembles the situation for the example of elastic neutron scattering discussed in section 7.

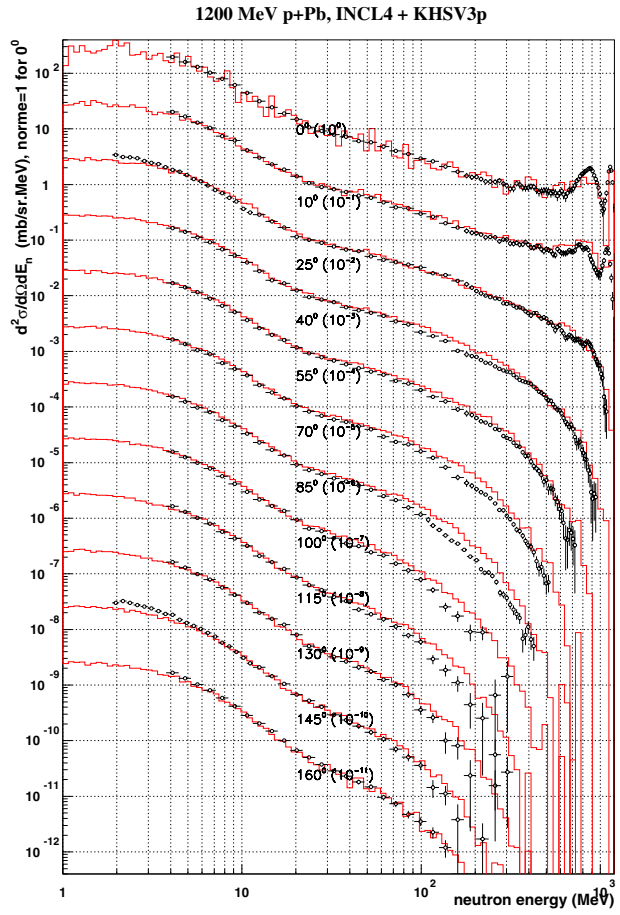

Figure 7: Differential cross sections for the ^{208}Pb(p,xn) reaction [22]. The histograms are calculations with the Liège intra-nuclear cascade (INC) model plus the KHSV3p evaporation-fission model [23, 24].

With this combination of methods, high-resolution neutron emission spectra from 2 MeV up to the incident energy, has been measured on several targets at 800, 1200 and 1600 MeV. Data on proton-induced neutron production on ^{208}Pb [22] are displayed in figure 7. These measurements will be discussed in some detail in another contribution to this workshop [5].

9.6 Fission

Although being a rather small cross section for all but the heaviest nuclei, fission plays a major role in ADS, even in places where you at first might not think about it. At low energies, fission is restricted to a few fissile nuclei, like ^{235}U, while at higher energies also much lighter nuclei - like lead - have sizeable fission branches. As an example, in a realistic ADS equipped with a lead spallation target irradiated with 1.6 GeV protons, 10–15% of the overall residual activity will be due to fission products after one year of cooling [25].

Among the most common degrees of freedom studied are the fission cross section and the relative yields of different fission products. At low neutron energies, plenty of data exist, while at energies above 50 MeV, only a few data on fission cross sections have been published, and fission yield data are virtually absent. There are good experimental reasons for this. At thermal energies, the fission process is easy to recognize, because essentially no other reactions producing large nuclear fragments are prevalent. At higher energies, however, effects of, e.g., multiple ion production can produce signals in a detector similar to those of fission fragments. Finding detectors sensitive to fission fragments but insensitive to lighter ions is therefore of high priority in these experiments.

Recently, experimental programs on fission cross section measurements using thin-film breakdown counters (TFBC) have been carried out [26, 27]. Such detectors have low intrinsic background and they are not sensitive to background from spallation residues which are produced in competition with fission. Up to now, data on one actinide, ^{238}U, and a few nuclei in the spallation-target regime, like ^{208}Pb and ^{209}Bi, have been published, while results on gold, tungsten and tantalum are underway.

10 The normalization of it all - *np* scattering

Last - but not least - we have to spend some efforts on determining the length of the yardstick with which all other information is measured. The *np* scattering cross section - in particular at 180° (C.M.), which corresponds to proton emission at 0° in the lab - is used to normalize measurements of other neutron-induced cross sections, i.e., it is the primary standard cross section. In addition, it plays an important role in fundamental physics, because it can be used to derive a value of the absolute strength of the strong interaction in the nuclear sector, commonly expressed as the pion-nucleon coupling constant, $g^2_{\pi NN}$. (See Ref. [6] for a review.) Large uncertainties for such an important cross section are therefore unacceptable.

Unfortunately, there are severe discrepancies in the data base on *np* scattering in the 100–1000 MeV range [28]. Uncertainties of 10 % or more are common, and thereby no other neutron-induced cross sections are known to better than that. Clearing up this mess should therefore be of high priority.

10.1 Backward *np* scattering

Backward *np* data have previously been measured by proton detection in the magnetic spectrometer LISA (Light Ion Spectrometer Assembly) at 96 MeV [29, 7] and 162 MeV [30, 8]. Relative angular distributions in the range 74°/72° (96/162 MeV, resp.) to 180° (c.m.) were obtained.

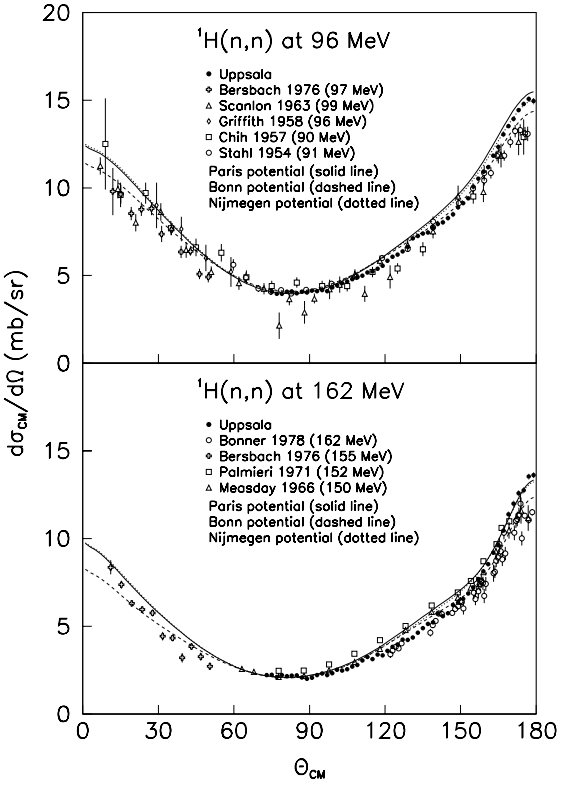

Figure 8: Differential np scattering cross sections at 96 and 162 MeV (filled circles). Also plotted are other data from the literature at energies close to 96 MeV [31, 32, 33, 34] (upper panel) and 162 MeV [35, 34, 36, 37] (lower panel). The lines show predictions for the Paris [38] (solid), Bonn [39] (dashed) and Nijmegen [40] (dotted) NN potentials.

Absolute np scattering cross sections were obtained by normalization to the total np cross section. The total cross section σ_T has been experimentally determined around 100–160 MeV by several groups, and is considered to be well known (about 1 % uncertainty). If the entire angular range, i.e., from 0° to 180°, had been measured, it would have been possible to normalize the data to the total cross section directly by integration. Since that was not the case, the angular distribution was considered as a measurement of a *fraction* (F) of the total cross section, i.e., the part between 74°/72° and 180°. By using a number of partial-wave analyses (PWA's) or potential models, it was possible to estimate the magnitude of this fraction, to which the data should be normalized.

The spread in F for the various PWA's and NN potential models has been used to estimate the precision of this normalization procedure, which was found to be $\pm 1.9\%$ and $\pm 2.3\%$ at 96 and 162 MeV, respectively.

The final data are presented in figure 8. A general feature is that the new data are about 10% higher at 180° and have a steeper slope in the $150° - 180°$ angular region than most of the older data in the same energy region. As a consequence, the slope is also steeper than several of the current PWA's and NN potential models, because these were to some extent

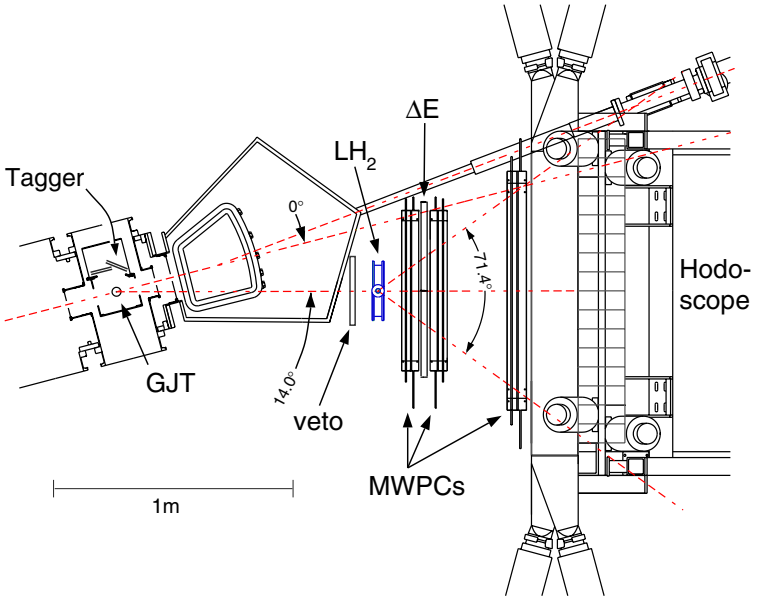

Figure 9: Overview of the IUCF tagged neutron setup [9].

fitted to the older data. A similar situation is also present at higher energies, where large data sets disagree significantly in shape. The shape of the TSL data is, however, in very good agreement with the new Franz *et al.* data [41].

10.2 Forward *np* scattering

As was mentioned above, if the entire angular range, i.e., from 0° to 180°, were known, it would have been possible to normalize the data to the total cross section directly by integration. This has motivated a recent experiment with SCANDAL (see section 9.1) on forward *np* scattering to cover the missing part of the angular distribution.

Subtraction of data obtained with CH_2 and carbon targets has been used to obtain the *np* differential cross section. Data analysis is in progress. The ambition is to provide a full angular distribution from 10° to 180° (c.m.), thereby obtaining a purely experimental *np* scattering cross section as reference for future measurements of neutron-induced cross sections.

This method provides a second, purely experimental normalization method, as outlined in section 6.1.3. By measuring CH_2 and carbon in the same experiment, the elastic cross section ratio of hydrogen versus carbon can be obtained. The elastic cross section of carbon can be determined absolutely by a combination of total and reaction cross section measurements. Both the total cross section and the reaction cross section can be determined in relative measurements of beam attenuation. The only important difference is the geometry used. The integrated elastic cross section can then be derived from the difference of the total and reaction cross sections. The elastic differential cross section on carbon falls dramatically with angle. With the present SCANDAL setup, essentially all the elastic differential cross section is covered. Thereby, the differential cross section can be related to the integrated

elastic cross section, and a second, independent normalization can be established.

As a byproduct of this, it is possible to obtain the C(n,n) elastic cross section as a secondary standard. This is very useful in elastic scattering experiments on heavier nuclei, because the C(n,n) cross section is relatively large, which allows good statistics for normalization in a rather short beam time, and carbon is easy to handle.

10.3 Tagged neutrons

Tagging (see section 6.1.1) provides another technique to obtain absolute normalization of neutron-induced cross sections. Such a facility has recently been developed at the cooler storage ring at Indiana University Cyclotron Facility (IUCF) [9] (see figure 9).

A circulating proton beam impinges on a deuterium gas-jet target. Neutrons are produced in the D(p,n)^{2}He reaction, where ^{2}He denotes two unbound protons in a relative $^1S_0$ state. By detection of these two low-energy protons, the neutron energy and angle are determined, which makes absolute cross section measurements feasible.

A setup for backward *np* cross section measurements is located close to the tagging facility. Test data have been obtained, and recently a large production run was performed.

It is interesting to compare the backward *np* measurements with LISA and the tagging experiment. The former is relatively easy experimentally, while the latter is very complicated. There is, however, a tradition at IUCF of successful completion of technically very challenging experiments.

It is tempting to speculate about the possible inpact of the IUCF experiment. If it turns out to agree with the TSL data, a new standard will be established, which would deviate significantly from the old one. If, on the other hand, the IUCF experiment corroborates the older measurements (and thereby the PWAs and *NN* models built upon those data), the TSL experiment has to be scrutinized or even repeated. If the IUCF data falls somewhere in between the TSL and old data, a re-evaluation of the systematic uncertainties in all measurements would probably be undertaken.

Acknowledgments

Many stimulating discussions with Nils Olsson are gratefully acknowledged. I want to thank Arjan Koning for providing some figures. This work was supported by the Swedish Natural Science Research Council, Vattenfall AB, Swedish Nuclear Fuel and Waste Management Company, Swedish Nuclear Power Inspectorate, Barsebäck Power AB, the EU Council, and the Swedish Defence Research Agency.

References

[1] R. Rhodes, *Dark sun - The making of the hydrogen bomb* (Simon & Schuster, New York, 1995).

[2] H.W. Lewis, *Technological risk* (W.W. Norton & Company, New York, 1990).

[3] J. Rapaport and E. Sugarbaker, Ann. Rev. Nucl. Part. Sci. **44**, 109 (1994).

[4] L. Tassan-Got, in these proceedings.

[5] S. Leray, in these proceedings.

[6] Critical Issues in the Determination of the Pion-Nucleon Coupling Constant, ed. J. Blomgren, Phys. Scr. **T87** (2000).

[7] J. Rahm, J. Blomgren, H. Condé, S. Dangtip, K. Elmgren, N. Olsson, T. Rönnqvist, R. Zorro, A. Ringbom, G. Tibell, O. Jonsson, L. Nilsson, P.-U. Renberg, T.E.O. Ericson and B. Loiseau, Phys. Rev. **C57**, 1077 (1998).

[8] J. Rahm, J. Blomgren, H. Condé, K. Elmgren, N. Olsson, T. Rönnqvist, R. Zorro, A. Ringbom, G. Tibell, O. Jonsson, L. Nilsson, P.-U. Renberg, T.E.O. Ericson and B. Loiseau, Phys. Rev. **C 63**, 044001 (2001).

[9] T. Peterson, L.C. Bland, J. Blomgren, W.W. Jacobs, T. Kinashi, A. Klyachko, P. Nadel-Turonski, L. Nilsson, N. Olsson, J. Rapaport, T. Rinckel, E.J. Stephenson, S.E. Vigdor, S.W. Wissink, Y. Zhou, Nucl. Phys. **A 663&664**, 1057c (2000).

[10] C. Johansson, J. Blomgren, A. Ataç, B. Bergenwall, S. Dangtip, K. Elmgren, J. Klug, N. Olsson, S. Pomp, A. Prokofiev, T. Rönnqvist, U. Tippawan, O. Jonsson, L. Nilsson, P.-U. Renberg, P. Nadel-Turonski, A. Ringbom, contribution to International Conference on Nuclear Data for Science and Technology, Tsukuba, Japan, Oct. 7-12, 2001.

[11] J. Thun, J. Blomgren, K. Elmgren, J. Källne, N. Olsson, J.F. Lecolley, F. Lefebvres, C. Varignon, F. Borne, X. Ledoux, Y. Patin, O. Jonsson, P.-U. Renberg, accepted for publication in Nucl. Instr. Meth. **A**.

[12] R.W. Finlay, W.P. Abfalterer, G. Fink, E. Montei, T. Adami, P.W. Lisowski, G.L. Morgan, R.C. Haight, Phys. Rev. **C47**, 237 (1993).

[13] S. Benck, I. Slypen, J.P. Meulders, V. Corcalciuc, Eur. Phys. J. **A3**, 149 (1998).

[14] H. Condé, S. Hultqvist, N. Olsson, T. Rönnqvist, R. Zorro, J. Blomgren, G. Tibell, A. Håkansson, O. Jonsson, A. Lindholm, L. Nilsson, P.-U. Renberg, A. Brockstedt, P. Ekström, M. Österlund, F.P. Brady, and Z. Szeflinski, Nucl. Instr. and Meth. **A292**, 121 (1990).

[15] J. Klug, J. Blomgren, A. Ataç,B. Bergenwall, S. Dangtip, K. Elmgren, C. Johansson, N. Olsson, J. Rahm, O. Jonsson, L. Nilsson, P.-U. Renberg, P. Nadel-Turonski, A. Ringbom, A. Oberstedt, F. Tovesson, C. Le Brun, J.-F. Lecolley, F.-R. Lecolley, M.

Louvel, N. Marie, C. Schweitzer, C. Varignon, Ph. Eudes, F. Haddad, M. Kerveno, T. Kirchner, C. Lebrun, L. Stuttgé, I. Slypen, A. Prokofiev, A. Smirnov, R. Michel, S. Neumann, U. Herpers, to be published.

[16] S. Dangtip, A. Ataç, B. Bergenwall, J. Blomgren, K. Elmgren, C. Johansson, J. Klug, N. Olsson, G. Alm Carlsson, J. Söderberg, O. Jonsson, L. Nilsson, P.-U. Renberg, P. Nadel-Turonski, C. Le Brun, F.-R. Lecolley, J.-F. Lecolley, C. Varignon, Ph. Eudes, F. Haddad, M. Kerveno, T. Kirchner, C. Lebrun, Nucl. Instr. Meth. **A452**, 484 (2000).

[17] A. Letorneau, J. Galin, F. Goldenbaum, B. Lott, A. Péghaire, M. Enke, D. Hilscher, U. Jahnke, K. Nünighoff, D. Filges, R.D. Neef, N. Paul, H. Schaal, G. Sterzenbach, A. Tietze, Nucl. Instr. Meth. **B170**, 299 (2000).

[18] S. Neumann, R. Michel, F. Sudbrock, U. Herpers, P. Malmborg, O. Jonsson, B. Holmqvist, H. Condé, P.W. Kubik, M. Suter, Proceedings of International Conference on Nuclear Data for Science and Technology, Trieste, Italy, 1997, p. 379.

[19] R. Michel, private communication, available from the OECD Nuclear Energy Agency, www.nea.fr.

[20] A. Koning and S. Hilaire, to be published.

[21] T. Enqvist, *et al.*, contribution to International Conference on Nuclear Data for Science and Technology, Tsukuba, Japan, Oct. 7-12, 2001.

[22] X. Ledoux, F. Borne, A. Boudard, F. Brochard, S. Crespin, D. Drake, J.C. Duchazeaubeneix, D. Durand, J.M. Durand, J. Fréhaut, F. Hanappe, L. Kowalski, C. Lebrun, F.R. Lecolley, J.F. Lecolley, F. Lefebvres, R. Legrain, S. Leray, M. Louvel, E. Martinez, S.I. Meigo, S. Ménard, G. Milleret, Y. Patin, E. Petitbon, F. Plouin, P. Pras, L. Stuttgé, Y. Terrien, J. Thun, M. Uematso, C. Varignon, D.M. Whittal, W. Wlasło, Phys. Rev. Lett. **82**, 4412 (1999).

[23] A. Boudard, J. Cognon, S. Leray, C. Volant, to be published.

[24] A.R. Junghans, M. de Jong, H.-G. Clerc, A.V. Ignatyuk, G.A. Kudyaev, K.-H. Schmidt, Nucl. Phys. **A629**, 635 (1998).

[25] Yu.N. Shubin, A.V. Ignatyuk, A. Yu. Konobeev, V.P. Lunev, E.V. Kulikov, Proceedings of 2nd International Conference on Accelerator-Driven Transmutation Technologies, Kalmar, Sweden, 1996, p. 953.

[26] V.P. Eismont, A.V. Prokofyev, A.N. Smirnov, K. Elmgren, J. Blomgren, H. Condé, J. Nilsson, N. Olsson, T. Rönnqvist, E. Tranéus, Phys. Rev. **C53**, 2911 (1996).

[27] A.V. Prokofiev, thesis, Uppsala university (2001).

[28] J. Blomgren, N. Olsson, J. Rahm, Phys. Scr. **T87**, 33 (2000).

[29] T. Rönnqvist, H. Condé, N. Olsson, R. Zorro, J. Blomgren, G. Tibell, O. Jonsson, L. Nilsson, P.-U. Renberg and S.Y. van der Werf, Phys. Rev. C **45**, R496 (1992).

[30] T.E.O. Ericson, B. Loiseau, J. Nilsson, N. Olsson, J. Blomgren, H. Condé, K. Elmgren, O. Jonsson, L. Nilsson, P.-U. Renberg, A. Ringbom, T. Rönnqvist, G. Tibell, and R. Zorro, Phys. Rev. Lett. **75**, 1046 (1995).

[31] R.H. Stahl and N.F. Ramsey, Phys. Rev. **96**, 1310 (1954).

[32] C.Y. Chih and W.M. Powell, Phys. Rev. **106**, 539 (1957).

[33] J.P. Scanlon, G.H. Stafford, J.J. Thresher, P.H. Bowen, and A. Langsford, Nucl. Phys. **41**, 401 (1963).

[34] A.J. Bersbach, R.E. Mischke, and T.J. Devlin, Phys. Rev. **D13**, 535 (1976).

[35] B.E. Bonner, J.E. Simmons, C.L. Hollas, C.R. Newsom, P.J. Riley, G. Glass, and Mahavir Jain, Phys. Rev. Lett. **41**, 1200 (1978).

[36] J.N. Palmieri and J.P. Wolfe, Phys. Rev. C **3**, 144 (1971).

[37] D.F. Measday, Phys. Rev. **142**, 584 (1960).

[38] M. Lacombe, B. Loiseau, J.M. Richard, R. Vinh Mau, J. Côté, P. Pirès, and R. de Tourreil, Phys. Rev. C **21**, 861 (1980).

[39] R. Machleidt, K. Holinde, and Ch. Elster, Phys. Rep. **149**, 1 (1987), and R. Machleidt, private communication.

[40] V.G.J. Stoks, R.A.M. Klomp, C.P.F. Terheggen, and J.J. de Swart, Phys. Rev. C **49**, 2950 (1994).

[41] J. Franz, E. Rössle, H. Schmitt, L. Schmitt, Phys. Scr. **T87**, 14 (2000).

NEUTRONS FOR SCIENCE AND INDUSTRY – THE UPPSALA NEUTRON BEAM FACILITY

J. Blomgren[*], *B. Bergenwall, C. Johansson, J. Klug, S. Pomp, U. Tippawan*
Department of Neutron Research, Uppsala University, Box 525, S-751 20 Uppsala, Sweden
K. Elmgren, N. Olsson
Swedish Defence Research Agency, S-172 90 Stockholm, Sweden
O. Jonsson, L. Nilsson, A. Prokofiev, P.-U. Renberg
The Svedberg Laboratory, Uppsala University, Box 535, S-751 21 Uppsala, Sweden
M. Österlund
Department of Physics, University of Jönköping, Box 1026, S-551 11 Jönköping, Sweden
S. Dangtip
Fast Neutron Research Facility, Department of Physics, Faculty of Science, Chiang Mai University, 50200 Thailand

Abstract

The 20-180 MeV neutron beam at the The Svedberg Laboratory (TSL), Uppsala, Sweden, is used to provide data for a large number of applications. These involve transmutation, fundamental physics, medicine, dosimetry and electronics effects. The comparatively high flux, good energy resolution, precise monitoring and easy access to the beam has resulted in a large user community, which presently comprises about 70 users from about 10 countries.

1 INTRODUCTION

Recently, a large number of applications involving neutrons above 20 MeV have become important, like transmutation of nuclear waste, fast-neutron cancer therapy, dose effects for airflight personnel as well as electronics failures due to cosmic-ray neutrons.

2 THE NEUTRON BEAM FACILITY

2.1 Neutron production

At the 20-180 MeV neutron facility at the The Svedberg Laboratory (TSL), Uppsala, Sweden [1,2] (see fig. 1), almost mono-energetic neutrons are produced by the reaction ^{7}Li(p,n)^{7}Be in a target of 99.98 % ^{7}Li. After the target, the proton beam is bent by two magnets into an 8 m concrete tunnel, where it is focused and stopped in a well-shielded carbon beam-dump. A narrow neutron beam is formed in the forward direction by a system of three collimators, with a total thickness of more than four metres.

The energy spectrum of the neutron beam is shown in fig. 2. About half of all neutrons appear in the high-energy peak, while the rest are roughly equally distributed in energy, from the maximum energy and down to zero. The low-energy tail can be reduced by time-of-flight measurements (see fig. 2). Typical intensities and energy resolutions are 10^{6} s^{-1}, and 1 MeV (FWHM), respectively.

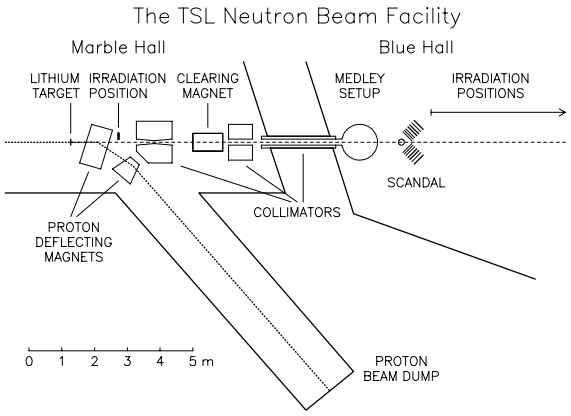

Figure 1 The neutron beam facility at the The Svedberg Laboratory, Uppsala, Sweden.

2.2 Base equipment

Two major experimental setups are semi-permanently installed. The MEDLEY detector telescope array for light-ion production measurements is housed in a vacuum chamber [3]. At the exit of this chamber, a 0.1 mm stainless steel foil terminates the vacuum system. Immediately after MEDLEY follows SCANDAL (SCAttered Nucleon Detection AssembLy) [2], a setup designed for large-acceptance neutron and proton detection. MEDLEY and SCANDAL are presented in more detail in the contribution by S. Pomp *et al.*

[*] Corresponding author. Tel: +46 18 471 3788; Fax: +46 18 471 3853; E-mail address: jan.blomgren@tsl.uu.se

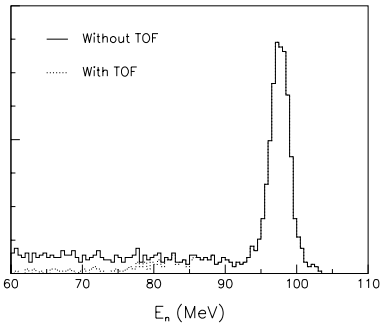

Figure 2 The neutron energy spectrum, with and without time-of-flight rejection of low-energy neutrons.

2.3 Monitoring

Absolute normalization of the neutron flux is a notorious problem in all high-energy neutron-beam applications. For direct neutron monitoring, fission counters are available, which have been calibrated relative to np scattering, allowing an uncertainty of about 10 %. Relative monitoring is also provided by charge integration of the primary proton beam.

3 DATA FOR APPLICATIONS

3.1 Transmutation

It is known today that spent fuel from nuclear power reactors and surplus nuclear weapons material can be incinerated by irradiation of neutrons, leading to dramatically reduced storage time. For spent fuel, such treatment would reduce the time until the material reaches natural radiotoxicity from about 100 000 years to less than 1000 years, i.e., it moves the issue from geological to technological time scales.

Presently, this can be carried out in laboratories with small amounts to high costs. Whether it can be achieved also on industrial scale to a reasonable cost remains to be proven. Research on these issues is rapidly expanding all over the world.

Almost all proposed transmutation techniques involve high-energy neutrons created in proton-induced spallation of a heavy target nucleus. Therefore, the neutron spectrum in a transmutation core will contain one significant difference compared to present reactors: neutrons at very high energies. The nuclear data libraries developed for reactors of today go up to about 20 MeV, which covers all available energies for that application, but with a spallator coupled to a core, neutrons with energies up to 1-2 GeV will be present.

Today, several groups are working on transmutation-related cross sections at TSL. Elastic scattering of neutrons is studied with SCANDAL. Hydrogen and helium production is measured with a combination of SCANDAL and MEDLEY, residue production by activation techniques, and fast-neutron fission by thin-film breakdown counters and ionization chambers.

3.2 Medical applications

Cancer treatment with fast neutrons is performed routinely at several facilities around the world, and today it represents the largest therapy modality besides the conventional treatments with photons and electrons. For a review of this field, see e.g. ref. [4].

The interaction of neutrons with tissue is very complex, and to a large extent unknown. Thus, the existing methods and techniques employed are based on experience, rather than on knowledge on fundamental physics. Because of the recent development of neutron beams with good intensity and energy resolution, it is today possible to study all the processes involved in detail, and thus dramatically improve the dose and radiation quality planning in connection with tumour therapy. The neutron facility at the The Svedberg laboratory (TSL) in Uppsala has unique properties in this respect.

In the commonly used energy range (up to about 70 MeV), it is unfortunately difficult to describe nuclear processes theoretically in a simple way, and in addition, the data base is meagre.

A substantial improvement in the knowledge of fundamental nuclear data is therefore needed for a better understanding of the processes occurring on a cellular level, which is required for optimization of the radiation therapy. Besides the applications in cancer treatment, these data will improve the understanding of fast neutron dosimetry for airplane crew, which has recently received widespread attention.

3.3 Fundamental physics

The TSL neutron beam facility has now been running for about a decade. The main activity up to now has been studies of the (n,p) reaction at about 100 MeV on a series of nuclei ranging from ^{9}Be to ^{208}Pb [5-9] and np scattering at 96 and 162 MeV [10-13]. Besides their fundamental importance, the (n,p) data on nuclei support code development for transmutation core design, and the np scattering cross section has been used to normalize other neutron-induced data, and thus this cross section is important also for applications.

Recently, the np scattering cross section in this energy range has been under intense debate, because it is used for determinations of the absolute strength of the strong interaction, and this also has cosmological relevance. These issues have motivated a critical re-examination of the entire np data situation [14]. New experiments are underway to resolve the discrepancy [15].

4 RESEARCH PROGRAMME

4.1 Elastic neutron scattering

Elastic neutron scattering is of utmost importance for a vast number of applications. Besides its fundamental

importance as a laboratory for tests of isospin dependence in the nucleon-nucleon, and nucleon-nucleus, interaction, knowledge of the optical potentials derived from elastic scattering come into play in virtually every application where a detailed understanding of nuclear processes are important.

Given the time and cost for such experiments, the focus must be on developing theoretical models rather than systematically measuring all nuclei. The obvious nuclei to study are then the magic or semi-magic nuclei. ^{12}C and ^{208}Pb have already been studied, ^{56}Fe is underway, and ^{16}O, ^{40}Ca and ^{90}Zr are future targets. Here it is fortunate that lead and zirconium are also important materials in future transmutation facilities, and carbon, oxygen and calcium are all of medical relevance (because the nuclear recoils account for 10-15 % of the dose), so the gain is twofold. In addition, H(n,n) has been studied for normalization purposes.

4.2 Charged-particle production

About half the dose in fast-neutron cancer therapy comes from np scattering, 10-15 % from elastic neutron scattering and the remaining 35-40 % from neutron-induced emission of charged particles, such as protons, deuterons, tritons, ^{3}He- and α-particles.

Double-differential cross sections for all these reactions in carbon and oxygen have been measured with the MEDLEY setup at 96 MeV, and nitrogen and calcium are planned.

MEDLEY is a multipurpose detector, which has turned out to be useful for many different applications. One of these is hydrogen and helium production in a transmutation core, which is important for safety as well as material swelling and embrittlement. Iron, lead and uranium data are under analysis.

4.3 Fast-neutron fission

About half the fission power in a transmutation core would be due to neutrons born at energies above 20 MeV. Very little data exist on high-energy fission, but the situation is under rapid improvement. Fission cross sections have been measured at many actinides and a few sub-actinide nuclei [16].

4.4 Residue production

Production of residual nuclei in neutron-induced nuclear reactions are studied by activation techniques [17]. These experiments are carried out at a second target station close to the neutron production, thereby allowing higher flux.

4.5 Neutron-induced electronics failures

Recently, the importance of cosmic radiation effects in aircraft electronics has been highlighted. (For reviews, see e.g. refs. [18,19] and references therein.) When an electronic memory circuit is exposed to particle radiation, the latter can cause a flip of the memory content in a bit, which is called a single-event upset (SEU). This induces no hardware damage to the circuit, but evidently, unwanted re-programming of aircraft computer software can have fatal consequences.

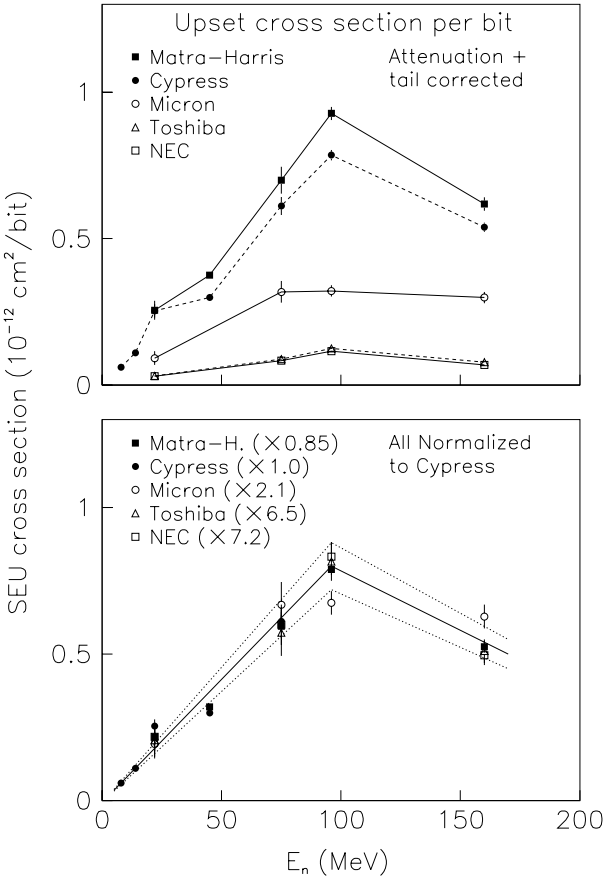

Figure 3 The energy dependence of the SEU cross section for a few devices. The upper panel shows the sensitivity for a few devices. In the lower panel, all devices have been re-normalized to the same total sensitivity, illustrating that the energy dependence is very similar for all devices. See the text for details.

At flight altitudes, as well as at sea level, the cosmic ray flux is dominated by neutrons and muons. The latter do not interact strongly with nuclei, and therefore neutrons are most important for SEU.

Since neutrons have no charge, they can only interact via violent, nuclear electronics. If the neutron-induced charged-particle production cross sections were known, and thus the energy deposition on a microscopic level, it might be possible to calculate the SEU reactions, in which charged particles are created, that occasionally induce an SEU. Thus, knowledge of the nuclear interaction of neutrons with silicon is needed to obtain a full understanding of the SEU problem.

Firm experimental information about neutron-induced cross sections is very scarce. Thus, one has had to rely heavily on calculations based on nuclear models, which have a poor and essentially unknown precision.

Measurements of neutron-induced charged particle-production cross sections are therefore of utmost importance for a full understanding of the SEU problem in aviation rate with reasonable precision also for any future components.

Up to now, in-beam testing of components has been carried out to characterize the effect, especially its neutron energy dependence [20,21]. As can be seen in fig. 3, the probability for upsets rises slowly with energy and seems to peak or saturate at about 100 MeV. This seems to imply that production of heavy ions is most important; if light ions, like α particles, were dominant, the cross section should rise and peak at lower energies. This conclusion is corroborated by simple estimates of the ionization required to obtain a bit change. It is evident that newer devices (Matra-Harris, Cypress) are more sensitive than older ones. Also this can be understood from knowledge of the circuit characteristics. New circuits require less charge for a bit flip, which makes them more sensitive to SEU.

There is a limit how much information that can be obtained from component testing. To get a full understanding of the problem, measurements of nuclear cross sections are required. Such experiments have been performed with MEDLEY to study light-ion production on silicon [22], and a new facility is being planned for heavy-ion production experiments.

4.6 Dosimetry research

Nuclear data measurements for dosemeter modelling are to be carried out using the SCANDAL and MEDLEY setups. In addition, direct testing of existing dosemeters are regularly undertaken, involving national radiation protection institutes from a number of European countries. The large number of simultaneous users has been a great asset in this research, because it has provided good normalization possibilities, but also interdisciplinary collaboration. A good example of the latter is the development of dosemeters based on fission in bismuth, which has benefitted very much on the fast-fission programme.

5 SUMMARY

The quasi-monoenergetic 20-180 MeV neutron beam at the The Svedberg Laboratory (TSL), Uppsala, Sweden, has been - and will be used - to provide data for a large number of applications. These involve transmutation, fundamental physics, medicine, dosimetry and electronics effects. The comparatively high flux, good energy resolution, precise monitoring and easy access to the beam has resulted in a large user community (presently about 70 users from about 10 countries). Two major multi-purpose experiment setups, MEDLEY and SCANDAL, are available.

The largest research programmes involve studies of elastic neutron scattering, neutron-induced light ion production, fast-neutron fission and in-beam testing of electronics devices.

This work was financially supported by the Development and Promotion of Science and Technology Talents Project of Thailand, Vattenfall AB, Swedish Nuclear Fuel and Waste Management Company, Swedish Nuclear Power Inspectorate, Barsebäck Power AB, Swedish Defense Research Establishment, Swedish Cancer Society, and Swedish Research Council.

REFERENCES

[1] H. Condé, *et al*., Nucl. Instr. Meth. A292 (1990) 121.
[2] J. Klug, *et al*., submitted to Nucl. Instr. Meth. A.
[3] S. Dangtip, *et al*., Nucl. Instr. Meth. A452 (2000) 484.
[4] M. Tubiana, J. Dutreix and A. Wambersie, Introduction to Radiobiology, (Taylor & Francis, 1990).
[5] H. Condé, *et al*., Nucl. Phys. A545 (1992) 785.
[6] N. Olsson, *et al*., Nucl. Phys. A559 (1993) 368.
[7] T. Rönnqvist, *et al*., Nucl. Phys. A563 (1993) 225.
[8] A. Ringbom, *et al*., Nucl. Phys. A617 (1997) 316.
[9] S. Dangtip, *et al*., Nucl. Phys. A677 (2000) 3.
[10] T. Rönnqvist, *et al*., Phys. Rev. C45 (1992) R496.
[11] T.E.O. Ericson, *et al*., Phys. Rev. Lett. 75 (1995) 1046.
[12] J. Rahm, *et al*., Phys. Rev. C57 (1998) 1077.
[13] J. Rahm, *et al*., Phys. Rev. C63 (2001) 044001.
[14] Workshop on "Critical Points in the Determination of the Pion-Nucleon Coupling Constant", Physica Scripta T87 (2000), ed. J. Blomgren.
[15] T. Peterson, *et al*., Nucl. Phys. A663&664 (2000) 1057c.
[16] V.P. Eismont, *et al*., Proceedings of International Conference on Nuclear Data for Science and Technology, Tsukuba, Japan, Oct. 7-12, 2001.
[17] W. Glasser, *et al*., Proceedings of International Conference on Nuclear Data for Science and Technology, Tsukuba, Japan, Oct. 7-12, 2001.
[18] J.F. Ziegler, IBM J. Res. Develop. 40 (1996) 19.
[19] H.H.K. Tang, IBM J. Res. Develop. 40 (1996) 91.
[20] K. Johansson, *et al*., IEEE transactions on Nuclear Science 45 (1998) 2195.
[21] K. Johansson, *et al*., IEEE transactions on Nuclear Science 46 (1999) 1427.
[22] U. Tippawan, *et al*., Proceedings of International Conference on Nuclear Data for Science and Technology, Tsukuba, Japan, Oct. 7-12, 2001.

MEDLEY AND SCANDAL – TWO FACILITIES FOR STUDIES OF NEUTRON-INDUCED NUCLEAR REACTIONS

S. Pomp[*], *B. Bergenwall, J. Blomgren, C.Johansson, J.Klug and U. Tippawan*
Department of Neutron Research, Uppsala University, Sweden
S. Dangtip
Fast Neutron Research Facility, Chiang Mai University, Thailand
K. Elmgren and N.Olsson
Swedish Defence Research Agency, Stockholm, Sweden
O. Jonsson, L. Nilsson, A.V. Prokofiev and P.-U. Renberg
The Svedberg Laboratory, Uppsala University, Sweden
M. Österlund
Department of Physics, University of Jönköping, Sweden

Abstract

Two complementary facilities for studies of neutron-induced nuclear reactions are currently in operation at the neutron beam facility of the The Svedberg Laboratory, Uppsala, Sweden. The SCANDAL (SCAttered Nucleon Detection AssembLy) detector was designed for the measurement of elastic neutron scattering but can also be used for (n,p) reaction studies, and the MEDLEY detector is used for studies of neutron-induced light charged-particle (lcp) production.

1 INTRODUCTION

In recent years, several growing research fields have evolved, which need high quality data on neutron-induced nuclear reactions at high energies. Examples are fast-neutron cancertherapy [1], single event effects (SEE) in microelectronic devices due to cosmic-ray neutrons [2] and accelerator-driven systems (ADS) for transmutation of nuclear waste [3]. In addition, the quest for the strength of the strong interaction recently gained new actuality [4].

This has led to growing experimental activities at the neutron beam facility of the The Svedberg Laboratory (TSL) in Uppsala, Sweden [5, 6].

2 NEUTRON PRODUCTION

A quasi-monoenergetic neutron beam is produced by the ^{7}Li(p,n)^{7}Be reaction in a target of 99.98% ^{7}Li (Fig.1) [7]. The protons are delivered by the Gustaf Werner cyclotron, which allows for neutron beams in the range from 20 to 180 MeV. After the Li target, a

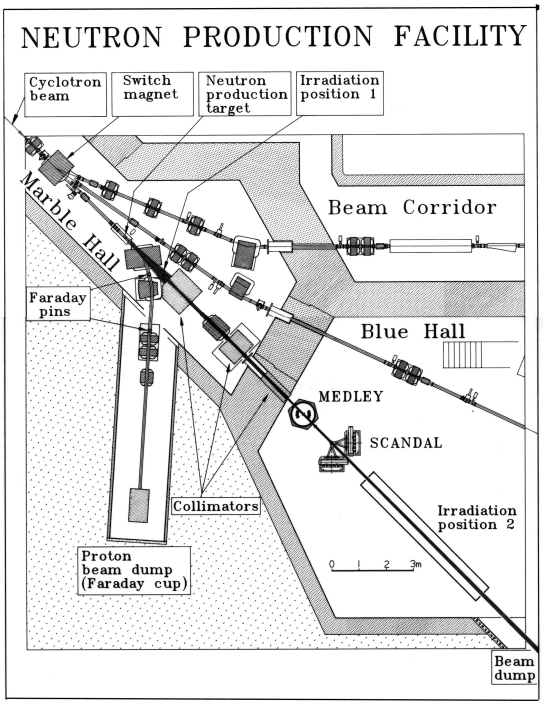

Figure 1: Layout of the neutron beam facility at the The Svedberg Laboratory in Uppsala.

[*] Corresponding author. Tel: +46 18 471 6850; Fax: +46 18 471 3853; E-mail address: Stephan.Pomp@tsl.uu.se

clearing magnet deflects the remaining proton beam into a well-shielded beam dump. A set of collimators shapes a neutron beam with a diameter of about 8 cm, which is delievered into the experimental hall. For a 100 MeV proton beam of 5μA and a 4 mm Li target, a flux of $3 \cdot 10^4$ neutrons $s^{-1}cm^{-2}$ is achieved.

The neutron spectrum (Fig. 2) exhibits a high-energy peak containing about 40% of all the neutrons and a flat tail, which can be suppressed by time-of-flight (TOF) techniques [8].

In order to monitor the neutron flux, the proton beam current is measured by means of a Faraday Cup located in the beam dump. In addition, a thin-film breakdown counter (TFBC), mounted in the experimental hall, monitors the number of neutron-induced fissions in ^{238}U [9].

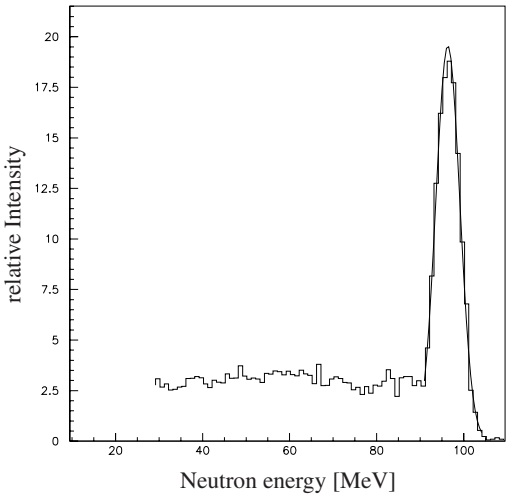

Figure 2: Neutron spectrum down to 30 MeV as measured with one telescope of the MEDLEY detector described below.

3 THE SCANDAL DETECTOR

The SCANDAL (SCAttered Nucleon Detection AssembLy) detector has been designed for measurements of elastic neutron scattering but can also be used for (n,p) reaction studies [10]. The layout and the detection principle are shown in Fig. 3. The device consists of two identical systems, which can be rotated around a fixed pivot point.

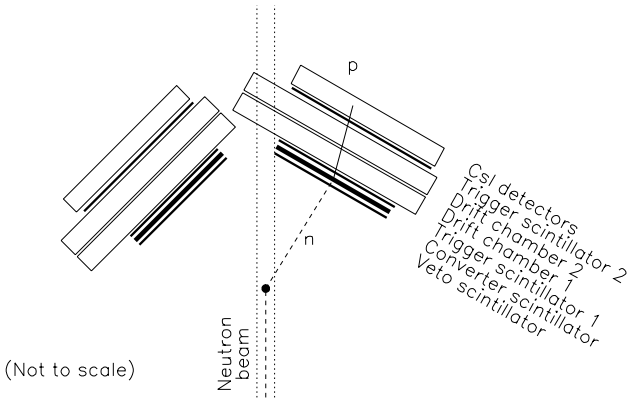

Figure 3: Layout of the SCANDAL detector illustrating the detection principle.

In neutron detection mode, each arm consists of a 2 mm thick veto scintillator for fast charged-particle rejection, a neutron-to-proton converter which is a 10 mm thick plastic scintillator, a 2 mm thick plastic scintillator for triggering, two drift chambers for proton tracking, a 2 mm thick ΔE plastic scintillator which is also part of the trigger, and an array of CsI detectors for energy determination. The trigger is provided by a coincidence of the two trigger scintillators, vetoed by the front scintillator.

Since the converter scintillator contains both hydrogen and proton, an unambiguous measurement is only possible down to 12 MeV below the incident energy. Therefore, only events with a conversion angle of less than 15^o are accepted.

In a typical experiment, the two arms will be located such as to cover $10\text{-}50^o$, and $30\text{-}70^o$, respectively. For a one-week run on ^{208}Pb, the total number of counts for a one-degree angular bin is expected to be about 5000 at 10^o and 1 at 70^o, illustrating the rapid fall of the cross section with the angle.

At present, data have been taken on ^{12}C and ^{208}Pb. In addition, ^{1}H has been studied for normalisation purposes. The full resolution is in the 3-4 MeV range.

In addition to the analysis of the obtained data, current projects include the measurement of $^{56}Fe(n,n)$ and a feasiblity study for (n,xn) measurements.

If used for (n,p) studies, the veto and converter scintillators can be removed and additional drift chambers can be mounted if desired. Fig. 4 shows preliminary results for the

^{208}Pb(n,xp) cross section at 40° as obtained by SCANDAL compared with another measurement with MEDLEY.

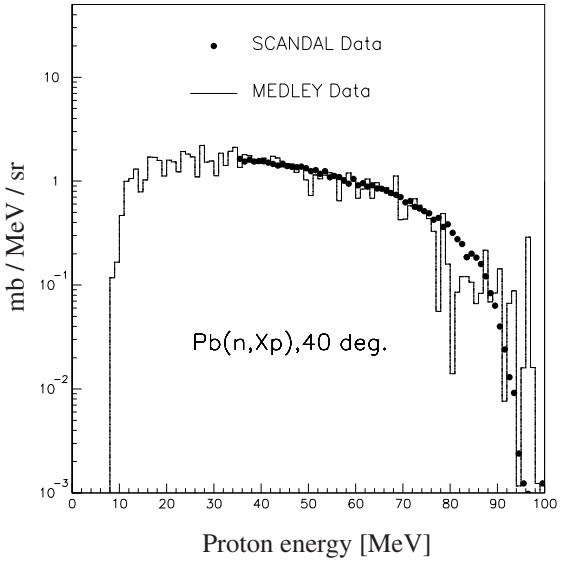

Figure 4: Comparision of preliminary cross section results for ^{208}Pb(n,xp) at 40° obtained by SCANDAL and MEDLEY [11].

4 THE MEDLEY FACILITY

The MEDLEY detector is used for studies of neutron-induced light charged-particle (lcp) production [12]. Eight three-detector telescopes are arranged in an evacuated scattering chamber, covering emission angles from 20 to 160 degrees in 20 degree intervalls (Fig. 5).

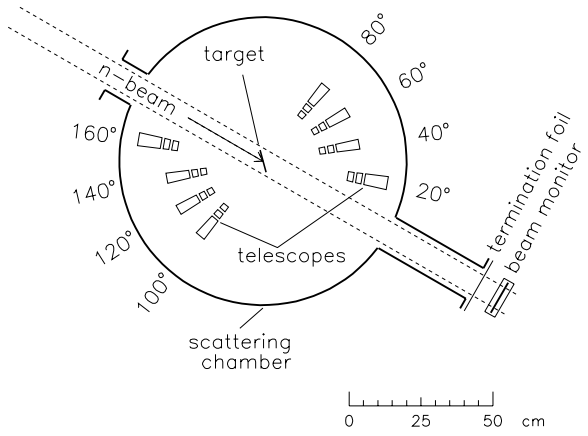

Figure 5: Schematic view of the MEDLEY setup.

Each telescope consists of a thin Si detector (~50 μm), a thick Si detector (~400 μm) and a CsI crystal (~3 cm). This arrangement allows for detection and identification of light ions up to α particles by ΔE-ΔE-E techniques. Active collimators made of plastic scintillators define the solid angle of each telescope (Fig. 6).

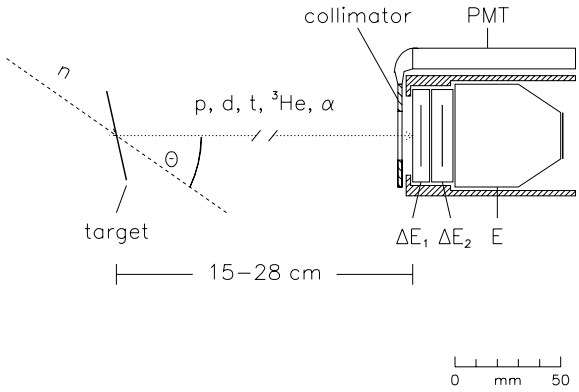

Figure 6: Cross-section of a telescope. Depicted are the thin silicon detector (ΔE_1), the thick silicon detector (ΔE_2), the CsI detector (E), the collimator with its photo-multiplier tube (PMT) and the detector housing.

Fig. 7 shows a calibrated pulse height spectrum of the energy deposition in the thin versus the thick silicon detector of the 20° telescope for ^{28}Si(n,lcp). Bands for protons, deuterons, tritions, ^{3}He and alpha particles are clearly separated. In addition, we could even identify a few ^{28}Si(n,xLi) events. A similar two-dimensional plot of ΔE_2 versus E (CsI) allows further particle identification.

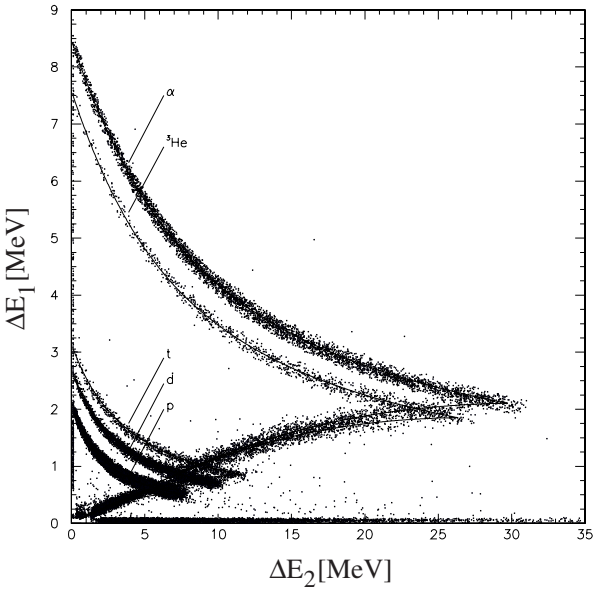

Figure 7: Calibrated pulse height spectrum of the energy deposit in the 50 μm silicon detector (ΔE_1) versus the 400 μm detector (ΔE_2).

The calibration at high energies is then checked using distinct peaks corresponding to direct reactions to the ground-state or low excitation-energy states in, *e.g.*, ^{28}Si(n,d)^{27}Al.

The time difference between the trigger signal from either of the silicon detectors and the cyclotron RF is, after correction for the charged particle time of flight, used to reject low-energy neutrons. The absolute, double-differential cross sections are then obtained by normalising to the number of recoil protons emerging from a CH_2 target, assuming that the *np* scattering cross section is well known. A preliminary energy spectrum for Si(n,xd) at a production angle of 20° is shown in Fig. 8.

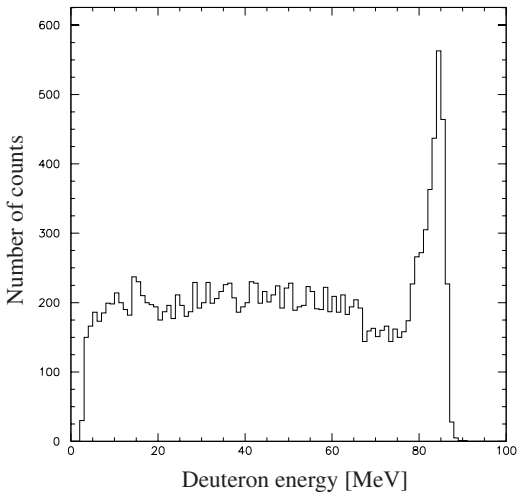

Figure 8: Preliminary energy spectrum for deuterons from Si(n,xd) at 20° (from [13]).

A first study of ^{12}C(n,lcp) showed that current evaluations severly underestimate, *e.g.*, proton production [14]. This is now under more detailed investigation. Further projects include measurements of (n,lcp) in ^{16}O, ^{28}Si, ^{56}Fe, ^{208}Pb and ^{238}U.

ACKNOWLEDGEMENTS

The authors wish to thank the The Svedberg Laboratory, the EU Council and the HINDAS collaboration, the Thailand Research Fund, the Swedish Research Council, the Swedish Cancer Foundation, Vattenfall AB, Swedish Nuclear Fuel and Waste Management Company, Swedish Nuclear Power Inspectorate, Barsebäck Power AB and the Swedish Defence Research Agency for their support.

REFERENCES

[1] Nuclear data for neutron therapy: Status and future needs, IAEA-TECDOC-992 (1997).
[2] See, *e.g.*, H. H. K. Tang, IBM J. Res. Develop. **40** (1996) 91.
[3] See, *e.g.*, Proc. of the 4th Int. Conf. on Accelerator Driven Transmutation Technology and Applications (ADTTA '01), Reno, United States, November 12-15, 2001.
[4] Critical Issues in the Determination of the Pion-Nucleon Coupling Constant, ed. J. Blomgren, Phys. Scr. **T87** (2000).
[5] J. Blomgren *et al.*, these proceedings.
[6] TSL homepage: www3.tsl.uu.se/~edberg/
[7] H. Condé *et al.*, Nucl. Instr. Meth. **A292** (1990) 121.
[8] A. V. Prokofiev *et al.*, Proc. of the Int. Conf. on Nuclear Data for Science and Technology (ND2001), Tsukuba, Japan, October 7-12, 2001.
[9] A. V. Prokofiev *et al.*, TSL Report, TSL/ISV-99-0203.
[10] J. Klug *et al.*, submitted to Nucl. Instr. Meth.
[11] V. Blideanu, private communication.
[12] S. Dangtip *et al.*, Nucl. Instr. Meth. **A452** (2000) 484.
[13] U. Tippawan *et al.*, Proc. of the Int. Conf. on Nuclear Data for Science and Technology (ND2001), Tsukuba, Japan, October 7-11, 2001.
[14] S. Dangtip, Ph.D. thesis, Uppsala University, 2000.

FOI
TOTALFÖRSVARETS
FORSKNINGSINSTITUT

Datum

2002-06-13
FOI MEMO

Vid korrespondens åberopa FOI beteckning

nr 02-2030
Sida 1 (6)

Miljödepartementet
MK-enheten
103 33 Stockholm

Er referens

Vår handläggare

Nils Olsson, FOI
Tomas Lefvert, Vattenfall AB

Minnesanteckningar från möte med

OECD/NEA Nuclear Science Committee (NSC)

Paris, 2002-06-03—05

Detta dokument utgör en kort och sammanfattande rapport över de viktigaste besluten och rapporteringarna till rubricerade möte. Svenska delegater till NEA/NSC är T. Lefvert och N. Olsson. T. Lefvert är dessutom NSC:s ordförande för närvarande. Ytterligare information eller kopior av underliggande dokument kan fås från någon av dessa två.

Dagordningen för mötet framgår av Bil. 1, medan en lista över mötesdeltagarna återfinns i Bil. 2.

1. NEA:s Generaldirektör, L. Echàvarri, hälsade kommittéledamöterna välkomna, samt rapporterade bl a följande från NEA:s Steering Committee:
   - Slovenien deltar i mötet som observatör.
   - Informationsutbytet, liksom mötesfrekvensen, om kärnenergisäkerhet har ökat markant efter 11 september förra året.
   - NEA:s förslag till program för 2003-2004 har mottagits väl. Budget på samma nivå som tidigare har allokerats för två år och kommer att följas upp årligen.
   - Beslut om Slovakiens medlemskap i NEA kommer att fattas i juni 2002.
   - Tre nya projekt inom säkerhet har startats under året.
   - På kärnavfallsområdet har mycket hänt, bl a kan nämnas President Bushs beslut att godkänna Yucca Mountain-förvaret, och Finlands djupförvars-beslut.
   - Satsningarna på vetenskap och teknikutveckling kommer att öka som resultat av USA:s satsning på Generation IV, liksom av Finlands beslut att bygga en femte reaktor.

Postadress	Besök	Telefon	Telefax	e-mail	www.foi.se
SE-172 90 Stockholm	Enköpingsvägen 126 Sundbyberg	08-55 50 33 86	08-55 50 34 94	nils.olsson@foi.se	

- NEA avser att hålla koordinationsmöten med samtliga tekniska kommittéer.
- NEA har fått förslag på nytt regelverk för kärnteknisk verksamhet från ICRP på remiss.

2. Dagordningen godkändes med en del smärre ändringar i ordningsföljden.

3. Summary Record från förra mötet, NEA/SEN/NSC(2001)3, godkändes.

4. Lägesrapporter för kommitténs projekt, NEA/SEN/NSC(2002)2, samt muntliga presentationer:

   4.1 NSC-finansierade workshops och möten.
   - "Second information exchange meeting on basic studies in the field of high temperature engineering", NEA, oktober 2001. Proceedings kom ut i maj. Man planerar ett tredje möte i Japan 2003, med stöd från JAERI. IAEA påpekade betydelsen av att inbjuda också Kina.
   - "Second workshop on advanced reactors with innovative fuels" (ARWIF-2001), Storbritannien, oktober 2001. Dominerande teman var: Inert matrix fuels, Thorium fuels, Minor actinide target design and fabrication. Trenden är en tyngdpunktsförskjutning mot: High temperature gas reactors and fuels, Accelerator-driven sub-critical systems, Molten salt reactors, Pb-Bi cooled fast reactors. De flesta bidragen var teoretiska.
   - "Shielding aspects of accelerators, targets and irradiation facilities" (SATIF-6), USA, april 2002. Nästa möte i denna serie kommer att hållas i Portugal 2004. Det föreslogs att acceleratorer för medicinskt bruk ska inkluderas, eftersom intresset för dessa ökat markant. Det rekommenderades att förslagsställaren (Qaim) lämnar en proposal om en sådan utvidgning till arbetsutskottet före dess möte i december.
   - "Reliability of high power accelerators", USA, maj 2002. Workshopen var fr a inriktad mot acceleratordrivna energisystem, och samlade 75 deltagare från 11 länder. Huvuddelen av bidragen var teoretiska. Nästa workshop kommer att hållas i Korea (eller Japan) våren 2004.
   - "Reactor noise" (SMORN), Sverige, maj 2002. Samlade färre deltagare, speciellt från kraftföretagen, än tidigare workshops.
   - "Meeting on the international reactor physics benchmark experiments project" (IRPhE), Ungern, maj 2002. 14 deltagare från sju länder och två organisationer. Syftet med mötet var att granska och analysera arbetet med att evaluera och validera data från de reaktorfysikexperiment som gjorts genom åren, samt att rädda den dokumentation som finns. Speciellt kan nämnas Kritz2-experimentet från Studsvik. Kommittén godkände också en revision av IRPhE-aktivitetens omfattning och mål.

   4.2 Kommittéaktiviteter (WP = working party, EG = expert group):
   - Kommittén stödjer förslaget att anordna en Workshop om R&D needs in Nuclear Science i Paris i november 2002.
   - WP on Physics of plutonium fuel and innovative fuel cycles (WPPR) föreslog att ändra sin uppdragsbeskrivning för att bredda verksamheten till att omfatta alla "innovativa" bränslecykler. Ett utkast till nya beskrivningen tas fram av K Hesketh, och P D´hondt i

tid till decembermötet med NSC arbetsutskott. Det slutliga dokumentet diskuteras vid kommittens möte i juni 2003.

- Kommittén diskuterade också att lägga ihop WPPR och EG on Reactor-Based Pu Disposition till en grupp. Frågan kommer att diskuteras vid nästföljande möten med dessa grupper.
- WP on Scientific issues in partitioning and transmutation (WPPT). Fyra arbetsgrupper har organiserats inom detta breda område för att behandla specifika problem, nämligen inom Acceleratorutnyttjande och -tillförlitlighet, Kemisk separation, Bränsle och material, samt Fysik och säkerhet hos transmutationssystem. Grupperna kommer att hålla sina egna möten och workshops, och det totala arbetet kommer att koordineras genom gemensamma möten.
- Kommittén godkände ett förslag att Working Party on Nuclear Criticality Safety (WPNCS) får ansvaret att föreslå tidpunkt och plats för kommande internationella konferenser på området.
- WP on Nuclear data evaluation cooperation (WPEC). Arbetet bedrivs inom arbetsgrupperna: Standarder, Aktiveringstvärsnitt, Evaluering av kovariansdata, Neutrontvärsnitt för merparten av fissionsprodukter, samt Kärndata för förbättrade LWR reaktivitetsberäkningar. Det syftar till att förbättra kvalitet och täckningsgrad hos evaluerade kärndatabibliotek, samt att koordinera experimentella insatser för att nå dessa mål.
- Ordföranden presenterade ett svenskt förslag för en ny aktivitet inom området för teoretisk simulering av strålningsinducerade skador i material. Flera medlemsländer uttryckte intresse att delta och skall ge synpunkter på förslaget och ange en kontaktperson före slutet av september 2002.
- Basic phenomena in fuel behaviour: Ett dokument distribuerades vid mötet där man föreslog två års förlängning av nuvarande mandat. Kommitten noterade att ehuru denna verksamhet är viktig har den huvudsakligen karaktären av datainsamling, liksom IRPhE-projektet, och därför är det tveksamt om man skall bilda en EG. Kommitten godkände ändå fortsatt verksamhet i två år.
- Reactor stability and LWR transient benchmarks: Det föreslogs att NSC deltar i de EU-stödda aktiviteterna CRISSUE-S och VALCO t ex genom att organisera nästa möte med gruppen för CRISSUE-S 5-6 september 2002. Kommitten stödde detta under förutsättning att ev juridiska aspekter på NEA deltagande i EU-aktiviteter först klargörs.
- Resultaten från ett uppstartmöte om en Benhcmark för kylmedelstransient i VVER-1000 redovisades. Man beslöt bl a att lägga till en arbetsuppgift avseende tillämpning av CFD-metoder.
- Radiation shielding. SINBAD – en internationell databas för integrala strålskyddsexperiment presenterades. Databasen innehåller data för både 2- och 3-dimensionell strålningstransport, och är användbar för reaktorer och i fusions- och acceleratorsammanhang.

4.3 NSC-finansierade workshops och möten 2002-2003:

- ”Workshop on computing radiation dosimetry”, Portugal, juni 2002. Workshopen fokuserar på beräkningsfrågor och state-of-the-art-teknik inom dosimetri, strålskydd, skärmning, biofysik, medicinsk fysik, etc. Man förväntar sig 40 deltagare från 22 organisationer i 11 länder, plus 12 inbjudna föreläsare från 6 länder. Workshopen följs av en träningskurs på mellannivå om MCNP-X.

- "Seventh information exchange meeting on actinide and fission product partitioning and transmutation", Korea, oktober 2002. Mötet kommer att ha sex tekniska sessioner, två poster sessioner och en inledande och en avslutande session i plenum, den senare följd av en paneldiskussion om fortsatt utveckling. De tekniska sessionerna behandlar: Bränslecykelstrategi och framtida reaktorer, Separation och avfallsformer, Bränslen och strålmål, Spallationsstrålmål och avancerade kylmedia, Fysik och kärndata, Design och säkerhet avseende transmutationssytem. Hittills har man tagit emot 118 abstracts från 16 länder.
- "Seminar on pellet-clad mechanical interaction", Frankrike, hösten 2002.
- Ett förslag om att anordna "Second workshop on nuclear production of hydrogen, USA, hösten 2003, godkändes av kommittén.

5. Fördjupad diskussion:

   5.1 Aktinidkemi. Charles Madic hade satt samman ett program med sex korta föredrag: "Actinide coordination and organometallic chemistry" (M. Ephritikhine, CNRS, CEA), "Actinide solid chemistry" (M. Beauvy, CEA), "Actinide environmental chemistry" (E. Simoni, Orsay), "Experimental thermodynamics of actinides in aqueous solutions" (P. Moisy, CEA), "Chemistry of actinides in molten salts" (G. Picard, CNRS), "Actinide theoretical chemistry" (J.-P. Dognon, CEA). På dessa presentationer följde en diskussion om kopplingar mellan olika aspekter, exempelvis vattenbaserad kemi – pyrokemi, separation – slutförvar, etc.

   5.2 Bränsle med hög utbränning. W. Wiesenack från Halden i Norge talade om problemen med att öka utbränningen från dagens 40-60 MWd/kg till 70-80 MWd/kg. Man får då problem med svällning och gasproduktion, den senare resulterar också i ett ökande tryck i kapslingen. På sikt vill man gärna öka utbränningen till uppåt 100 MWd/kg, vilket kräver högre anrikning. De ekonomiska frågorna är naturligtvis avgörande. Utveckling av både bränsle och kapsling kommer att krävas. Kommittén uppdrog åt ordföranden att tillsammans med de engelska och schweitziska representanterna framlägga ett förslag på en aktivitet inom detta område till arbetsutskottets möte i december.

6. Möten, konferenser, publikationer och NSC Websidor.
   Refererades till Annex 1 och 2 i NEA/SEN/NSC(2002)2.

7. Rapport från elfte mötet med Executive Group.
   P. D'Hondt, ordförande i Executive Group (EG), rapporterade från mötet 2002-06-03. EG har till uppgift att monitorera verksamheten vid NEA Nuclear Data Bank (NEADB). NSC godkände programförslag och budget för åren 2003 och 2004. Budgeten ligger på samma nivå som för de senaste åren.

8. Huvuddrag i NEA:s program och budget för 2003 och 2004.

9. Ämnen för fördjupad diskussion på nästa NSC möte. Flera förslag förelåg, bl a:
   - High-Priority Request List (HPRL) för nya kärndata.
   - Medicinska tillämpningar av radioisotoper (föreslogs av S. Qaim, Tyskland).

- Modellering av reaktortransienter (föreslogs av R. Chawla, Schweitz).

Dessa tre förslag står kvar sedan tidigare. Dessutom föreslogs:

- Aspekter på skärmning av acceleratorer (Italien).
- Nukleär toxokologi (Frankrike).
- Materialvetenskap och strålskador (Sverige).

Förslagsställarna uppmanades att skriva en sida som konkretiserar förslagen, vilka sedan kommer att diskuteras av arbetsutskottet i december.

10. Information om NEA:s engagemang i Generation IV projektet.
    T. Dujardin informerade om det amerikanska Generation IV projektet, där man har som målsättning att utveckla och demonstrera åtminstone ett reaktorsystem före år 2030. De aspekter som ska beaktas är ekonomi, säkerhet och uthållighet. Förutom USA deltar nio länder i arbetet.

11. Rapporter från andra NEA-avdelningar och andra internationella organisationer.
    Rapporter gavs från NEA Nuclear Safety Division och NEA Nuclear Development Division. Rapporter gavs också från IAEA Nuclear Power Division och IAEA Division of Physical and Chemical Science. Vidare gavs en rapport från EU och IRMM, Geel, Belgien. Avslutningsvis presenterades det finska beslutet att bygga en femte reaktor.

12. Datum för nästa NSC möte beslutades till 2003-06-04—06, medan nästa möte med arbetsutskottet kommer att hållas 2002-12-03.

13. Det sittande arbetsutskottet i NSC, dvs T. Lefvert, Sverige, P. D'Hondt, Nederländerna, A. Zaetta, Frankrike, T. Osugi, Japan, och N. Haberman, USA, omvaldes på ett år, med Lefvert som ordförande.

14. Mötet avslutades.

Nils Olsson
Forskningschef
FOI

Sändlista:

Jan Blomstrand, Avd. för reaktorteknologi, KTH, 100 44 Stockholm
Wiktor Frid, Avd. för reaktorteknologi, KTH, 100 44 Stockholm
Raj Sehgal, Avd. för kärnkraftsäkerhet, KTH, 100 44 Stockholm
Peter Ekström, Inst. för fysik, Lunds universitet, Sölvegatan 14, 223 63 Lund
Waclav Gudowski, Avd. för reaktorfysik, SCFAB/KTH, 106 91 Stockholm
Börje Johansson, Avd. för tillämpad materialfysik, KTH, 100 44 Stockholm
Jan Blomgren, Inst. för neutronforskning, Uppsala universitet, Box 525, 751 20 Uppsala
Ane Håkansson, Inst. för strålningsvetenskap, Uppsala universitet, Box 535, 751 21 Uppsala
Jan. Källne, Inst. för neutronforskning, Uppsala universitet, Box 525, 751 20 Uppsala
Jan-Olov Liljenzin, Avd för Kärnkemi, Chalmers Tekniska Högskola, 412 96 Göteborg
Lembit Sihver, Avd för Kärnkemi, Chalmers Tekniska Högskola, 412 96 Göteborg
Imre Pázsit, Avd. för reaktorfysik, Chalmers Tekniska Högskola, 412 96 Göteborg

Gustaf Löwenhielm, Statens kärnkraftinspektion, 106 58 Stockholm
Oddbjörn Sandervåg, Statens kärnkraftinspektion, 106 58 Stockholm
Benny Sundström, Statens kärnkraftinspektion, 106 58 Stockholm
Ulf Bäverstam, Statens strålskyddsinstitut, 171 16 Stockholm

Per-Erik Ahlström, Svensk kärnbränslehantering AB, Box 5864, 102 40 Stockholm
Sten-Olof Andersson, Studsvik Nuclear AB, 611 82 Nyköping
Stig Andersson, Westinghouse Atom AB, 721 63 Västerås
Stig-Erik Larsson, Sycon AB, 205 09 Malmö
Jan Almberger, Vattenfall Bränsle, 16287 Stockholm
Agneta Wellmar, Barsebäck Kraft AB, Box 524, 246 25 Löddeköpinge
Fredrik Winge, Barsebäck kraft AB, Box 524, 240 21 Löddeköpinge

Lena Oliver, FOI Ursvik
Anders Ringbom, FOI Ursvik
Björn Sandström, FOI Umeå
Katarina Wilhelmsen Rolander, FOI Ursvik

UU-NF 02#04
(May 2002)
UPPSALA UNIVERSITY NEUTRON PHYSICS REPORT

MCNP CALCULATIONS OF BETA-GAMMA COINCIDENCE DETECTORS FOR MONITORING OF RADIOACTIVE XENON

CECILIA JOHANSSON

Department of Neutron Research, Uppsala University

THESIS FOR THE DEGREE OF LICENTIATE OF TECHNOLOGY

ABSTRACT

Monte Carlo simulations of two systems for detection of radioactive xenon have been performed, using the MCNP code. These systems, designed for monitoring violations of the Comprehensive Nuclear-Test-Ban Treaty, are based on coincident detection of electrons and gamma rays, emitted in beta decay of xenon nuclides produced in nuclear weapons explosions. In general, the simulations describe test data well, and the deviations from experimental data are understood.

UPPSALA UNIVERSITY
DEPARTMENT OF NEUTRON RESEARCH
PROGRAM OF APPLIED NUCLEAR PHYSICS
UPPSALA, SWEDEN

Preface

In this report, I present MCNP calculations on two beta-gamma coincidence detectors for xenon monitoring. This licentiate thesis is a report of these calculations, as well as a deteiled description of the detecting systems. To be able to simulate detector responses, it is necessary to have a good knowledge of the detector design. I have gained this knowledge by joining one of the experimental detector teams, taking part in the installation procedure. To give the reader a better understanding of the modelled detectors, also the full monitoring systems they belong to are described in the report.

My main work has been to model the geometry of the detectors, and to perform efficiency calculations and simulations of beta-gamma coincidences. For the latter task, special procedures have been developed in order to track the simulated particles and record coincidence events (which is not a default option in MCNP). The largest time fraction has been spent on the procedures and results described in section 7.2. I have also collaborated with the International Data Centre of CTBTO in Vienna to develop subroutines for MCNP.

Some of the results reported here have been presented at a workshop on xenon detection, organized by the Swedish Defence Research Agency in April 2001. My work will also be reported in two scientific papers;

- A. Ringbom, T. Larsson, A. Axelsson, K. Elmgren and C. Johansson, *SAUNA - a System for Automatic Sampling, Processing, and Analysis of Radioactive Xenon*, to be published.
- W.K. Pitts, T.W. Bowyer, J.I. McIntyre, P.L. Reeder, A. Ringbom, C. Johansson, *Gain Calibration of a Beta-Gamma Coincidence Spectrometer for Automated Radioxenon Analysis*, to be published.

Uppsala, May 2002

Cecilia Johansson

Contents

1 Introduction

Detection of radioactive xenon is used to monitor nuclear weapons tests. This report describes Monte Carlo simulations of two beta-gamma coincidence detectors with different geometry, intended for such monitoring by low activity measurements of gaseous samples. The main objectives for simulating these detector systems are to ensure that the experimental spectra can be understood, to see how detector and other materials influence the results, and to compute detector efficiencies.

In section 2, an introduction to the Comprehensive Nuclear-Test-Ban Treaty is given, as well as an overview of techniques used for monitoring violations of the treaty. Section 3 is focused on one of these techniqes, i.e., xenon detection, and the principles for collecting and detecting radioactive xenon isotopes are outlined. In sections 4 and 5, detailed information is given on SAUNA and ARSA, two xenon systems, and the code used for the simulations, MCNP, is described in section 6. The results of the calculations performed are presented and compared with experimental data in section 7, and finally, a summary, the conclusions and an outlook are given in section 8.

2 The Comprehensive Nuclear-Test-Ban Treaty

The Comprehensive Nuclear-Test-Ban Treaty (CTBT) is an important component for the non-proliferation of nuclear weapons. It was opened for signature in September 1996, and has so far been signed by 165 nations. The treaty bans any nuclear tests, in all environments, and constrains the development and improvement of existing weapons.

An important step towards the CTBT was taken in 1963, when the Partial Test-Ban Treaty (PTB) was signed. It banned nuclear tests in the atmosphere, underwater and in space, but not underground. This treaty, however, was never signed by the two nuclear weapon states China and France. In 1968, another step towards nuclear disarmament was taken with the Non-Proliferation Treaty (NTP). It prohibited non-nuclear states to possess, acquire, or manufacture nuclear weapons.

Under strong support from the UN, negotiations for the CTBT began in 1993, and on September 24, 1996, it was signed by the first states, including the five confirmed nuclear weapons states of that time. However, for the treaty to enter into force, also ratification is mandatory. In particular, it is required that the 44 states with "nuclear capacity" ratify the treaty. Among these, one finds the five classical nuclear weapon states (USA, Russia, Great Britain, France, and China) as well as India, Israel, and Pakistan. So far, 90 states have ratified the treaty, including the three nuclear weapon states Russia, Great Britain and France [1].

The Preparatory Commission for the Comprehensive Nuclear-Test-Ban Treaty Organization (CTBTO) monitors compliance with the treaty. Through its Provisional Technical Secretariat (PTS), the CTBTO is setting up an International Monitoring System (IMS). Using different techniques, the IMS will be able to detect nuclear explosions in all environments and on all continents.

Furthermore, states which have signed the treaty have the right to request on-site inspections to clarify if a nuclear test has taken place, and to collect environmental data which can help in identifying violations of the treaty.

2.1 The International Monitoring System

The monitoring regime within the CTBTO is the International Monitoring System (IMS). This is a worldwide control system, consisting of seismic, infrasound, hydro-acoustic and radionuclide detectors, placed in a network around the globe. In total, there will be 337 monitoring facilities (see Fig. 1), many of which are placed in remote areas. It is therefore important that the stations are reliable and automatic, and that they continuously report to the International Data Centre (IDC) of CTBTO in Vienna, Austria.

The four monitoring techniques rely on two basic phenomena that occur in a nuclear detonation - energy release and radionuclide production. The energy from an explosion propagates as waves through earth, air, and water, while the physical products are distributed to the surrounding environment and transported by winds and water. Three of the monitoring techniques rely on wave detection in different media - seismology in solid earth, hydro-acoustics in water, and infrasound in air. For the detection of different radionuclide products, the network uses aerosol stations and noble gas collection systems.

Once fully equipped, the monitoring system will have 50 primary seismic stations, reporting to the IDC in real time, and 170 auxiliary stations, providing data on demand from the data centre. The main use of the seismic verification system is to detect underground nuclear explosions and the main difficulty is to clearly distinguish between these and commonly occuring earthquakes.

Sound waves can travel very long distances in water, and as a result, only 11 hydroacoustic monitoring stations are needed to cover the entire ocean surface of the Earth. However, hydroacoustic signals are created from many man-made and natural sources, such as submarines, explosions, and earthquakes, presenting a measurement background.

The infrasound network will consist of 60 stations that use acoustic pressure sensors to detect low-frequency sound waves in the atmosphere. The IDC will use data from these stations to distinguish between nuclear explosion events and other man-made or natural phenomena, such as rocket launches, meteorites, and explosive volcanoes.

For radionuclide measurements, the network will consist of 80 aerosol stations that use air samplers to collect and detect radioactive particles released from explosions in the atmosphere, or transported through rock or water from underground and underwater explosions. The relative abundance of different isotopes can be used to rule out other sources, such as nuclear reactors and medical facilities. Of the 80 radionuclide stations, 40 will include xenon detection systems. The remaining 40 will be equipped later, after a decision taken by the conference of state parties. In addition to the sampling stations, the IMS also has 11 radionuclide laboratories to its disposal for further analysis of aerosol filters and noble gas samplers.

2.2 The collaboration on noble gas sampling and detection

In order to evaluate systems for noble gas sampling and detection, an international collaboration has been formed. It consists of four laboratories, which have each developed a xenon detection system:

- The Swedish Defence Research Agency (FOI), Sweden. Xenon system: SAUNA.
- The Pacific Northwest National Laboratory (PNNL), USA. Xenon system: ARSA.
- Commissariat à l´Energie Atomique, Direction des Applications Militaires, Département Analyses Surveillance Environnement (CEA/DASE), France. Xenon system: SPALAX.

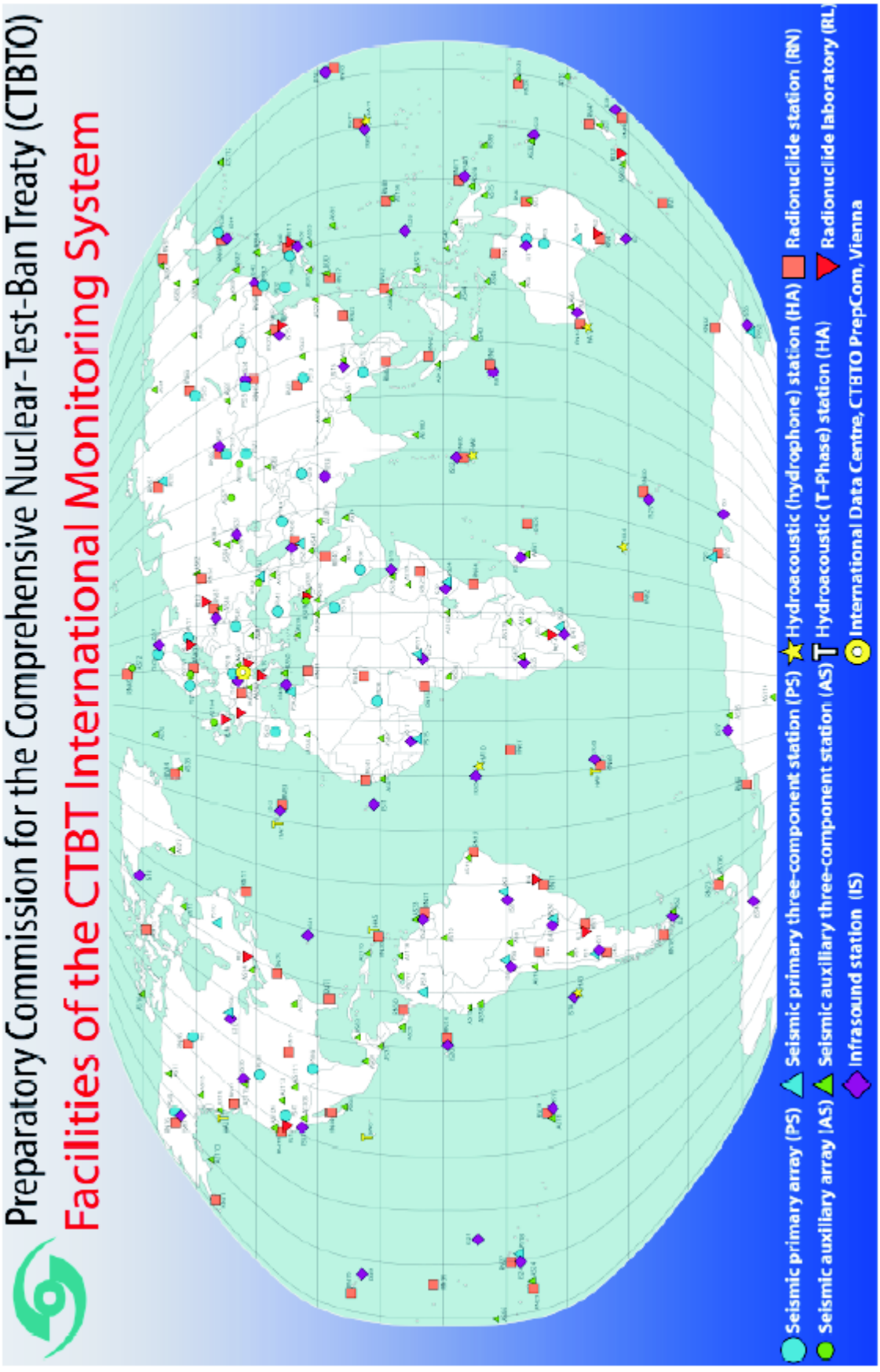

Figure 1: The detection facilities in the CTBT International Monitoring System.

- Khlopin Radium Institute (KRI), Russia. Xenon system: ARIX.

In October 2000, all systems were installed together at the Institut für Atmosphärische Radioaktivität (IAR), in Freiburg, Germany. The objective was to compare the systems under similar conditions, and also to perform a collective calibration test by injecting a ^{133}Xe sample with a known activity of around 10 Bq.

At present, the four xenon acquisition systems are being field tested in different environments around the globe. The Swedish system is stationed in Spitzbergen (Norway), the American in Guangzhou (China), the Russian in Rio de Janeiro (Brazil), and the French in Papeete (Tahiti). The goal of these tests is to demonstrate long-term, unattended, operation to gain experience on measurements without trained operators. For more information on the international noble gas programme, see ref. [2].

3 Detection of radioactive xenon

Airborne radioactive noble gases are released from several man-made sources, including nuclear explosions, nuclear reactors, fuel reprocessing plants, and nuclear medicine facilities. These noble gases are produced in fission of uranium and plutonium, both directly and as daughter nuclides from decay of other fission products. In this work, mainly various stable and radioactive isotopes of xenon are considered.

Xenon is a chemically inert gas which is volatile in the environment. This makes it difficult to confine xenon from a nuclear explosion, and therefore, detection of atmospheric xenon could be a sensitive tool for monitoring nuclear weapons tests, also those performed underground. Xenon does not easily condense on atmospheric particles, which means that aerosol stations cannot be used for collection. Instead, other sampling techniques are used (see sections 4 and 5).

The xenon isotopes of interest for monitoring of nuclear weapons tests are ^{131m}Xe, ^{133}Xe, ^{133m}Xe, and ^{135}Xe. They have half-lives of the order of days and are produced in amounts large enough to be relatively easy to detect, also at large distances. The most important background for monitoring measurements comes from release of xenon from nuclear power plants. However, it is possible to distinguish between xenon from power plants and from nuclear explosions by inspecting the ratios between the different isotopes. A simple calculation, taking into account relevant direct and cumulative fission yields, indicates that the ratio ^{135}Xe/^{133}Xe is about four orders of magnitude larger for an explosion release than for a reactor release, and the ratio ^{133m}Xe/^{133}Xe will differ by about a factor of 100 [3].

The most important decay modes for the relevant xenon isotopes are listed in Table 1. Here, it can be seen that ^{133}Xe and ^{135}Xe decay through beta emission, followed by gamma decay or internal conversion (i.e., low-energy electron emission) accompanied by x-ray emission. The metastable isotopes, ^{131m}Xe and ^{133m}Xe, decay to the xenon ground states by gamma emission or internal conversion electrons and x-rays. The detection techniques studied in this work all rely on beta-gamma coincidence measurements.

The most prominent gamma line in the ^{133}Xe spectrum is found at 81 keV. The corresponding beta decay has an endpoint energy of 346 keV. In 54% of the decays, internal conversion takes place, resulting in a 45 keV electron, followed by a cesium x-ray, with an energy of around 30 keV. The decay scheme is shown in Fig. 2.

Also ^{135}Xe has several possible beta decay modes. The most probable one has an endpoint energy of 910 keV and it populates an excited state of 250 keV. This state

Isotope	Half life	Energy (keV)	Intensity (%)	Decay type
^{131m}Xe	11.8 days			
		29.46	15.5	x-ray
		29.78	28.9	x-ray
		33.61	7.8	x-ray
		34.61	1.85	x-ray
		163.9	1.96	gamma
		129.0	60.7	ic
^{133}Xe	5.24 days			
		346.0 (max)	100	beta
		30.62	14.1	x-ray
		30.97	26.0	x-ray
		34.97	7.1	x-ray
		36.01	1.74	x-ray
		79.61	0.239	gamma
		80.99	37.0	gamma
		45.0	54.1	ic
^{133m}Xe	2.19 days			
		29.46	16.2	x-ray
		29.78	30.1	x-ray
		33.61	8.1	x-ray
		34.61	1.92	x-ray
		233.2	10.3	gamma
		199.0	63.1	ic
^{135}Xe	8.38 days			
		910.0 (max)	100	beta
		30.62	1.5	x-ray
		30.97	2.77	x-ray
		34.97	0.76	x-ray
		36.01	0.185	x-ray
		249.8	90.0	gamma
		608.2	2.90	gamma
		214.0	5.70	cc

Table 1: Decay properties of radioactive xenon isotopes relevant for monitoring. Note that not all possible transitions are listed here.

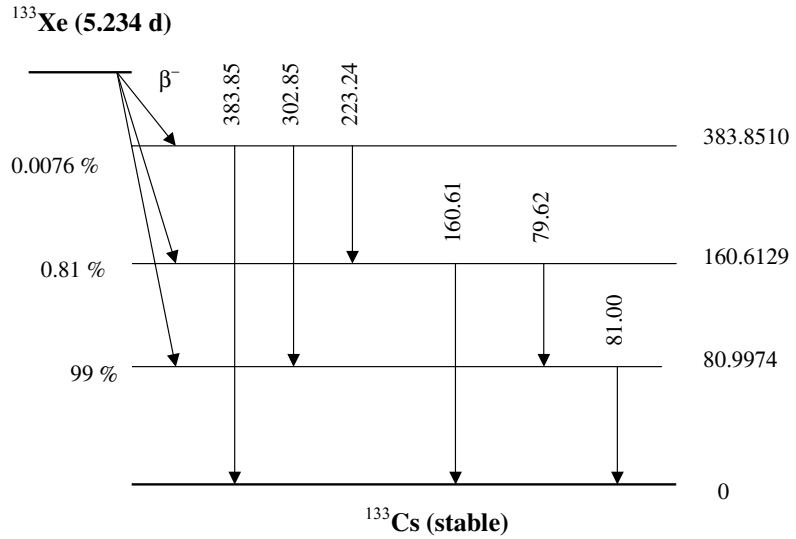

Figure 2: Decay scheme for ^{133}Xe. Energies are given in keV.

decays mainly by gamma emission, but in 5.7% of the cases internal conversion takes place, resulting in emission of an electron of 214 keV followed by emission of a cesium x-ray of around 30 keV. A decay scheme is shown in Fig. 3.

The decays of ^{131m}Xe and ^{133m}Xe are less complicated, since each of the metastable states only emit one gamma ray, or an internal conversion electron in association with a xenon x-ray.

Beta energies always form a continuum up to a maximum energy. Thereby, beta energy measurements cannot be used on an event-by-event basis to identify a certain isotope in a mixture of beta-active elements. Beta detection alone could in principle be used to detect the presence of a certain nuclide, but this requires good statistics in combination with a very low background. Therefore, a combination of beta and gamma detection, i.e., a coincidence technique, is preferred, because it facilitates isotope identification with much less statistics.

All the xenon isotopes involved emit x-rays at about the same energy, which is not surprising because the energies of these x-rays are determined by electron shell properties. Thus, these x-rays might be useful for detecting the presence of xenon, but not for isotope identification. When inspecting the decay properties (see Table 1), it can be found that all the four isotopes emit gamma rays, with energy differences larger than the detector energy resolution, thus allowing isotope identification.

4 SAUNA - Swedish Automatic Unit for Noble gas Acquisition

SAUNA - Swedish Automatic Unit for Noble gas Acquisition - is a system for automatic sampling, processing, quantification and activity determination of radioactive xenon in the atmosphere. It has been developed at the Swedish Defence Research Agency (FOI), Department for Nuclear Weapon Issues and Detection, Ursvik, Stockholm. Continuous sampling of ^{133}Xe has been performed since 1990 using an older semi-automatic technique.

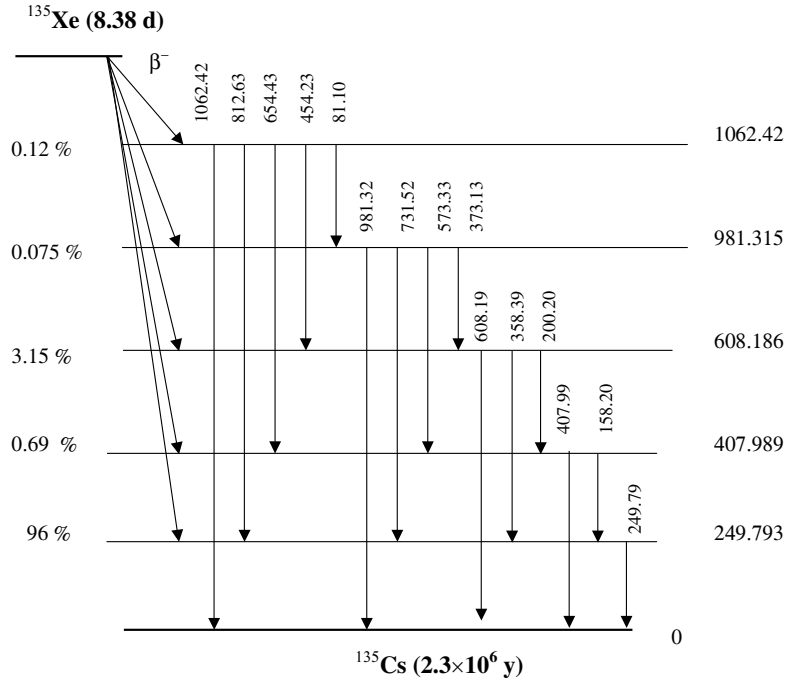

Figure 3: Decay scheme for ^{135}Xe. Energies are given in keV.

Xenon yields determined in measurements between 1990 and 1998 are presented in Fig. 4. The high reading indicated with an arrow is xenon from the most recent Soviet nuclear test in Novaja Zemlja in October 1990. The other peaks are due to xenon from nuclear power plants. This older system could not meet all the requirements of CTBTO, however, and therefore SAUNA was built.

The SAUNA system collects air, extracts a xenon sample, measures the activity of the four isotopes, ^{131m}Xe, ^{133}Xe, ^{133m}Xe, and ^{135}Xe, and automatically produces data files which can be sent to the IDC in Vienna.

4.1 Principles for collection of atmospheric xenon

A photograph of SAUNA, installed at its permanent location at Spitzbergen, is shown in Fig. 5, and the collection principle is outlined in Fig. 6. The first part of SAUNA is the air inlet, through which about 0.6 m^3 of air is pumped per hour. To remove moisture, the incoming air is cooled to a few degrees below 0 ℃ using a small freeze trap. Carbon dioxide and the remaining water is removed in molecular sieves. These are synthetical adsorbents characterised by pores and crystalline cavities of extremely uniform dimensions. Molecular sieves are commercially available in different grades, which adsorb molecules of different sizes. E.g., grade 4A adsorbs molecules of sizes up to four Ångström.

In the next step, the xenon is enriched by adsorption on activated charcoal. Adsorption is more effective at low temperatures, but at higher temperatures, this can be partially compensated for by using larger charcoal columns.

To allow for uninterrupted sampling, SAUNA uses two parallel sampling ovens, collecting air for 6 hours each. The sample is transferred to the first process oven by heating the charcoal in the sampling oven to more than 300 ℃ , using helium as a carrier gas. In

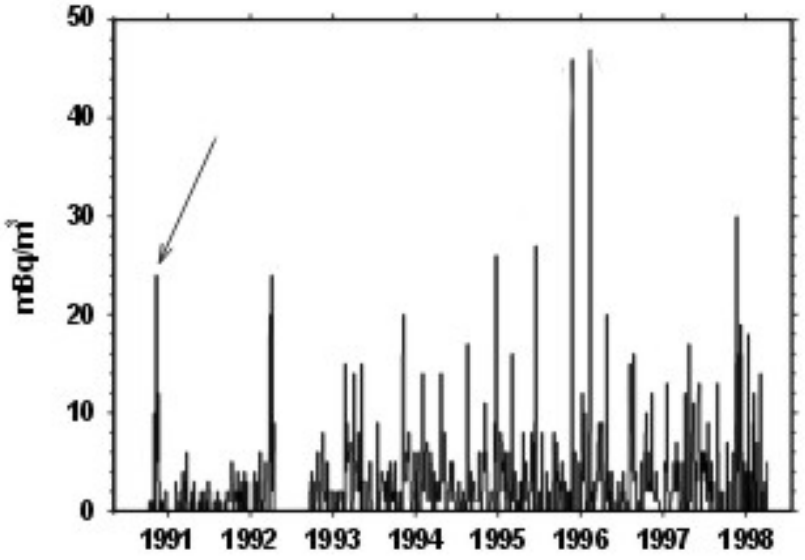

Figure 4: Measurements of ^{133}Xe activity at FOA, Ursvik, between 1990 and 1998. Note the xenon peak indicated with an arrow, which corresponds to the most recent Soviet nuclear bomb test. The other peaks are xenon discharges from nuclear power plants.

this process oven, two samples are also combined using a second charcoal column.

To separate and concentrate the xenon, the sample is further transported through molecular sieves in the second process oven. At the end of the processing procedure, the amount of xenon is determined using a gas chromatograph. It measures the resistance in the sample gas relative to a reference gas (in this case helium). The resistance is proportional to the thermal conductivity which differs for different gases. A time window around the xenon peak is applied to allow only this part of the sample into the detector (see Fig. 7). This is crucial in order to achieve efficient removal of radon, which otherwise could interfere severely with the activity measurement. The gas chromatograph also provides quantification of the amount of detected xenon, by integrating the obtained peak.

For transport into the detector, helium is again used as carrier gas. Typically 0.5 ml of stable xenon is collected from a 12 hour cycling. The atmosphere contains 0.087 ppm stable xenon, thus the collection yield corresponds to more than 90%.

After the activity measurement, the gas in the detector cell can be flushed out and transferred to an archive bottle. Control measurements of these archive bottles can be performed at the radio-nuclide laboratories belonging to the IMS network.

4.2 The SAUNA beta-gamma detector

The detector part of SAUNA consists of two identical beta-gamma detectors working in parallel. While one detector is measuring a sample, the other records background data after being flushed with helium gas to reduce xenon contamination from the previous sample.

The SAUNA beta detector is a 6.4 mm^3 plastic scintillator cylinder that contains the gas sample. The thickness of the cylinder walls are 1.2 mm, and in each end a 3/4" PM-tube is attached. The cylinder and the PM-tubes are mounted in a plastic support. The

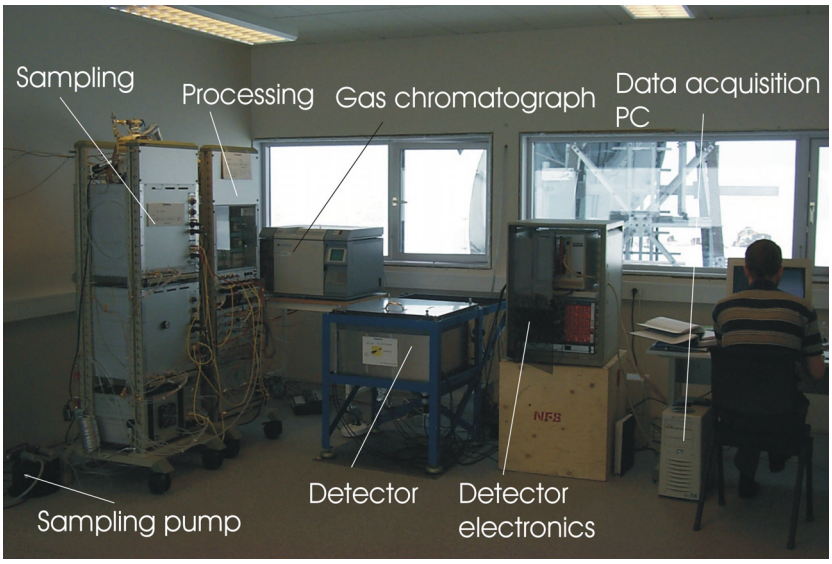

Figure 5: The SAUNA xenon system, photographed at Spitzbergen. The "processing" refers to process ovens 1 and 2 (see Fig. 6).

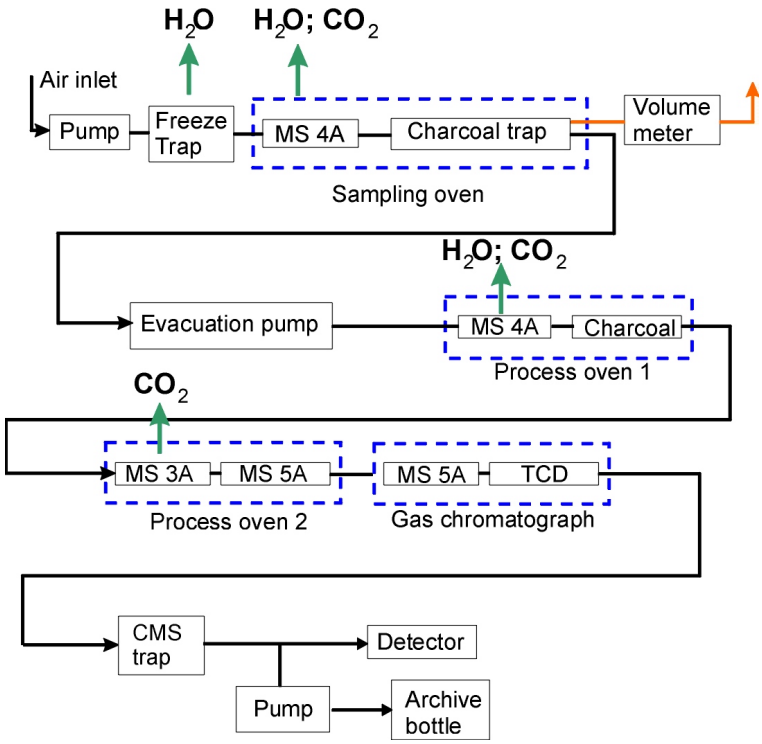

Figure 6: A schematic description of the principle for the SAUNA xenon sampling and concentration process. See the text for details.

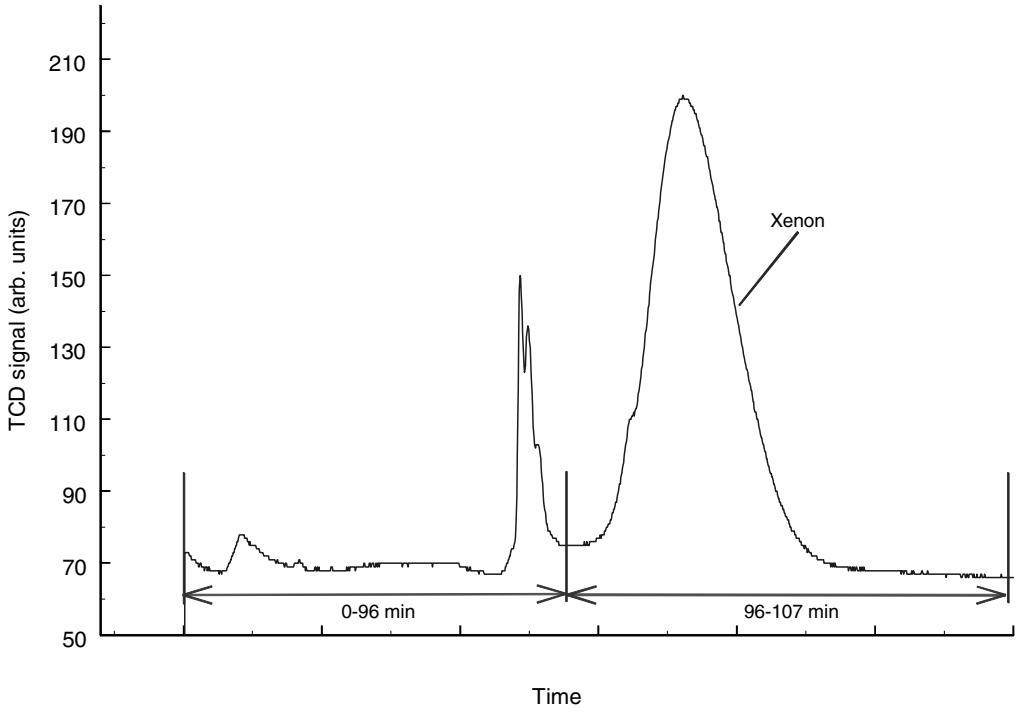

Figure 7: A gas chromatogram, showing the measured thermal conductivity (TCD signal) versus time (note that the scale is broken). The xenon peak is separated in time from the rest of the sample.

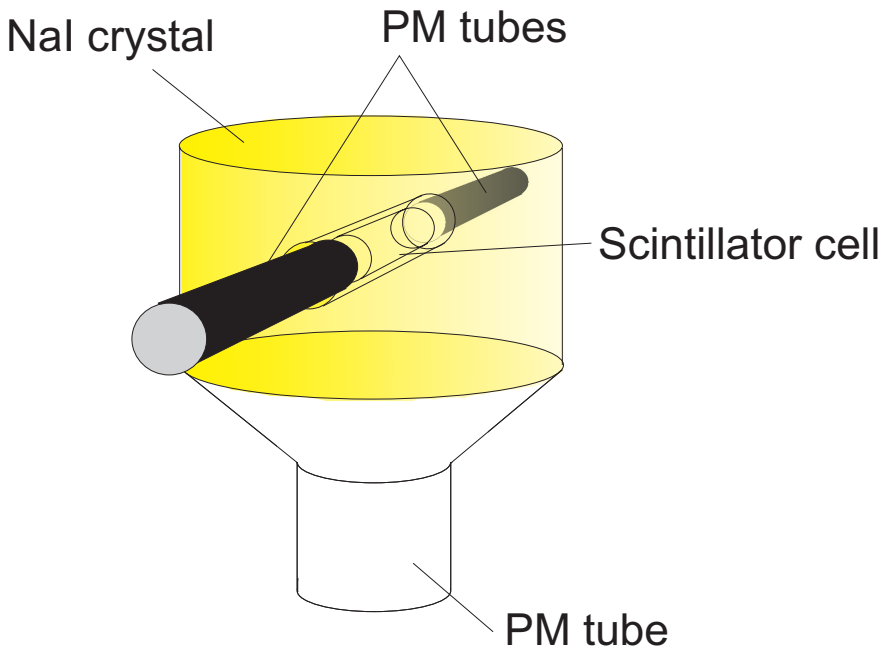

Figure 8: The SAUNA beta-gamma detector. The scintillating beta cell with its two PM tubes is inserted into a drilled hole in the NaI crystal.

Isotope	Decay	Beta interval	Gamma interval
^{133}Xe	x-ray	16-35 keV	0-410 keV
^{133}Xe	gamma	70-95 keV	0-370 keV
^{135}Xe	gamma	225-275 keV	0-950 keV

Table 2: The different regions of interest (ROI) used for efficiency calculations.

beta cell is surrounded by a 4" × 5" cylinder NaI crystal, acting as a gamma detector. It has a 35 mm hole drilled through the centre, into which the beta cell in its plastic support has been inserted (see Fig. 8). The NaI crystal has an outer aluminium layer of 1 mm, and the drilled hole has an inner 0.25 mm aluminium cover. The crystal is read out by one single PM-tube.

Each of the two detector systems is placed inside a 5 cm thick lead shield, with an inner copper layer of 5 mm, and a top lid layer of 5 mm iron (see Fig. 9). The lead shield consists of low-activity lead bricks, and the copper layer protects the detectors from lead x-rays.

Standard CAMAC and NIM electronics are used for the electronic read-out of the detectors. The trigger of the system is a triple coincidence between the two beta PM tubes and the gamma PM tube, i.e., a beta-gamma coincidence. The beta energy deposited in the plastic is obtained by summing the signals from the two PM tubes.

The main uncertainties in the determination of the activity of a xenon isotope are due to proper identification of events to the relevant activity, and due to the detector efficiency. Since a few isotopes can contribute with signals in the detector, regions of interest (ROI) have been pre-defined, in which the yield is used for activity determination for a specific

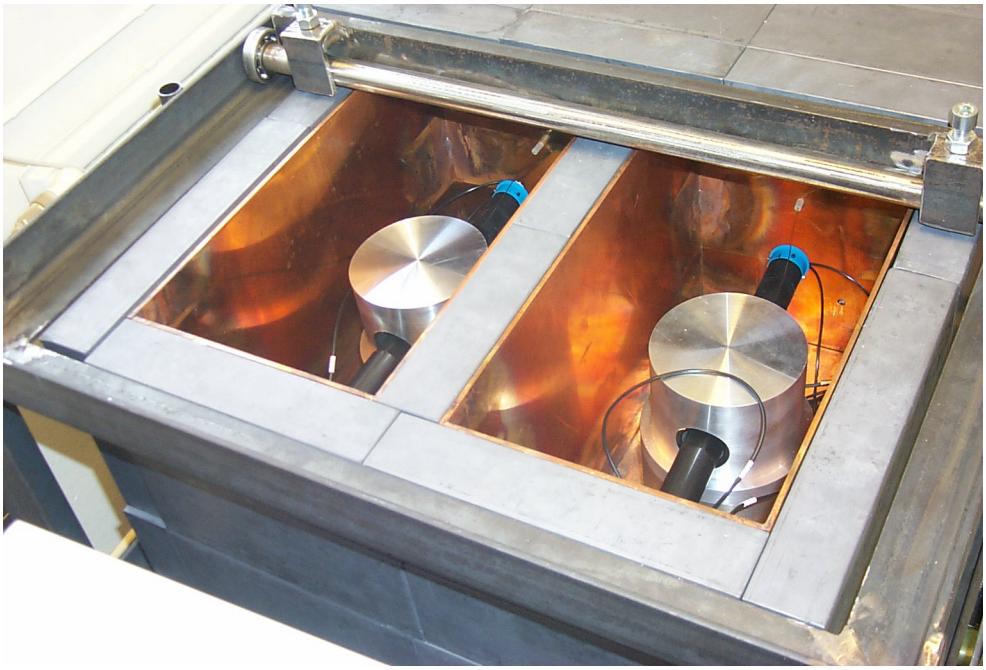

Figure 9: A photo of the two identical SAUNA beta-gamma detectors, seen from above. The two detectors are separated and shielded by a 5 cm thick lead box with an inner layer of copper. The NaI crystal is covered by aluminium.

nuclide (see Table 2). When determining these yields, a background measurement followed by a sample measurement is performed. The background measurement will include both xenon left from the previous sample and the ambient background.

Known characteristics of detector response functions are used to estimate from each measured two-dimensional (2D) histogram (sample or background) a "net number of counts" for each ROI. Such known characteristics are ratios of counts in different regions, relating for instance the amount of ^{133}Xe counts in the 80 keV region to the 30 keV region, as well as background regions adjacent to the ROI, used to estimate the contribution of uncorrelated, approximately flat background (as in the case of ^{135}Xe). The thus estimated net number of counts in the sample and background measurements, respectively, are then combined to estimate a decay-corrected, background-subtracted number of counts, which then are used to determine the concentration of each isotope in the sample.

The detector efficiencies in the different ROIs are difficult to measure. One way of finding the efficiencies is to use simulations, which is a motivation for the present work, see section 7.3.

4.3 Energy calibration of the SAUNA detector

Energy calibration of the NaI crystal was performed using standard point sources (^{133}Ba, ^{241}Am, ^{152}Eu, and ^{22}Na). The sources were placed inside the lead shield and the electronics were adjusted to trig on NaI signals only. The relative resolution has been found to be 23% at 30 keV, decreasing nearly linearly to 8.9% at 511 keV.

Calibration of the beta detector is more complicated than for the gamma detector. The beta cell is contained inside a plastic cover, making it difficult for electrons from a source emitting conversion electrons to reach the detector. Therefore, a technique based

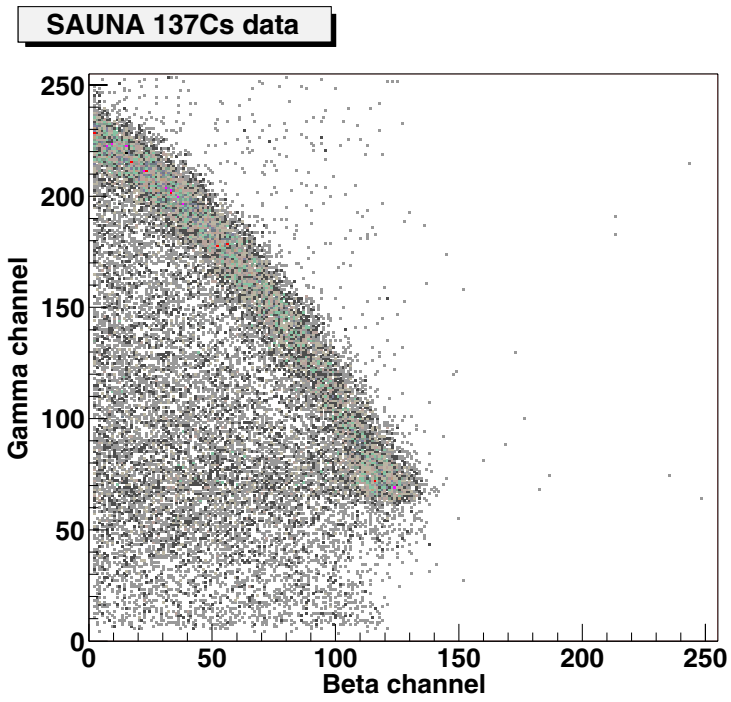

Figure 10: Spectrum obtained with a ^{137}Cs point source. The diagonal corresponds to the total energy (662 keV) being deposited in the detectors, and these events are used for energy calibration of the beta scale.

on Compton scattering of gamma rays from ^{137}Cs has been developed [4]. A cesium point source is placed inside the lead shield, above the gamma cylinder, approximately 20 cm from the detector centre. It turns out that the electrons created by Compton scattering in the plastic scintillator material can be used for calibration of the beta scale over the entire energy range used (see Fig. 10).

When an incident gamma ray undergoes one or several Compton scatterings in the NaI crystal, or in the beta cell, coincidences are created in the detector. The diagonal distribution going from left to right in Fig. 10 corresponds to the full energy of the gamma rays (662 keV) being deposited in the detectors. No photo-peak is visible in the spectrum, since photoelectric absorption would not cause beta-gamma coincidences in the detector. Multiple Compton scattering in the NaI gives rise to events above the Compton edge in the gamma spectrum. The distribution ends at 478 keV beta energy, corresponding to backscattering in the beta cell followed by absorption of the remaining 184 keV gamma ray in the NaI crystal. Events below the diagonal are due to beta particles not fully stopped in the beta cell.

The calibration of the beta energy scale is performed using the events corresponding to $E_\beta + E_\gamma = 662$ keV (the diagonal in Fig. 10). The energy scale is not fully linear due to the electronics, and to the fact that the light output function from the scintillator is non-linear at electron energies below 125 keV. The resolution of the beta detector is approximately 30 keV over the full energy scale [5].

4.4 Efficiency calibration of the SAUNA detector

Efficiency calibration of the detector has been performed by injecting a strong sample of ^{133}Xe into the beta cell. The beta efficiency was then obtained by comparing NaI spectra recorded in singles and coincidence mode. Using this method, the beta efficiency has been determined to be around 95% for the 30 keV peak, and 80% for the 81 keV peak. Beta efficiencies have not been explicitly measured for the other xenon isotopes, but they are expected to be around 85% for the 250 keV peak in ^{135}Xe, and nearly 100% for the decay of the metastable states [5].

There are no well-defined peaks in the beta spectra, and therefore the use of a xenon sample to measure the gamma efficiency is not as straightforward as in the beta case above. The energy-integrated gamma efficiency for a specific sample can, however, be measured by comparing the total number of counts in the ungated and gamma-gated beta spectra. This is done using the same sample as in the beta-efficiency measurement, resulting in an energy-integrated gamma efficiency of 63%. By comparing with an efficiency function calculated using MCNP (see section 7.1), it has been conjectured that the photo-peak efficiency can be determined within an absolute uncertainty of 10–15% [5].

5 ARSA - Automatic Radioxenon Sampler-Analyzer

The Automatic Radioxenon Sampler-Analyzer (ARSA) has been built by the Pacific Northwest National Laboratory (PNNL), Richland, Washington, USA. ARSA and SAUNA are fairly similar when it comes to the xenon decay detection, while there are some significant differences in the gas acquisition techniques. The ARSA xenon collection and purification stages are based on adsorption at -150 ℃, a temperature achieved by compressors. This makes the collection more efficient than for SAUNA, which works at room temperature, but at the expense of a more complex technique. The collection time is 8 hours, and during this time 48 m^3 of gas is collected, i.e., about a factor of ten more than SAUNA. For more information on the ARSA system, see ref. [6].

5.1 The ARSA beta-gamma detector

As was metioned above, the SAUNA and ARSA detectors are very similar. The beta cell was designed by PNNL, and adopted by FOI when developing SAUNA. Both systems are also equipped with NaI gamma detectors, and both utilize beta-gamma coincidences.

The ARSA detector (see Fig. 11) has two rectangular 7" × 4" × 1.5" NaI crystals which are sandwiched together and covered with a 1 cm aluminium layer. Each NaI crystal is read out by two 3" PM-tubes. In the plane adjoining the crystals, four holes with a radius of 0.625" are drilled, 1.5" apart. In these holes, four identical beta cells, each with two PM-tubes, have been placed. The reason for having four beta cells is the ARSA sampling cycle, which produces a new sample every 8 hours. The ARSA detector is - like the SAUNA detector - surrounded by a 5 cm lead box with a 5 mm inner copper layer to provide shielding from lead x-rays.

The energy calibration of the ARSA detector is performed in the same way as for the SAUNA system [4]. The only difference is the placement of the ^{137}Cs source for beta energy calibration. For ARSA measurements, the source is placed inside the plastic support close to one beta cell, but the measurement is done in the adjacent cell. The

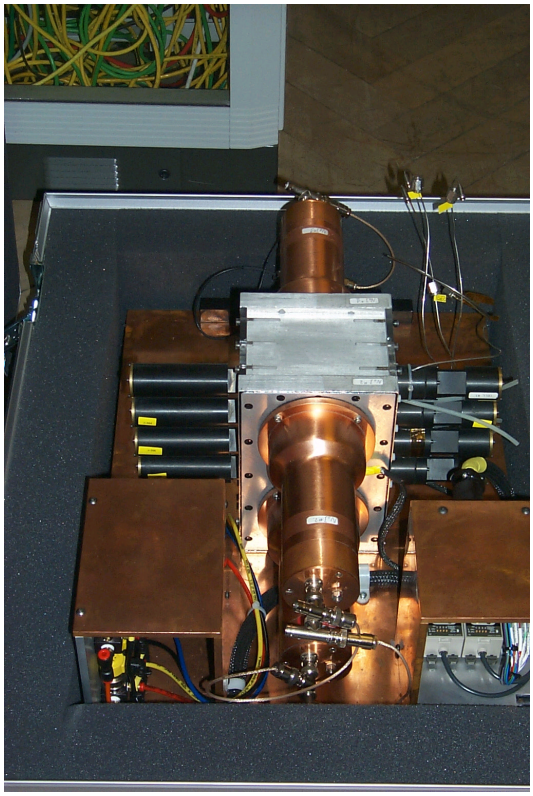

Figure 11: The ARSA beta-gamma detector as seen from above.

reason for this is to get a more homogenous illumination of the cell, although at the expense of a lower counting rate.

6 MCNP calculations

Computer simulations of detector systems are important for many reasons. They can give insight into the details of experimental spectra and a deeper understanding of the detector response in different energy ranges. The work presented below aims at modelling the detector systems as realistically as possible, calculating the photo-peak efficiency in the gamma crystal and simulating two-dimensional beta-gamma spectra from calibration runs (^{137}Cs) and data taking runs (^{133}Xe and ^{135}Xe).

MCNP was chosen since it is a well-established and well-documented code for these kinds of calculations, and since its source code is provided to users. The latter has enabled modifications of the particle source definition according to our specific needs.

6.1 The MCNP code

MCNP is an acronym for Monte Carlo N-Particle Transport Code, and it is a Monte Carlo code developed at Los Alamos National Laboratory (LANL). The program language is mainly FORTRAN, but in developing the code, also C++ has been used. The first version, which was released in 1969, treated neutrons only, but later versions also include transport of photons and electrons. The version used for this work is MCNP4C, which was the most recent version when the simulation project started in April 2000. Since

then, a few versions have been released, among which is MCNPX, which transports also particles like protons and alphas.

With the Monte Carlo techniques, each created particle can be followed in a pre-defined geometry from its source to its termination, caused by, e.g., absorption or escape from the defined geometry. At each step of the life of the particle, probability distributions are randomly sampled and used together with data libraries to determine the fate of the particle. When secondary particles are created, these are stored in the memory (banked) for later transport.

The non-deterministic approach of MCNP means that the average behaviour of the simulated particles is recorded, and certain requested aspects (tallies) of the behaviour are presented to the user. Since the problem is not analytically solved, no other information than that requested can be obtained once the code has been run for a problem.

The user can select the number of source particles (histories) to be simulated by the code. Every time an interaction occurs in some material, a new track (event) starts. The code follows one history at a time, event by event, until the cut-off energy (default = 1 keV) is reached, or the particle disappears out from the defined geometry.

6.2 Photon physics of MCNP

MCNP has two photon interaction models, a simple and a detailed one. In the detailed mode, all photon collisions are taken into account. These are:

- Thomson (coherent) scattering, where no energy loss occurs. This means that no secondary electron is created, and that only the deflection angle of the incoming photon is of interest.

- photoelectric effect, which is the process where the incident photon is completely absorbed by an atom. In the process, a photoelectron is ejected from one of the bound electron shells. MCNP differentiates between zero, one, or two fluorescent photons being emitted. For elements with $Z < 12$, a photoelectric event is terminated, since the possible fluorescent energy is below 1 keV, which is the MCNP cut-off energy. Single fluorescence takes place for $12 < Z < 31$, while double fluorescence is possible for elements with $Z > 31$. In all cases, the fluorescent photons are assumed to be emitted isotropically.

- Compton (incoherent) scattering, where the incoming photon is deflected through an angle θ with respect to its original direction. A portion of the photon energy is transferred to an electron in the absorbing material. The energy transferred to this recoil electron can vary from zero to a large fraction of the original photon energy.

- pair production, which only takes place for energies above 1.022 MeV. This case is of no importance for the present work.

When secondary electrons are created, which is the case for all processes except coherent scattering, these are banked and transported later by the code. Form factors are used to account for electron binding effects.

The simple mode ignores coherent (Thomson) scattering and fluorescent photons from photoelectric absorption, and is intended for high-energy photons. For photons with energies below 100 MeV, detailed treatment is default.

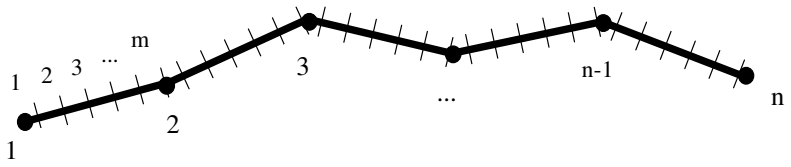

Figure 12: Illustration of steps (n) and substeps (m) used by MCNP in electron physics.

6.3 Electron physics of MCNP

Since electrons are electrically charged, they are subject to long-range Coulomb forces which induces many small collisions when entering a material. Compared to a photon, an electron undergoes more than five orders of magnitude more collisions per path length. This complexity makes single-collision electron transport unfeasible, and in most transport problems, multi-scattering theories are used. These aim at using fundamental cross sections, together with statistical representations of transport processes, to predict the probabilities for energy loss and angular deflection.

When an electron is transported by MCNP, its track is divided into several energy steps. Each step is long enough to encompass several collisions, but short enough to keep the energy loss small compared with the electron energy. The path length for every step is chosen so that

$$\frac{E_n}{E_{n-1}} = k, \tag{1}$$

where k is a constant. The default in MCNP is $k = 2^{-1/8}$, which allows an energy loss of 8.3% per step, but this number can be changed by the user.

To make the trajectory of the electron more accurate, every step is further divided into a number of equally long substeps. Appropriate numbers of substeps for different materials have been empirically determined, and a guiding rule is to use at least ten substeps for any material of importance to the transport problem.

For every electron track, MCNP computes non-radiative energy loss and energy straggling at every main step, while angular deflection and production of secondary particles are computed at every substep.

6.4 Geometry modelling

The geometry modelling for the SAUNA and ARSA detectors have been done by defining surfaces and cells in the MCNP format, described in appendix A.1.

It is very time-consuming to define a complete and exact geometry, and that is in general not necessary. Simplifications can of course be made where the impact on the result is small, but sometimes also more crucial changes to the actual geometry must be made. A simple geometry speeds up the calculations, but a more precise geometry definition can potentially expose important features.

Since the ARSA and SAUNA detectors are very similar, they have been modelled in a similar way (see Figs. 13 and 14). For both systems, the commercial materials used are BC404 for the plastic scintillator and ABS plastic for the support. For the optical light output material, soda-lime glass was used. The measuring beta cell is filled with a gaseous mixture of helium and xenon.

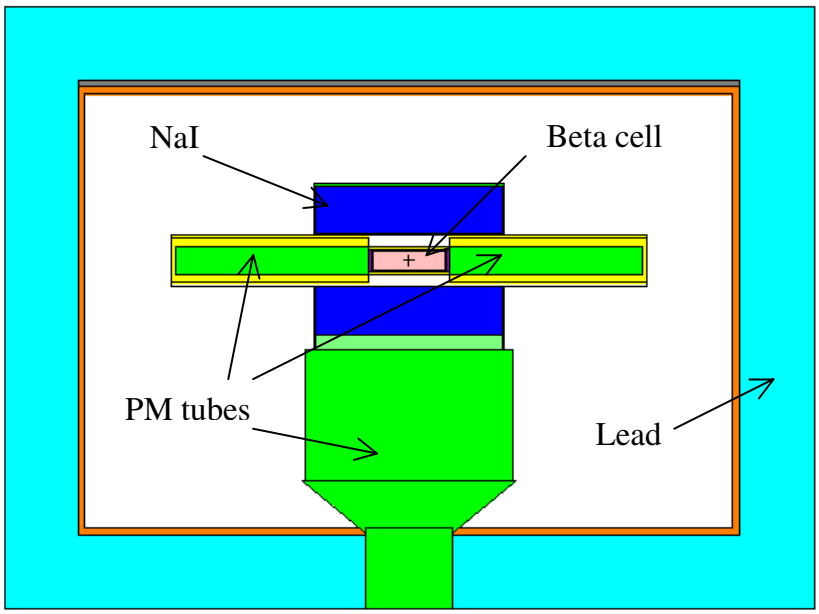

Figure 13: The SAUNA detector geometry modelled in MCNP. View from the side. See the text for details.

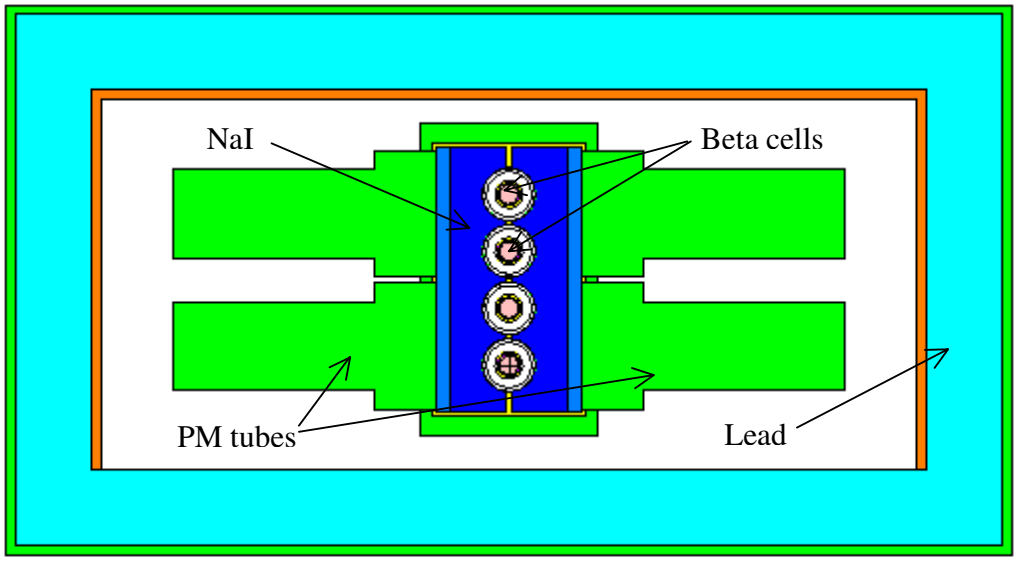

Figure 14: The ARSA detector geometry modelled in MCNP. View from the side.

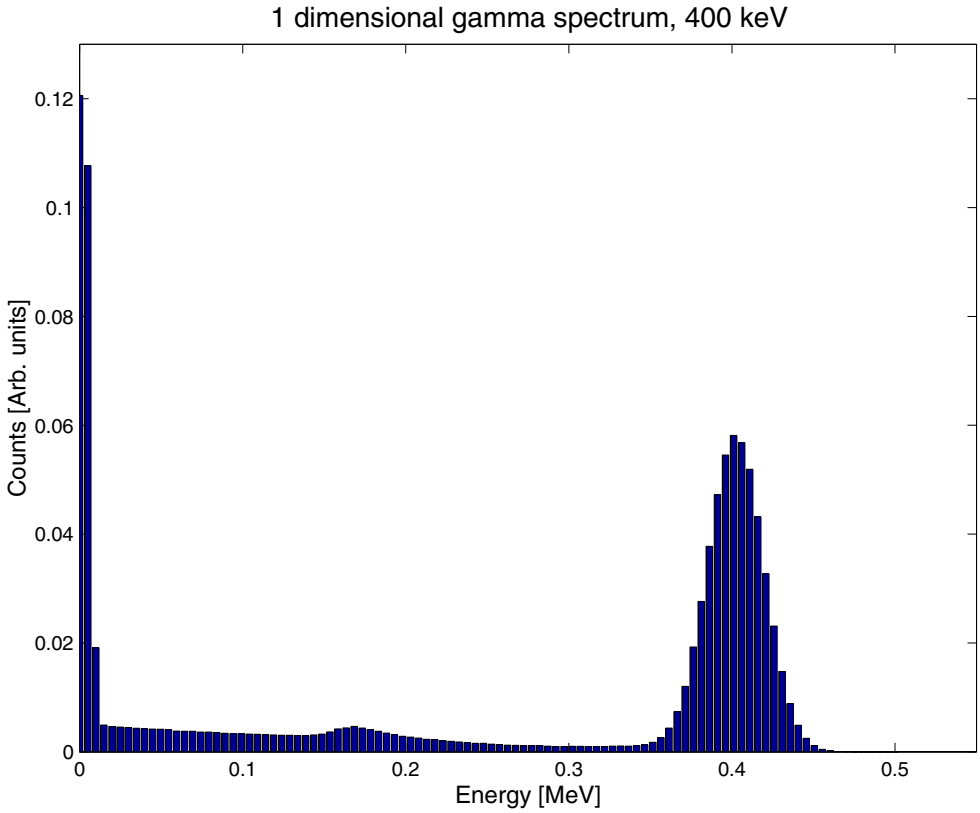

Figure 15: The SAUNA NaI response function simulated for a 400 keV gamma source energy.

The geometry modelling is done very accurately in the close vicinity of the beta cell. Further away, some simplifications have been made, the most important one being the modelling of the PM tubes. They are treated as being solid cylinders of aluminium, which was chosen for being representative of a medium-heavy material. Control runs were made with other materials, but the difference was very small.

7 Results and discussion

7.1 Photo-peak efficiencies

For calculation of the photo-peak efficiency of the NaI detectors, several separate runs with different mono-energetic gamma energies were performed. In the SAUNA case, the gamma source was placed inside the beta cell with an extension equal to the cell volume. The detector energy resolution was taken from experimental data. For the SAUNA gamma detector it has been found that

$$\Gamma = 0.076\sqrt{E}, \tag{2}$$

where Γ is the full width at half maximum, and E is the source particle energy, both in MeV.

In Fig. 15, one example of the MCNP output for gamma energy deposited in the NaI crystal is shown. The input source energy is 400 keV, and at this energy the photo-peak efficiency is about 50%. At 400 keV, Γ is around 40 keV (see ref. [5]), and hence a 40 keV broadening has been applied to the spectrum. Due to the relatively large detector

volume, the continuum goes all the way to the full-energy peak. This effect is due to multiple Compton events.

For the ARSA detector, the photo-peak efficiency was calculated in a similar way. The gamma source was placed outside one of the outer beta cells. The ARSA resolution is approximately given by

$$\Gamma = 0.067\sqrt{E}. \tag{3}$$

The results for the photo-peak efficiency are similar for the ARSA and SAUNA detectors at energies up to 100 keV (see Fig. 16). The absolute photo-peak efficiency is 80 – 90 % in the energy range 30 to 300 keV, meaning that the gamma rays deposit almost all their energy in the crystal. When going towards lower energies, the efficiency decreases rapidly due to absorption of gamma rays in the scintillator cells and in the aluminium layer. The sharp dip at around 30 keV is related to the K-shell absorption edge in iodine in the crystal. What actually happens is that above about 30 keV, ionization of K-electrons becomes possible. This results in emission of 28 keV photons when L-electrons fill the vacancy in the K-shell, plus lower-energy photons from rearrangements, predominantely in the L- and M-shells. The 28 keV photons are emitted close to isotropically, which means that the probability for loss of ionization in the detector increases, due to 28 keV photons leaving the detector through the hole in the NaI crystal.

At higher energies, the efficiency decreases since many photons escape from the crystal before the photoabsorption occurs. At these energies, Compton scattering is the dominant mechanism for photon interaction with the crystal. Above 100 keV, the ARSA efficiency is lower than that of the SAUNA, due to the larger amount of NaI material close to the cell in the SAUNA case.

7.2 Energy calibration spectra

As described earlier (see section 4.4), ^{137}Cs was used for energy calibration of the detectors. In the simulations of the SAUNA detector, the calibration source was placed 8 cm above the centre of the gamma cylinder, and for computational reasons, the source was biased, i.e., only emissions into a cone covering the NaI were considered. In the ARSA detector simulations, the ^{137}Cs source was placed inside one of the drilled holes in the NaI, 1 cm away from one cell, and the beta measurement was performed in the neighbouring cell. In this case, the source was modelled as an isotropic point source.

Both the ARSA and SAUNA detectors trigger on coincident gamma-beta signals. In order to simulate such coincidences in MCNP, it is necessary to follow each source particle and to track those particles that undergo reactions in both the beta cell and the gamma crystal. To obtain a two-dimensional (2D) spectrum similar to the experimental result, the energy deposited in the beta cell must be plotted versus the energy in the gamma cell. Such coincident 2D plots cannot be produced by default with MCNP, even though the tracking information for each source particle is contained in the output runfile. One way to extract the coincident beta and gamma events is to use the PTRAC card.

The PTRAC card writes position, energy and other vital parameters for every step in all histories of every source particle to a file named ptrac. The ptrac-file must then be sorted with respect to hit pattern and energy, so that the coincidence information can be extracted. The result is a number of coincidence events with energy deposition in both the beta cell and the gamma crystal. The sorting of the ptrac-files was performed using

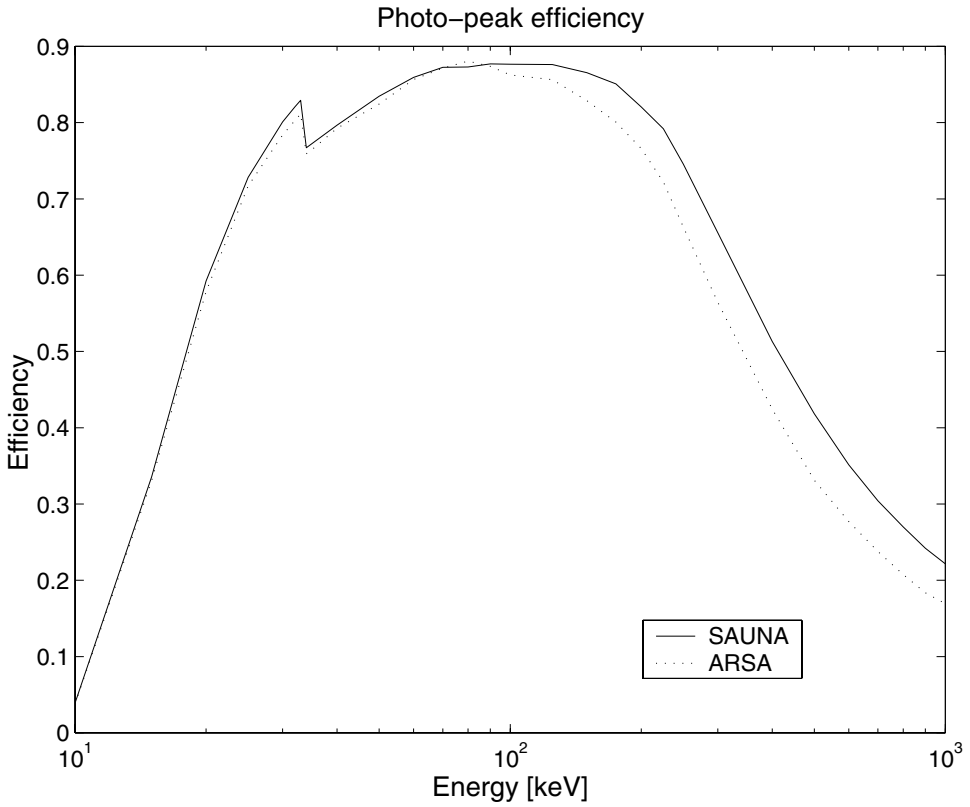

Figure 16: Photo-peak efficiencies for SAUNA and ARSA. See the text for details.

a program written in PERL, which is a program language very suitable for sorting large text files. For more detailed information on the sorting procedure, see Appendix A.2.

The procedure described here is very time consuming, since a majority of the simulated particles do not give rise to gamma-beta coincidences. On average, approximately 1 in 10 000 source particles generates a coincidence event. This is a number found to be in agreement with experiment. To speed up the computations, MCNP contains various variance reduction techniques, e.g., biasing of source particles, time cut-off, etc. Many of these, however, have the drawback of a less precise tracking of the individual particles, making it impossible to use the PTRAC option. Therefore, no variance reduction techniques have been used in this work.

The MCNP calculations for the SAUNA detector are shown together with experimental data in Figs. 17 and 18. The calculations have been performed with about 8.5 millon source particles, resulting in around 40 000 coincidence events. The calculated data were folded with the experimental resolutions, i.e., for the gamma detector, Eq. 2 was used, while a constant resolution of 30 keV was used for the beta detector.

In the 2D plot (Fig. 17), the experimental curve is bent at low beta energies, while the calculated curve is not. This bending is due to non-linearities in the electronics and light output of the plastic scintillator below 125 keV. None of these features have been considered in the simulations. The bending can also be seen in the experimental projected 1D beta spectrum (Fig. 18, upper panel) at low energies, where there is a dip in the distribution. The simulated beta spectrum peaks at the lowest energies since the bending is missing.

The gamma spectra (Fig. 18, lower panel) show a prominent peak at around 200

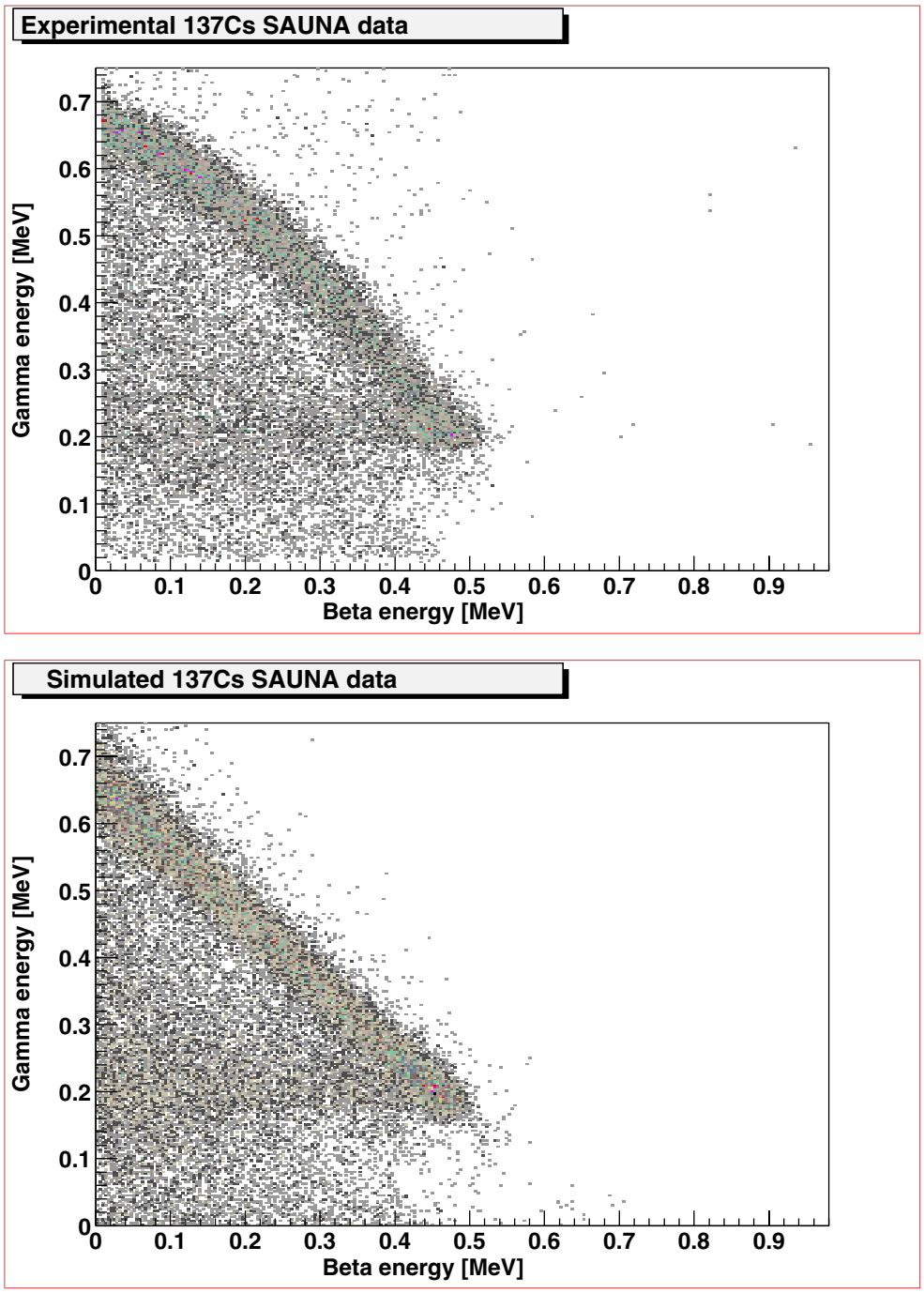

Figure 17: Two-dimensional experimental (upper panel) and simulated (lower panel) spectra from Compton scattering of ^{137}Cs obtained with SAUNA.

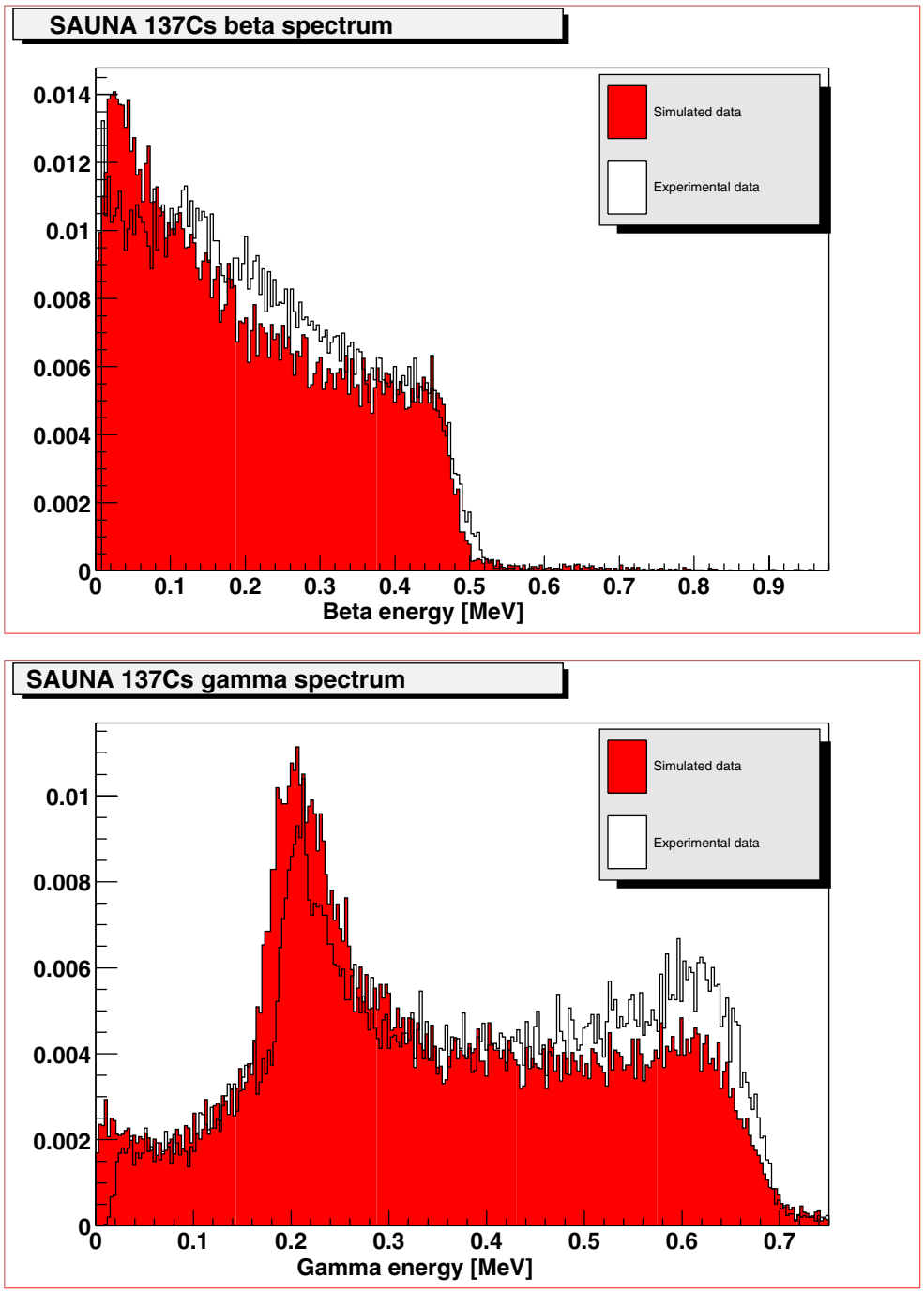

Figure 18: Beta (upper panel) and gamma (lower panel) spectra due to Compton scattering of gamma rays from ^{137}Cs obtained with SAUNA and compared with simulations.

keV, corresponding to backscattering of the source photons. The gamma distributions end at 662 keV, which is the full energy of the incoming photons. The beta spectrum, on the other hand, ends at 478 keV, which is the maximum remaining energy from the backscattering events.

The calculations with a ^{137}Cs source that were made for SAUNA, were also performed for the ARSA detector (see Figs. 19 and 20). Due to a more complicated geometry, the calculations are even more time consuming, and the 20 million transported source particles only give rise to about 40 000 coincidence events. The gamma resolution in the simulations was the one given in Eq. 3, and the beta resolution was chosen to fit the experimental beta spectrum. It was found that a constant beta energy resolution of 59 keV FWHM made the best fit between experimental and simulated data.

In the 2D experimental ARSA spectrum, the distribution is bent at low beta energies (see Fig. 19, upper panel). This is again due to electronics and a non-linear light output at beta energies below 125 keV, which have not been modelled in MCNP. The experimental 2D spectra from SAUNA and ARSA both have bendings, but they are bent in different directions. This can be explained by different electronics setups. When comparing the beta spectra (see Fig. 20, upper panel) the bending is visible in the experimental spectrum as a peak at the lowest energies. This peak is much less prominent in the simulated spectrum, where the bending is missing.

When looking at gamma spectra (Fig. 20, lower panel) there is again the backscattering peak at around 200 keV in both histograms. However, there is also a second peak from an additional backscattering, resulting in a peak at around 110 keV. This peak shows up in both the experimental and simulated spectra for ARSA, but it is not visible in either of the corresponding SAUNA spectra. The reason for this is the placement of the cesium source in the two cases. In the SAUNA case, the source is placed outside the NaI, so particles backscattered in the surrounding material are less likely to reach the beta cell. The ARSA source, on the other hand, is placed inside the NaI crystal, close to an adjacent beta cell. Therefore, backscattering close to the source results in about 200 keV gamma rays which are backscattered a second time in the beta cell, and give rise to the peak at around 110 keV.

As in the SAUNA case, and as expected, the gamma distribution ends at 662 keV, and the beta spectrum ends at 478 keV.

7.3 Xenon spectra

Radioactive xenon isotopes emit coincident beta and gamma particles. Thus, standard MCNP cannot be used, for reasons described in section 7.2. However, since the MCNP developers provide the full source code to users, it is possible to link a user-defined source subroutine to the rest of the code. The user-defined routine will automatically be called by MCNP if the standard source, SDEF, is omitted.

The source routine used in this work has been developed together with Romano Plenteda at the CTBTO. A similar approach has been used in calculations of germanium spectrometers [8]. The source is a FORTRAN routine, which reads a xenon decay, scheme and samples the relevant particles with correct energy and particle type. In addition, a user-defined tally routine for addition of coincident particles (i.e., gamma cascades) has been developed. Some changes have also been made to the pulse height routine that scores pulse height tallies at the end of each history.

Calculations of xenon spectra, using the special user-defined source routine, were only

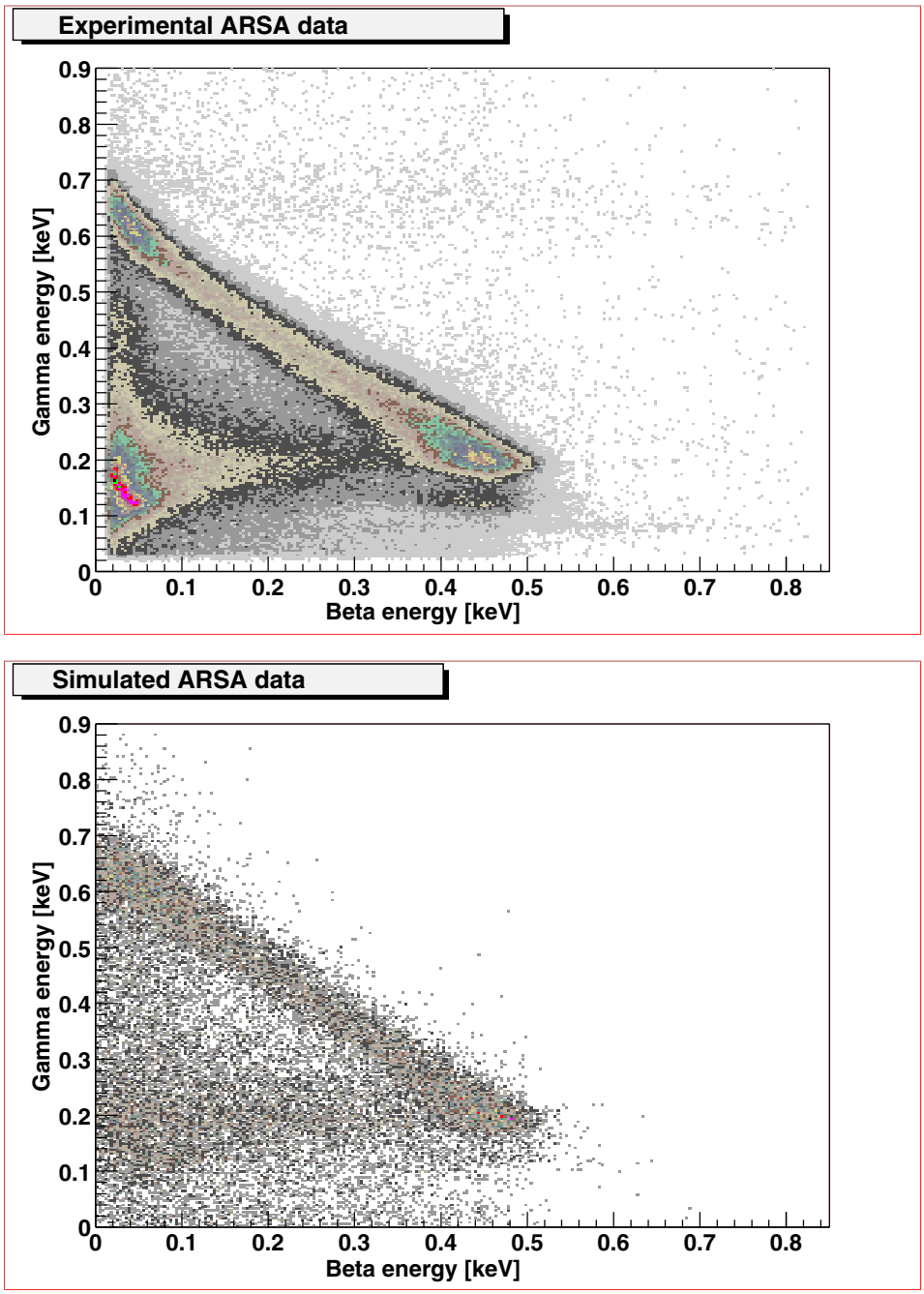

Figure 19: Two-dimensional experimental (upper panel) and simulated (lower panel) spectra from Compton scattering of ^{137}Cs obtained with ARSA.

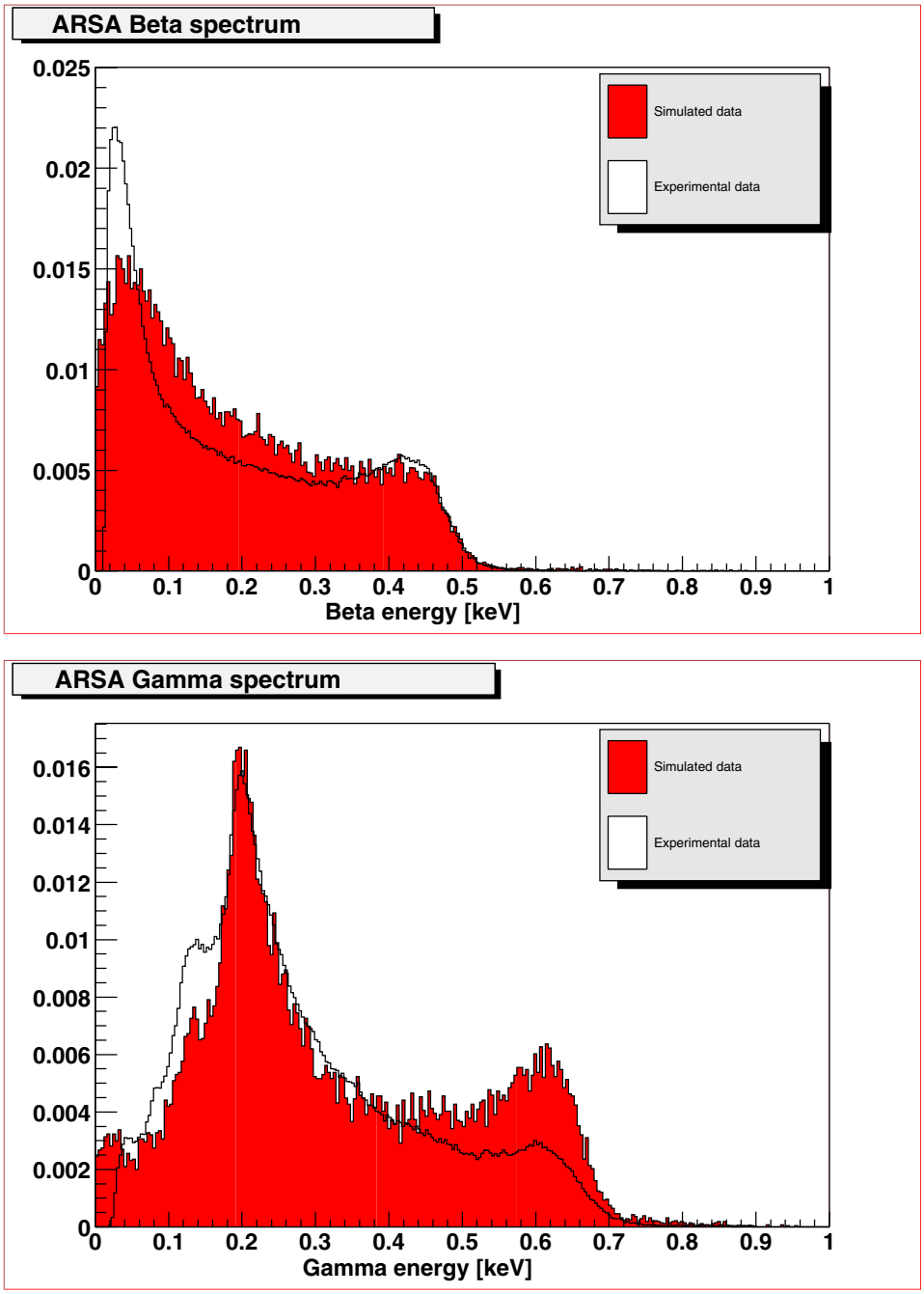

Figure 20: Beta (upper panel) and gamma (lower panel) spectra due to Compoton scattering of gamma rays from ^{137}Cs obtained with ARSA and compared with simulations.

performed for the SAUNA detector. Since the output is direct and does not require the PTRAC sorting, these calculations are much faster than the ones for ^{137}Cs decribed in section 7.2. Approximately 50 000 source particles are needed for sufficient statistics. The same values for the gamma and beta energy resolution were used as in the other calculations.

In Fig. 21, 2D spectra of a ^{133}Xe measurement and a calculation are shown. There are two prominent gamma distributions in both plots, one at around 30 keV gamma energy, corresponding to cesium x-rays, and one at 81 keV gamma energy. In the simulated spectra (lower panel), also higher excited states are visible (e.g., one at 160 keV). The gamma rays from these states are not obvious in the experimental spectrum, due to poor statistics and the instrumental background. Note that the x-ray distribution does not extend all the way down to zero beta energy in the experimental spectrum (the upper panel). This is due to coincidence summing in the electronics of one electron from beta decay, and one from internal conversion (the life-time of the 81 keV level is only around 3 ns). This effect has not been modelled in MCNP, which is clearly seen in the lower panel.

The projected beta and gamma spectra for both the measured data and the calculations are shown in Fig. 22. The dominant beta decay in ^{133}Xe has an endpoint energy of 346 keV, which can be clearly seen in the simulated histogram (the upper panel of Fig. 22) . The experimental data display a peak at around 130 keV, which is missing in the calculations. It is due to decay of ^{131m}Xe, which was also present in the measured sample but not included in the modelling.

The gamma projections in the lower panel of Fig. 22 exhibit two dominant peaks, in both the experimental and the simulated spectra. These are due to the gamma emission from the 81 keV excited state in ^{133}Cs, and the x-rays around 30 keV from internal conversion of the same state. The contribution from ^{131m}Xe can also be seen in the experimental spectrum, contributing to the peak at around 30 keV.

In Fig. 23, simulations of ^{135}Xe are shown. There are no experimental data containing pure ^{135}Xe available for comparison, but the result obtained with MCNP is the expected one. The dominant beta decay has an endpoint energy of 910 keV, and it populates the 250 keV excited state (see the upper panel of Fig. 23). A weaker band can also be seen at around 608 keV gamma energy. The middle panel shows the beta spectrum, which is expected to end at 910 keV. In the lower panel, the dominant peak is the 250 keV gamma ray, and also the 608 keV transition can be seen. The peak at around 30 keV comes from cesium x-rays associated with internal conversion of the 250 keV state.

In all the experimental xenon spectra, there is a background contribution from decay of ^{40}K in construction materials, etc. ^{40}K emits gamma rays of 1460 keV, which results in a Compton distribution representing a background at the energies of the xenon mesurements. This ^{40}K decay has been measured outside the lead shieldning with a germanium detector, and has been found not to be an important problem.

For the computation of the detector efficiencies, various regions of interest (ROI) have been defined (see Table 2). These correspond to regions in the different xenon spectra, where prominent peaks are expected to appear, and where it is of special importance to know the counting efficiency of the detector.

Experimentally, the beta distribution in the x-ray region results in higher, or comparable, beta-gamma efficiency compared with the 81 keV region, even though the photo-peak efficiency is lower in that region (see Fig. 16). The reason for this is addition in the electronics of a coincident electron from internal conversion and the beta particle, reulting the x-ray distribution starting at around 45 keV beta energy instead of zero (see Fig.

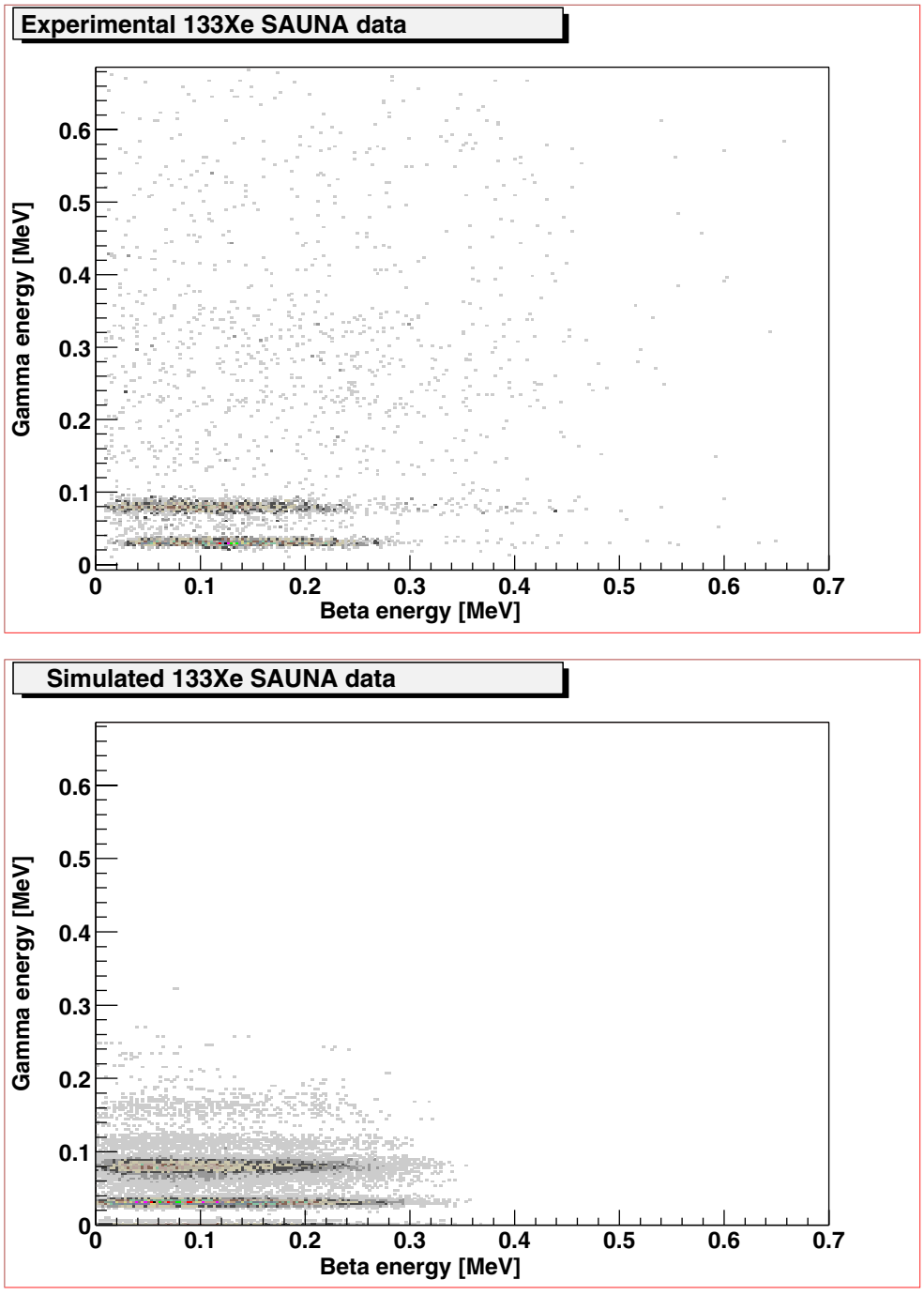

Figure 21: Comparison between measured (upper panel) and simulated (lower panel) ^{133}Xe spectra in SAUNA. The faint two bands at about 110 and 160 keV gamma energy in the simulation are not visible in the experimental data due to poor statistics. (The simulation has almost a factor 10 more events.)

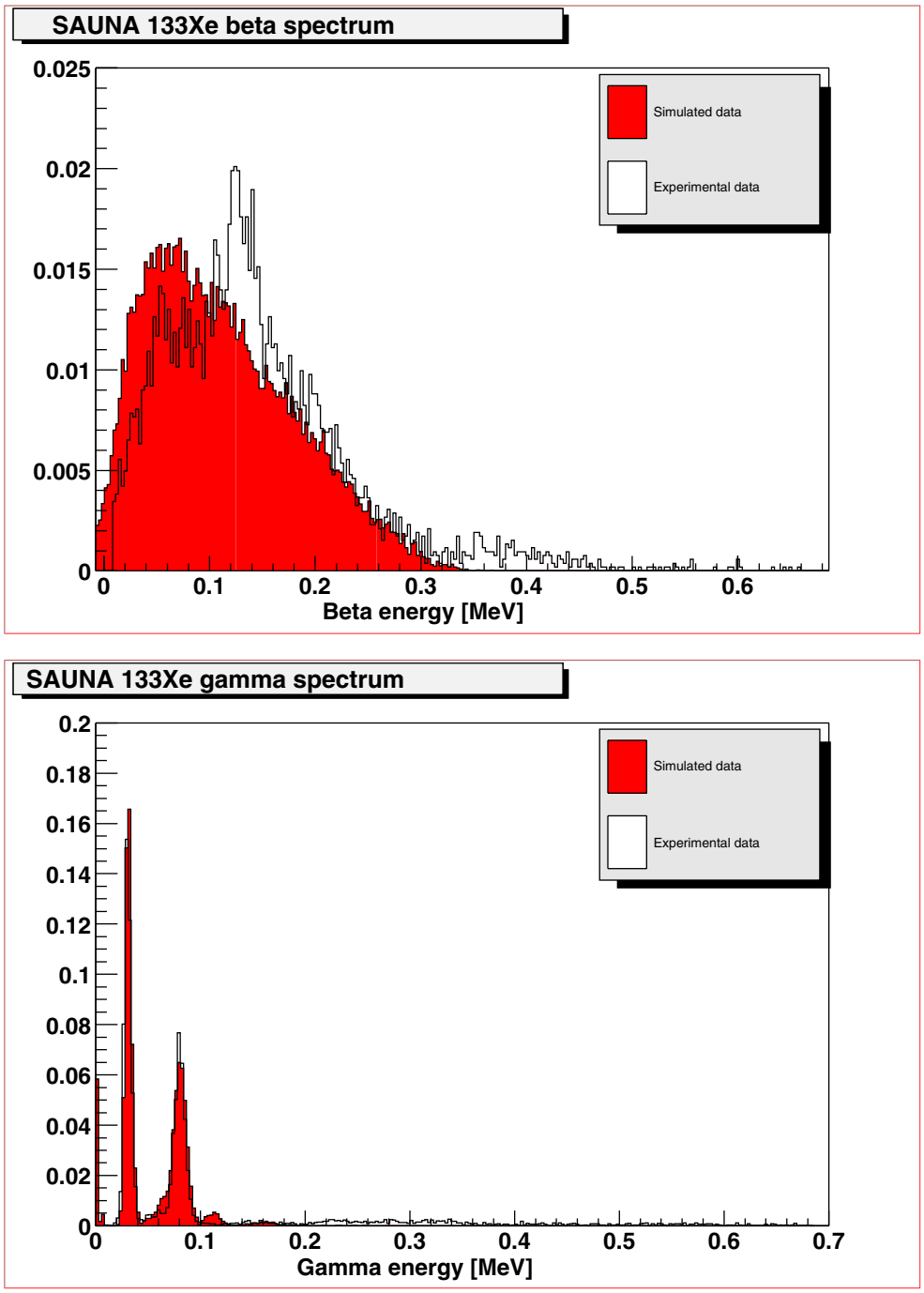

Figure 22: Beta (upper panel) and gamma (lower panel) projections of ^{133}Xe spectra. Experimental and simulated spectra are shown together.

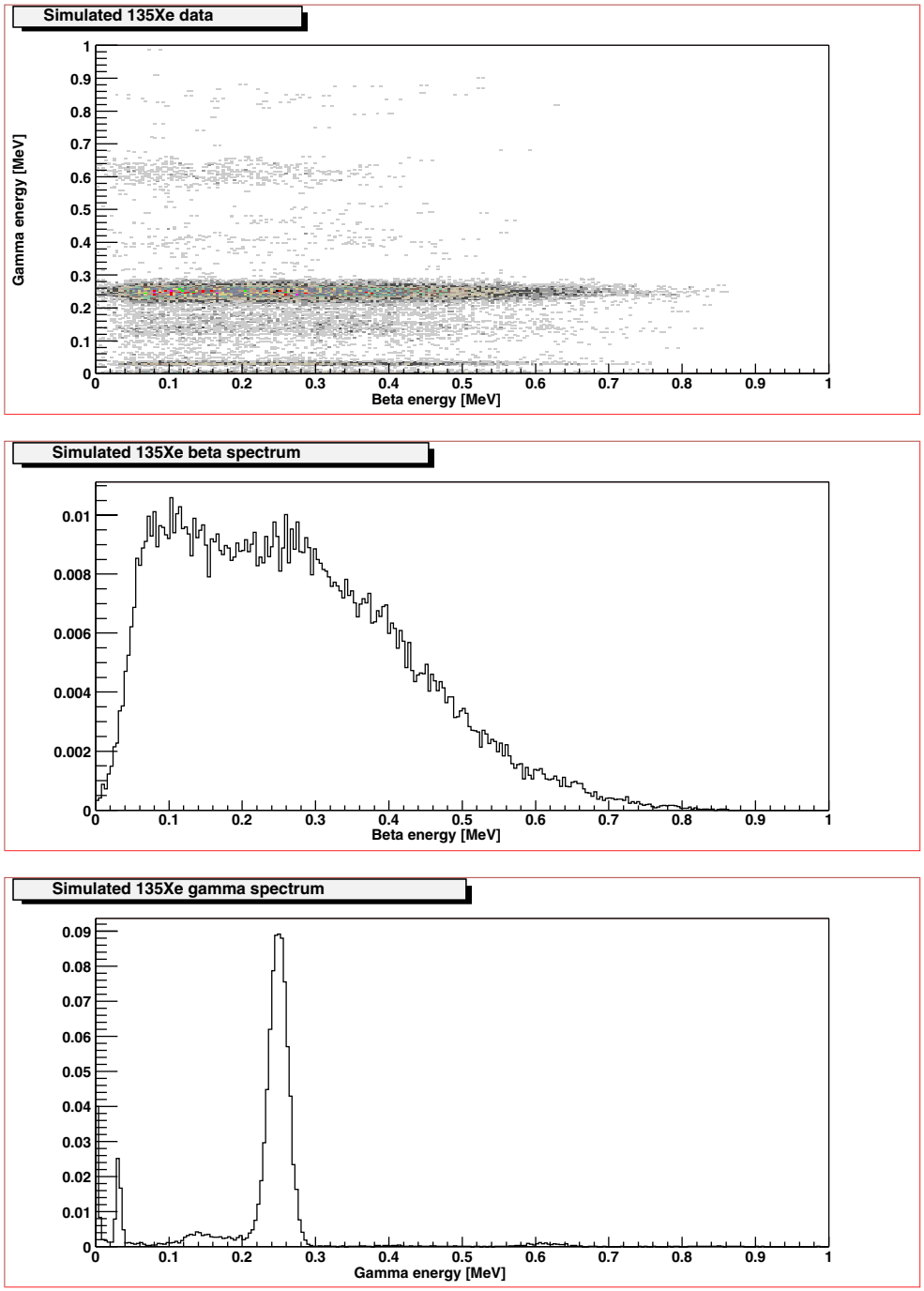

Figure 23: MCNP calculations of ^{135}Xe decay detected by SAUNA. The upper panel shows gamma energy plotted versus beta energy, the middle panel shows the beta energy spectrum, and the lower panel the gamma energy spectrum.

	^{133}Xe		^{135}Xe
Gamma energy	30 keV	80 keV	250 keV
Beta threshold	0 keV	0 keV	0 keV
Calculated efficiency	**71%**	**75%**	**68%**
Beta threshold	10 keV	10 keV	10 keV
Calculated efficiency	**70%**	**74%**	**68%**
Beta threshold	20 keV	20 keV	20 keV
Calculated efficiency	**67%**	**71%**	**67%**
Measured efficiency	**50%**	**40%**	-

Table 3: Calculated and measured beta-gamma efficiencies in various regions of interest.

21, upper panel). This also makes the 30 keV region less sensitive for variations in the discriminator level on the beta energy, which is typically below 50 keV. For comparison, some typical experimental efficiencies used in the concentration analysis of SAUNA data are shown in Table 3. These efficiencies are based on a combination of measured beta efficiencies and earlier MCNP calculations [9]. The main reason for the relatively large discrepancy between these efficiencies and the ones calculated in the present work, is due to the fact that neither the internal conversion electrons nor the light output function are taken into account in the calculations. Since the trigger is based on a triple coincidence between the two beta PM tubes and the NaI detector, a signal with a deposited energy above threshold still might be lost, if the beta particle interacts in the plastic cylinder close to the edge. This results in a small signal in the other PM tube, and as a result no trigger will be produced. This effect is not included in the calculations.

When comparing the results for the NaI detector efficiency in Fig. 16 with those for the total efficiency in Table 3, it is possible to calculate the beta detector efficiency through the relation $\epsilon_{\beta\gamma} = \epsilon_\beta \cdot \epsilon_\gamma$. At the energies 30 keV, 80 keV and 250 keV, ϵ_γ is 80%, 87%, and 74%, respectively (see Fig. 16). A simple calculation assumuing a 0 keV beta threshold, gives the values 89%, 86%, and 92% for the beta efficiencies of the energies 30 keV, 80 keV, and 250 keV, respectively.

8 Summary, conclusions and outlook

This report describes MCNP simulations of the response of two detectors with slightly different geometries. These are the SAUNA and ARSA systems for detection of radioactive xenon as a means to monitor violations of the Comprehensive Nuclear-Test-Ban Treaty. The detectors measure beta-gamma coincidences, with a similar trigger and electronics setup. Coincidences between beta particles and gamma rays are not recorded in the MNCP default output, so special methods have been developed for treatment of coincidences. In the case of simulating Compton scattering of gamma rays from ^{137}Cs, the tracking information contained in the MCNP output was extracted and sorted with respect to energy deposition in the beta and gamma cells. When simulating xenon isotopes, on the other hand, a user-defined particle source routine was linked to the MCNP code to create coincident source events.

In addition to these simulations, detector efficiencies have been studied. The gamma detector efficiency was simulated using simple non-coincident gamma sources of different energies, and the total beta-gamma efficiency was obtained from the count rates in various

regions of interest defined in the detector energy range.

The obtained results agree well with experimental data and have been useful to understand the detector response. Deviations from experimental data can be understood from known differences between the detectors and the modelled geometries.

As a continuation of this work, it would be interesting to model the user-defined source for xenon decays even more carefully. One improvement could be to add transport of conversion electrons, and thereby be able to reproduce the beta energy coincidence effects in 2D plots. This would enable a more accurate calculation of detector efficiencies. Also a modelling of the light output for the beta detector could help in this respect.

In addition, the metastable xenon states could be modelled, as well as combinations of xenon isotopes. The xenon expected from fission of heavy elements is a combination of various isotopes, and therefore it would be interesting to investigate different ratios and combinations.

It would also be beneficial to see the effect in simulated spectra of the ^{40}K background from surrounding material seen in the experimental data.

Finally, it would be valuable to investigate if the sorting procedure for ^{137}Cs Compton scattering coincidences could be improved, especially if it would enable a larger number of particles to be transported, resulting in better statistics.

Acknowledgements

The work I have performed is the result of a collaboration between the Department of Neutron Research (INF), Uppsala University and the Swedish Defence Research Agency (FOI). It was initially planned to be a two-month project within the AIM Research School, but as time went on and new interesting fields opened, it grew and eventually became a licentiate thesis.

The people who have made it possible for me to work with this interesting project are most of all my supervisors, Jan "Bumpen" Blomgren (UU) and Anders Ringbom (FOI). Thank you Bumpen for letting me spend a lot of time with the FOI and still supporting my work, and thank you Anders for introducing me to the work, guiding me through it, and (not the least) for letting me come to Spitzbergen!

I am also very grateful for the help and inspiring company of the xenon team at FOI: Anders R., Anders A., and Klas. We had a great time in Longyearbyn! I am especially thankful to Klas who saved me many hours of work by revealing many secrets of LaTeX and the postscript format. Everyone else at FOI should also be acknowledged for nice company at the coffee table and for creating a stimulating atmosphere. I am also very thankful to those of you who transported me between Uppsala and FOI, Anders, Klas, Nisse, and Pär. Nisse is also acknowledged for valuable advice on this report.

Another person who has helped me a lot by letting me use and develop his FORTRAN routines is Romano Plenteda at CTBTO. Thank you for a good cooperation!

Most of my working time I have spent at the INF in Uppsala, and I will yet spend a lot of time there. Therefore, all my nice colleagues at INF will have to wait for their thanks until my doctoral thesis! But you have all done pretty well so far...

References

[1] Homepage of the Comprehensive Nuclear-Test-Ban Treaty Organization, http://www.ctbto.org.

[2] M. Auer, *et al.*, *The international programme to test and evaluate CTBT/IMS noble gas equipment*, to be published.

[3] R.W. Perkins and L.A. Casey, *DOE/RL-96-51,* (June 1996).

[4] W.K. Pitts, T.W. Bowyer, J.I. McIntyre, P.L. Reeder, A. Ringbom, C. Johansson, *Gain Calibration of a Beta-Gamma Coincidence Spectrometer for Automated Radioxenon Analysis*, to be published.

[5] A. Ringbom, T. Larsson, A. Axelsson, and K. Elmgren, *SAUNA - Swedish Automatic Unit for Noble Gas Acqusition, Operational manual*, to be published.

[6] T.W. Bowyer, *et al.*, *Journal of Radioanalytical and Nuclear Chemistry*, **235, No:s 1-2** (1998) 77-81.

[7] A. Ringbom, T. Larsson, A. Axelsson, K. Elmgren and C. Johansson, *SAUNA - a System for Automatic Sampling, Processing, and Analysis of Radioactive Xenon*, to be published.

[8] R. Plenteda, *A Monte Carlo Based Virtual Gamma Ray Spectroscopy*, to be published.

[9] A. Ringbom, *FOA Report*, 00905-861 (1998).

[10] J.F. Briesmeister, MCNP - A General Monte Carlo N-Particle Transport Code, Version 4B, March 1997.

A Appendix

A.1 The MCNP input file

The MCNP input is defined by cards which are interpreted by the code. These can be divided into three classes: surface cards, cell cards, and data cards. If nothing else is defined, the default units are cm, MeV, grams, and barn.

The first entry on a surface card is the surface number. Second comes an alphabetical mnemonic defining the type of surface, and the following entries are the numerical coefficients of the equation describing the surface type. Examples:

```
1 pz -5
2 s 0 0 0 3
3 cx 1
```

The three surfaces above define, (1) a plane orthogonal to the z-axis, at z = -5 cm, (2) a sphere with radius 3 cm centred at (0,0,0), and (3) an infinite cylinder on the x-axis with radius 1 cm.

The cell cards define cells bounded by the surfaces. The first entry is the cell number, then comes the material number with its density, and last a list of the surfaces that confine the cell. Examples:

```
1 1 -7.86 1
2 0 -2
3 2 -3.0 -3 -1
```

Cell number 1 contains material 1 with density 7.86 g/cm^3 and is located to the right of surface 1. Cell 2 is void (has no density) and is the volume inside the spherical surface 2. Finally, cell 3 is made out of material number 2 with a density of 3.0 g/cm^3, and defines the space inside the cylinder 3 and to the left of the plane surface 1. When the density is given as a negative number, the unit is g/cm^3, whilst if the entry is positive, the unit is interpreted as atoms/cm^3. A minus sign preceding the surface number indicates that the cell is located on the negative side of the surface.

Data cards are all other cards that are used to define a MCNP problem. Some of the most important are:

- MODE, which defines the problem mode. Choices are n (neutron transport), p (photon transport), e (electron transport), or combinations of these.
- Mn, material card, defining material n, by giving relative atomic abundancies.
- SDEF, the general source card. The entries here define, e.g., the source position, extent, direction, particle type, and energy type. An example of a simple source is:

  ```
  SDEF POS=0 0 0 ERG=0.662, PAR=p
  ```

  which emits photons of 0.662 MeV from the point (0,0,0).

- Fn, tally cards. Tallies display the requested output information. There is a number of standard MCNP tallies, defined by different values of n, for example F8, which is energy distribution in a chosen cell.

- PTRAC, the particle track output card. It generates an output file, (a ptrac-file), which contains user-filtered tracks of particle events and histories. PTRAC is a useful card when the user wants to follow individual particle tracks, but the created ptrac-files tend to be very large.

For a complete description of MCNP methods, theory and input, see the MCNP manual [10].

An example of a MCNP input file for SAUNA

```
4"x5" NaI crystal, point source (Cs) outside NaI
c
c cell cards
c
1 0 -4 6 fill=1 imp:e,p=1
2 2 -3.67 5 u=1 imp:e,p=1
3 3 -2.70 -5 u=1 imp:e,p=1
4 3 -2.70 4 31 -7 6 #20 imp:e,p=1
5 0 -6 12 -11 #13 fill=2 imp:e,p=1
6 9 -2.2 -3 22 -21 u=2 imp:e,p=1
7 4 -1.0 -10 24 -23 #6 u=2 imp:e,p=1
8 3 -2.70 -8 u=2 imp:e,p=1
9 3 -2.70 -9 u=2 imp:e,p=1
10 4 -1.0 8 -13 23 u=2 imp:e,p=1
11 4 -1.0 9 -13 -24 u=2 imp:e,p=1
12 0 #6 #7 #8 #9 #10 #11 u=2 imp:e,p=1
13 0 -2 24 -23 fill=3 imp:e,p=1
14 5 -0.002 -1 u=3 imp:e,p=1
15 1 -1.032 1 22 -21 u=3 imp:e,p=1
16 1 -1.032 #14 #15 u=3 imp:e,p=1
17 6 -11.35 -14 15 #21 imp:e,p=1
18 8 -7.87 -15 16 #21 imp:e,p=1
19 7 -8.96 -16 17 #21 #22 imp:e,p=1
20 3 -2.70 -18 imp:e,p=1
21 3 -2.70 -19 imp:e,p=1
22 3 -2.70 -30 #21 18.3 imp:e,p=1
23 0 -17 7 #5 #20 #22 #24 imp:e,p=1
24 10 -2.5 -31 imp:e,p=1
50 0 14 imp:e,p=0

c
c surface cards
c
1 rcc 0 -2.42 0 0 4.84 0 0.635
2 cy 0.7557
21 py 2.54
22 py -2.54
23 py 2.74
24 py -2.74
3 cy 0.7577
4 rcc 0 0 -5.08 0 0 10.16 6.35
5 cy 1.7754
6 cy 1.75
7 rcc 0 0 -6.1325 0 0 11.3125 6.45
8 rcc 0 2.74 0 0 13.1 0 0.9525
9 rcc 0 -2.74 0 0 -13.1 0 0.9525
10 cy 0.932
```

```
11 py 16.14
12 py -16.14
13 cy 1.51
14 box 16.5 -27.5 -23.7 -33 0 0 0 55 0 0 0 40.9
15 box 11.5 -22.5 -18.7 -23 0 0 0 45 0 0 0 30.9
16 box 11.5 -22.5 -18.7 -23 0 0 0 45 0 0 0 30.5
17 box 11 -22 -18.2 -22 0 0 0 44 0 0 0 29.5
18 rcc 0 0 -14.98 0 0 8.9475 7
19 rcc 0 0 -23.7 0 0 5.5 3
30 kz -21 1.450 1
31 rcc 0 0 -5.08 0 0 -0.9525 6.35

c
c data cards
c
mode p e
M1 1000 0.5236 6000 0.4764
M2 11000 0.5 53000 0.5
M3 13000 1.
M4 1000 0.529 6000 0.441 7000 0.03
M5 2000 -0.083 54000 -0.917
M6 82000 1.0
M7 29000 1.0
M8 26000 1.0
M9 6000 0.33 9000 0.67
M10 14000 0.25 11000 0.1 20000 0.05 8000 0.6
sdef pos=0 0 8 erg=0.662 vec=0 0 -1 dir=D1 par=2
SI1 L 1 0.95 0.9 0.8 0.85 0.7
SP1 D 0.3 0.3 0.2 0.1 0.1 0.1
FT8 GEB -7.7e-3 75.7e-3
f8:p,e (2 ¡ 1)
e8 0 1e-5 0.01 138l 1.4
FT18 GEB 0.03 0
f18:e (15 ¡ 13)
e18 0 1e-5 0.01 98l 1.0
f4:e (15 ¡ 13)
sd4 1
dbcn 1011
nps 8000000
c print 85
ptrac file=asc write=all max=10000000 cell=15 type=e filter=2,15,icl
tally=4 value=0
```

A.2 The PTRAC output and sorting procedure

The output obtained with the PTRAC card is an ASCII or binary file containing the chosen information specified in the input file. The information is presented history by history (i.e., source particle by source particle), and within each history, every event is presented with position, direction, energy, weight and time. Each event is also described by more parameters, like a type code and the cell in which the event takes place. The type codes of most importance for the sorting procedure are

- **1000**, source event, i.e., a new history starts.
- **2000 + L**, bank event. These are events that give rise to new particles which are saved for later transport (banked). Among these are photo electric events, Compton events, etc. The various event types are defined by the number **L**, so, for instance, the type code **2012** signals the creation of a Compton electron.
- **3000**, surface event. This means that a surface has been crossed. Usually this does not involve a "true" reaction and has no energy loss associated with it.
- **5000**, termination event. The prexent event is terminated when the energy is below the cut-off energy, or if it has escaped out of the geometry. After a termination event, the next bank event is transported.
- **9000**, last history event, i.e., after this event the next history begins.

To obtain the coincidence information, i.e., energy deposition in the beta cell and the gamma cell for the same history, a sorting procedure has been developed. It consists of a program written in PERL language and goes through the ptrac-file to find events with energy deposition in the wanted cells. It then sums the deposited beta and gamma energies for each history, respectively. The final output is two vectors containing the beta and gamma energies.